MOLECULAR MECHANISMS OF ATHEROSCLEROSIS IN THE MOUSE

INVESTIGATING THE MOLECULAR MECHANISMS OF ATHEROSCLEROSIS DEVELOPMENT IN THE MOUSE: EMPHASIS ON THE MACROPHAGE SPHINGOSINE-1-PHOSPHATE RECEPTOR 1.

By LETICIA A. GONZALEZ JARA, M.SC

A Thesis Submitted to the School of Graduate Studies in Partial Fulfillment of the Requirements for the Degree Doctor of Philosophy

McMaster University

McMaster University DOCTOR OF PHILOSOPHY (2016) Hamilton, Ontario

(Biochemistry and Biomedical Sciences)

TITLE:	Investigating the molecular mechanisms of atherosclerosis development in the mouse: emphasis on the macrophage sphingosine-1-phosphate receptor 1.
AUTHOR:	Leticia A. Gonzalez Jara, M.Sc (Universidad de Chile)
SUPERVISOR:	Dr. Bernardo Trigatti
NUMBER OF PAGES:	288

Abstract

Atherosclerosis is a chronic inflammatory disease affecting large- and medium-sized arteries and is considered the major cause behind cardiovascular diseases (CVD). Elevated low-density lipoprotein (LDL)-cholesterol and low high-density lipoprotein (HDL)-cholesterol are considered major risk factors for the CVD. HDL mediates a variety of atheroprotective actions, many of them involving the interaction with the scavenger receptor class B, type 1 (SR-B1).

Despite the efforts placed in raising HDL-cholesterol, no improvement has been achieved in reducing CVD risk, suggesting that other components of the HDL particles may be responsible for HDL-mediated atheroprotection. One of these may be sphingosine-1-phospate (S1P).

In this thesis, the role of S1P receptors (S1PRs) in atherosclerosis is explored, with emphasis in macrophage apoptosis. In particular, the importance of the macrophage S1PR1 and its role in apoptosis and atherosclerosis was evaluated. We demonstrated that diabetes exacerbates atherosclerosis development and myocardial infarction in SR-B1 KO/apoE-hypomorphic mice and that treatment with FTY720, a S1PR agonist, protects against diabetes pro-atherogenic effects. We also show that S1PR1 agonists protected macrophages against apoptosis through phosphoinositide 3-kinase (PI3K)/AKT, and that HDL failed to protect S1PR1 deficient macrophages against apoptosis. *In vivo*, macrophage S1PR1 deficiency translated into increased atherosclerosis, necrotic core formation and numbers of apoptotic cells in the atherosclerotic plaque.

BIM deficiency in BM cells was protective against atherosclerosis development and HDL treatment reduced BIM protein levels in cells exposed to ER stressors, suggesting that the pro-apoptotic protein may be an important target for HDL in macrophages.

We conclude that signaling through the S1PRs, in particular S1PR1 is important in controlling macrophage apoptosis and atherosclerosis development. Our data suggests that S1PR1 signaling axis and the pro-apoptotic protein BIM play an important role in mediating HDL anti-apoptotic signaling, however further studies are required to clarify the interaction between all of these factors.

Acknowledgements

I would like to start by thanking my supervisor Dr. Bernardo Trigatti for his constant support since the very first day I joined his lab. Dr. Trigatti was always patient and generous with his knowledge and I am grateful I had a chance to learn from him.

I would also extent my thanks to my supervisory committee: Dr. Trigatti, Dr. Werstuck and Dr. Liaw for their support and guidance throughout this journey towards my PhD. Thank you for all the encouraging words and helpful advice.

Many thanks to all the members of the Trigatti lab and everyone at the TaARI, you always made me feel welcomed and working along all of you has been a pleasure. I wish you all the best in your future career and sincerely hope that the future brings nothing but happiness to your life.

To all my friends here in Canada and around the world, thank you for always listening to my complaints when things were not going the way I wanted. Thank you for all the moments we spent together laughing and enjoying life and thank you for being my family away from home. Special thanks to Guayaberos and the Paradise fam, I love you guys.

A mi familia y mis amigos del alma en Chile, se que estos años que hemos estado separados no han sido fáciles y quisiera agradecerles desde el fondo de mi corazón por siempre estar a mi lado, apoyandome. Gracias por creer en mi y alentarme cuando las ganas me faltaban y por amarme a pesar de todo. Los extraño siempre.

Andres, thank you for coming to my life and for staying. I love you and I'm excited for what the future has prepared for us.

And finally to Sarahi, because you were here for as long as you could and I will never forget you.

The years I spent in McMaster were nothing but happy and satisfactory and I will always remember them as one of the best moments in my life. Thank you to everyone from the bottom of my heart, I am a much better person now than what I was before.

The future is bright.

Leticia

Table of contents

List of Figures and Tables

List of abbreviations

ABC	ATP binding cassette
AGE	Advanced Glycation End products
AIM	Apoptosis Inhibitor of Macrophage
ALdKO	ApoA1/LDLR dKO
AMPK	5' Adenosine Monophosphate-activated Protein Kinase
ANOVA	Analysis of Variance
Apaf-1	Apoptotic Protease Activating Factor 1
Apo	Apolipoprotein
apoE-hypo	Apolipoprotein E-hypomorphic
ATF6	Activating Transcription Factor 6
Bad	Bcl-2-associated Death Promoter
Bak	Bcl-2 Homologous Antagonist/Killer
Bax	Bcl-2-associated X Protein
Bcl-2	B-cell Lymphoma 2
Bcl-XL	B-cell Lymphoma-extra large
Bid	BH3-interacting Domain Death Agonist
BIM	The BCL-2 homology Domain 3 (BH3)-only Protein, B-cell lymphoma 2 Interacting Mediator of Cell Death
BM	Bone Marrow
BMT	Bone Marrow Transplantation

BW	Body weight
CA	Coronary Artery
CAD	Coronary Artery Disease
CCL5	Chemokine (C-C Motif) Ligand 5
CCR1	C-C chemokine receptor type 1
CCR5	C-C chemokine receptor type 5
CD3	Cluster of Differentiation 3
CD36	Cluster of Differentiation 36
CETP	Cholesteryl Ester Transfer Protein
CHD	Coronary Heart Disease
CHOP	CCAAT-enhancer Binding Protein Homologous Protein
COX2	Cyclooxygenase Type 2
CVD	Cardiovascular Disease
DAPI	4', 6'-diamidino-2-phenylindole
DISC	Death-Inducing Signaling Complex
dKO	Double Knockout
DMEM	Dulbecco's Modified Eagle Medium
EC	Endothelial Cells
ECL	Enhanced Chemiluminescence
EDTA	Ethylenediaminetetraacetic Acid
eIF2α	Eukaryotic Initiation Factor 2α
eNOS	Endothelial Nitric Oxide Synthase

EPO	Erythropoietin
ER	Endoplasmic Reticulum
ERK	Extracellular Signal-Regulated Kinases
ERO1α	ER Oxidase 1α
FADD	Fas-associated Protein Death Domain
FasL	Fas Ligand
FasR	Fas Receptor
FBS	Fetal Bovine Serum
FOXO3A	Forkhead Box O3
FPLC	Fast Protein Liquid Chromatography
GAPDH	Glyceraldehyde 3-Phosphate Dehydrogenase
GRP78	Glucose-Regulated Protein 78
H&E	Hematoxylin/Eosin
HDL	High-density Lipoprotein
HDL-C	HDL Cholesterol
HF	High fat
HFC	High Fat/High Cholesterol
HRP	Horseradish Peroxidase
HtrA2	HtrA Serine Peptidase 2
HW	Heart Weight
ICAM1	Intercellular Adhesion Molecule 1
IDL	Intermediate-Density Lipoprotein

IRE1α	Inositol-Requiring Protein 1α
KLF4	Krüpel-Like Factor 4
KO	Knockout
LCAT	Lecithin:Cholesterol Acyl Transferase
LDL	Low-Density Lipoprotein
LDL-C	LDL Cholesterol
LDLR	LDL receptor KO
LPS	Lipopolysaccharide
LY	LY294002
MAPK	Mitogen-Activated Protein Kinases
Mcl-1	Myeloid Cell Leukemia 1
MCP-1	Monocyte Chemoattractant Protein-1
MerTK	MER Proto-Oncogene, Tyrosine Kinase
MKO	Macrophage KO
Mph	Macrophages
MPT	Mitochondrial Permeability Transition
NADPH	Nicotinamide Adenine Dinucleotide Phosphate-Oxidase
NCLPDS	Newborn Calf Lipoprotein Deficient Serum
NF-κB	Nuclear Factor κ B
NFAT	Nuclear Factor of Activated T-cells
NO	Nitric Oxide
ORO	oil Red O

oxLDL	Oxidized LDL
PAR-1	Protease Activated Receptor 1
PBS	Phosphate-buffered Saline
PCR	Polymerase Chain Reaction
PDZK1	PDZ-domain Containing Protein
PERK	Protein kinase RNA-like ER Kinase
PI3K	Phosphoinositide 3-Kinase
PKC	Protein Kinase C
PPRs	Pattern Recognition Receptors
PUMA	p53 Upregulated Modulator of Apoptosis
qRT-PCR	Quantitative Real Time PCR
RAC1	Ras-related C3 Botulinum Toxin Substrate 1
RAGE	Receptor for AGE
RCT	Reverse Cholesterol Transport
ROS	Reactive Oxygen Species
S1P	Sphingosine-1-phosphate
S1PR	S1P receptor
SEM	Standard Error of the Mean
SMCs	Smooth Muscle Cells
SphK	Sphingosine Kinase
SPP	S1P Selective Phosphatase
SR-B1	Scavenger Receptor Class B, Type 1

SRA	Scavenger Receptor A
STZ	Streptozotocin
T1D	Type 1 Diabetes
T2D	Type 2 Diabetes
TF	Tissue Factor
Thap	Thapsigargin
Tiam1	T-cell Lymphoma Invasion and Metastasis 1
TLR4	Toll-like Receptor 4
TN	Tunicamycin
TNF-α	Tumor Necrosis Factor α
TNFR1	TNF receptor 1
TUNEL	Terminal Deoxynucleotidyl Transferase dUTP Nick End Labeling
TxA2	Thromboxane A2
UPR	Unfolded Protein Response
VCAM1	Vascular Cell Adhesion Molecule 1
VLDL	Very Low-density Lipoprotein
WT	Wild Type

Chapter 1: General Introduction

1.1 Cardiovascular diseases

Cardiovascular diseases (CVD) account for over 17 millions deaths yearly dominating as one of the major contributors to global mortality; these numbers are expected to increase to approximately 20 million deaths by 2030[i]. Management of CVD risk factors such as obesity, hypertension, dyslipidemia and diabetes are key steps in the prevention of clinical manifestation of CVD, like myocardial infarction and stroke (Wong, 2014). In Canada, 30% of the registered deaths in 2008 were attributed to CVD, half of which were associated with ischemic heart disease[ii]. Atherosclerosis is a chronic inflammatory disease affecting the artery wall and represents the main underlying cause of ischemic heart disease (Tabas et al., 2015). Due to the high incidence of mortality associated with atherosclerosis, efforts are concentrated not only in prevention but also in understanding the mechanisms that govern the development of this disorder.

1.2 Atherosclerosis

Formation of the atherosclerotic plaque, the hallmark of atherosclerosis, is the result of a combination of factors including inflammation, accumulation of lipids and immune cell

[i] Mendis, S., Puska, P. & Norrving, B. (Eds) Global Atlas on Cardiovascular Disease Prevention and Control (WHO, 2011)
[ii] Statistics Canada. Mortality, Summary List of Causes 2008. Data summarized at Heart and Stroke foundation of Canada.

infiltration in the vessel wall (Hansson and Libby, 2006). In humans, early lesions can be classified as either intimal xanthomas or intimal thickening, and tend to be small and asymptomatic (Bui et al., 2009). These early lesions, also known as fatty streaks, can be detected in the aorta as early as the first decade of life and can evolve into more complex and advanced plaques (Lusis, 2000). The first step in disease development is the retention of apolipoprotein (apo) B containing lipoproteins, including the low-density lipoprotein (LDL), in the sub-endothelial space (Hansson and Libby, 2006) (see Figure 1.1). This local accumulation of lipoproteins is triggered by the activation and dysfunction of endothelial cells (EC) lining the vessel wall in areas where the vessels curve or branch (Tabas et al., 2015). The altered blood flow along with changes in endothelial cell morphology is thought to increase the permeability of these atherosclerosis-prone regions to macromolecules facilitating lipoprotein infiltration (Tabas et al., 2015).

It is widely accepted that the oxidative modification of the LDL particles retained in the vessel wall is an initiating event in atherosclerosis development (Lusis, 2000). Oxidized (ox) LDL is pro-inflammatory, stimulating EC to secrete cytokines and chemokines and to increase the expression of adhesion molecules on the cell surface (Lusis, 2000). Collectively, these changes in the endothelium trigger the recruitment of monocytes that differentiate into macrophages once in the vessel wall (Hansson and Libby, 2006). The uptake of oxLDL by macrophages, via scavenger receptors, leads to the formation of macrophage foam cells that can further secrete cytokines amplifying the inflammatory response (Hansson and Libby, 2006). As the disease progresses,

cholesterol overload results in the death of foam cells through apoptosis or secondary necrosis, releasing the cholesterol content in the intima (Tabas, 2010a). The inefficient clearance of dead cells promotes the accumulation of cell debris and extracellular lipids, generating a lipid rich region known as the necrotic core (Tabas, 2010a). The transition to more complex lesions also involves the activation and migration of smooth muscle cells (SMCs) from the medial layer to the sub-endothelium (Libby et al., 2011). Activated SMCs on top of the lesion secrete extracellular matrix proteins- such as collagen and elastin- forming the fibrous cap, which helps keep the lesion stable (Libby et al., 2011). Over time, secretion of matrix metalloproteases by plaque resident macrophages degrades and weakens the fibrous cap that prevents the exposure of the pro-thrombotic content of the plaque to circulation (Libby, 2009). Clinical manifestations of atherosclerosis usually arise as consequence of vessel stenosis due to the enlargement of the atherosclerotic plaque, or due to plaque rupture and the activation of the coagulation cascade (Tabas et al., 2015). The formation of a thrombus on top of the lesion can block the normal blood flow in the arteries resulting in myocardial infarction and/or stroke (Libby, 2009).

Figure 1.1: Atherosclerotic plaque development

A. The formation of the atherosclerotic plaque starts with changes in endothelium permeability that allows the accumulation of lipoproteins in the subendothelium. Once inside the vessel wall, these lipoproteins undergo modifications such as oxidation, which in turn induces the expression of adhesion molecules on the surface of EC and the release of chemokines. The pro-inflammatory environment attracts circulating monocytes and the presence of adhesion molecules facilitates their capture and transmigration into the vessel wall. Monocytes differentiate into macrophages (Mph) and take up modified proteins becoming foam cells. Both, macrophages and foam cells are able to secrete cytokines further amplifying the inflammatory response. **B.** The pro-inflammatory environment and the release of cytokines stimulate the activation and migration of SMCs. Activated SMCs secrete collagen and both help to create the fibrous cap covering the lesion. Foam cells, cells undergoing apoptosis and lipid droplets coalesce in the center of the lesion forming the necrotic core, which is rich in tissue factor (TF). **C.** The continuous growth of the necrotic core and macrophage-derived matrix proteases degrade and weaken the fibrous cap, rendering the plaque unstable. The fracture of the fibrous cap and the exposure of its contents to circulation activate the generation of a thrombus and the consequent risk of an ischemic event.

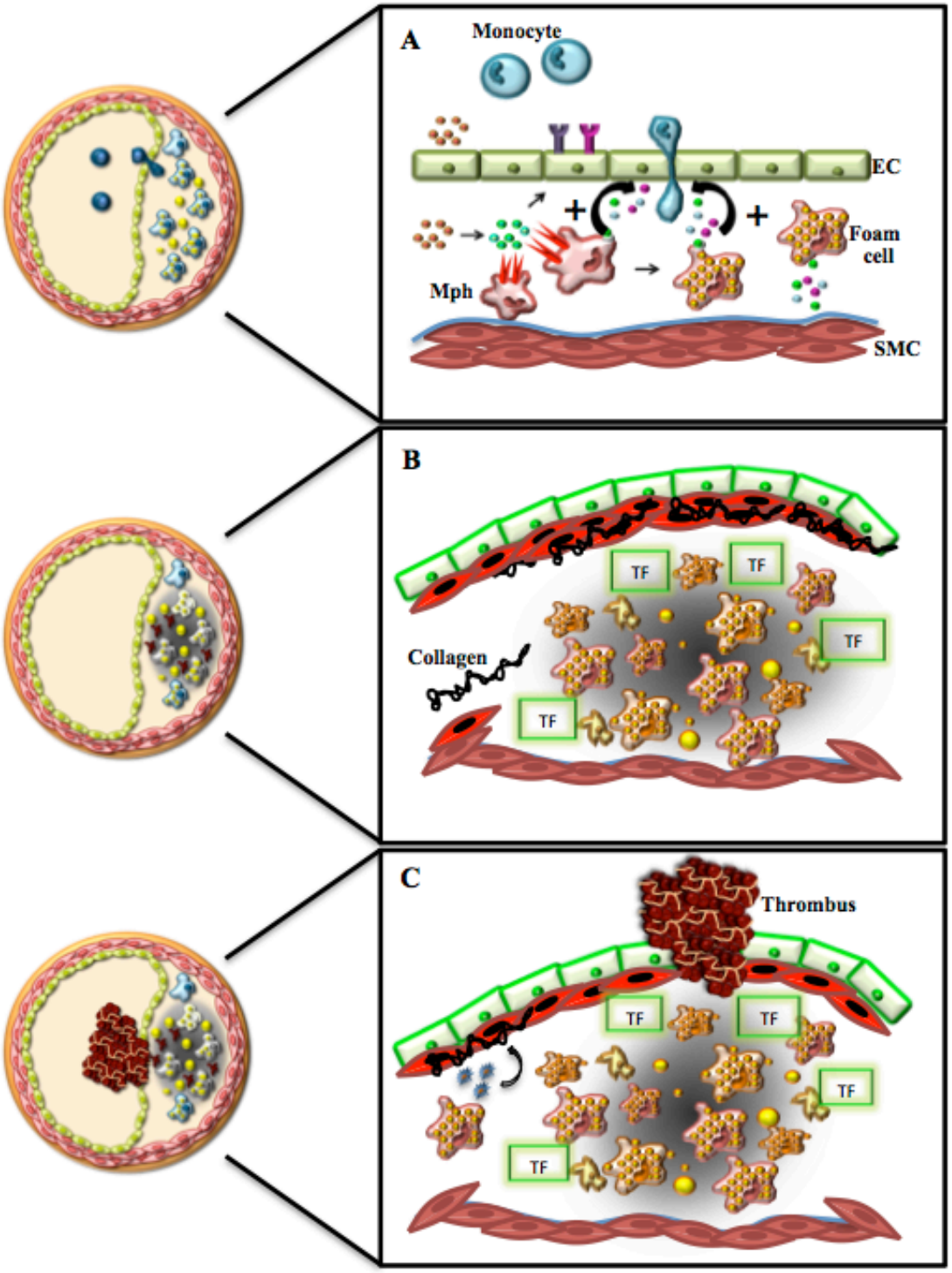
A
Monocyte
EC
Foam cell
Mph
SMC
B
TF
TF
TF
Collagen
TF
C
Thrombus
TF
TF
TF
TF

1.3 Diabetes, a risk factor for atherosclerosis development

Several risk factors, among them diabetes, have been linked to atherosclerosis development contributing to either the onset or progression of plaque formation (Zeadin et al., 2013). Diabetes is a metabolic disease characterized by a deficiency in insulin production (type 1, T1D) or defective insulin signaling (type 2, T2D) – also known as insulin resistance – resulting in hyperglycemia (Zeadin et al., 2013). Studies estimate that by 2030, almost 4.5% of the population will suffer from diabetes (Maahs et al., 2010). The most common complication in diabetes patients is CVD, affecting over 80% of the diabetic population (Winer and Sowers, 2004). Atherosclerotic lesions in diabetic patients tend to start earlier and develop faster (Voulgari et al., 2010). In fact by the age of 55, 35% of T1D patients (of both sexes) have died of coronary artery disease (CAD) compared to 8% and 4% for non-diabetic male and women respectively (Voulgari et al., 2010).

A significant amount of data exists linking hyperglycemia with atherosclerosis development in T1D patients. Studies have shown that children suffering from T1D present enhanced aortic and carotid intima-media thickness compared to the normal population (Jarvisalo et al., 2001; Jarvisalo et al., 2002). Hyperglycemia has also been shown to increase atherosclerosis development in mouse models. In the LDL receptor (*Ldlr*) knockout (LDLR KO) GP model, where diabetes is induced through viral-induced destruction of the insulin producing β-cells of the pancreas, early atherosclerotic lesions appearance has been reported in the absence of changes in plasma lipids (Renard et al.,

2004). Diabetic apolipoprotein E (*Apoe*) KO (apoE KO) mice develop significantly more atherosclerosis but also present a significant increase in plasma cholesterol compared to non-diabetic apoE KO mice (Park et al., 1998; Werstuck et al., 2006). Similarly, hyperlipidemic pigs also develop larger plaques under high blood glucose conditions (Gerrity et al., 2001).

Hyperglycemia induces endothelial dysfunction (Funk et al., 2012). Endothelial cells exposed to high glucose showed reduction in nitric oxide production and an increase in leukocyte infiltration and inflammation (Du et al., 2001; Morigi et al., 1998). The effect of hyperglycemia can be explained by several alterations including promotion of reactive oxygen species (ROS) production, generation of advance glycation end products (AGE) and changes in metabolic/signaling pathways (Funk et al., 2012). The increase in ROS in response to high glucose levels is related to diverse mechanisms including endothelial nitric oxide synthase (eNOS) uncoupling and mitochondrial dysfunction (Cai et al., 2005; Funk et al., 2012). AGE have also been reported to increase intracellular production of ROS through interaction with the surface receptor for AGE (RAGE) (Yan et al., 1994). The redox status of the cell can further be altered through the activation of the polyol pathway due to depletion of the antioxidant sources (Gleissner et al., 2008).

High intracellular glucose levels also activate the hexosamine pathway resulting in the generation of glucosamine (Beriault and Werstuck, 2012). In hyperglycemic apoE KO mice, high levels of glucosamine in macrophage foam cells correlates with increased atherosclerosis (Zeadin et al., 2013). Glucosamine has also been described to increase the production of inflammatory cytokines in the endothelium by increasing nuclear factor-κB

(NF- κB) activity (Werstuck et al., 2006), and to induce the accumulation of unfolded proteins leading to endoplasmic reticulum (ER) stress (Beriault and Werstuck, 2012). The compensatory response under conditions of ER stress is known as the unfolded protein response (UPR), which restores the equilibrium in the ER (Tabas, 2010b). There are three important sensors of ER stress located in the ER membrane: protein kinase RNA-like ER kinase (PERK), activating transcription factor 6 (ATF6) and the inositol-requiring protein 1α (IRE1α) (Ron and Walter, 2007). Under normal conditions, the sensors are kept inactive by interaction with the chaperone glucose-regulated protein 78 (GRP78)/Bip in the lumen of the ER (Zhou and Tabas, 2013). GRP78 dissociates from the sensors when misfolded proteins accumulate, triggering the activation in the UPR signaling cascade (Zhou and Tabas, 2013). The UPR helps relieve stress by decreasing protein synthesis, increasing the production of chaperones and facilitating degradation of the protein aggregates (Hetz, 2012).

1.4 Macrophage apoptosis and necrotic core formation

Monocytes are the driving force behind atherogenesis. Studies specifically targeting monocytes in transgenic mice have shown that reduced number and function of monocytes is associated with inhibition of early lesion development but did not affect the progression of already established atherosclerotic plaques (Stoneman et al., 2007). Similarly, mice deficient in chemokines and chemokine receptors crucial for monocyte recruitment, such as chemokine (C-C Motif) Ligand 5 (CCL5)/ C-C chemokine receptor

(CCL) type 1 and 5 (CCR1, CCR5), confirmed the importance of monocyte infiltration for plaque development (Zernecke et al., 2008). In circulation, monocytes can be roughly classified in two groups: Ly6C^{hi}, thought to be pro-inflammatory; and Ly6C^{lo}, thought to be involved in patrolling the inside of blood vessels (Moore et al., 2013). *In vivo* studies have shown that Ly6C^{hi} monocytes readily bind and infiltrate the activated endothelium compared to the Ly6C^{lo} counterpart (Swirski et al., 2007; Tacke et al., 2007). Moreover, hypercholesterolemia has been shown to promote Ly6C^{hi}-rich monocytosis in mice (Swirski et al., 2007). Once in the vessel wall, monocytes differentiate into macrophages. *In vitro*, macrophages can be classified in different subsets. M1 or classically activated macrophages differentiate in response to toll-like receptor ligands (like lipopolysaccharide (LPS), which reacts with TLR4) and interferon-γ (Moore et al., 2013). They are considered pro-inflammatory, as the main cytokines secreted are interleukin (IL)-1β and tumor necrosis factor α (TNF-α). On the other hand, M2, or alternatively activated macrophages differentiate in response to IL-4 and IL-13 and help with inflammation resolution and repair as they secrete mainly anti-inflammatory cytokines like IL-10 among other factors that help with tissue repair (Moore et al., 2013). Several studies have suggested that M2 polarization of macrophages is atheroprotective. Administration of IL-13 to LDLR KO mice inhibited atherosclerosis progression (Cardilo-Reis et al., 2012). Similarly, deletion of the M2 polarization factor Krüppel-like factor 4 (KLF4) promoted M1 macrophage activation and accelerated atherosclerosis in apoE KO mice (Liao et al., 2011).

Macrophages contribute to several changes in plaque morphology. The necrotic core is generated through a combination of several processes: macrophage apoptosis, secondary necrosis and impaired phagocytic clearance (efferocytosis) (Tabas, 2010a). Apoptosis is a form of programmed cell death involved in both homeostatic and defense mechanisms (Elmore, 2007). There are two main apoptotic pathways: the extrinsic and the intrinsic (mitochondrial) pathway, both converging in the same execution pathway characterized by the cleavage of caspase-3 (Elmore, 2007) (Figure 1.2). The activation of caspase-3 finally results in DNA fragmentation, formation of apoptotic bodies and expression of ligands for phagocytic cell receptors to facilitate clearance of the apoptotic cell (Elmore, 2007). The extrinsic pathway is characterized by the activation of death receptors, the Fas ligand (FasL)/Fas receptor (FasR) and TNF-α/tumor necrosis factor receptor 1 (TNFR1) models being the best characterized (Locksley et al., 2001). Upon activation of the death receptors, several cytoplasmic adaptor proteins are recruited and bind the receptors through the death domains. Association of the Fas-associated protein death domain (FADD) protein to procaspase-8 generates the death-inducing signaling complex (DISC) and results in the autocatalytic activation of procaspase-8 (Kischkel et al., 1995). The activation of caspase-8 leads then to the execution pathway and cell death (Elmore, 2007).

The intrinsic pathway is not receptor dependent and it is triggered by stimuli that induce changes in the inner mitochondrial membrane resulting in the opening of mitochondrial permeability transition (MPT) pores (Elmore, 2007). Formation of MPT pores alters the transmembrane potential facilitating the release of mitochondrial pro-

apoptotic proteins such as cytochrome c, Smac/DIABLO and HtrA serine peptidase 2 (HtrA2)/OMI (Saelens et al., 2004). Cytochrome c interacts with the apoptotic protease activating factor 1 (Apaf-1) and procaspase-9 forming the apoptosome leading to caspase-9 activation leading once again to the activation of the execution pathway (Chinnaiyan, 1999). The members of the B-cell lymphoma 2 (Bcl-2) family of proteins tightly control the mitochondrial pathway (Cory and Adams, 2002). Members of the Bcl-2 family regulate not only mitochondrial membrane permeability but can also be classified as pro- and anti-apoptotic (Cory and Adams, 2002). Bcl-2 and B-cell lymphoma-extra large (Bcl-XL) are examples of anti-apoptotic proteins; while Bcl-2-associated X protein (Bax), Bcl-2-associated death promoter (Bad) and Bcl-2 homology domain 3 (BH-3)-only protein, Bcl-2 interacting mediator of cell death (BIM) are examples of pro-apoptotic Bcl-2 members (Cory and Adams, 2002). The main mechanism through which Bcl-2 family members are important in apoptosis is by regulating cytochrome c release from the mitochondria (Elmore, 2007). Studies have also suggested the existence of a cross-talk between the extrinsic and intrinsic pathway mediated by the cleavage of the BH3-interacting domain death agonist (Bid) (generating tBid) activating the intrinsic pathway, by caspase 8, a member of the extrinsic pathway (Li et al., 1998).

Figure 1.2: Schematic representation of the main apoptotic pathways

Apoptosis can be triggered by the activation of the extrinsic (death receptor) or intrinsic (mitochondrial) pathways, both culminating in the activation of the effector caspases 3 and 7. Binding of death ligands, such as FasL or TNF-α, to death receptors activates the extrinsic pathway and the formation of the DISC complex, leading to activation of procaspase 8. Active caspase 8 leads to the subsequent activation of effector caspases 3 and 7 and apoptosis. The intrinsic pathway is activated in response to cellular stressors such as growth factor withdrawal or irradiation leading to the activation of the pro-apoptotic members of the Bcl-2 family of proteins (Bad, Bax, BIM), which in turn neutralize the anti-apoptotic members (Bcl-2, Bcl-XL, Myeloid cell leukemia 1 (Mcl-1)), resulting in disruption of the mitochondrial membrane integrity and the release of mitochondrial components including cytochrome c and Smac/DIABLO. Cytochrome c, Apaf-1 and caspase-9 will form a complex called the apoptosome, finally leading to the activation of caspase 3 and 7. Cleavage of Bid by caspase 8 acts as a point of cross talk between these two apoptotic pathways. IAPs: inhibitor of apoptosis proteins.

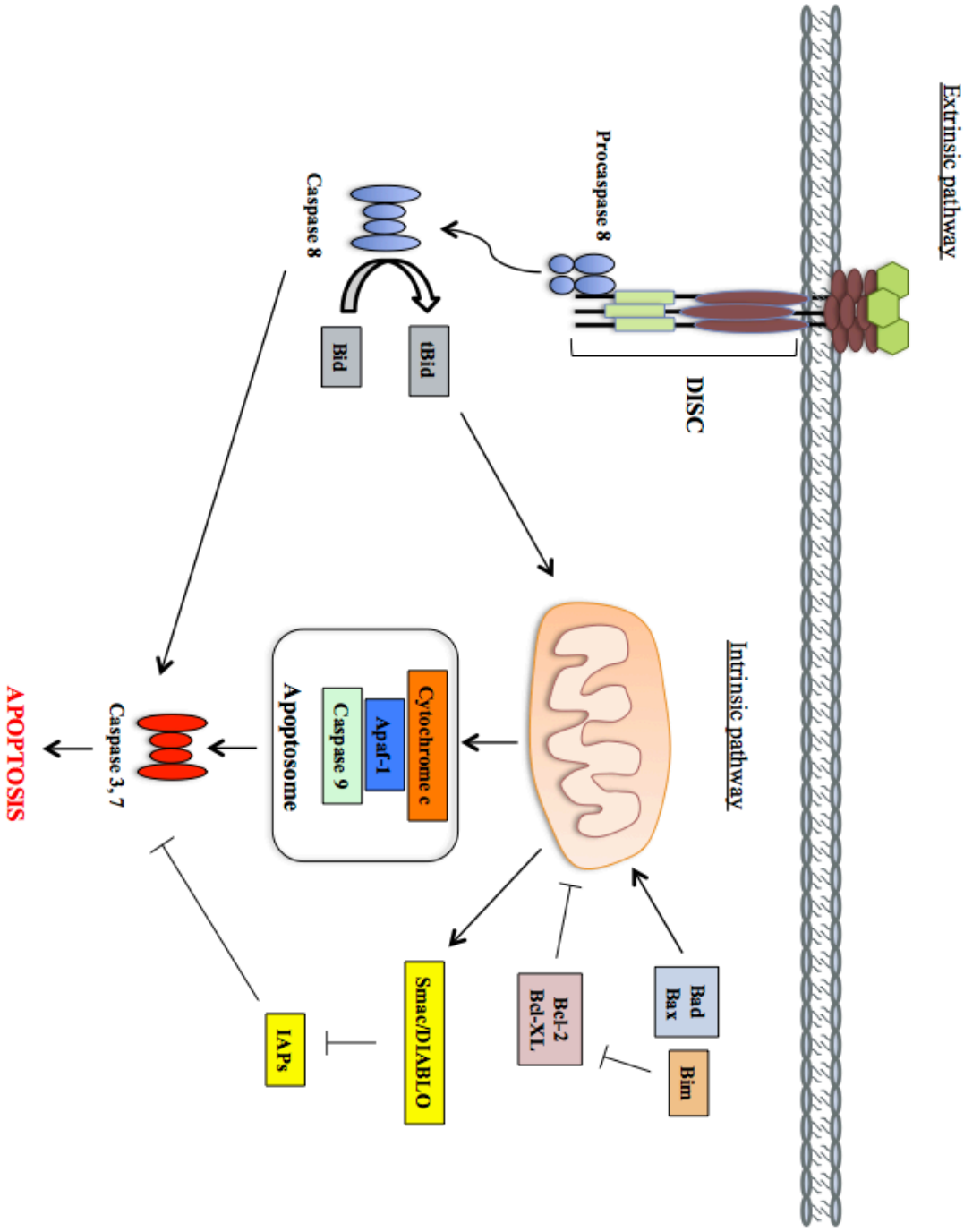
Extrinsic pathway
Procaspase 8
DISC
Caspase 8
Bid
tBid
Intrinsic pathway
Cytochrome c
Apaf-1
Caspase 9
Apoptosome
Caspase 3, 7
APOPTOSIS
Bad
Bax
Bcl-2
Bcl-XL
Bim
Smac/DIABLO
IAPs

At early stages of plaque development (prior to necrotic core formation), macrophage apoptosis contributes to reduce plaque cellularity limiting the expansion of the size of the plaque (Seimon and Tabas, 2009). LDLR KO mice reconstituted with Bax deficient bone marrow present reduced macrophage apoptosis and increased atherosclerosis (Liu et al., 2005). Similarly, LDLR KO macrophages deficient in the apoptosis inhibitor of macrophages (AIM) were more susceptible to apoptosis and dKO mice were protected against atherosclerosis development (Arai et al., 2005). As the disease progresses, clearance of apoptotic cells becomes defective leading to secondary necrosis in which macrophages release their cellular content amplifying the inflammatory response and leading to necrotic core formation (Seimon and Tabas, 2009). In this context, apoE KO mice deficient in the MER proto-oncogen, tyrosine Kinase (MerTK) (receptor for apoptotic cells) presented a significant increase in total plaque apoptosis and non-macrophage-associated apoptotic cells indicating defective efferocytosis (Thorp et al., 2008). MerTK/apoE dKO mice also presented a significant increase in plaque necrosis (Thorp et al., 2008). Similar results have also been observed in model deficient in other molecules involved in efferocytosis such as apoE, complement protein C1q (Seimon and Tabas, 2009), and the scavenger receptor class B type 1 (SR-B1) (Tao et al., 2015).

Cholesterol toxicity, oxidized phospholipids and oxysterols are known to contribute to macrophage apoptosis by inducing ER stress and activating the UPR (Feng et al., 2003; Myoishi et al., 2007). The UPR functions as a response mechanism to reestablish ER homeostasis by reducing protein synthesis, inducing chaperones to assist

in folding of the accumulated unfolded proteins and facilitating degradation of proteins that cannot be folded (Tabas, 2010b). However under conditions of prolonged ER stress, continuous expression of the UPR transcription factor CCAAT-enhancer binding protein homologous protein (CHOP) can induce apoptosis (Tabas, 2010b). Levels of expression of CHOP strongly correlate with the stage of plaque development in human CA disease (Myoishi et al., 2007). Deletion of CHOP in apoE KO and LDLR KO mice not only results in reduction in total lesion area but also a marked reduction in necrotic core size (Thorp et al., 2009). CHOP deficiency also led to a reduction in plaque rupture further confirmed a role for this protein in plaque instability (Tsukano et al., 2010). Furthermore, CHOP deficiency in bone marrow-derived cells was enough to decrease plaque rupture (Tsukano et al., 2010). Tabas and colleagues have also introduced the theory of the "two-hit" apoptotic process based on the premise than ER stress *in vivo* may not be enough to induce large-scale apoptosis (Tabas, 2010b). This secondary hit involves the activation of the pattern recognition receptors (PPRs), which are cell surface receptors that recognize pathogens, foreign agents and modified lipids among others (Seimon and Tabas, 2009). Scavenger receptors and toll-like receptors are examples of PPRs (Seimon and Tabas, 2009). The combined deficiency of the scavenger receptor class A (SRA) and the cluster of differentiation 36 (CD36), both scavenger receptors, in apoE KO mice prevented advanced plaque macrophage apoptosis and plaque necrosis confirming a role of these receptors in plaque progression (Manning-Tobin et al., 2009).

1.5 High-density lipoprotein (HDL)

Lipoproteins are central players in the pathogenesis of atherosclerosis. CVD risk is directly related to the levels of LDL cholesterol (LDL-C) in circulation, while the opposite relationship is found with HDL cholesterol (HDL-C) levels (Hegele, 2009). In fact, HDL-C levels below 35 mg/dl is one of the most common lipid abnormalities found in patients under 60 years of age and it is considered and independent risk factor for coronary heart disease (Genest et al., 1992). However, recent therapies focusing on increasing HDL-C levels in humans have failed to reduce CHD risk, indicating that other components in the HDL particle beyond the cholesterol levels might play a more significant role in translating HDL anti-atherogenic properties (Kingwell et al., 2014).

The HDL fraction groups a heterogeneous population of lipoproteins differing in several aspects including protein and lipid content. The main protein found in HDL is apoA1, which is produced in both the liver and small intestine in humans (Kingwell et al., 2014). Nascent HDL, also known as pre-β HDL, is composed of a discoidal phospholipid bilayer surrounded by apoA1 (Wu et al., 2007). After cholesterol loading, the HDL matures into and spherical particle with a core of cholesteryl esters and triglycerides (Daniels et al., 2009). The increase in cholesteryl esters not only gives the particle the characteristic spherical shape but also generates a positive gradient that favors the addition of more unesterified cholesterol from tissues (Daniels et al., 2009). Besides apoA1, HDL has also been described to carry other apo such as apoA2, apoD, apoE and apoM among others (Kontush et al., 2015). HDL also carries important enzymes

involved in lipid metabolism like lecithin:cholesterol acyl transferase (LCAT), cholesteryl ester transfer protein (CETP) and phospholipid transfer protein (Kontush et al., 2015). Along with them, HDL also serves as a carrier for some bioactive lipids, including sphingosine 1-phosphate (S1P) (Scanu and Edelstein, 2008).

One of the main mechanisms through which HDL is thought to protect against atherosclerosis development is reverse cholesterol transport (RCT). This process refers to the ability of HDL to collect cholesterol from peripheral tissues - including macrophage foam cells- and deliver it to the liver for it to be reused or excreted. RCT starts with the flux of cholesterol from tissues to pre-β HDL in a process aided by the ATP-binding cassette (ABC) transporter A1. Mature HDL can also accept excess cholesterol from cells through interaction with another member of the ABC family of transporters, ABCG1. The delivery of cholesterol to hepatocytes, also known as selective lipid uptake, is mediated by the reversible binding of HDL to its receptor SR-B1. Contrary to the endocytosis-mediated delivery of cholesterol from LDL, the uptake of cholesterol from HDL involves transfer of cholesterol without net internalization and degradation of the lipoprotein.

In addition to RCT, HDL has many other properties that can contribute to its anti-atherogenic activity. HDL has been described to have anti-inflammatory, anti-oxidant and anti-thrombotic properties, each of which contribute to its ability to protect against atherosclerosis and CVD (Nofer et al., 2002). HDL can inhibit cytokine-induced expression of adhesion molecules on endothelial cells (Assmann and Nofer, 2003) and expression and/or activation of their cognate integrin receptors on monocytes (Murphy et

al., 2008; Smythies et al., 2010), effectively preventing monocyte interaction with the endothelium. HDL has also been described to promote prostacyclin production in endothelial cells, inducing vasorelaxation (van der Stoep et al., 2014). Studies have also shown that HDL prevents endothelial dysfunction and promotes endothelial cells proliferation while protecting against apoptosis, which can directly impact plaque stability (Nofer et al., 2002). As mentioned previously, oxLDL is a pro-inflammatory factor critical in monocyte/macrophage recruitment to the nascent atherosclerotic plaque. In this context, HDL has been described to inhibit LDL oxidation in a process mediated by both apoA1 and paraoxonase 1, an enzyme carried by HDL that catalyzes the breakdown of oxidized phospholipids found in LDL (Assmann and Nofer, 2003; Rosenblat et al., 2006). The important role of paraoxonase 1 on this process has been confirmed by studies in mice lacking the enzyme. Animals were significantly more prone to atherosclerosis development and HDL isolated from these mice failed to prevent LDL oxidation (Shih et al., 1998).

Regarding the anti-thrombotic role of HDL, it has been shown that it can modulate different components of the coagulation pathway and affect thrombus formation by interfering with platelet activation (Nofer et al., 2002; van der Stoep et al., 2014). It is important to notice that the human HDL fraction is composed by a wide array of particles varying in size, composition and surface charge (Rye et al., 1999). Conversely, different components and subpopulation of HDL may account for the atheroprotective properties of this lipoprotein and further knowledge concentrated in identifying this factors might help to develop more effective therapies.

1.6 SR-B1 in atherosclerosis

Many of the atheroprotective actions of HDL are mediated by the interaction with SR-B1. Scavenger receptors are transmembrane proteins that can bind modified lipoproteins as substrate (Trigatti et al., 2003). SR-B1 is a 509 amino acid protein that contains a large extracellular loop and two transmembrane domains (Rigotti et al., 2003). The extracellular domain is rich in N-glycosylation sites and contains a cysteine-rich carboxy-terminal half. SR-B1 has also been reported to be subject to fatty acylation (Babitt et al., 1997; Vinals et al., 2003). On the cell surface, SR-B1 seems to be located in the plasma membrane caveolae where selective lipid uptake occurs (Babitt et al., 1997). However studies have also shown that absence of caveolin 1, main protein component of caveolae, does not affect SR-B1 mediated lipid uptake (Wang et al., 2003) indicating that localization of the receptor on these membrane structures might not be required for cholesterol transfer (Briand et al., 2003). SR-B1 is mainly expressed in the liver and steroidogenic tissue (Acton et al., 1996), but has also been detected in the intestine, testes and mammary glands in rats (Landschulz et al., 1996). Expression of SR-B1 in the liver can be regulated by several hormonal, pharmacological and dietary interventions (Rigotti et al., 2003). Another factor regulating hepatic expression of SR-B1 is the PDZ-domain containing 1 (PDZK1) protein, which binds to the intracellular C-terminus of SR-B1 (Kocher and Krieger, 2009). PDZK1 deficiency results in a 95% reduction on SR-B1 levels in the liver but with no impact on the steroidogenic tissue, macrophages or endothelial cells (Kocher et al., 2003; Kocher et al., 2008; Zhu et al., 2008).

SR-B1 plays a critical role in HDL metabolism. SR-B1 deficient mice are characterized by significantly larger HDL particles and reduced biliary cholesterol (Rigotti et al., 1997). Conversely, overexpression of hepatic SR-B1 notably reduced HDL cholesterol by increasing clearance and transport of cholesterol from the liver to the bile (Kozarsky et al., 1997). In addition to its role in cholesterol clearance, SR-B1 has also been reported to mediate bi-directional movement of cholesterol from cells to HDL (Brundert et al., 2005; Connelly et al., 2003; Jian et al., 1998). Besides its role in cholesterol handling, SR-B1 is involved in HDL signaling in several cell types and the downstream activation of AKT and mitogen-activated protein kinases (MAPK) seems to be a common factor on its signaling pathway (Nofer, 2015). eNOS expression in endothelial cells and aortas in response to HDL involves the activation of both AKT and MAPK (Yuhanna et al., 2001) (Mineo et al., 2003). Also, proliferation of mesenchymal stem cells in response to HDL involves both binding to SR-B1 and activation of phosphoinositide 3-kinase (PI3K)/AKT/MAPK pathways (Xu et al., 2012). Furthermore, SR-B1 activation of AKT and the 5' adenosine monophosphate-activated protein kinase (AMPK) in adipocytes promotes glucose uptake, indicating that SR-B1 might contribute to the insulin-sensitizing effect of HDL (Zhang et al., 2011). Expression of SR-B1 is required for HDL-mediated inhibition of TNF-α dependent adhesion molecule expression in endothelial cells as well (Kimura et al., 2006). Absence of SR-B1 has also been reported to affect erythrocyte maturation (Holm et al., 2002), platelet structure (Dole et al., 2008) and to affect HDL's antioxidant properties (Van Eck et al., 2007).

As a receptor for HDL and also mediator of several cellular effects of this lipoprotein, the role of SR-B1 in atherosclerosis has been explored in both knockout (KO) and transgenic mouse models. Overexpression of SR-B1 in LDL receptor (LDLR) KO mice significantly reduced pre-existing lesions probably through a reduction in HDL cholesterol levels (Kozarsky et al., 2000). Hepatic overexpression of SR-B1 in heterozygous LDLR KO mice fed a high fat/high cholesterol diet also resulted in decreased plaque development and lipoprotein cholesterol content, however the results were not replicated in homozygous LDLR KO fed a similar diet (Arai et al., 1999). Krieger and colleagues were the first ones to report the effect of SR-B1 deficiency in atherosclerosis development (Trigatti et al., 1999). SR-B1/apoE double KO (dKO) mice presented a striking increase in very low-density lipoprotein (VLDL) cholesterol along with abnormally large HDL particles. SR-B1/apoE dKO mice spontaneously develop significant aortic sinus atherosclerosis (Trigatti et al., 1999). Furthermore, coronary artery (CA) atherosclerosis, myocardial fibrosis, heart failure detected in these mice resulted in 50% mortality by 6 weeks of age (Braun et al., 2002). Similar results were also seen in the SR-B1 KO/apoE-hypomorphic mouse model, which is characterized by the reduced (around 5% of normal) expression of a mutant form of apoE (Zhang et al., 2005b). SR-B1 KO/apoE-hypomorphic mice are healthy while on a normal chow diet, but readily develop extensive aortic root and CA atherosclerosis mimicking the phenotype observed in SR-B1/apoE dKO mice (Zhang et al., 2005b). Accelerated atherosclerosis has also been reported in high fat diet-fed SR-B1/LDLR dKO mice (Covey et al., 2003). Larger necrotic cores, enhanced CA atherosclerosis and platelet

accumulation in the CA were also detected in the SR-B1/LDLR KO mouse model while challenged with several atherogenic diets (Fuller et al., 2014). In the same context, PDZK1 deficiency in apoE KO mice also results in increased atherosclerosis when mice are challenged with a high fat, high cholesterol diet though disease was not as aggressive as seen in SR-B1/apoE dKO mice (Kocher et al., 2008).

Expression of SR-B1 in bone marrow derived cells is also critical for atheroprotection as evidenced by bone marrow transplantation (BMT) experiments (Covey et al., 2003; Tao et al., 2015; Van Eck et al., 2004). BMT experiments performed by Pei and colleagues in SR-B1 KO/apoE-hypomorphic mice also show that expression of SR-B1 in the BM compartment was crucial for atherosclerosis protection (Pei et al., 2013). The reduction in plaque formation was explained mainly by a reduction in monocyte recruitment in mice receiving SR-B1 containing BM (Pei et al., 2013).

1.7 Sphingosine-1-phosphate in atherogenesis

Sphingolipids are structural components of the cell membrane that also play important roles in several cellular processes (Alewijnse and Peters, 2008). They are derived from sphingomyelin and the metabolites sphingosine, ceramide and sphingosine-1-phosphate (S1P) also act as bioactive lipids playing rather important role in cell fate through the interconversion into one another (Alewijnse and Peters, 2008; Cuvillier et al., 1996) (Figure 1.3). S1P is generated by the action of sphingosine kinase (SphK) on sphingosine (Schuchardt et al., 2011); the two identified isoforms of SphK differ in tissue

distributions, subcellular localization and catalytic properties (Pitson, 2011) and despite being intracellular enzymes, they can also be secreted (Venkataraman et al., 2006). Levels of S1P in the cell are also regulated by S1P-selective phosphatase (SPP) and S1P lyase, both enzymes involved in the degradation step (Brindley, 2004; Kumar and Saba, 2009).

Figure 1.3: The sphingolipid rheostat

Sphingosine-1-phosphate is derived from the membrane lipid sphingomyelin. Sphingosine, ceramide and sphingosine-1-phosphate are interconvertible metabolites playing an important role in several cell processes, especially cell survival. Ceramide and sphingosine are associated with cell cycle arrest and apoptosis, while sphingosine-1-phosphate promotes both proliferation and survival. Levels of sphingosine-1-phosphate are controlled by the action of both sphingosine-1-phosphate phosphatase and sphingosine-1-phosphate lyase.

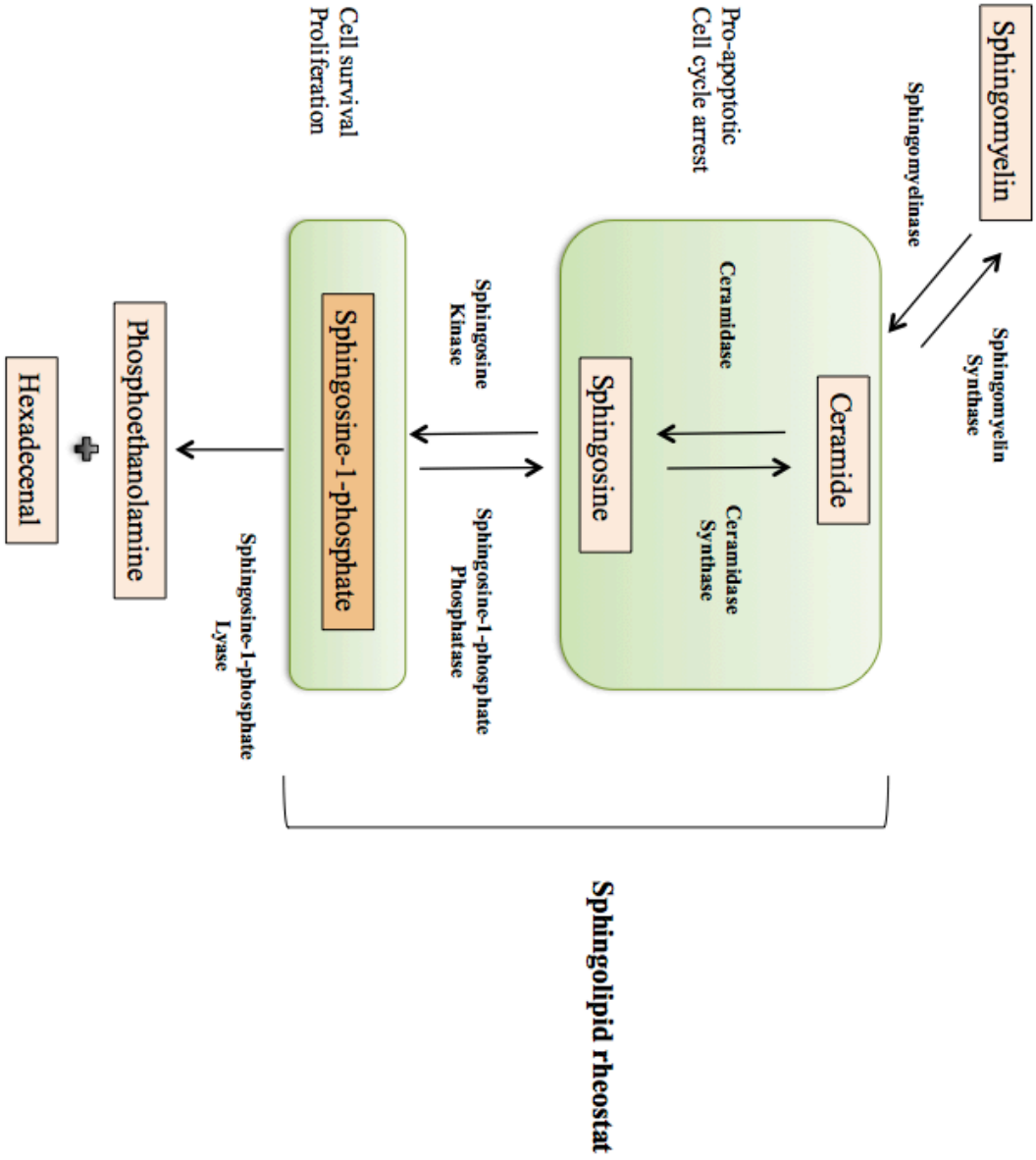
Sphingomyelin
Sphingomyelinase
Sphingomyelin Synthase
Ceramide
Ceramidase
Ceramidase Synthase
Sphingosine
Sphingosine Kinase
Sphingosine-1-phosphate Phosphatase
Sphingosine-1-phosphate
Sphingosine-1-phosphate Lyase
Phosphoethanolamine
Hexadecenal
✓ Pro-apoptotic
✓ Cell cycle arrest
✓ Cell survival
✓ Proliferation
Sphingolipid rheostat

S1P is found at micromolar concentrations in plasma and nanomolar concentrations in tissues creating a concentration gradient important for cell signaling (Daum et al., 2009; Rivera et al., 2008). The main sources of S1P in circulation are the erythrocytes and platelets. Erythrocytes are considered the main supplier since they lack the enzymes involved in S1P degradation so they serve as a buffer system (Ito et al., 2007; Pappu et al., 2007). Platelets, on the other hand, release S1P upon activation (Okajima, 2002). The release of S1P from erythrocytes depends on the availability of protein acceptors such as HDL and albumin (Takuwa et al., 2011). Most S1P in circulation is bound to HDL (60-70%), while the remaining associates with albumin (30%) and other lipoproteins; only a very small amount travels in a free state (Alewijnse and Peters, 2008; Schuchardt et al., 2011). Signaling by S1P is mediated by activation of five different G protein-coupled receptors (S1PR1-5) (Sanchez and Hla, 2004) (Figure 1.4). The receptors have different patterns of expression with S1PR1-3 widely expressed in several tissues in both humans and mice, S1PR4 mainly expressed in the hematopoietic and lymphoid tissue and S1PR5 confined to the nervous system (Sanchez and Hla, 2004). All S1PRs have different G protein coupling efficacy. S1PR1 couples exclusively with the G_i protein, while the remaining S1PRs tend to fluctuate between G_i, G_q and $G_{12/13}$ depending on the cell type and signaling pathway activated (Schuchardt et al., 2011).

Figure 1.4: Sphingosine-1-phosphate receptors and signaling pathways

Sphingosine-1-phosphate signals through five different G-protein coupled receptor, S1PR1-5. The expression pattern of the receptors varies in different tissues. Similarly, all receptors have different G-protein coupling preferences. S1PR1 only interacts with the G_i protein, while the others tend to fluctuate among several G proteins depending on the tissue where they are expressed. Once activated, S1PRs can activated a wide variety of signaling pathways allowing for the control of several different cellular processes, depending on the cell type, including control of: cell survival, proliferation and migration. Sphingosine-1-phosphate signaling is also involved in regulation of endothelial cell barrier integrity and platelet production.

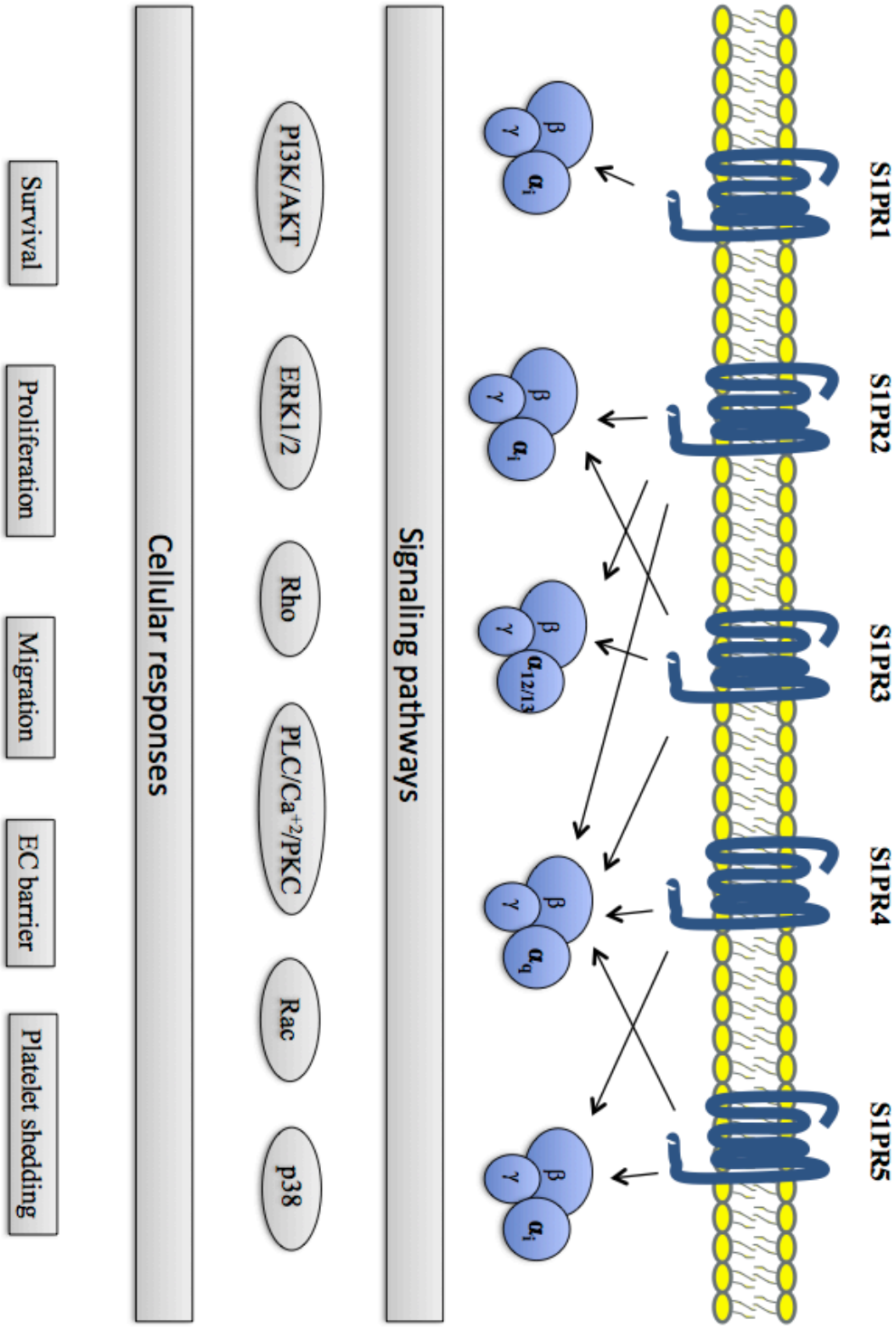
S1PR1
S1PR2
S1PR3
S1PR4
S1PR5
β
γ
α_i
$\alpha_{12/13}$
α_q
Signaling pathways
PI3K/AKT
ERK1/2
Rho
PLC/Ca^{+2}/PKC
Rac
p38
Cellular responses
Survival
Proliferation
Migration
EC barrier
Platelet shedding

Sphingolipid metabolism is altered in diabetes but most studies have focused on the role of ceramides (Deevska and Nikolova-Karakashian, 2011; Summers, 2010), with fewer studies addressing S1P. Ceramide has been linked with the induction of insulin resistance (T2D) in a mechanism involving inhibition of AKT, which is required for insulin signaling (Deevska and Nikolova-Karakashian, 2011; Summers, 2010). On the other hand, adiponectin – an insulin sensitizing hormone – stimulates ceramidase activation and generation of S1P (Holland et al., 2011). Production of S1P might be associated with survival of pancreatic β cells, however no direct correlation has been established (Holland et al., 2011). *In vivo*, increased S1P levels have been detected in models of T1D although the source is unknown (Fox et al., 2011). Also, an antagonist of the S1PR2 prevented the onset of diabetes in a streptozotocin (STZ)-induced diabetes mouse model and S1PR2 deficiency in pancreatic β cells protected them against STZ-induced apoptosis (Imasawa et al., 2010).

The high concentration of S1P found in HDL and also the positive correlation between HDL cholesterol and S1P levels suggests that this sphingolipid might mediate some of HDL's atheroprotective effects (Zhang et al., 2005a). Clinical studies have shown that HDL-S1P inversely correlates with ischemic heart disease but no correlation is seen with free S1P (Argraves et al., 2011). Inverse correlation with the severity of CAD has also been reported (Sattler et al., 2014). In fact, HDL-S1P is lower in patients that suffered myocardial infarction and CAD, when compared to the healthy population (Sattler et al., 2010). S1P binds HDL through interaction with apoM (Christoffersen et al., 2011). This apolipoprotein belongs to the lipocalin superfamily of proteins (Duan et

al., 2001), characterized by the presence of a hydrophobic pocket that allows for binding small lipophilic ligands (Sevvana et al., 2009). Studies have shown that S1P is absent in HDL obtained from apoM KO mice, while a significant increase in HDL-S1P is detected in transgenic mice overexpressing human apoM (Christoffersen et al., 2011). Moreover, only HDL-S1P is able to activate S1P/S1PR1 responses in endothelial cells, further supporting the role of apoM in S1P binding to HDL (Christoffersen et al., 2011). ApoM also seems to play an important role in atherosclerosis prevention; overexpression of apoM reduces atherosclerosis development, enhances formation of pre-β HDL and promotes cholesterol efflux from foam cells (Christoffersen et al., 2008).

Initial studies on the role of S1P in atherosclerosis development involved the use of S1P mimetics. Nofer and colleagues (Nofer et al., 2007) and Keul and colleagues (Keul et al., 2007), simultaneously reported that FTY720 – an S1P analogue that binds all S1PRs except S1PR2 – effectively reduces atherosclerosis development in high fat, high cholesterol diet fed-LDLR and apoE KO respectively. LDLR KO mice treated with FTY720 also shown a reduction in necrotic core formation (Nofer et al., 2007). The atheroprotective effect seen after FTY720 administration seems to be explained by the ability to reduce the pro-inflammatory state and also to the reduction in circulating T cells. Unexpectedly, FTY720 was unable to protect apoE KO mice fed a normal diet from atherosclerosis (Klingenberg et al., 2007). Similar lack of protection has been reported in mildly hypercholesterolemic LDLR KO mice as well, despite the changes in T cell distribution (Poti et al., 2012). Together these results suggest that perhaps FTY720 atheroprotective properties develop only under conditions of chronic inflammation.

The effect of specific S1PRs in atherosclerosis has also been explored by using receptor-deficient mouse model. Keul and colleagues were the first one to explore the role of S1PR3 in atherosclerosis (Keul et al., 2011). Despite having no effect on plaque formation, S1PR3 deficiency was associated with reduction in the monocyte/macrophage content in the lesions – while SMCs and neointima formation were significantly increased – hinting at both pro- and anti-atherogenic properties (Keul et al., 2011). S1PR2, on the other hand, seems to be strictly pro-atherogenic. ApoE KO mice deficient in S1PR2 developed fewer lesions and presented reduced macrophage foam cells compared to controls, suggesting that S1PR2 might be involved in macrophage recruitment and retention in the atherosclerotic plaque (Skoura et al., 2011). On a different approach, Bot and colleagues showed that S1P lyase deficiency in hematopoietic cells altered S1P gradients elevating its levels in plasma, inducing monocytosis and increased cytokine release (Bot et al., 2013). Despite the pro-inflammatory environment, S1P lyase deficiency in the bone marrow compartment was associated with reduced atherosclerosis in LDLR KO mice (Bot et al., 2013).

In vivo studies addressing the role of the S1PR1 are difficult because global S1PR1 deficiency renders a phenotype that is lethal in utero due to massive hemorrhages, complicating studies involving the receptor (Liu et al., 2000). This lethal phenotype is also reproduced when the S1PR1 is knocked out in EC, indicating the importance of this receptor in vascular development (Allende et al., 2003). In an attempt to elucidate the role of the S1PR1 in plaque formation, Poti and colleagues administered the selective S1PR1 agonist KRP203 to LDLR KO mice (Poti et al., 2013). In this animal model, both

early and advanced lesions were significantly reduced as were circulating levels of activated T cells and pro-inflammatory cytokines and chemokines, after treatment with KRP203. S1PR1 activation also resulted in reduced cytokine secretion by macrophages and markers of endothelial activation in plasma. Moreover, both expression of the vascular cell adhesion molecule 1 (VCAM1) and the intercellular adhesion molecule 1 (ICAM1) and monocyte adhesion were reduced in endothelial cells treated with KRP203 (Poti et al., 2013). Altogether, these results suggest that the S1P/S1PR1 axis might play a central role in atheroprotection.

Several studies *in vitro* also support a potential role for S1P in protection against atherosclerosis. In the following, I summarize some of the anti-atherogenic effects HDL and its cargo S1P in vascular cells.

1.7.1 Role of S1P in endothelial cells

Endothelial dysfunction is characterized by the imbalance of the factors regulating vessel vasodilation, favoring contraction and a pro-inflammatory state (Hadi et al., 2005). A dysfunctional endothelium has been identified as one of the first steps in atherosclerosis development (Libby et al., 2011). EC express S1PR1-3, with the S1PR1 being the most abundant (Lucke and Levkau, 2010). S1P signaling has been found to be critical for the maintenance of the endothelial barrier. S1P-induced enhancement of the endothelial barrier in pulmonary EC was mediated by recruitment of S1PR1 to caveolin-enriched microdomains and activation of PI3K/T-cell lymphoma invasion and metastasis 1

(Tiam1)/Ras-related C3 botulinum toxin substrate 1 (Rac1) pathway (Singleton et al., 2005). Animals lacking plasma S1P show increased vascular leakage, a phenotype that is rescued by administration of an S1PR1 agonist (Camerer et al., 2009). Similarly, HDL-S1P was unable to enhance endothelial barrier integrity in the presence of an S1PR1 antagonist (Sanna et al., 2006). In the same context, Wilkerson and colleagues were able to demonstrate that HDL-S1P was more efficient than albumin-S1P in maintaining endothelial barrier function due to reduced degradation of the S1PR1 in the presence of HDL associated S1P (Wilkerson et al., 2012).

HDL-S1P is also involved in the control of cell proliferation and survival in endothelial cells through the extracellular signal-regulated kinases (ERK) activation (Kimura et al., 2001). Later on, the same authors also demonstrated that HDL-S1P control endothelial cell migration through S1PR1/3, and also survival through S1PR1 activation (Kimura et al., 2003). Activation of the MAPK signaling cascade by HDL-S1P has also been associated with endothelial cell tube formation (Miura et al., 2003). Furthermore, HDL-mediated inhibition of adhesion molecule expression in EC requires not only SR-B1 expression but also S1PR1, suggesting that HDL might signal simultaneously through both receptors by delivering S1P (Kimura et al., 2006). Overexpression of VCAM1 in the diabetic endothelium is also prevented by S1P/S1PR1-mediated inhibition of NF-κB, resulting in a significant reduction in monocyte adhesion (Whetzel et al., 2006). EC exposed to high glucose levels presented a significant increase in S1PR2 and a decrease in S1PR1 expression levels (Chen et al., 2015). These changes resulted in increased ROS and reduced production of nitric oxide (NO) suggesting that

S1PRs are involved in hyperglycemia-induced endothelial cells dysfunction (Chen et al., 2015).

HDL-S1P can also protect endothelial cells against apoptosis. HDL prevented growth factor deprivation-induced apoptosis in endothelial cells by AKT-mediated inactivation of Bad (Nofer et al., 2001). As a consequence, HDL-S1P prevented mitochondrial potential disruption, cytochrome c release and activation of caspases 3 and 9 hence protecting against apoptosis (Nofer et al., 2001). Finally, HDL-S1P partially accounts for HDL-mediated activation of eNOS and NO production in endothelial cells in an S1PR3-dependent manner (Nofer et al., 2004). Treatment of endothelial cells with statins significantly increased S1PR1 expression levels enhancing the effect of HDL on eNOS activation (Igarashi et al., 2007; Kimura et al., 2008). Increased eNOS and AKT activity along with higher levels of S1PR1 and S1PR3 were also described in fenofibrate-treated mice, which presented higher levels of HDL and S1P in circulation (Krishna et al., 2012).

Thrombin – a key component of the coagulation cascade and direct activator of thrombus formation – reacts with its receptor protease activated receptor 1 (PAR-1) in endothelial cells, effectively disrupting endothelial barrier integrity (Garcia et al., 1996). Thrombin signaling also involves cross talk activation of the S1P/S1PR1 signaling pathway (Niessen et al., 2009) in order to protect against vascular leakage and edema formation, limiting its own actions (Tauseef et al., 2008). Nevertheless, S1P has also been described to synergistically promote thrombin-induced tissue factor production in endothelial cells thereby increasing thrombin generation (Takeya et al., 2003).

1.7.2 Role of S1P in SMCs

In response to the pro-inflammatory environment in the atherosclerotic plaque, SMCs respond by switching from a contractile to a synthetic phenotype, which allows them to both migrate and secrete extracellular matrix proteins (Orr et al., 2010). SMCs isolated from human pulmonary arteries were shown to express S1PR2 and 3 preferentially but S1PR1 expression in response to mitogenic factors has also been described (Birker-Robaczewska et al., 2008). The S1P component of HDL has been reported to control SMCs migration. HDL inhibits SMCs migration in a process that requires expression of the S1PR2 (Tamama et al., 2005). Additionally, HDL-S1P blocks monocyte chemoattractant protein-1 (MCP-1) production in SMCs by activating S1PR3/Rac1 and reducing nicotinamide adenine dinucleotide phosphate-oxidase (NADPH)-dependent ROS production (Tolle et al., 2008). HDL can also induce up-regulation of cyclooxygenase type 2 (COX2), increasing prostacyclin levels in vascular SMCs in an S1PR2-3/p38/ERK dependent fashion (Gonzalez-Diez et al., 2008).

1.7.3 Role of S1P in platelets

Several studies agree on the fact that HDL prevents platelet activation (Mineo and Shaul, 2013). The inhibition seems to be in part explained by the effects of HDL on the endothelium, such as eNOS activation (Yuhanna et al., 2001) and prostacyclin production (Mineo and Shaul, 2013). HDL can also inhibit tissue factor production through PI3K

activation in EC (Viswambharan et al., 2004). However, HDL has also been reported to directly modulate platelet function. HDL has been shown to reduce platelet aggregation (Nofer et al., 2010) and to attenuate intracellular calcium mobilization (Knorr et al., 1988); the effect of HDL on platelets seems to be mediated by interaction with its receptor SR-B1 (Nofer and van Eck, 2011). Megakaryocytes – precursors of platelets – express S1PR1, 2 and 4 but only S1PR1 has been identified as critical for two important steps in platelet formation: pro-platelet elongation and shedding (Hla et al., 2012). S1P is released upon platelet activation increasing its local concentration in plasma, however the role of platelet-derived S1P is still not fully understood (Mahajan-Thakur et al., 2015), with some studies hinting at a role in the initiation phase of platelet aggregation (Yatomi et al., 1995) but not others (Nugent and Xu, 2000; Ulrych et al., 2011).

1.7.4 S1P role in monocyte/macrophages

The expression patterns of S1PRs in monocytes/macrophages are species specific. Human monocytes express S1PR1, 2 and 4 while human macrophages express S1PR1-4 (Weigert et al., 2009). In mice, macrophages have been reported to express receptors 1 to 4 (Poti et al., 2014). S1P has been reported to protect macrophages against apoptosis. During phagocytosis, S1P released from apoptotic cells protected phagocytic cells by activating PI3K, ERK and calcium signaling and controlling Bcl-2 protein dynamics (Weigert et al., 2006). Inhibition of SphK1 favors LPS-induced apoptosis in RAW macrophages suggesting that S1P is required for protection against cell death (Wu et al.,

2004). Similarly, SphK1 knock down sensitizes macrophages to TNF-induced apoptosis (Hammad et al., 2008). The role of individual S1PRs in this process has not been investigated. Regarding the role of HDL-S1P, Dueñas and colleagues showed that both HDL and S1P were able to prevent the inflammatory response of murine monocytes after incubation with Toll-like receptor 2 agonists (Duenas et al., 2008). The direct role of the S1P cargo in this response, however, requires further confirmation. Recently, we showed that FTY720 induces murine macrophage migration and that S1PR1 antagonists were able to block HDL-induce migration of macrophages, suggesting that activation of the S1P/S1PR1 axis is required for HDL signaling in macrophages (Al-Jarallah et al., 2014). In this context, S1P has been suggested to act as a chemoattractant for monocytic cell lines and human monocyte/macrophages as well (Weigert et al., 2009).

1.8 Overall context and objective

Abundant literature has provided evidence of the inverse correlation between HDL-C levels and CVD risk. However, clinical efforts to increase HDL-C in circulation have shown that plain elevation is not enough to reduce cardiovascular risk, suggesting that other components of HDL might play a significant role on its atheroprotective properties. S1P is a bioactive sphingolipid involved in the regulation of a wide variety of cell processes in several tissues, including the cardiovascular system. S1P has also been identified as an important component of HDL and studies have shown that it can mediate

some of HDL's atheroprotective actions. Furthermore, the use of S1P mimetics and receptor agonists has suggested a role for S1P in protection against atherosclerosis.

The role of HDL-S1P in macrophages is less clear but we have been able to show that HDL-induced migration of macrophages involves S1PR1 activation, suggesting that both signaling pathways might act synergistically in macrophages. The objective of this thesis is to explore the role of the S1P signaling pathway in protection against atherosclerosis, with emphasis on studying the role of macrophage S1PR1 in HDL-protection against apoptosis, necrotic core formation and plaque development.

1.9 Hypothesis

The S1P/S1PR1 axis plays a crucial role in protection against apoptosis in macrophages and HDL is unable to protect S1PR1 deficient macrophages against pro-apoptotic stimuli. The protective role of S1P/S1PRs extends to the *in vivo* setting, effectively protecting against atherosclerosis development in the context of diabetes. Moreover, S1PR1 expression in macrophages not only protects against atherosclerosis development but also necrotic core formation by reducing plaque apoptosis.

1.10 Specific aims

Chapter 2

Evaluate the effect of hyperglycemia on aortic sinus and CA atherosclerosis development in the context of systemic SR-B1 deficiency and test if FTY720 administration can prevent the detrimental effects of hyperglycemia on plaque progression.

Chapter 3

Evaluate the role of the S1P/S1PR1 axis in macrophage protection against pro-apoptotic stimuli, and test the role of S1PR1 expression in HDL-mediated protection of macrophages against apoptosis. Also, test *in vivo* the impact of macrophage S1PR1 deficiency on atherogenesis and necrotic core formation.

Chapter 4

Evaluate the role of the pro-apoptotic Bcl-2 family protein BIM on macrophage apoptosis, atherosclerosis development and necrotic core formation *in vivo*.

Chapter 2

Hyperglycemia aggravates and FTY720 protects against diet induced atherosclerosis and coronary heart disease in SR-B1 KO/apoE-hypomorphic mice.

Author list: Leticia Gonzalez, Melissa MacDonald and Bernardo L. Trigatti

Foreword

This manuscript studies the effect of diabetes in coronary artery atherosclerosis development in HFC diet-fed SR-B1 KO/apoE-hypo mice and if FTY720 – a S1P analogue – can prevent the detrimental effects of diabetes on atherosclerosis progression. We show that diabetes is associated with increased plasma cholesterol, reduced HDL cholesterol and increased plasma IL-6 in mice fed a HFC diet. Diabetes also induced accelerated atherosclerosis development in the aortic sinus and the formation of larger necrotic cores in the aortic sinus atherosclerotic plaques and platelet accumulation in atherosclerotic coronary arteries. This phenotype was accompanied by increased myocardial fibrosis and a reduction in survival. FTY720 treatment increased HDL cholesterol levels and reduced IL-6 plasma levels in HFC diet-fed SR-B1 KO/apoE-hypo mice. It also significantly reduced the size of the atherosclerotic plaque and the necrotic core sizes in the aortic sinus. We also detected a significant reduction in CA

atherosclerosis and platelet accumulation on atherosclerotic CA and in myocardial fibrosis.

This manuscript was submitted for publication to *Atherosclerosis*. The experiments were designed by Leticia Gonzalez under the guidance of Bernardo L. Trigatti. Leticia Gonzalez performed the experiments and collected the majority of the data. Melissa MacDonald assisted in animal care and collecting some of the glucose data for Figure 2.1. Data was analyzed and interpreted by Leticia Gonzalez under the guidance of Bernardo L. Trigatti. The manuscript was written by Leticia Gonzalez with guidance from Bernardo L. Trigatti.

2.1 Abstract

Objective: Several epidemiological studies have established diabetes as an independent risk factor for the development of cardiovascular disease. Diabetic animal models have shown increased development of aortic atherosclerosis, however the impact on coronary artery (CA) disease is less clear. Sphingosine-1-phosphate, a component of HDL, has been shown to play an important role in atheroprotection.

Methods and results: To investigate the role of diabetes in coronary artery atherosclerosis and if FTY720 – a sphingosine-1-phosphate analog – can prevent the detrimental effects of diabetes on the development of atherosclerosis and resulting heart disease, we use a mouse model of diet-induced atherosclerotic coronary heart disease, the high fat/high cholesterol diet-fed SR-B1 KO/apoE-hypomorphic mouse. Diabetes induction with STZ treatment was associated with increased plasma total cholesterol and cholesterol associated with non-HDL lipoproteins, reduced HDL cholesterol and increased high fat/high cholesterol diet induced plasma IL-6 levels. Diabetes induction with STZ accelerated the development of atherosclerosis and the formation of larger necrotic cores in the atherosclerotic plaques in the aortic sinus and the accumulation of platelets in atherosclerotic coronary arteries. This was accompanied by an increase in myocardial fibrosis and a reduction in the survival of the high fat/high cholesterol diet-fed mice. Administration of FTY720 in the drinking water was associated with increased plasma HDL-cholesterol and reduced plasma IL-6 in high fat/high cholesterol diet-fed diabetic SR-B1 KO/apoE-hypomorphic mice. FTY720 treatment significantly reduced the sizes

of atherosclerotic plaques and cellular apoptosis, and necrotic core sizes within atherosclerotic plaques in the aortic sinus. We also observed a slight reduction in the numbers of atherosclerotic coronary arteries and more striking reductions in platelet accumulation within atherosclerotic coronary arteries and in myocardial fibrosis. Conclusion: In summary, our data shows that diabetes can accelerate and that FTY720 can partially protect diabetic mice from the development of cardiac fibrosis associated with coronary disease.

Key words: coronary arteries, diabetes, FTY720, atherosclerosis.

2.2 Introduction

Type I diabetes (T1D) patients present an increased risk of developing cardiovascular diseases relative to the general population (1). Furthermore, coronary artery (CA) disease represents the leading cause of death among patients with diabetes mellitus (2). In fact, children with T1D exhibit increased aortic intima-media thickness, an early marker of subclinical atherosclerosis (3). Atherosclerotic plaque development results from the abnormal lipid deposition in the arterial intima due to a complex mechanism involving immune cells, lipoproteins and the vessel wall (4). Several prospective studies have shown that levels of high-density lipoprotein (HDL) cholesterol inversely correlate with cardiovascular disease (CVD) risk in patients with normal or high levels of low-density lipoprotein (LDL) cholesterol (5). However, recently it has been suggested that the

amount and function of HDL particles rather than their cholesterol concentrations might be a superior predictor of CVD risk hinting at other components of the HDL particle playing a role in atheroprotection (6; 7).

Sphingosine-1-phosphate (S1P) – an sphingolipid with diverse biological properties – travels in circulation bound to HDL (8). *In vitro* studies have attributed several atheroprotective effects of HDL to the S1P cargo, including inhibition of endothelial cell adhesion molecule expression (9; 10), promotion of endothelial survival (11) and inhibition of smooth muscle cells migration (12; 13). Furthermore, HDL-bound S1P levels are reduced in patients that suffered myocardial infarction and CA disease compared to healthy individuals and inversely correlate with the severity of CA disease symptoms (14; 15). Mice deficient in sphingosine kinase 1 (SphK1) develop severe diabetes when challenged with a high-fat diet and presented reduced insulin levels and reduced beta pancreatic cell mass, indicating an important role of S1P in glucose metabolism (16).

FTY720, an agonist of diverse S1P receptors, has been reported to exhibit a variety of beneficial effects. It leads to immunosuppression by blocking lymphocyte egress from lymphatic tissues (17; 18), and it has been reported to reduce atherosclerosis in apolipoprotein E (apoE) knockout (KO) and LDL receptor (LDLR) KO mice (19; 20). Furthermore, S1P signaling has been reported to attenuate pancreatic β cell dysfunction (21) and both FTY720 and S1P have been reported to protect pancreatic β cells against apoptosis (16; 22). Recently, FTY720 administration to diabetic rats was shown to

significantly improve coronary flow reserve, however the impact of FTY720 in CA stenosis was not evaluated (23).

Hyperglycemic mice more readily develop aortic sinus atherosclerosis compared to normoglycemic controls but effects of hyperglycemia on CA atherosclerosis have not been reported (24; 25) in part, because conventional mouse atherosclerosis models, such as apoE or LDLR deficient mice, do not develop substantial CA atherosclerosis or subsequent myocardial infarction (26). Mice deficient in the scavenger receptor class B, type 1 (SR-B1) – a multiligand HDL receptor – exhibit substantially increased HDL cholesterol as a result of impaired hepatic HDL cholesterol clearance (27). When SR-B1 deficiency was combined with apoE deficiency, the resulting double knockout (dKO) exhibited substantially accelerated aortic sinus atherosclerosis development (28) as well as spontaneous development of extensive, occlusive atherosclerosis in CAs and myocardial infarction resulting in early death (~6-8 weeks of age) (29). We have reported similar results for SR-B1 deficiency in LDLR KO mice fed high fat/high cholesterol atherogenic diets (30; 31). SR-B1 KO mice homozygous for a hypomorphic mutant apoE allele have also been reported to develop high fat/high cholesterol (HFC) diet induced CA disease that is sensitive to environmental conditions (32). ApoE-hypomorphic (apoE-hypo) mice express a mutant form of the murine apoE (Thr61→Arg61) gene that also harbors an intronic neomycin resistance gene cassette that induces a hypomorphic phenotype, resulting in 95-98% reductions in both the apoE gene expression and the accumulation of protein in plasma, compared to wild type controls (32; 33). Feeding these mice HFC diets results in dramatic accumulation of very low-density lipoprotein

(VLDL) and intermediate density lipoprotein (IDL)/LDL sized and reduced HDL sized lipoproteins due to altered lipoprotein clearance (34), which can be reversed by switching the mice back to normal chow diets (34; 35). SR-B1 KO/apoE-hypo mice, when fed a high fat, high cholesterol atherogenic diet, develop extensive diet dependent occlusive CA atherosclerosis, myocardial fibrosis and cardiac dysfunction similar to the SR-B1/apoE double KO mice (36). Taking advantage of the inducible nature of the coronary heart disease (CHD) phenotype in SR-B1 KO/apoE-hypo mice, we tested whether the induction of diabetes in these mice affected the development of the diet induced CHD phenotype and whether treatment with FTY720 protected the diabetic mice from diet induced CHD.

We report that treatment with multiple low doses of streptozotocin (STZ) induced hyperglycemia and increased the extent of atherosclerosis development in the aortic sinus but only marginally in CAs. STZ induced hyperglycemia substantially increased cardiac fibrosis, and reduced the symptom-free survival of HFC diet-fed SR-B1 KO/apoE-hypo. Treatment of diabetic HFC diet-fed SR-B1 KO/apoE-hypo mice with FTY720 did not affect the degree of hyperglycemia, but reduced atherosclerosis development in the aortic sinus and CAs, reduced necrotic core size and apoptosis in plaques in the aortic sinus, and reduced platelet accumulation in the atherosclerotic CAs. FTY720 treatment was also associated with reduced mean levels of myocardial fibrosis but did not result in prolonged symptom-free survival of diabetic SR-B1 KO/apoE-hypo mice.

2.3 Materials and Methods

2.3.1 Materials

FTY720 (Fingolimod HCl) was purchased from Selleck Chemicals (Houston, Texas, USA). Citrate buffer was purchased from Electron Microscopy Sciences (Hatfield, PA, USA). STZ and all other materials were purchased from Sigma Aldrich (St. Louis, Missouri, USA) unless indicated otherwise.

2.3.2 Animals

All animal-related procedures were approved by the McMaster University Animal Research Ethics Board and were in accordance with the Canadian Council on Animal Care. All animals were bred and housed in vented cages at the Thrombosis and Atherosclerosis Research Institute animal facility at McMaster University under controlled light (12 h light/dark) and temperature conditions, and had free access to normal rodent chow (Harlan Teklad TD2918, Madison, WI, USA) and water. Unless otherwise indicated, mice received automatic watering. SR-B1 KO/apoE-hypo mice (C57BL/6:129 mixed background) were originally obtained from Dr. Monty Krieger (MIT, Cambridge, USA). SR-B1$^{-/-}$/apoE-hypo male and SR-B1$^{+/-}$/apoE-hypo female mice were bred and male SR-B1$^{-/-}$/apoE-hypo offspring were selected for experiments. Experimental mice were housed 2-4 mice per cage. Diabetes was induced in male mice

(5 weeks old) by injecting STZ intraperitoneally at a dose of 40 mg/kg of body weight (BW) following the multiple low-dose injections method as previously described (25). Briefly, mice received daily injections of STZ for five consecutive days, were rested for one week, and then received another series of STZ injections for 5 days. Control mice received an equivalent volume of vehicle solution (20 mM citrate buffer) following the same schedule. Non-fasting blood glucose was monitored weekly using a commercial glucometer (Contour meter, Bayer). For FTY720 treatment, diabetes was induced under the conditions described above. Animals were given bottled water either containing FTY720 (0.0036 g/l), or control water alone. Treatment was started on the day of the first STZ injection (Week -3 in Figure 3A). The average dose of FTY720 per animal was estimated at 0.3 mg/kg per day, based on water consumption (37). At the beginning of week 4 of the study (Time 0 weeks in Figures 2.1A and 2.3A), mice with confirmed hyperglycemia were switched to a HFC diet (Harlan Teklad TD94059, Madison, WI, USA) for four weeks. At the end of the feeding period (4 weeks), animals were fasted for 4 hours prior to anesthesia and euthanasia. Blood was collected by cardiac puncture and tissues were perfused with heparinized saline (10 U/ml) followed by 10% formalin. Hearts were harvested, weighed and fixed overnight in 10% formalin and embedded in Cryomatrix (Thermo Fisher Scientific, Ottawa, Canada). Plasma was obtained by centrifugation of blood at 4000 rpm for 15 minutes and stored at -80°C until further analysis. For survival studies, mice were left on the HFC diet until they reached endpoint (30) (panting, hunched posture, ruffled fur, inactivity when disturbed) at which point they were euthanized.

2.3.3 Plasma lipid analysis

Commercial enzymatic assays were used to determine total cholesterol (Infinity Cholesterol Reagent, Thermo Fisher Scientific), free cholesterol (Free Cholesterol E, Wako Diagnostics, Mountain view, CA, USA), triglycerides (L-type Triglyceride M, Wako Chemicals, Richmond, VA, US) and HDL-Cholesterol (HDL- cholesterol E, Wako Diagnostics, Mountain view, CA, USA) in plasma following manufacture's protocols. Non-HDL cholesterol was calculated as the difference between total cholesterol and HDL cholesterol measurements. Cholesteryl ester levels were calculated as the difference between total cholesterol and free cholesterol measurements for each sample.

2.3.4 Enzyme-linked immunosorbent assay

Plasma levels of interleukin (IL)-6 were measured using the ELISA Max Deluxe kit (BioLegend, San Diego, CA, USA).

2.3.5 Histology

For neutral lipids, cryosections (10μm) of the top of the heart and the aortic sinus were stained with oil red O (ORO). Aortic sinus atherosclerosis was measured as previously described (30) using quantitative morphometry with ImageJ software. For necrotic core size, aortic sinus cryosections were stained with hematoxylin/eosin (H&E) stain.

Necrotic core area was defined as the a-nuclear and a-cellular area within the plaque and was normalized against plaque area. For CA atherosclerosis, ORO-stained transverse sections from the middle to the heart up to the sinus in 0.5 mm intervals were analyzed and numbers of CAs scored as either lacking atherosclerosis (plaque free), containing fatty streaks, or which were <50% occluded, >50% occluded or 100% occluded by atherosclerotic plaques were determined and expressed as % of total CAs counted. For myocardial fibrosis, transverse sections were stained with Masson's Trichrome, which stains collagen-rich tissue blue and healthy myocardium red, following the manufacture's protocol (38). Fibrotic area was measured manually using the outline function in ImageJ across 5 transverse sections from each mouse near the top of the heart spaced 0.5mm apart and expressed as average cross-sectional area per section. All images were collected with a Zeiss Axiovert 200M inverted microscope with a 5X objective (Carl Zeiss Canada Ltda., Toronto, Canada).

2.3.6 Immunofluorescence

Tissue sections were stained with rat anti-mouse CD41 antibody (BD Pharmingen, Mississauga, Canada) followed by goat anti-rat Alexa 488 (Molecular Probes, Burlington, Canada). CD41-positive CAs were counted across five tissue sections. Results were expressed as the average number of CD41-positive CAs per tissue section. Apoptosis in the atherosclerotic plaque was assessed by terminal deoxynucleotidyl transferase dUTP nick end labeling (TUNEL) staining, using the ApopTag In Situ Apoptosis Detection Kit

(Millipore, Etobicoke, Canada). The number of TUNEL + cells within the atherosclerotic plaques were counted and normalized to the atherosclerotic plaque area. 4', 6'-diamidino-2-phenylindole (DAPI) was used as counterstain to visualize nuclei. All images were acquired with a Zeiss Axiovert 200M inverted microscope with a 20X objective.

2.3.7 Statistical Analysis

Results are presented as mean ± SEM. Data was subjected to the D'Agostino & Pearson omnibus normality test prior to the selection of the appropriate statistical test. When data fit a normal distribution, the Student's T test was used for statistical analysis. If data did not fit a normal distribution, it was analyzed using the Mann Whitney U test. To analyze significant differences between more than two groups, one-way ANOVA followed by Newman-Keuls post-hoc test or two-way ANOVA followed by Bonferroni post-hoc test were used. All data analysis was done using the PRISM software (GraphPad Software Inc, La Jolla, CA, USA). $P<0.05$ was considered to be significant.

2.4 Results

2.4.1 Effects of STZ-treatment of SR-B1 KO/apoE-hypo mice on hyperglycemia and plasma lipids

To evaluate the impact of hyperglycemia on atherosclerosis development in SR-B1 KO/apoE-hypo mice, we used the multiple, low-dose STZ treatment, which has been used previously to demonstrate that hyperglycemia accelerates atherosclerosis development in the aortic sinus of apoE deficient mice (25). SR-B1 KO/apoE-hypo mice were treated with 5 consecutive daily intraperitoneal injections of 40 mg/kg STZ or control citrate buffer vehicle. Mice were fed an atherogenic, HFC diet starting from 8 weeks of age (Figure 2.1A). STZ treatment, beginning in mice aged 5 weeks, increased blood glucose levels from 10.9 ± 06 to a maximum of 24.0 ± 0.8 mM after the second round of injections. Blood glucose levels remained elevated in the STZ-treated mice over the entire time-course of the study (Figure 2.1B). Immunofluorescence analysis of sections of the pancreas confirmed reduced numbers of insulin-positive β cells in pancreatic islets in the STZ treated mice (Supplementary Figure 2.6). Occasionally, we observed individual mice whose blood glucose levels rose after STZ treatment but returned to baseline levels after STZ treatment was discontinued. Those individuals were removed from the study. In contrast, blood glucose levels did not increase in control mice injected with citrate buffer vehicle (Figure 2.1B). STZ treatment had similar effects, as expected, when mice were maintained on a normal chow diet (Supplementary Figure 2.7B).

STZ-treated mice that were maintained on normal chow diet did not exhibit differences in plasma total cholesterol, unesterified cholesterol, cholesteryl ester or non-HDL cholesterol, but increases in plasma triglyceride and HDL cholesterol were detected (Table 2.1). HFC diet feeding increased levels of all lipid parameters measured, except for triglyceride levels, which were unchanged, and HDL-cholesterol levels, which were reduced compared to normal chow fed mice (Table 2.1). Diabetic mice that were fed the HFC diet exhibited 20-40% increases in plasma total cholesterol, plasma cholesterol ester, and plasma non-HDL cholesterol levels but exhibited no statistically significant differences in plasma free cholesterol, triglycerides or HDL cholesterol levels relative to non-diabetic mice fed the HFC diet (Table 2.1). Diabetic mice fed the HFC diet also had increased plasma IL-6 levels compared to HFC diet fed normoglycemic mice (Table 2.1).

2.4.2 Effect of STZ-treatment on survival of SR-B1 KO/apoE-hypo mice

STZ-treated mice that were fed the HFC diet exhibited reduced survival (Figure 2.1C, average symptom free survival of 42 days of feeding) when compared to the control mice that were fed the same diet (average symptom free survival of 58 days comparable, to what has been previously reported for SR-B1 KO/apoE-hypo and SR-B1/LDLR dKO mice fed the same diet (30; 35)). STZ treatment, alone, did not appear to reduce the survival of SR-B1 KO/apoE-hypo mice that were maintained on a low fat, low cholesterol chow diet (Supplementary Figure 2.7C). Thus, STZ treatment appears to accelerate the onset or development of HFC diet-induced disease in SR-B1 KO/apoE-hypo mice.

2.4.3 Effect of STZ-induced hyperglycemia on HFC diet-induced atherosclerosis in SR-B1/apoE-hypo mice

To evaluate aortic sinus and CA atherosclerosis, STZ or control treated and HFC diet-fed mice were euthanized and analyzed 4 weeks after the initiation of HFC feeding. This precedes the initiation of early death in the HFC diet fed SR-B1 KO/apoE-hypo mice (Figure 2.1C). Figures 2.1D and E show representative images of atherosclerotic plaques in the aortic sinus of control and STZ-treated, HFC diet-fed mice. STZ treatment significantly increased the average plaque size in aortic sinuses of HFC diet fed SR-B1 KO/apoE-hypo mice compared to control treated mice receiving the same diet (Figure 2.1F). STZ-treated, HFC diet-fed mice also developed increased necrotic core sizes in atherosclerotic plaques, compared to those in control-treated HFC diet-fed mice (Figures 2.1G-I). No differences were observed in numbers of apoptotic nuclei detected within the plaques from the two groups of mice (Figures 2.1J-L).

Figure 2.1: STZ-induced diabetes is associated with reduced survival and increased aortic sinus atherosclerosis and necrotic core area in HFC diet-fed SR-B1 KO/apoE-hypo mice

A. At the start of the experiment (marked weeks -3), 5 week old male SR-B1 KO/apoE-hypo mice received two rounds of injections of STZ (5 daily injections of 40 mg/kg of body weight/week) with one week of rest in between. 3 weeks later, after hyperglycemia was confirmed, mice were fed a high fat, high cholesterol (HFC) diet (beginning if HFC diet feeding marked as week 0) either for four weeks before euthanasia and analysis of atherosclerosis and cardiac pathology, or until they reached human endpoint (survival study, panel C). **B.** Non-fasting glucose levels. Open circles, control mice (n=11) treated with citrate buffer alone; solid circles, STZ (in citrate buffer)-treated mice (n=15). Glucose was measured weekly until week +3 of the study (***$p<0.001$). **C.** Kaplan-Meier survival curves for control- or STZ-treated mice as in A. Symptom-free survival is plotted against the length of time of HFC diet feeding (**$p<0.01$ by Mantel-Cox Log-rank test). **D-E.** Representative images of oil red O/hematoxylin-stained cross sections of the aortic sinus of control and diabetic mice respectively. **F.** Quantification of plaque area (n=14-15; *$p<0.05$). **G-H.** Representative images of hematoxylin/eosin-stained atherosclerotic plaques in the aortic sinus of control and diabetic mice respectively, showing necrotic cores devoid of nuclei and cells. **I.** Quantification of necrotic core area (n=14-15; **$p<0.01$). **J-K.** Representative images of TUNEL-stained cross sections of the aortic sinus of control and diabetic mice respectively. Apoptotic $TUNEL^+$ nuclei appear green; DAPI was used as a nuclear counterstain (blue). The dashed line represents

the boundary between the media and neointima of the vessel wall. **L.** Quantification of $TUNEL^+$ nuclei in the aortic sinus plaque (n=10).

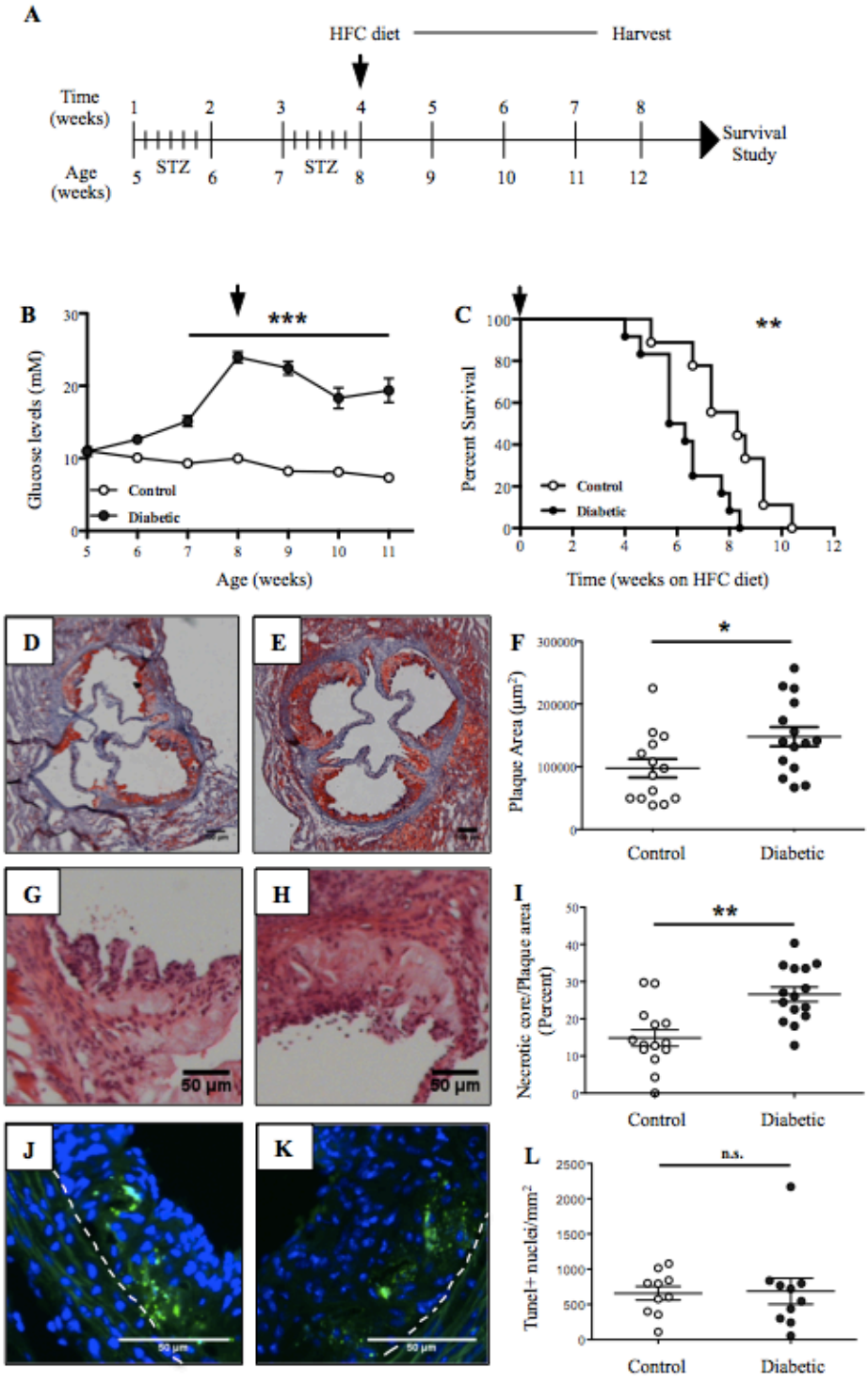
A
HFC diet
Harvest
Time (weeks)
Age (weeks)
STZ
STZ
Survival Study
B
***
Glucose levels (mM)
Control
Diabetic
Age (weeks)
C
**
Percent Survival
Control
Diabetic
Time (weeks on HFC diet)
D
E
F
*
Plaque Area (μm²)
Control
Diabetic
G
H
50 μm
50 μm
I
**
Necrotic core/Plaque area (Percent)
Control
Diabetic
J
K
50 μm
50 μm
L
n.s.
Tunel+ nuclei/mm²
Control
Diabetic

Table 2.1: Plasma lipids in control and diabetic SR-B1 KO/apoE-hypo mice

Plasma was prepared from blood collected by cardiac puncture from chow diet fed- and HFC diet fed-SR-B1 KO/apoE-hypo mice at the moment of harvest. Plasma lipids were determined as described in materials and methods. Results are expressed as mean ± SEM. Sample size is indicated in parenthesis on the group column: a, $p<0.05$ vs Control chow diet; b, $p<0.05$ vs Diabetic chow diet; c, $p<0.05$ vs Control High fat/High cholesterol diet, One-way ANOVA. ¶, $p<0.05$ vs Control High fat/High cholesterol diet Student's T test, § $p=0.0513$ vs Control chow diet, Mann Whitney test.

	Chow diet		**High fat/High cholesterol diet**	
	Control (7)	**Diabetic (6)**	**Control (14)**	**Diabetic (15)**
Total Cholesterol (mmol/l)	9.92 ± 1.59	8.45 ± 0.70	34.82 ± 2.02[a,b]	42.08 ± 1.96[a,b,c]
Free Cholesterol (mmol/l)	6.16 ± 0.78	4.78 ± 0.25	22.52 ± 1.81[a,b]	25.10 ± 1.96[a,b]
Cholesterol Ester (mmol/l)	3.76 ± 0.88	3.66 ± 0.59	12.30 ± 1.29[a,b]	16.98 ± 1.32[a,b,c]
Triglycerides (mmol/l)	0.61 ± 0.11	1.20 ± 0.22[§]	0.65 ± 0.10	0.82 ± 0.13
HDL-cholesterol (mmol/l)	3.3 ± 0.61	5.35 ± 1.23[a]	0.88 ± 0.10[a,b]	0.52 ± 0.06[a,b,¶]
Non HDL-cholesterol (mmol/l)	6.63 ± 1.61	3.10 ± 0.80	33.94 ± 2.00[a,b]	40.57 ± 2.06[a,b,c]
IL-6 (pg/ml)	116.6 ± 35.63	37.73 ± 15.93	177.8 ± 23.05[b]	273 ± 38.43[a,b,c]

To evaluate the effects of STZ treatment on atherosclerosis development in CAs in HFC diet fed SR-B1 KO/apoE-hypo mice, the proportions of CAs scored for the degree of occlusion (Figure 2.2A) were determined. STZ treatment was associated with a slight but statistically significant reduction in the proportion of CAs scored as "plaque free" (Figure 2.2B, 51 ± 2 % vs 62 ± 2 %, respectively). We saw trends towards slightly increased proportions of CAs containing atherosclerotic plaques, scored as <50%, >50% and 100% occluded (Figure 2.2B, 27 ± 2 % vs 22 ± 2 %) in the STZ-treated vs control HFC-diet fed mice, although the differences did not reach statistical significance. This suggests that STZ treatment did not substantially increase the HFC-diet induced atherosclerosis development in the CAs of SR-B1 KO/apoE-hypo mice. The STZ-dependent increase in atherosclerosis in the aortic sinus and the development of atherosclerosis in CAs of SR-B1 KO/apoE-hypo mice appeared to be specific to mice fed the atherogenic HFC diet, because when we subjected a second cohort of SR-B1 KO/apoE-hypo mice to STZ or control treatment and then maintained them on a normal chow diet until they were 22 weeks of age (approximately 10 weeks older than the HFC diet-fed mice), we observed smaller atherosclerotic plaque sizes in the aortic sinus and much lower numbers of atherosclerotic CAs (Supplementary Figure 2.8). Surprisingly, STZ treatment was accompanied by an approximate 50% reduction in average atherosclerotic plaque sizes in the aortic sinus and slightly increased proportion of CAs that were scored as plaque free (with corresponding, though not statistically significant trends towards decreases in the small numbers of CAs scored as >50% or 100% occluded) in the normal chow diet fed mice (Supplementary Figure 2.8A-C). Thus, STZ treatment

increased HFC diet-induced but not spontaneous atherosclerosis in the aortic sinus of SR-B1 KO/apoE-hypo mice.

2.4.4 STZ treatment increases platelet accumulation in atherosclerotic CAs and myocardial fibrosis in HFC diet fed SR-B1 KO/apoE-hypo mice

We have previously reported detecting CD41 staining in atherosclerotic CAs in HFC atherogenic diet fed SR-B1/LDLR dKO mice, suggesting that at least some of the atherosclerotic plaques in occluded CAs in those mice contain platelets (30). CD41 immunostaining was performed on cardiac sections from STZ- and control-treated and HFC diet fed SR-B1 KO/apoE-hypo mice, revealing that some of the completely occluded CAs in HFC diet fed SR-B1 KO/apoE-hypo mice were positive for this marker of platelets, consistent with our previous findings in SR-B1/LDLR dKO mice. Representative sections showing CAs negative or positive for platelets are shown in Figure 2.2 (C and D respectively). STZ treated mice exhibited, on average, approximately 4-fold increased numbers of CAs that were positive for CD41, indicating increased platelet accumulation in atherosclerotic CAs from STZ- compared to control-treated SR-B1 KO/apoE-hypo mice after HFC diet feeding (Figure 2.2E).

Figure 2.2: HFC diet-induced atherosclerosis and platelet accumulation in CAs of control and STZ-treated SR-B1 KO/apoE-hypo mice

A. Heart cross sections were stained with oil red O/hematoxylin and coronary arteries (CAs) were classified as having no atherosclerotic plaques ("no plaque"), oil red O staining within the wall without the presence of raised plaque ("fatty streak"), or containing raised atherosclerotic plaques occluding <50 %, >50 % or 100 % of the artery lumen (as shown). **B.** Quantification of the average proportions of CAs per section classified according to the degree of occlusion (n=14-15; ***$p<0.001$). **C-D.** Representative images of CAs stained for activated platelets (CD41, green) and nuclei (DAPI, blue). The dashed line represents the vessel wall. **E**. Quantification of platelet-positive CAs (n=11-14; *$p<0.05$).

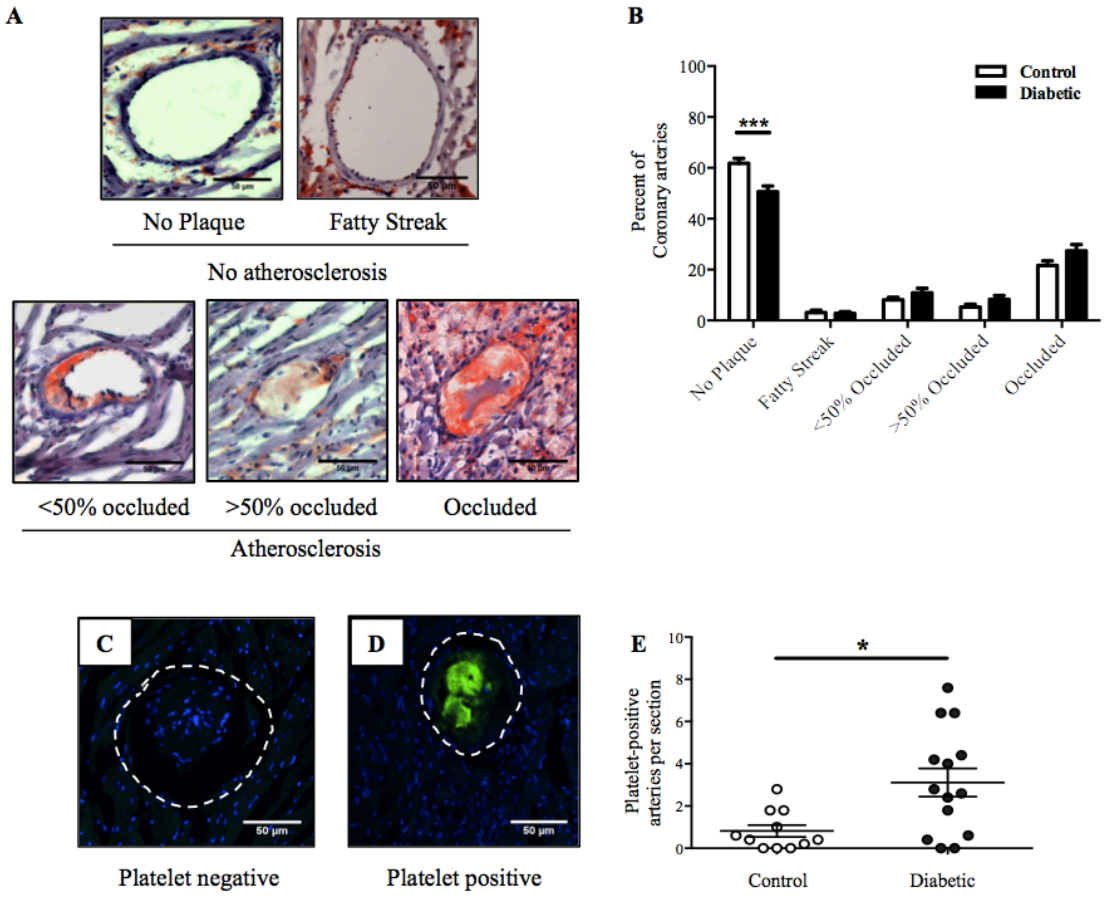
A
No Plaque
Fatty Streak
No atherosclerosis
<50% occluded
>50% occluded
Occluded
Atherosclerosis
B
Control
Diabetic
***
Percent of Coronary arteries
100
80
60
40
20
0
No Plaque
Fatty Streak
<50% Occluded
>50% Occluded
Occluded
C
D
50 µm
Platelet negative
Platelet positive
E
*
Platelet-positive arteries per section
10
8
6
4
2
0
Control
Diabetic

2.4.5 Treatment of diabetic SR-B1 KO/apoE-hypo mice with FTY720 attenuates HFC diet induced atherosclerosis development

FTY720 has been reported in independent studies to reduce aortic sinus atherosclerosis in normoglycemic mice (19; 20) and to protect against pancreatic β cell dysfunction (21) and preserve coronary flow in diabetic rodents (23). We therefore tested if treatment of diabetic SR-B1 KO/apoE-hypo mice affected the development of HFC-diet induced atherosclerosis. As before, we first subjected 5 week old mice to two rounds of multiple low dose STZ treatment, with the exception that these mice were provided with bottled water (control) or bottled water containing FTY720 (0.0036 g/l, Figure 2.3A). Mice were then placed on the HFC diet at 8 weeks of age and one cohort was monitored for the onset of cardiovascular endpoints, whereas another cohort was euthanized at 12 weeks of age, i.e. after 4 weeks of HFC diet feeding. Weekly glucose monitoring revealed that FTY720 treatment did not affect the onset of STZ induced hyperglycemia (Figure 2.3B). FTY720 treatment did not prolong the symptom-free survival of the diabetic SR-B1 KO/apoE-hypo mice fed the HFC diet (Figure 2.3C). Curiously, this cohort of control diabetic mice (given water in water bottles) exhibited reduced survival compared to the cohort of HFC-fed diabetic mice maintained on automatic watering (Figure 2.1C; both survival curves re-plotted on the same graph in Supplementary Figure 2.9). This suggests that housing conditions may alter the survival of the diabetic SR-B1 KO/apoE-hypo mice and is reminiscent of previous reports that the number of mice per cage affected the survival of atherogenic diet-fed non-diabetic SR-B1 KO/apoE-hypo mice (35).

We analyzed the effects of FTY720 treatment on plasma lipids in mice fed the HFC diet for 4 weeks. FTY720 treatment did not significantly impact plasma total, unesterified or esterified cholesterol, or non-HDL cholesterol (Table 2.2). HDL cholesterol, which represented only a minor fraction of total cholesterol in plasma, was nevertheless significantly increased in the FTY720-treated diabetic HFC-diet fed mice (Table 2.2). A significant reduction in plasma IL-6 was also detected in the FTY720 treated mice (Table 2.2, $p<0.05$), suggesting anti-inflammatory effects.

FTY720-treatment of diabetic mice resulted in a 32% reduction in the average size of the atherosclerotic plaques in the aortic sinus (74,000 ± 8,000 μm^2 in FTY720-treated mice compared with 108,000 ± 12,000 μm^2 in controls, figure 2.3D-F). FTY720-treatment was also associated with a 51% reduction in mean relative necrotic core size in atherosclerotic plaques in the aortic sinus (Figure 2.3G-I). Because macrophage apoptosis has been reported to contribute to necrotic core development, we examined the extent of apoptosis in atherosclerotic plaques using TUNEL staining for nuclei with damaged DNA. Plaques from FTY720-treated diabetic mice exhibited fewer TUNEL positive nuclei than those from control treated diabetic mice (274 ± 59 vs. 481 ± 121 TUNEL positive nuclei per mm^2, figure 2.3J-L). This suggests that FTY720-treatment reduced the level of apoptosis within atherosclerotic plaques of diabetic HFC diet fed SR-B1 KO/apoE-hypo mice and that this may contribute to the reduced necrotic core development.

Figure 2.3: FTY720-treatment reduces HFC diet-induced aortic sinus atherosclerosis and necrotic core formation in diabetic SR-B1 KO/apoE-hypo mice

A. Time course of the study STZ-treatment of 5 week old SR-B1 KO/apoE-hypo mice and HFC diet feeding (black arrow) was as described in the legend to Figure 1A, with the exception that from the start and throughout the experiment, mice were provided with water bottles containing either FTY720 (0.0036 g/l, ~0.3 mg/kg/day based on water consumption) in the drinking water, or control water lacking FTY720. Time (weeks) is relative to the start of HFC-diet feeding. The age of mice (weeks) is indicated at the bottom. **B.** Non-fasting glucose levels. Open circles, diabetic mice receiving control water (n=14); solid circles, diabetic mice treated with FTY720 (n=15). Glucose was measured weekly with a commercial glucometer. **C.** Kaplan-Meier survival curves of diabetic mice treated with FTY720 or receiving control water (n=7-10). Symptom-free survival is plotted against the length of time of HFC diet feeding. **D-E.** Representative images of oil red O/hematoxylin-stained aortic sinus cross sections from diabetic and diabetic mice treated with FTY720 respectively. **F**. Quantification of plaque area in the aortic sinus (n=14-15; *$p<0.05$). **G-H.** Representative images of hematoxylin/eosin-stained atherosclerotic plaques in the aortic sinus of control and FTY720-treated diabetic mice respectively, showing necrotic cores devoid of nuclei and cells. **I.** Quantification of necrotic core area (n=14-15; **$p<0.01$). **J-K.** Representative images of TUNEL-stained cross sections of the aortic sinus of control and FTY720-treated diabetic mice respectively. Apoptotic $TUNEL^+$ nuclei appear green; DAPI was used as a nuclear counterstain (blue). The dashed line represents the boundary between the media and

neointima of the vessel wall. **L.** Quantification of TUNEL + nuclei per atherosclerotic plaque area (n=10-11; *p<0.05).

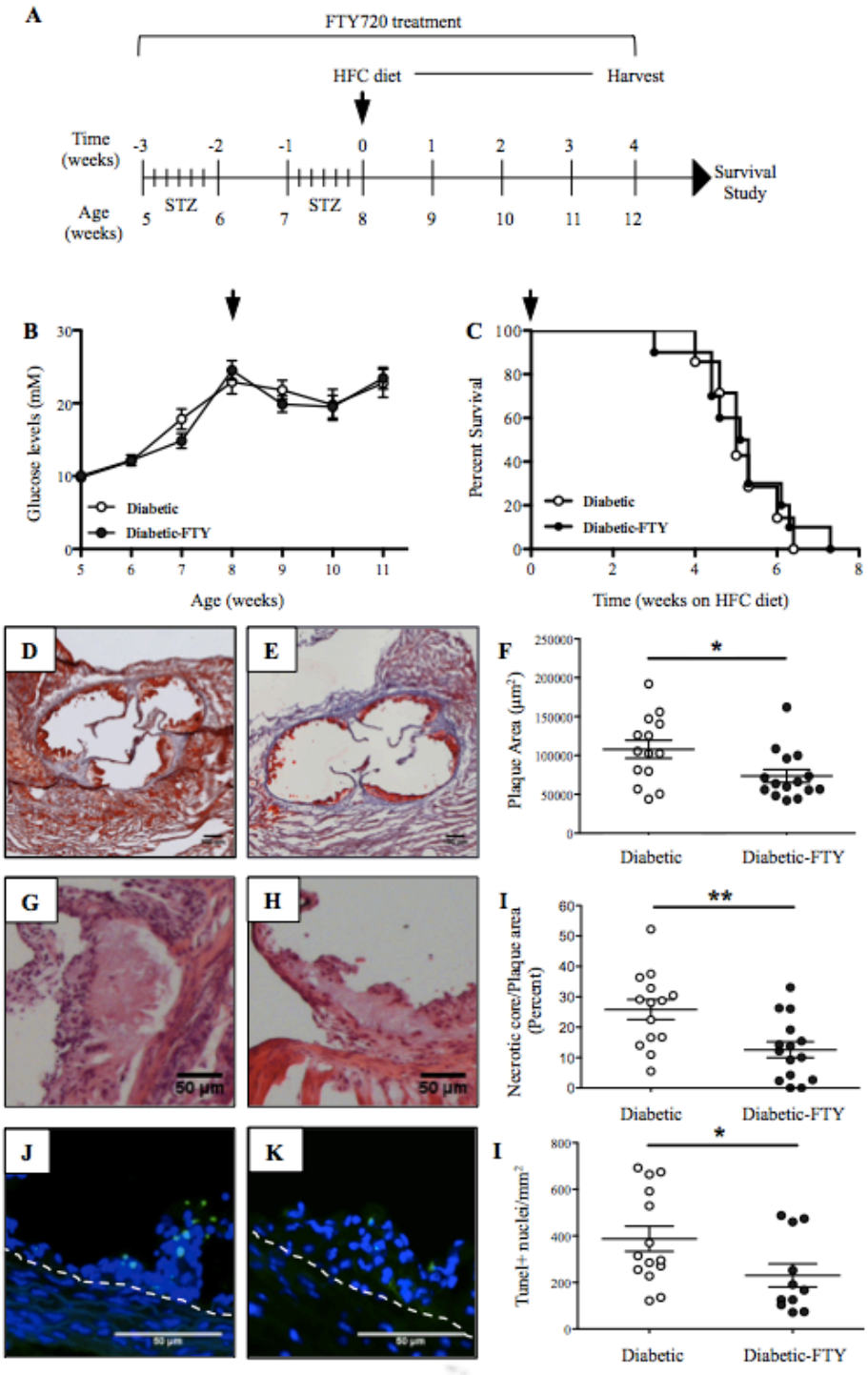
A
FTY720 treatment
HFC diet
Harvest
Time (weeks)
-3 -2 -1 0 1 2 3 4
Survival Study
Age (weeks)
5 STZ 6 7 STZ 8 9 10 11 12
B
Glucose levels (mM)
Diabetic
Diabetic-FTY
Age (weeks)
C
Percent Survival
Diabetic
Diabetic-FTY
Time (weeks on HFC diet)
D
E
F
Plaque Area (μm²)
*
Diabetic
Diabetic-FTY
G
H
50 μm
I
Necrotic core/Plaque area (Percent)
**
Diabetic
Diabetic-FTY
J
K
I
Tunel+ nuclei/mm²
*
Diabetic
Diabetic-FTY

Table 2.2: Plasma lipids in diabetic SR-B1 KO/apoE-hypo mice treated with FTY720 or vehicle

Plasma was prepared from blood collected by cardiac puncture from chow diet fed- and HFC diet fed-SR-B1 KO/apoE-hypo mice at the moment of harvest. Plasma lipids were determined as described in materials and methods. Results are expressed as mean ± SEM. Sample size for each group is indicated in parenthesis: a, $p<0.05$ vs Vehicle, Student's T test.

	Vehicle (14)	**FTY720 (15)**
Total Cholesterol (mmol/l)	60.47 ± 8.32	54.81 ± 5.68
Free Cholesterol (mmol/l)	39.49 ± 4.21	40.09 ± 3.71
Cholesterol Ester (mmol/l)	20.98 ± 4.94	14.72 ± 2.65
Triglycerides (mmol/l)	1.92 ± 0.49	1.37 ± 0.45
HDL-cholesterol (mmol/l)	0.55 ± 0.09	1.27 ± 0.17[a]
Non HDL-cholesterol (mmol/l)	59.92 ± 8.33	53.54 ± 5.68
IL-6 (pg/ml)	390.9 ± 89.57	182.7 ± 50.17[a]

2.4.6 FTY720 treatment reduced platelet accumulation in atherosclerotic CAs in diabetic HFC diet-fed SR-B1 KO/apoE-hypo mice.

Treatment with FTY720 resulted in a slight but statistically significant increase (Figure 2.4B, 64 ± 1 % vs 59 ± 2 %) in the proportion of CAs that were free of atherosclerosis ("plaque free"), and a corresponding, statistically significant decrease in the proportion of CAs that were completely occluded by the atherosclerotic plaque (Figure 2.4B, 20 ± 1 % vs 25 ± 2 %), compared to the control-treated diabetic mice (Figure 2.4A-B). No changes in the small proportions of arteries with fatty streaks or atherosclerotic plaques occluding <50 % or >50 % of the artery lumen were observed in FTY720-treated mice. FTY720-treatment was associated with a more striking, 43% reduction in the numbers of atherosclerotic CAs that exhibited CD41 staining (Figure 2.4C-E), indicating that FTY720 reduced platelet accumulation in atherosclerotic CAs.

Figure 2.4: HFC-diet induced atherosclerosis and platelet accumulation in CAs of control and FTY720-treated diabetic SR-B1 KO/apoE-hypo mice

A. Heart cross sections were stained with oil red O/hematoxylin and CAs were classified as having no atherosclerotic plaques ("no plaque"), oil red O staining within the wall without the presence of raised plaque ("fatty streak"), or containing raised atherosclerotic plaques occluding <50 %, >50 % or 100 % of the artery lumen (as shown). **B.** Quantification of the average proportions of CAs per section classified according to the degree of occlusion (n=14-15; *p<0.05). **C-D.** Representative images of CAs stained for activated platelets (CD41, green) and nuclei (DAPI, blue). The dashed line represents the vessel wall. **E**. Quantification of platelet-positive coronary arteries (n=10; *p<0.05).

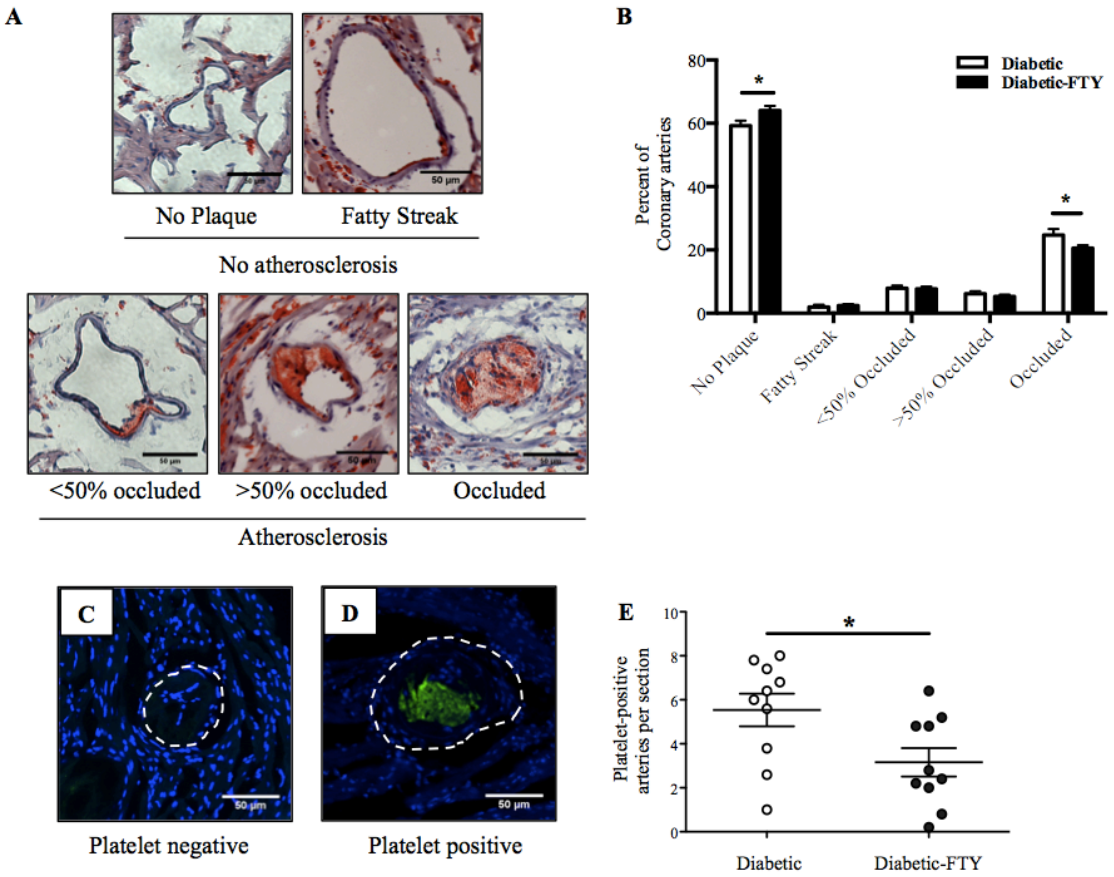
A
No Plaque
Fatty Streak
No atherosclerosis
<50% occluded
>50% occluded
Occluded
Atherosclerosis
B
Diabetic
Diabetic-FTY
Percent of Coronary arteries
80
60
40
20
0
*
*
No Plaque
Fatty Streak
<50% Occluded
>50% Occluded
Occluded
C
D
Platelet negative
Platelet positive
E
Platelet-positive arteries per section
10
8
6
4
2
0
*
Diabetic
Diabetic-FTY

2.4.7 STZ induced diabetes increases and FTY720-treatment reduces cardiac fibrosis in diabetic HFC diet fed SR-B1 KO/apoE-hypo mice

Ventricular fibrosis is a common process detected in the aftermath of myocardial infarction. To detect cardiac fibrosis, frozen transverse sections of hearts were stained with Mason's trichrome, which stains collagen fibers blue/purple and healthy myocardium red. Trichrome staining in sections from control, normoglycemic SR-B1 KO/apoE-hypo mice that were fed the HFC diet for 4 weeks revealed collagen deposition in the myocardium, averaging approximately 4 ± 1 % of the myocardial cross sectional area (Figure 2.5A). More extensive fibrosis (averaging 12 ± 3 % of the myocardial cross sectional area) was detected in cross sections from the hyperglycemic, STZ-treated SR-B1 KO/apoE-hypo mice that were fed the HFC diet mice (Figure 2.5B,C). The increased HFC diet-induced cardiac fibrosis observed in the hyperglycemic STZ-treated vs normoglycemic control-treated SR-B1 KO/apoE-hypo mice is consistent with previously reported effects of diabetes increasing cardiomyophathy in surgical models of coronary ligation (39; 40). Treatment of diabetic SR-B1 KO/apoE-hypo mice with FTY720, on the other hand, was associated with an approximately 50 % reduction in the level of HFC-diet induced cardiac fibrosis (14 ± 2 % for control diabetic vs 7 ± 2 % for FTY720-treated diabetic mice; Figure 2.5D-F). This suggested that FTY720-treatment could at least partially attenuate the effects of diabetes induction on HFC diet-induced cardiac fibrosis in SR-B1 KO/apoE-hypo mice.

Figure 2.5: Effects of STZ-induced diabetes and FTY720-treatment on myocardial fibrosis in HFC diet-fed SR-B1 KO/apoE-hypo mice

Heart cross sections were stained with Mason's trichrome which stains healthy myocardium red and collagen blue. **A-B.** Representative images of control-and STZ-treated mice after 4 weeks of HFC diet feeding. **C**. Quantification of average fibrotic area per section (n=14-15; **p<0.01). **D-E**. Representative images of control- and FTY720-treated diabetic SR-B1 KO/apoE-hypo mice after 4 weeks of HFC diet feeding. **F**. Quantification of myocardial fibrosis per section (n=14-15; *p<0.05).

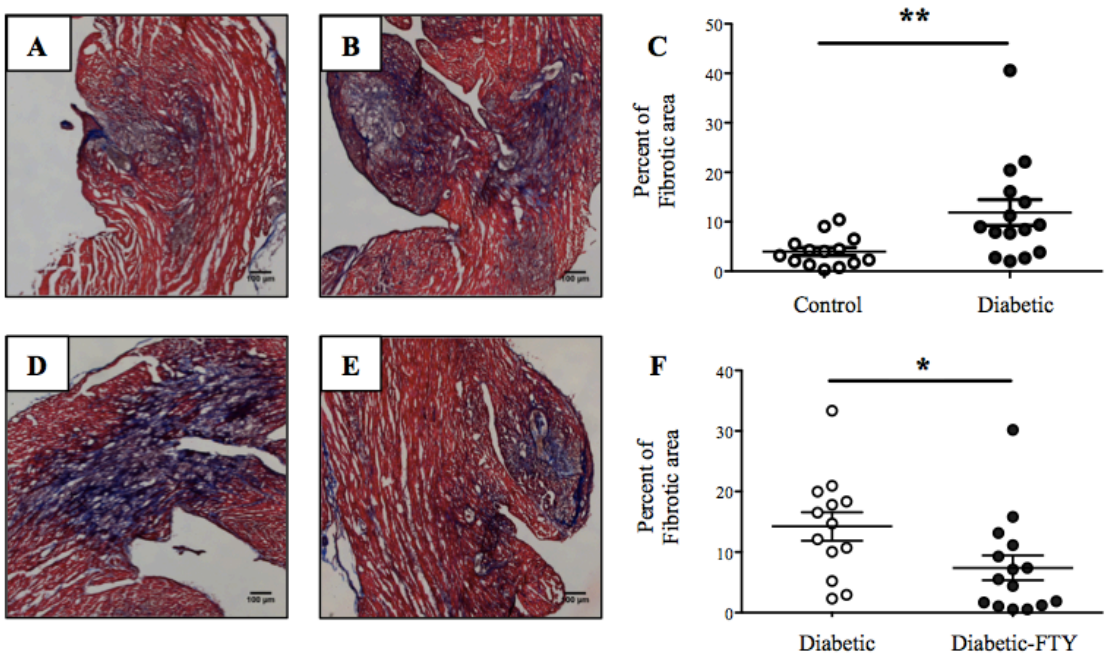
A
B
C
**
Percent of Fibrotic area
50
40
30
20
10
0
Control
Diabetic
D
E
F
*
Percent of Fibrotic area
40
30
20
10
0
Diabetic
Diabetic-FTY

Despite the increased HFC diet-induced cardiac fibrosis in diabetic vs normoglycemic control mice and reduced HFC diet-induced cardiac fibrosis in FTY720-treated vs control diabetic mice, we did not observe differences in heart weights (HW) (Supplementary Figure 2.10A,D). We did, however observe a trend (not statistically significant) towards reduced body weight (BW) in diabetic vs control mice (Supplementary figure 2.10B), and a statistically significant increase in BW of FTY720-treated vs control diabetic mice (Supplementary Figure 2.10E), which resulted in a trend towards decreased HW/BW ratios of FTY720-treated vs control diabetic mice (Supplementary Figure 2.10F). These differences in average HW/BW ratios were driven by changes in BWs rather than changes in HW. This suggests that the 4 week HFC feeding period may not have been long enough for the development of cardiomegaly, consistent with our previous observations that cardiomegaly appears to develop after cardiac fibrosis and late in the disease process, closer to the sudden death of these mice (41).

2.5 Discussion

In this study we show that STZ-induced diabetes increased the development of diet-induced CHD in SR-B1 KO/apoE-hypo mice and that FTY720-treatment was able to prevent some of the detrimental effects triggered by diabetes. Diabetes induction increased the sizes of atherosclerotic plaques and of necrotic cores in atherosclerotic plaques in the aortic sinus (Figure 2.1). Surprisingly, diabetes induction did not appear to

significantly affect the numbers of atherosclerotic CAs; however it did substantially increase platelet accumulation in atherosclerotic CAs of HFC diet-fed mice (Figure 2.2). Diabetic mice also exhibited more extensive myocardial fibrosis (Figure 2.5A-C) and reduced survival compared to control-treated mice, after HFC diet feeding (Figure 2.1C). FTY720 was able to reduce the sizes of atherosclerotic plaques in the aortic sinus, the degree of cell apoptosis and the sizes of necrotic cores within those plaques (Figure 2.3). FTY720-treatment was also associated with a slight but significant reduction in the proportion of CAs that were atherosclerotic, and a substantial reduction in platelet accumulation within atherosclerotic CAs (Figure 2.4). FTY720 also reduced the degree of myocardial fibrosis (Figure 2.5D-F). Despite the beneficial effects, however, it did not extend the survival of diabetic SR-B1 KO/apoE-hypo mice fed the HFC diet (Figure 2.3C). This suggests either that the reduced survival of diabetic versus control HFC diet fed SR-B1 KO/apoE-hypo mice may have been the consequence of pathways other than acute CA atherosclerosis/myocardial infarction, or that the burden on occlusive CA atherothrombosis/myocardial infarction, though less in FTY720-treated mice, may still have been sufficient to trigger fatality.

Previous studies have suggested that hyperglycemia can directly increase atherosclerosis development in the absence of dyslipidemia (42) ; however in our hands, in the normal chow diet-fed SR-B1 KO/apoE-hypo mice, hyperglycemia had the opposite effect, reducing atherosclerosis in the aortic sinus and CAs (Supplementary Figure 2.8). Therefore in SR-B1 KO/apoE-hypo mice, hyperglycemia increased HFC diet-induced but not spontaneous atherosclerosis in the aortic sinus. The observed diabetes-dependent

increase in HFC diet-induced atherosclerosis is most likely the consequence of several factors in addition to the observed hyperglycemia, including the increased total cholesterol, reduced HDL cholesterol and increased IL-6 in plasma (tables 2.1 and 2.2). FTY720-treatment was able to reduce the levels of aortic sinus atherosclerosis to that of non-diabetic mice and also slightly but statistically significantly reduced CA atherosclerosis levels, despite having no effect on hyperglycemia and plasma total cholesterol. The effects we observed on aortic sinus atherosclerosis are consistent with results published by Nofer and colleagues (19) and Keul and colleagues (20) but differ from results obtained in mice fed a low cholesterol diet where FTY720-treatment did not protect against atherosclerosis (43; 44). The experimental conditions we used involved HFC diet, reported to increase systemic markers of inflammation (30). Indeed we observed a trend (though not statistically significant) towards higher plasma IL-6 levels in the HFC diet-fed mice compared to those fed a normal diet, and a statistically significant 1.5-fold increase in plasma IL-6 levels in diabetic versus control HFC diet-fed mice (Table 2.1), whereas IL-6 levels were reduced in diabetic HFC diet-fed mice that were also treated with FTY720 (Table 2.2). This is consistent with the reported reductions in circulating lymphocytes numbers in plasma cytokine levels in FTY72-treated mice (19; 20), and may, at least in part, contribute to the atheroprotective effects of FTY720 we observed. Protection against CA atherosclerosis by FTY720 has also been detected in a model of cardiac transplantation possibly due to inhibition of macrophage activation (45).

Macrophage apoptosis plays a central role in the formation of necrotic cores and defective insulin signaling in macrophages reportedly renders them more susceptible to

apoptosis due to altered AKT signaling (46). Furthermore, defective efferocytosis has also been reported in macrophages from diabetic obese mice (47). Nevertheless, we found no significant differences in numbers of apoptotic cells in atherosclerotic plaques of the hyperglycemic and normoglycemic mice even though necrotic cores were significantly enlarged (Figure 2.1). A deficiency of SR-B1, itself, has also been shown to impair macrophage efferocytosis in atherosclerotic plaques (48); this may explain, at least in part, why hyperglycemia did not appear to increase the accumulation of apoptotic cells in plaques in the aortic sinus of the HFC diet-fed SR-B1 KO/apoE-hypo mice. In agreement with results in FTY720-treated apoE and LDLR KO mice (19; 20), HFC diet-fed diabetic SR-B1 KO/apoE-hypo mice that were treated with FTY720 developed smaller necrotic cores in the aortic sinus atherosclerotic plaques (Figure 4I). We have previously reported that FTY720 induces macrophage migration *in vitro*, which could influence plaque growth and/or regression (49). FTY720 has also been shown to reduce cholesterol toxicity in human macrophages (50), which might explain the reduction in plaque apoptosis detected in mice treated with FTY720. The reduced plaque apoptosis may contribute for the reduction in necrotic core size in FTY720-treated mice however future studies are required to confirm if this is the case.

Studies in humans have shown increased incidence of coronary thrombosis in diabetic patients (51). Consistent with this, we have detected increased incidence of atherosclerotic CAs positive for CD41, a marker of activated platelets, in diabetic compared to control SR-B1 KO/apoE-hypo mice. We have also reported the detection of CD41, a marker of activated platelets, in atherosclerotic CAs of HFC diet-fed SR-

B1/LDLR dKO mice (30). Our findings suggest that hyperglycemia might exacerbate platelet activation in mice already prone to thrombosis. Excessive platelet activation could be explained by the increased production of thromboxane A2 (TxA_2), which has been reported previously in diabetic subjects and animal models of diabetes (52). The apparent increase in thrombotic events seen in the diabetic HFC diet-fed SR-B1 KO/apoE-hypo mice could also be the result of altered AKT activation due to dysregulation of the insulin growth factor I pathway (53). We and others have reported that SR-B1 mediates beneficial HDL dependent AKT1 activation in macrophages, endothelial cells and other cell types (49; 54; 55), however others have reported that AKT1 exhibits detrimental cardiovascular effects in the context of SR-B1 deficiency (56). Alternatively, the increased platelet accumulation in atherosclerotic CAs in diabetic SR-B1 KO/apoE-hypo mice may reflect increased thrombosis secondary to plaque rupture. This is consistent with the increased size of necrotic cores (one feature of unstable plaques) observed in plaques in the aortic sinuses of diabetic SR-B1 KO/apoE-hypo mice fed the HFC diet (Figure 2.1G-I). In this context the reduced platelet staining in atherosclerotic CAs of FTY720-treated diabetic mice may reflect reduced platelet accumulation secondary to plaque stabilization, consistent with the reduced necrotic core sizes and macrophage apoptosis observed in aortic sinus plaques in the FTY720-treated diabetic mice fed the HFC diet (Figure 2.3G-L). Although it is tempting to speculate that this may be involved, it is important to point out that the small size of atherosclerotic plaques in CAs, even those completely occluding the CAs make it difficult to identify necrotic cores and other signs of plaque rupture in those vessels in HFC diet fed SR-B1

KO/apoE-hypo mice. Therefore further extensive research will be required to determine if this is indeed involved.

Increased CA atherosclerosis and platelet accumulation in SR-B1 KO/apoE-hypo mice was accompanied by increased myocardial fibrosis and reduced survival in diabetic mice (Figure 2.1C). Diabetes (both types 1 and 2) has been shown to induce diabetic cardiomyopathy, including enhancing myocardial fibrosis in rodent models of CA ligation induced ischemia/reperfusion injury (40; 57). Consistent with this, we have found substantially increased myocardial fibrosis in diabetic vs non-diabetic HFC diet-fed SR-B1 KO/apoE-hypo mice despite only slightly increased numbers of occluded CAs. On the other hand, FTY720-treated diabetic mice exhibited reduced myocardial fibrosis compared to untreated diabetic controls. Whether the reduced myocardial fibrosis in FTY720-treated mice was a consequence of reduced CA atherothrombosis or direct effects of FTY720 on myocardial fibrosis in not clear. FTY720-treated mice exhibited only slightly reduced numbers of completely occluded CAs, but more striking reductions in the numbers of occluded CAs positive for platelet CD41 staining, suggesting that while FTY720 did not substantially reduce the burden of CA atherosclerosis, it may have more strongly attenuated thrombosis in atherosclerotic CAs. FTY720 has been reported to directly influence cardiac fibrosis by reducing periostin production and cardiomyocyte nuclear factor of activated T-cells (NFAT) signaling (58), suggesting that this may have contributed to the reduced myocardial fibrosis observed in the FTY720-treated mice. Despite these protective effects, FTY720 treatment did not extend the survival of HFC diet-fed, diabetic SR-B1 KO/apoE-hypo mice. Thus the degree of reduction of CA

disease and myocardial infarction in the FTY720-treated diabetic mice was not sufficient to extend their survival, suggesting either factors other than CA occlusion and myocardial fibrosis contribute to reduced lifespan, or that the burden of CAD was still sufficiently high to be fatal. A recent paper reported that treatment of non-diabetic SR-B1 KO/apoE-hypo mice with FTY720 at a lower dose (0.05 mg/kg/d) than we used in this study, resulted in no atheroprotection but improved left ventricular function and extended the survival of the mice (37). It is possible that FTY720-treatment is able to extend the survival of normoglycemic (as in (37)) but not diabetic SR-B1 KO/apoE-hypo mice (analyzed herein). Alternatively it is possible that the higher dose of FTY720 that we used, exerted as yet uncharacterized negative effects that may have counteracted the beneficial effects on atherothrombosis and myocardial fibrosis; in this respect, Raffai and co-workers reported in their studies that treatment of SR-B1 KO/apoE-hypo mice with a dose of FTY720 equivalent to the one we used resulted in extensive mortality (37). Further experiments are required to understand the lack of effect of FTY720-treatment on survival of the diabetic HFC diet-fed SR-B1 KO/apoE-hypo mice in light of the reduced atherothrombosis and myocardial fibrosis.

We noted that, unexpectedly, the survival of the diabetic HFC diet-fed SR-B1 KO/apoE-hypo mice was significantly reduced when mice were given water via water bottles compared to those that received automatic watering (Supplementary Figure 2.9). This is reminiscent of reports by Krieger and co-workers that housing conditions affected the survival of atherogenic diet-fed SR-B1 KO/apoE-hypo mice (35). Specifically, they demonstrated that SR-B1 KO/apoE-hypo mice housed singly, and fed a diet equivalent to

the one we used, exhibited considerably reduced survival compared to similarly fed mice housed in groups of 2-5 (35). For our studies, all mice were housed in groups of 2-4 to avoid confounding effects of social isolation. Further studies are required to understand why these mice exhibited reduced survival when given water bottles.

In summary, we have shown that STZ treatment-induced diabetes exacerbates HFC diet-induced atherothrombosis and myocardial fibrosis and reduced survival of SR-B1 KO/apoE-hypo mice. This may therefore represent a useful, surgery-free model of diet inducible diabetic CA disease and diabetic cardiomyopathy. We also have shown that treatment of diabetic SR-B1 KO/apoE-hypo mice with FTY720 reduced the size of atherosclerotic plaques, the degree of apoptosis in atherosclerotic plaques and the sizes of plaque necrotic cores in the aortic sinus, the accumulation of platelets in atherosclerotic CAs as well as the degree of myocardial fibrosis, but did not extend the survival of the diabetic mice. FTY720 is an agonist for multiple S1P receptor types. Future studies, including the use of more specific S1P receptor agonists, will examine the contribution of specific S1P receptors to protection against diet-induced atherothrombosis and cardiac fibrosis in diabetic SR-B1 KO/apoE-hypo mice.

2.6 References

1. de Ferranti SD, de Boer IH, Fonseca V, Fox CS, Golden SH, Lavie CJ, Magge SN, Marx N, McGuire DK, Orchard TJ, Zinman B, Eckel RH: Type 1 diabetes mellitus and cardiovascular disease: a scientific statement from the American Heart Association and American Diabetes Association. *Circulation* **130**:1110-1130, 2014.

2. Secrest AM, Becker DJ, Kelsey SF, Laporte RE, Orchard TJ: Cause-specific mortality trends in a large population-based cohort with long-standing childhood-onset type 1 diabetes. *Diabetes* **59**:3216-3222, 2010.

3. Harrington J, Pena AS, Gent R, Hirte C, Couper J: Aortic intima media thickness is an early marker of atherosclerosis in children with type 1 diabetes mellitus. *J Pediatr* **156**:237-241, 2010.

4. Libby P, Ridker PM, Hansson GK: Progress and challenges in translating the biology of atherosclerosis. *Nature* **473**:317-325, 2011.

5. Tariq SM, Sidhu MS, Toth PP, Boden WE: HDL hypothesis: where do we stand now? *Curr Atheroscler Rep* **16**:398, 2014.

6. Akinkuolie AO, Paynter NP, Padmanabhan L, Mora S: High-density lipoprotein particle subclass heterogeneity and incident coronary heart disease. *Circ Cardiovasc Qual Outcomes* **7**:55-63, 2014.

7. Zanoni P, Khetarpal SA, Larach DB, Hancock-Cerutti WF, Millar JS, Cuchel M, DerOhannessian S, Kontush A, Surendran P, Saleheen D, Trompet S, Jukema JW, De Craen A, Deloukas P, Sattar N, Ford I, Packard C, Majumder A, Alam DS, Di Angelantonio E, Abecasis G, Chowdhury R, Erdmann J, Nordestgaard BG, Nielsen SF, Tybjaerg-Hansen A, Schmidt RF, Kuulasmaa K, Liu DJ, Perola M, Blankenberg S, Salomaa V, Mannisto S, Amouyel P, Arveiler D, Ferrieres J, Muller-Nurasyid M, Ferrario M, Kee F, Willer CJ, Samani N, Schunkert H, Butterworth AS, Howson JM, Peloso GM, Stitziel NO, Danesh J, Kathiresan S, Rader DJ, Consortium CHDE, Consortium CAE, Global Lipids Genetics C: Rare variant in scavenger receptor BI raises HDL cholesterol and increases risk of coronary heart disease. *Science* **351**:1166-1171, 2016.

8. Poti F, Simoni M, Nofer JR: Atheroprotective role of high-density lipoprotein (HDL)-associated sphingosine-1-phosphate (S1P). *Cardiovasc Res* **103**:395-404, 2014.

9. Bolick DT, Srinivasan S, Kim KW, Hatley ME, Clemens JJ, Whetzel A, Ferger N, Macdonald TL, Davis MD, Tsao PS, Lynch KR, Hedrick CC: Sphingosine-1-phosphate prevents tumor necrosis factor-{alpha}-mediated monocyte adhesion to aortic endothelium in mice. *Arterioscler Thromb Vasc Biol* **25**:976-981, 2005.

10. Kimura T, Tomura H, Mogi C, Kuwabara A, Damirin A, Ishizuka T, Sekiguchi A, Ishiwara M, Im DS, Sato K, Murakami M, Okajima F: Role of scavenger receptor class B type I and sphingosine 1-phosphate receptors in high density lipoprotein-induced

inhibition of adhesion molecule expression in endothelial cells. *J Biol Chem* **281**:37457-37467, 2006.

11. Kimura T, Sato K, Malchinkhuu E, Tomura H, Tamama K, Kuwabara A, Murakami M, Okajima F: High-density lipoprotein stimulates endothelial cell migration and survival through sphingosine 1-phosphate and its receptors. *Arterioscler Thromb Vasc Biol* **23**:1283-1288, 2003.

12. Tamama K, Tomura H, Sato K, Malchinkhuu E, Damirin A, Kimura T, Kuwabara A, Murakami M, Okajima F: High-density lipoprotein inhibits migration of vascular smooth muscle cells through its sphingosine 1-phosphate component. *Atherosclerosis* **178**:19-23, 2005.

13. Damirin A, Tomura H, Komachi M, Liu JP, Mogi C, Tobo M, Wang JQ, Kimura T, Kuwabara A, Yamazaki Y, Ohta H, Im DS, Sato K, Okajima F: Role of lipoprotein-associated lysophospholipids in migratory activity of coronary artery smooth muscle cells. *Am J Physiol Heart Circ Physiol* **292**:H2513-2522, 2007.

14. Sattler KJ, Elbasan S, Keul P, Elter-Schulz M, Bode C, Graler MH, Brocker-Preuss M, Budde T, Erbel R, Heusch G, Levkau B: Sphingosine 1-phosphate levels in plasma and HDL are altered in coronary artery disease. *Basic Res Cardiol* **105**:821-832, 2010.

15. Sattler K, Lehmann I, Graler M, Brocker-Preuss M, Erbel R, Heusch G, Levkau B: HDL-bound sphingosine 1-phosphate (S1P) predicts the severity of coronary artery atherosclerosis. *Cell Physiol Biochem* **34**:172-184, 2014.

16. Qi Y, Chen J, Lay A, Don A, Vadas M, Xia P: Loss of sphingosine kinase 1 predisposes to the onset of diabetes via promoting pancreatic beta-cell death in diet-induced obese mice. *FASEB J* **27**:4294-4304, 2013.

17. Yanagawa Y, Sugahara K, Kataoka H, Kawaguchi T, Masubuchi Y, Chiba K: FTY720, a novel immunosuppressant, induces sequestration of circulating mature lymphocytes by acceleration of lymphocyte homing in rats. II. FTY720 prolongs skin allograft survival by decreasing T cell infiltration into grafts but not cytokine production in vivo. *J Immunol* **160**:5493-5499, 1998.

18. Pinschewer DD, Ochsenbein AF, Odermatt B, Brinkmann V, Hengartner H, Zinkernagel RM: FTY720 immunosuppression impairs effector T cell peripheral homing without affecting induction, expansion, and memory. *J Immunol* **164**:5761-5770, 2000.

19. Nofer JR, Bot M, Brodde M, Taylor PJ, Salm P, Brinkmann V, van Berkel T, Assmann G, Biessen EA: FTY720, a synthetic sphingosine 1 phosphate analogue, inhibits development of atherosclerosis in low-density lipoprotein receptor-deficient mice. *Circulation* **115**:501-508, 2007.

20. Keul P, Tolle M, Lucke S, von Wnuck Lipinski K, Heusch G, Schuchardt M, van der Giet M, Levkau B: The sphingosine-1-phosphate analogue FTY720 reduces atherosclerosis in apolipoprotein E-deficient mice. *Arterioscler Thromb Vasc Biol* **27**:607-613, 2007.

21. Kurano M, Hara M, Tsuneyama K, Sakoda H, Shimizu T, Tsukamoto K, Ikeda H, Yatomi Y: Induction of insulin secretion by apolipoprotein M, a carrier for sphingosine 1-phosphate. *Biochim Biophys Acta* **1841**:1217-1226, 2014.

22. Moon H, Chon J, Joo J, Kim D, In J, Lee H, Park J, Choi J: FTY720 preserved islet beta-cell mass by inhibiting apoptosis and increasing survival of beta-cells in db/db mice. *Diabetes Metab Res Rev* **29**:19-24, 2013.

23. Xu H, Jin Y, Ni H, Hu S, Zhang Q: Sphingosine-1-phosphate receptor agonist, FTY720, restores coronary flow reserve in diabetic rats. *Circ J* **78**:2979-2986, 2014.

24. Park L, Raman KG, Lee KJ, Lu Y, Ferran LJ, Jr., Chow WS, Stern D, Schmidt AM: Suppression of accelerated diabetic atherosclerosis by the soluble receptor for advanced glycation endproducts. *Nat Med* **4**:1025-1031, 1998.

25. Werstuck GH, Khan MI, Femia G, Kim AJ, Tedesco V, Trigatti B, Shi Y: Glucosamine-induced endoplasmic reticulum dysfunction is associated with accelerated atherosclerosis in a hyperglycemic mouse model. *Diabetes* **55**:93-101, 2006.

26. Trigatti BL, Fuller M: HDL signaling and protection against coronary artery atherosclerosis in mice. *J Biomed Res* **30**2015.

27. Rigotti A, Trigatti BL, Penman M, Rayburn H, Herz J, Krieger M: A targeted mutation in the murine gene encoding the high density lipoprotein (HDL) receptor scavenger receptor class B type I reveals its key role in HDL metabolism. *Proc Natl Acad Sci U S A* **94**:12610-12615, 1997.

28. Trigatti B, Rayburn H, Vinals M, Braun A, Miettinen H, Penman M, Hertz M, Schrenzel M, Amigo L, Rigotti A, Krieger M: Influence of the high density lipoprotein receptor SR-BI on reproductive and cardiovascular pathophysiology. *Proc Natl Acad Sci U S A* **96**:9322-9327, 1999.

29. Braun A, Trigatti BL, Post MJ, Sato K, Simons M, Edelberg JM, Rosenberg RD, Schrenzel M, Krieger M: Loss of SR-BI expression leads to the early onset of occlusive atherosclerotic coronary artery disease, spontaneous myocardial infarctions, severe cardiac dysfunction, and premature death in apolipoprotein E-deficient mice. *Circ Res* **90**:270-276, 2002.

30. Fuller M, Dadoo O, Serkis V, Abutouk D, MacDonald M, Dhingani N, Macri J, Igdoura SA, Trigatti BL: The effects of diet on occlusive coronary artery atherosclerosis and myocardial infarction in scavenger receptor class B, type 1/low-density lipoprotein receptor double knockout mice. *Arterioscler Thromb Vasc Biol* **34**:2394-2403, 2014.

31. Covey SD, Krieger M, Wang W, Penman M, Trigatti BL: Scavenger receptor class B type I-mediated protection against atherosclerosis in LDL receptor-negative mice involves its expression in bone marrow-derived cells. *Arterioscler Thromb Vasc Biol* **23**:1589-1594, 2003.

32. Raffai RL, Dong LM, Farese RV, Jr., Weisgraber KH: Introduction of human apolipoprotein E4 "domain interaction" into mouse apolipoprotein E. *Proc Natl Acad Sci U S A* **98**:11587-11591, 2001.

33. Raffai RL, Weisgraber KH: Hypomorphic apolipoprotein E mice: a new model of conditional gene repair to examine apolipoprotein E-mediated metabolism. *J Biol Chem* **277**:11064-11068, 2002.

34. Raffai RL, Loeb SM, Weisgraber KH: Apolipoprotein E promotes the regression of atherosclerosis independently of lowering plasma cholesterol levels. *Arterioscler Thromb Vasc Biol* **25**:436-441, 2005.

35. Nakagawa-Toyama Y, Zhang S, Krieger M: Dietary manipulation and social isolation alter disease progression in a murine model of coronary heart disease. *PLoS One* **7**:e47965, 2012.

36. Zhang S, Picard MH, Vasile E, Zhu Y, Raffai RL, Weisgraber KH, Krieger M: Diet-induced occlusive coronary atherosclerosis, myocardial infarction, cardiac dysfunction,

and premature death in scavenger receptor class B type I-deficient, hypomorphic apolipoprotein ER61 mice. *Circulation* **111**:3457-3464, 2005.

37. Wang G, Kim RY, Imhof I, Honbo N, Luk FS, Li K, Kumar N, Zhu BQ, Eberle D, Ching D, Karliner JS, Raffai RL: The immunosuppressant FTY720 prolongs survival in a mouse model of diet-induced coronary atherosclerosis and myocardial infarction. *J Cardiovasc Pharmacol* **63**:132-143, 2014.

38. Al-Jarallah A, Igdoura F, Zhang Y, Tenedero CB, White EJ, MacDonald ME, Igdoura SA, Trigatti BL: The effect of pomegranate extract on coronary artery atherosclerosis in SR-BI/APOE double knockout mice. *Atherosclerosis* **228**:80-89, 2013.

39. Eguchi M, Xu G, Li RK, Sweeney G: Diabetes influences cardiac extracellular matrix remodelling after myocardial infarction and subsequent development of cardiac dysfunction. *J Cell Mol Med* **16**:2925-2934, 2012.

40. Eguchi M, Kim YH, Kang KW, Shim CY, Jang Y, Dorval T, Kim KJ, Sweeney G: Ischemia-reperfusion injury leads to distinct temporal cardiac remodeling in normal versus diabetic mice. *PLoS One* **7**:e30450, 2012.

41. Pei Y, Chen X, Aboutouk D, Fuller MT, Dadoo O, Yu P, White EJ, Igdoura SA, Trigatti BL: SR-BI in bone marrow derived cells protects mice from diet induced coronary artery atherosclerosis and myocardial infarction. *PLoS One* **8**:e72492, 2013.

42. Chait A, Bornfeldt KE: Diabetes and atherosclerosis: is there a role for hyperglycemia? *J Lipid Res* **50 Suppl**:S335-339, 2009.

43. Klingenberg R, Nofer JR, Rudling M, Bea F, Blessing E, Preusch M, Grone HJ, Katus HA, Hansson GK, Dengler TJ: Sphingosine-1-phosphate analogue FTY720 causes lymphocyte redistribution and hypercholesterolemia in ApoE-deficient mice. *Arterioscler Thromb Vasc Biol* **27**:2392-2399, 2007.

44. Poti F, Costa S, Bergonzini V, Galletti M, Pignatti E, Weber C, Simoni M, Nofer JR: Effect of sphingosine 1-phosphate (S1P) receptor agonists FTY720 and CYM5442 on atherosclerosis development in LDL receptor deficient (LDL-R(-)/(-)) mice. *Vascul Pharmacol* **57**:56-64, 2012.

45. Hwang MW, Matsumori A, Furukawa Y, Ono K, Okada M, Iwasaki A, Hara M, Sasayama S: FTY720, a new immunosuppressant, promotes long-term graft survival and inhibits the progression of graft coronary artery disease in a murine model of cardiac transplantation. *Circulation* **100**:1322-1329, 1999.

46. Han S, Liang CP, DeVries-Seimon T, Ranalletta M, Welch CL, Collins-Fletcher K, Accili D, Tabas I, Tall AR: Macrophage insulin receptor deficiency increases ER stress-induced apoptosis and necrotic core formation in advanced atherosclerotic lesions. *Cell Metab* **3**:257-266, 2006.

47. Li S, Sun Y, Liang CP, Thorp EB, Han S, Jehle AW, Saraswathi V, Pridgen B, Kanter JE, Li R, Welch CL, Hasty AH, Bornfeldt KE, Breslow JL, Tabas I, Tall AR: Defective phagocytosis of apoptotic cells by macrophages in atherosclerotic lesions of ob/ob mice and reversal by a fish oil diet. *Circ Res* **105**:1072-1082, 2009.

48. Tao H, Yancey PG, Babaev VR, Blakemore JL, Zhang Y, Ding L, Fazio S, Linton MF: Macrophage SR-BI mediates efferocytosis via Src/PI3K/Rac1 signaling and reduces atherosclerotic lesion necrosis. *J Lipid Res* **56**:1449-1460, 2015.

49. Al-Jarallah A, Chen X, Gonzalez L, Trigatti BL: High density lipoprotein stimulated migration of macrophages depends on the scavenger receptor class B, type I, PDZK1 and Akt1 and is blocked by sphingosine 1 phosphate receptor antagonists. *PLoS One* **9**:e106487, 2014.

50. Blom T, Back N, Mutka AL, Bittman R, Li Z, de Lera A, Kovanen PT, Diczfalusy U, Ikonen E: FTY720 stimulates 27-hydroxycholesterol production and confers atheroprotective effects in human primary macrophages. *Circ Res* **106**:720-729, 2010.

51. Silva JA, Escobar A, Collins TJ, Ramee SR, White CJ: Unstable angina. A comparison of angioscopic findings between diabetic and nondiabetic patients. *Circulation* **92**:1731-1736, 1995.

52. Siewiera K, Kassassir H, Talar M, Wieteska L, Watala C: Long-term untreated streptozotocin-diabetes leads to increased expression and elevated activity of prostaglandin H synthase in blood platelets. *Platelets*:1-9, 2015.

53. Stolla MC, Li D, Lu L, Woulfe DS: Enhanced platelet activity and thrombosis in a murine model of type I diabetes are partially insulin-like growth factor 1-dependent and phosphoinositide 3-kinase-dependent. *J Thromb Haemost* **11**:919-929, 2013.

54. Mineo C, Yuhanna IS, Quon MJ, Shaul PW: High density lipoprotein-induced endothelial nitric-oxide synthase activation is mediated by Akt and MAP kinases. *J Biol Chem* **278**:9142-9149, 2003.

55. Zhang Q, Yin H, Liu P, Zhang H, She M: Essential role of HDL on endothelial progenitor cell proliferation with PI3K/Akt/cyclin D1 as the signal pathway. *Exp Biol Med (Maywood)* **235**:1082-1092, 2010.

56. Kerr BA, Ma L, West XZ, Ding L, Malinin NL, Weber ME, Tischenko M, Goc A, Somanath PR, Penn MS, Podrez EA, Byzova TV: Interference with akt signaling protects against myocardial infarction and death by limiting the consequences of oxidative stress. *Sci Signal* **6**:ra67, 2013.

57. Greer JJ, Ware DP, Lefer DJ: Myocardial infarction and heart failure in the db/db diabetic mouse. *Am J Physiol Heart Circ Physiol* **290**:H146-153, 2006.

58. Liu W, Zi M, Tsui H, Chowdhury SK, Zeef L, Meng QJ, Travis M, Prehar S, Berry A, Hanley NA, Neyses L, Xiao RP, Oceandy D, Ke Y, Solaro RJ, Cartwright EJ, Lei M, Wang X: A novel immunomodulator, FTY-720 reverses existing cardiac hypertrophy and fibrosis from pressure overload by targeting NFAT (nuclear factor of activated T-cells) signaling and periostin. *Circ Heart Fail* **6**:833-844, 2013.

2.7 Supplementary materials

Supplementary Figure 2.6: Effect of STZ treatment in the pancreas of SR-B1 KO/apoE-hypo mice

Five week old male SR-B1 KO/apoE-hypo mice received two rounds of STZ (40 mg/Kg of body weight) as described in Materials and Methods and Figures 2.1A and 2.3A. After 4 weeks of HFC diet feeding (as in Figures 2.1 and 2.3), mice were euthanized. Pancreas tissue was embedded in paraffin and 4 μm sections were generated and stained with a primary antibody against insulin (Novus Biologicals, cat#182410), followed by a secondary antibody conjugated with Alexa Flour 488 (Life technologies, cat#A-11006) and DAPI. Representative images of pancreatic islets in sections from a control-treated (A-C) and an STZ-treated (D-F) mouse. **A,D**. DAPI staining for control pancreas. **B,E**. Insulin staining for control pancreas. **C,F**. Merge color images showing DAPI (blue) and insulin (green). Scale bar: 50 μm (20 x objective).

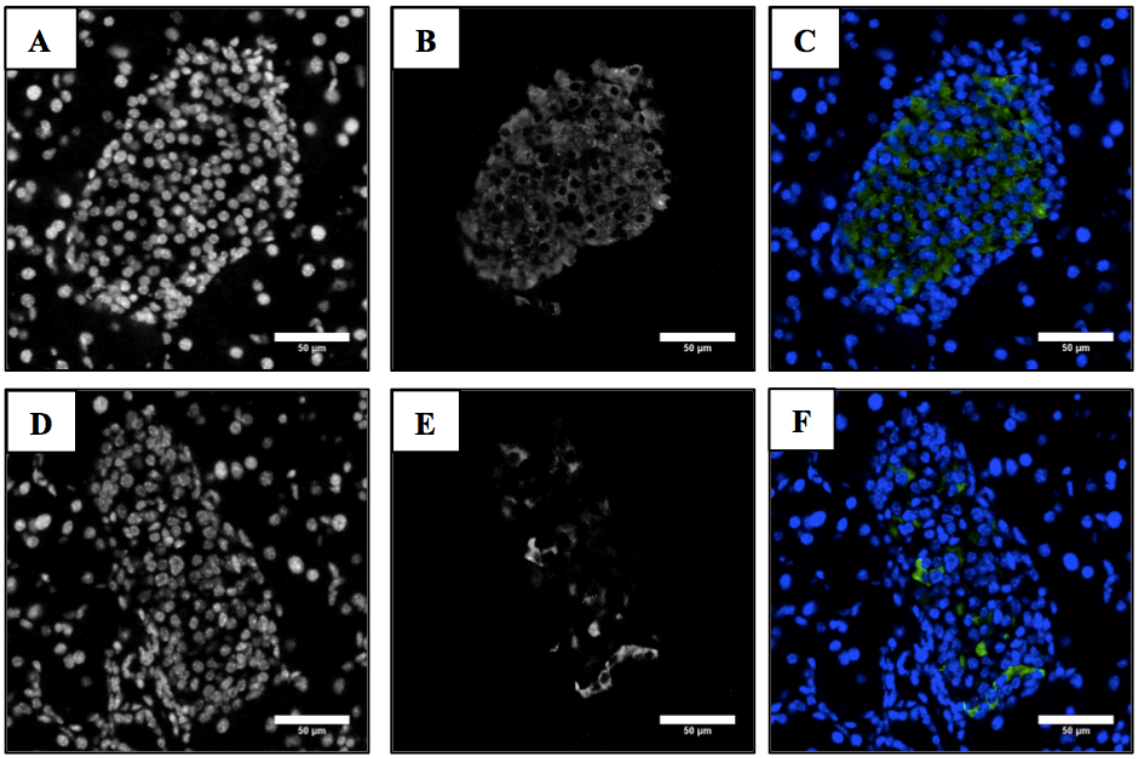
A
B
C
D
E
F
50 µm

Supplementary Figure 2.7: Effect of STZ administration on plasma glucose levels and survival in SR-B1 KO/apoE-hypo mice fed a normal chow diet

A. Male, 8 week old mice were treated with 2 rounds of 5 daily injections (with a rest weeks in between) of STZ (40 mg/kg BW/day in citrate buffer) or an equal volume of control citrate buffer intraperitoneally as described in Materials and Methods. Mice were maintained on a chow diet for 11 weeks before they were euthanized and tissues harvested. **B**. Plasma glucose was monitored weekly. Results are presented as mean ± SEM (n=6-7mice per group). ***$p<0.0001$ vs control, two-way ANOVA. **C.** Survival curve (100% survival for both groups).

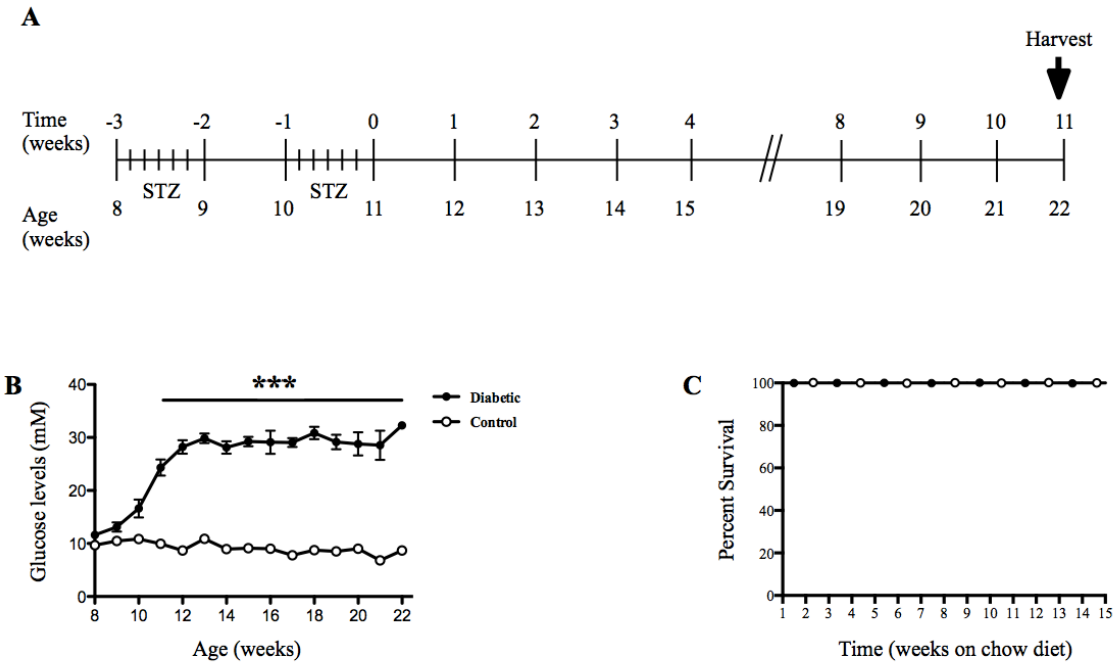
A
Harvest
Time (weeks)
-3 -2 -1 0 1 2 3 4 8 9 10 11
STZ
STZ
Age (weeks)
8 9 10 11 12 13 14 15 19 20 21 22
B
***
Diabetic
Control
Glucose levels (mM)
0 10 20 30 40
8 10 12 14 16 18 20 22
Age (weeks)
C
Percent Survival
0 20 40 60 80 100
1 2 3 4 5 6 7 8 9 10 11 12 13 14 15
Time (weeks on chow diet)

Supplementary Figure 2.8: Effect of STZ administration on aortic sinus and CA atherosclerosis in SR-B1 KO/apoE-hypo mice fed a normal chow diet

Normal chow diet fed mice were euthanized at 22 weeks of age, 14 weeks after the start of STZ treatment as described in the legend to Supplementary Figure 2.7. Representative images of oil red O/hematoxylin stained aortic sinus sections from **A.** a control mouse that received citrate buffer and **B.** an STZ-treated (diabetic) mouse. **C.** Quantification of aortic sinus atherosclerotic plaque cross sectional area (scale bar=100 μm, 5 x objective; n=6-7 mice per group). *$p<0.05$ vs Control, Mann Whitney U test. **D.** CA atherosclerosis assessed as the proportions of CAs in cross sections through the heart, with different levels of occlusion by atherosclerotic plaques, as described in the Materials and Methods section and the legends to Figure 2.2 and 2.4. Controls mice treated with citrate buffer (white bars); STZ-treated diabetic mice (black bars). Results are presented as mean ± SEM (n=6-7 mice per group); **$p<0.01$ vs Control, two-way ANOVA.

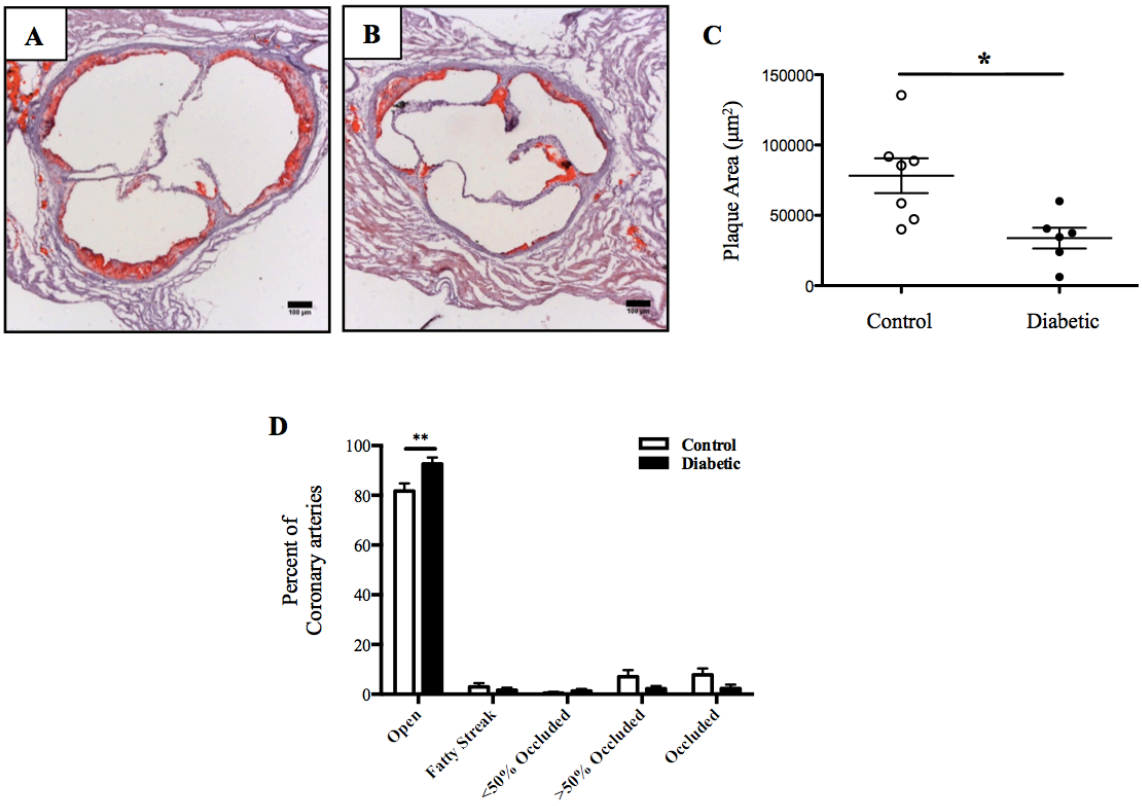
A
B
C
Plaque Area (µm²)
150000
100000
50000
0
*
Control
Diabetic
D
Percent of Coronary arteries
100
80
60
40
20
0
**
Control
Diabetic
Open
Fatty Streak
<50% Occluded
>50% Occluded
Occluded

Supplementary Figure 2.9: Comparison of survival curves for STZ-treated SR-B1 KO/apoE-hypo mice maintained on automatic watering versus given water in bottles

Kaplan-Meier survival curves for SR-B1 KO/apoE-hypo mice treated with STZ and maintained on an automated watering system (open circles) or given water in bottles (solid circles). Male 5 week old mice were treated with STZ as described in the legends to figures 2.1A and 2.3A and were put on HFC diet at 8 weeks of age. Survival to humane endpoint is plotted as the time (weeks) on the HFC diet. Mice were fed an HFC diet until endpoint. Data are replotted from figures 2.1A and 2.3A. *p<0.05 Log-rank test.

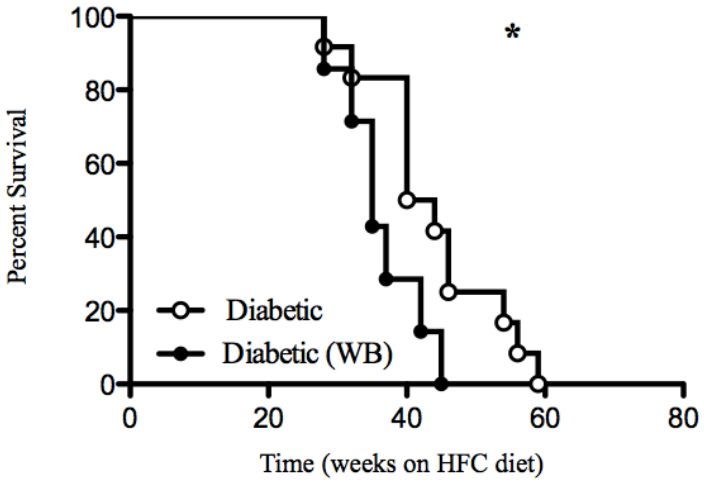

Supplementary Figure 2.10: Heart weights, body weights and heart weight:body weight ratios of control, STZ and FTY720-treated SR-B1 KO/apoE-hypo mice fed the HFC diet for 4 weeks

Male, 5 week old SR-B1 KO/apoE-hypo mice were treated (**A-C**) with STZ or control citrate buffer or (**D-F**) with STZ along with either control water or water containing FTY720 and placed on HFC diet for 4 weeks as described in Figures 2.1A and 2.3A, respectively. At harvest, heart weights (**A, D**) and body weights (**B, E**) were measured and heart weight/body weight ratios were determined (**C-F**). N=14-15 mice per group; *$p<0.05$, Student's T test.

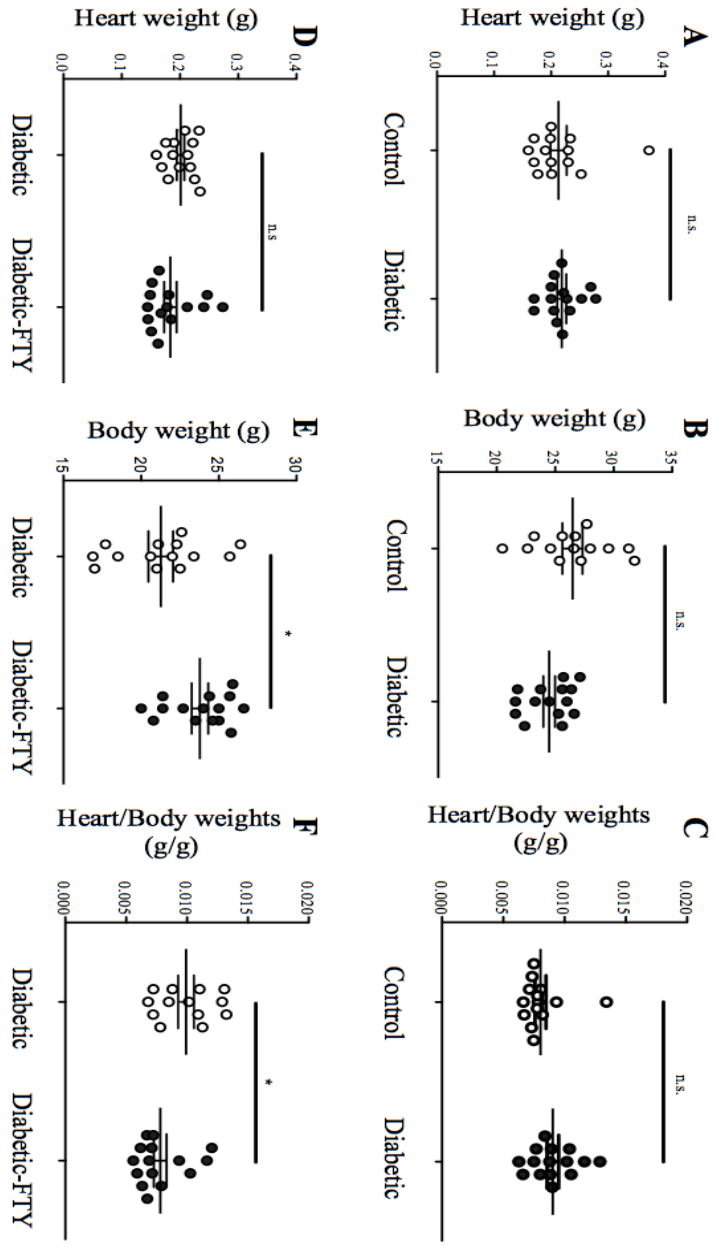
A
Heart weight (g)
0.0
0.1
0.2
0.3
0.4
n.s.
Control
Diabetic
B
Body weight (g)
15
20
25
30
35
n.s.
Control
Diabetic
C
Heart/Body weights (g/g)
0.000
0.005
0.010
0.015
0.020
n.s.
Control
Diabetic
D
Heart weight (g)
0.0
0.1
0.2
0.3
0.4
n.s
Diabetic
Diabetic-FTY
E
Body weight (g)
15
20
25
30
*
Diabetic
Diabetic-FTY
F
Heart/Body weights (g/g)
0.000
0.005
0.010
0.015
0.020
*
Diabetic
Diabetic-FTY

Chapter 3

Macrophage S1PR1 plays an important role in HDL protection against apoptosis and necrotic core formation in atherosclerotic plaque development

Author list: Leticia Gonzalez, Usama Tahir, Pei Yu, Melissa MacDonald and Bernardo L. Trigatti.

Foreword

This manuscript explores in more depth the role of S1P receptor signaling in atherosclerosis development, specifically the role of the macrophage S1PR1 in disease progression and cell survival. We show that activation of the S1PR1 axis in macrophages effectively prevents apoptosis under stress conditions in a PI3K/AKT dependent manner. S1PR1 deficiency in the macrophages also negatively impacted the ability of HDL to prevent macrophage apoptosis, suggesting that the S1P/S1PR1 axis is required for HDL-mediated protection. In the context of atherosclerosis progression, macrophage S1PR1 deficiency was associated with an increase in atherosclerotic plaque development and necrotic core formation in the aortic sinus atherosclerotic plaque at early stages. The increase in necrotic core formation was also associated with increased atherosclerotic

plaque apoptosis, suggesting that the S1PR1 might play an important role in preventing transition towards unstable plaques.

This manuscript will be submitted for publication in mid 2016. Experiments were designed by Leticia Gonzalez with guidance by Bernardo L. Trigatti. All *in vitro* data was collected and analyzed by Leticia Gonzalez. All animal procedures were done by Leticia Gonzalez. Melissa MacDonald assisted in animal care. Pei Yu assisted with the bone marrow transplantation procedure. Usama Tahir contributed to the collection of atherosclerosis and plasma data of the 9 weeks on high fat diet cohort and a portion of the 12 weeks high fat diet cohort. All atherosclerotic plaque TUNEL data and the remaining of the atherosclerosis and plasma data for the 12 weeks cohort was collected by Leticia Gonzalez. All data was analyzed and interpreted by Leticia Gonzalez under the guidance of Bernardo L. Trigatti. The manuscript was written by Leticia Gonzalez with guidance from Bernardo L. Trigatti.

3.1 Abstract

Objective: Sphingosine-1-phosphate has been identified as a factor that contributes to the atheroprotective function of high-density lipoproteins. Recently we demonstrated that sphingosine-1-phosphate receptor 1 (S1PR1) mediates high-density lipoprotein-induced macrophage migration. However the role of the S1PR1 in apoptosis and atherogenesis has yet to be explored.

Methods and results: To test if macrophage S1PR1 is involved in protection against apoptosis and atherosclerotic plaque development, we generated mice with myeloid specific inactivation of the gene encoding S1PR1. For *in vivo* studies, we performed bone marrow transplantation into LDLR KO mice and atherosclerosis was induced through high fat diet feeding. Activation of the macrophage S1PR1 protected macrophages against apoptosis signaling through the PI3K/AKT pathway. Absence of the S1PR1 also impaired the ability of high-density lipoprotein to protect cells against apoptosis suggesting that activation of the sphingosine-1-phosphate axis is required for high-density lipoprotein to function in macrophages. When translated into the context of atherosclerosis disease, absence of the S1PR1 resulted in the development of larger plaques with bigger necrotic cores. A significant increase in the plaque apoptosis in the context of S1PR1-deficient macrophages indicates that the receptor might play an important role in preventing the transition to unstable plaques.

Conclusion: In summary, our data suggests that macrophage S1PR1 is an important factor in high-density lipoprotein protection against apoptosis and a potential target in future therapies preventing atherosclerosis development.

Key words: Sphingosine; Sphingosine 1-phosphate receptor 1; atherosclerosis; macrophages; apoptosis.

3.2 Introduction

Atherosclerosis is a chronic inflammatory disease characterized by the accumulation of lipids and inflammatory cells in the vessel wall of large- and medium-sized arteries (1). Macrophage apoptosis is considered a key step in the transition from stable to unstable plaques, which are more prone to rupture and associated with myocardial infarction and stroke (2; 3). Studies have suggested that accumulation of apoptotic cells resulting from both increased apoptosis and defective clearance of apoptotic cells are directly implicated in necrotic core formation and plaque instability (4). Oxidative modification of the low-density lipoprotein (LDL) is a critical step in disease initiation and progression (5). Oxidized LDL (oxLDL) exhibits a wide array of pro-atherogenic properties: it promotes monocyte recruitment and limits their egress from the arterial wall (6) and it also promotes macrophage apoptosis which can lead to necrotic core formation (7). The accumulation of unesterified cholesterol in the endoplasmic reticulum (ER) of foam cells disrupts normal ER function, inducing ER-stress and macrophage apoptosis through

mechanisms involving prolonged activation of the unfolded protein response and overexpression of the transcription factor CCAAT-enhancer binding protein homologous protein (CHOP) (8).

High-density lipoprotein (HDL) protects against atherosclerosis development at least in part through the scavenger receptor class B, type 1 (SR-B1) (9). SR-B1 deficiency in mouse models of atherosclerosis accelerates the development of atherosclerosis (10-12). The absence of SR-B1 in bone marrow-derived cells also accelerates the development of atherosclerosis in LDL receptor (LDLR) knockout (KO) and apolipoprotein E (apoE) KO mice, suggesting the importance of SR-B1 expression in macrophages for atheroprotection (13; 14). HDL mediates a variety of atheroprotective effects including reverse cholesterol transport from the artery wall to the liver, anti-oxidative, anti-inflammatory and anti-apoptosis, in a number of tissues and cell types (15). These functions have been associated with the different components found in the HDL. For example, Fuhrman and colleagues have shown that in mice, deficiency of paraoxonase-1, an anti-oxidant enzyme found in HDL, leads to a reduction in macrophage SR-B1 expression and the consequent loss of HDL-mediated protection against apoptosis (16). Another component reportedly contributing to HDL's protective properties is sphingosine-1-phosphate (S1P).

S1P is a zwitterionic lysophospholipid, carried by HDL in circulation, essential for regulation of proliferation, migration, survival and vascular development (17-20). The intracellular balance between S1P/ceramide in the so-called S1P rheostat is at the center of the decision between cell death and survival (17). Most effects triggered by S1P

involve the activation of one of its 5 receptors. S1P receptors (S1PR) 1-5 are G-protein coupled receptors with different patterns of expression throughout different cell types (21). Murine macrophages have been reported to express receptors 1 to 4 (22). S1P has been described to protect macrophages from apoptosis, to modulate macrophage trafficking and also to favor an anti-inflammatory phenotype (23).

In the context of atherosclerosis, studies have shown that FTY720, an agonist of S1PR1 and S1PR 3-5, can protect against LDLR KO and apoE KO mice against atherosclerosis development in some studies (24; 25) but not in others (26). FTY720 has also been shown to decrease cholesterol toxicity in human macrophages by reducing the delivery of cholesterol to the ER and facilitating its release to extracellular acceptors (27). Furthermore, activation of the S1PR1 in endothelial cells reduces TNF-α induced expression of the vascular cell adhesion molecule-1 (VCAM-1) and the intercellular adhesion molecule 1 (ICAM-1) and the adhesion of monocytes to tumor necrosis factor α (TNF-α)-activated endothelial cells (28). HDL-mediated inhibition of adhesion molecule expression in endothelial cells was shown to be dependent on the activation of both SR-B1 and S1PR1, suggesting that SR-B1 and S1P might mediate HDL's effects in a concerted fashion (29). Similarly, we have shown that HDL, FTY720 and the S1PR1 specific agonist SEW2871 were each able to induce migration of macrophages *in vitro* and that S1PR1-selective antagonists could block HDL-induced macrophage migration, suggesting that S1PR1 was required for HDL signaling in macrophages (30).

In this study, we set out to test the hypothesis that S1PR1 in macrophages protects against atherosclerosis development *in vivo* in LDLR KO mice. We found that treatment

with S1PR1 selective agonists protects macrophages against apoptosis through a mechanisms involving activation of the phosphoinositide 3-kinase (PI3K)/AKT pathway, and that these effects were lost when S1PR1 was selectively inactivated in macrophages. Likewise, HDL treatment protected macrophages from apoptosis and this was also lost when S1PR1 was inactivated. Finally, we demonstrated that macrophage S1PR1 deficiency significantly increased early atherosclerosis development and necrotic core formation in LDLR KO mice fed a high fat diet. The increase in necrotic core size was accompanied by a significant increase in apoptosis in the atherosclerotic plaques in mice lacking S1PR1 in macrophages.

3.3 Materials and methods

3.3.1 Materials

SEW2871 and tunicamycin were purchased from Cayman Chemicals (Ann Arbor, Michigan, USA). OxLDL and HDL were purchased from Alfa Aesar (Ward Hill, MA, USA). LY294002 (PI3K inhibitor) was purchased from Biovision inc. (Milpitas, CA, USA). AKT inhibitor V (triciribine) was purchased from Millipore Corporation Canada (Etobicoke, ON, Canada). All other chemicals were purchased from Sigma Aldrich (St. Louis, Missouri, USA) unless indicated otherwise.

3.3.2 Mice

All procedures involving animals were approved by the McMaster University Animal Research Ethics Board and were in accordance with guidelines of the Canadian Council of Animal Care. All animals were bred and housed in vented cages at the Thrombosis and Atherosclerosis Research Institute animal facility at McMaster University under controlled light (12 hours light/dark cycle) and temperature conditions, and had free access to normal chow diet (Harlan Teklad TD2918, Madison, WI, USA) and automated watering. All mice were on a C57BL6/J background. LDLR KO mice and wild type C57BL/6 mice were each bred from founders from the Jackson Laboratories (Bar Harbor ME, USA). Macrophage-specific S1PR1 macrophage KO ($S1PR1^{MKO}$) mice were generated by breeding Lys2-Cre mice ($S1PR1^{wt/wt}$, Jackson laboratory) and S1PR1-floxed mice (generously provided by Professor Richard Proia, NIH/NIDDK, Maryland, USA) to homozygosity for both alleles ($Lys2^{cre/cre}$ $S1PR1^{lox/lox}$). $Lys2^{cre/cre}$ mice (hereafter referred to as $S1PR1^{wt/wt}$) were used as controls for the $S1PR1^{MKO}$ mice.

3.3.3 Bone marrow transplantation

Bone marrow (BM) was flushed out of femurs and tibias from female $S1PR1^{wt/wt}$ and $S1PR1^{MKO}$ female mice with Iscove's Modified Dulbecco's media (Gibco, Thermo Fisher, Ottawa, ON, Canada) containing 2 % heat inactivated FBS supplemented with 2 mM L-glutamine, 50 μg/ml penicillin and 50 U/ml streptomycin. Recipient mice (LDLR

KO, 10-12 weeks old) were exposed to 1300 rad of ^{137}Cs irradiation using a Gammacel 3000/small animal irradiator (Best Theratronics, Ottawa, Canada). BM (3×10^6 cells/mouse) was injected intravenously via the tail vein. Mice were allowed to recover for 4 weeks, after which, atherosclerosis was induced by feeding a high fat, Western type (HF) diet containing 21 % butter fat and 0.15 % cholesterol (Dyets Inc. 112286) for 9 or 12 weeks. At the end of the feeding period, mice were fasted for 4 hrs prior to anesthesia and euthanasia. Heparinized blood was collected by cardiac puncture and plasma was obtained by centrifugation at 4000 rpm. Tissues were collected after in situ perfusion with 10 U/ml heparinized saline followed by 10 % formalin, immersion fixed overnight in 10 % formalin, and embedded in Shandon Cryomatrix (Thermo Fisher Scientific, Ottawa, ON, Canada). Plasma and tissues were stored at -80 C until further analysis.

3.3.4 Plasma lipids

Total cholesterol, free cholesterol, triglycerides and HDL cholesterol in plasma were measured using enzymatic assay kits according to the manufacturer's protocols (total cholesterol: Infinity Cholesterol, Thermo Fisher Scientific, Ottawa, ON, Canada; free cholesterol: Free Cholesterol E, Wako diagnostics, Mountain view, CA, USA; triglycerides: L-type triglyceride M, Wako chemicals, Richmond, VA, USA; HDL cholesterol: HDL-cholesterol E, Wako diagnostics, Mountain view, CA, USA). Non-HDL cholesterol was calculated as the difference between total cholesterol and HDL

cholesterol measurements. Cholesteryl ester levels were calculated as the difference between total cholesterol and free cholesterol measurements for each sample.

3.3.5 Histology

Hearts were fixed in formalin overnight and frozen in Shandon cryomatrix (Thermo Fisher Scientific, Ottawa, ON, Canada). Transverse cryosections of the aortic sinus (10 μm) were collected and stained with oil red O for neutral lipids. Aortic sinus atherosclerosis was measured as previously described (31) using quantitative morphometry with ImageJ software. For necrotic core size, aortic sinus cryosections were stained with hematoxylin/eosin (H&E) stain. Necrotic cores were defined as the a-cellular, a-nuclear areas within the plaque and necrotic core sizes were normalized against total plaque area. All images were collected using a Zeiss Axiovert 200M inverted microscope using bright field illumination (Carl Zeiss Canada Ltda., Toronto, ON, Canada).

3.3.6 Cell preparation, culture and treatment

For macrophage collection, mice were injected with 10% thioglycollate. At day 4 post-injection, mice were anesthetized and euthanized. Macrophages were isolated by peritoneal lavage in Phosphate-buffered saline (PBS) containing 5 mM ethylenediaminetetraacetic acid (EDTA), centrifuged at 500 x g and resuspended in

dulbecco's modified eagle medium (DMEM) supplemented with 10 % fetal bovine serum (FBS), 2 mM L-glutamine, 50 μg/ml penicillin and 50 U/ml streptomycin. All experiments evaluating apoptosis were carried out on DMEM supplemented with 3 % newborn calf lipoprotein deficient serum (NCLPDS), 2 mM L-glutamine, 50 μg/ml penicillin and 50 U/ml streptomycin. For experiments evaluating protein phosphorylation, macrophages were incubated in serum-free DMEM containing 2 mM L-glutamine, 50 μg/ml penicillin and 50 U/ml streptomycin for 1 hr prior to addition of stimuli.

3.3.7 Immunofluorescence

For *in vitro* apoptosis experiments, cells were treated with tunicamycin (TN, 10 μg/mL) or oxidized LDL (oxLDL, 100 μg/mL) in the presence or absence of SEW2871 (SEW, 1 μM) or HDL (50 μg/mL) for 24 hrs at 37 °C before fixation with freshly prepared 4 % paraformaldehyde. Apoptosis was detected by terminal deoxynucleotidyl transferase dUTP nick end labeling (TUNEL) staining, using the ApopTag-fluorescein In situ apoptosis detection kit (EDM Millipore, Etobicoke, Canada). Nuclei were counterstained with 4', 6'-diamidino-2-phenylindole (DAPI). Fluorescent images were captured using a Zeiss Axiovert 200M inverted fluorescence microscope with a 40 x objective (Carl Zeiss Canada Ltd. Toronto, ON, Canada). Apoptosis was quantified by counting the numbers of $TUNEL^+$ nuclei and total numbers of nuclei in 3 fields per well for 4-8 wells per

treatment condition and dividing the number of $TUNEL^+$/total nuclei to determine the ratio of cells that were apoptotic.

For detection of apoptosis in the atherosclerotic plaque, 10 μm cryosections of the aortic sinus were stained using the ApopTag-fluorescein In situ apoptosis detection kit (Millipore, Etobicoke, Canada) and nuclei were counterstained with DAPI as above. All images were captures using a Zeiss Axiovert 200M inverted fluorescence microscope with a 20 x objective. $TUNEL^+$ cells within the atherosclerotic plaque were counted and normalized to the atherosclerotic plaque area.

3.3.8 SDS-PAGE and immunoblotting

Cells were lysed in RIPA buffer supplemented with protease (1 mM PMSF, 1 μg/ml pepstatin A, 1 mg/ml leupeptin, 2 μg/ml aprotinin) and phosphatase (phosSTOP, Roche Diagnostics, Mannheim, Germany) inhibitors. Protein concentration was determined using the BCA protein assay kit (Pierce Biotechnology, Rockford, Illinois, USA). Proteins (30 μg) were separated by sodium dodecylsulfate-12 % acrylamide gel electrophoresis (SDS-PAGE) and electrophoretically transferred to polyvinyldifluoride membranes as previously described (32). Membranes were blocked with 5% skim milk in TBST buffer (0.1% tween-20) for 1hr at room temperature prior to incubation with rabbit anti-mouse phospho-AKT and total AKT (both from Cell Signaling Technology, Danvers, MA, USA) overnight at 4 °C overnight. After incubation, membranes were washed and incubated with horseradish peroxidase (HRP) conjugated goat anti-rabbit

secondary antibody (Jackson Immunoresearch Laboratory, West Grove, Pennsylvania, USA) for 1 hour at room temperature. HRP activity was detected using the Amersham Enhanced Chemiluminescence (ECL) kit (GE Healthcare Life Sciences Baie d'Urfe Quebec, Canada) and band intensities were measured using a Gel Doc imaging system (Bio-Rad laboratories, Hercules, California, USA).

3.3.9 Statistical analysis

Results are presented as mean ± SEM. For the *in vitro* data, significant differences among groups were evaluated by unpaired Student's T-test, one-way ANOVA followed by Newman-Keuls post-hoc test or two-way ANOVA. For the *in vivo* experiments, data was subjected to the D'Agostino & Pearson omnibus normality test prior to the selection of the appropriate statistical test. When data fit a normal distribution, the Student's T test was used for statistical analysis. If data did not fit a normal distribution, it was analyzed using the Mann Whitney U test. All data analysis was done using the PRISM software (GraphPad Software Inc, La Jolla, CA, USA). $P<0.05$ was considered to be significant.

3.4 Results

3.4.1 Effect of SEW2871, an S1PR1 agonist, in protection of macrophages against apoptosis

Apoptosis plays a crucial role in atherosclerosis development and it is critically involved in shaping plaque morphology (33). To evaluate if the activation of S1PR1 could protect macrophages against apoptosis, we collected mouse peritoneal macrophages and induced apoptosis with TN (10 μg/mL) in the presence or absence of the S1PR1 agonist SEW (1 μM). No evidence of significant increase of apoptosis was detected in macrophages treated with SEW alone compared to the vehicle control-treated macrophages (Figure 3.1A-B). When macrophages were exposed to TN, a significant increase in apoptosis levels was detected (Figure 3.1A-B). Cells co-incubated with TN in presence of SEW exhibited significantly (~40 %) reduced levels of apoptosis compared to macrophages treated with TN alone. To further confirm the ability of SEW to protect cells from apoptosis, macrophages were treated with oxLDL (100 μg/mL). OxLDL treatment significantly increased apoptosis levels compared with the control condition (Figure 3.1C). Similar to the results obtained with TN-induced apoptosis, incubation of macrophages with SEW reduced oxLDL-induced apoptosis by approximately 60 % (Figure 3.1C). Together, these results suggest that activation of the S1PR1 in macrophages protects against apoptosis induced by either the ER stress-inducing agent TN or by oxLDL.

Figure 3.1: SEW2871 protects macrophages against tunicamycin- and oxidized LDL-induced apoptosis

Thioglycollate-elicited mouse peritoneal macrophages were collected and cultured overnight in 3% NCLPDS DMEM. The next day they were incubated with either tunicamycin (TN, 10 μg/mL) or oxidized LDL (oxLDL, 100 μg/mL) in the presence or not of SEW2871 (SEW, 1 μM) for 24 hours. **A.** Cells were fixed and DNA degradation was detected by TUNEL staining (green fluorescence). Nuclei were stained using DAPI (blue). Representative images of TUNEL-stained macrophages treated with TN in the presence or absence of SEW are shown (40 x objective, scale bar: 50 μm). "UN" indicates untreated control cells (cells received equivalent amount of vehicle). **B.** Quantification of TUNEL positive cells (%) after treatment with TN in presence or not of SEW (n= 6). **C.** Quantification of TUNEL positive cells (%) after treatment with oxLDL in presence or not of SEW (n=5). Results are shown as mean ± SEM. ***$p<0.001$, **$p<0.01$.

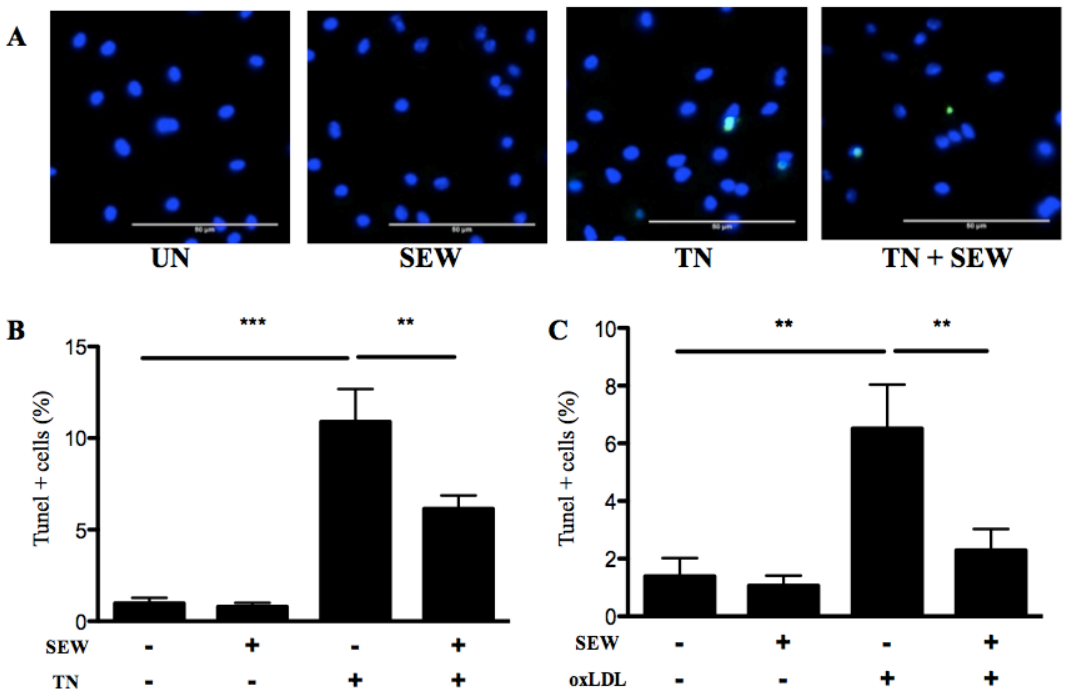
A
UN
SEW
TN
TN + SEW
B
***
**
Tunel + cells (%)
15
10
5
0
SEW - + - +
TN - - + +
C
**
**
Tunel + cells (%)
10
8
6
4
2
0
SEW - + - +
oxLDL - - + +

3.4.2 Role of the PI3K/AKT pathway in S1PR1 agonist-mediated protection against macrophage apoptosis

To test which signaling pathways might be involved in S1PR1 protection against apoptosis, WT peritoneal macrophages were incubated with S1PR1 agonists for different periods of time. We first tested the non-selective S1PR agonist, FTY720 (FTY, 1 μM). Figure 3.2A shows a representative blot and Figure 3.2B, the representative quantification of p-AKT (Ser473) in cells treated with FTY720 for different periods of time. FTY720 significantly increased AKT phosphorylation after 15 minutes of incubation. Similarly, SEW treatment also significantly, through transiently, increased the levels of AKT phosphorylation at Ser473 in macrophages after 15 minutes of incubation (Figure 3.2C-D). In both cases (FTY and SEW) the increased levels of p-AKT were transient, with levels returning back to baseline by 60 and 120 min of incubation (Figure 3.2A-D). The transient increase in p-AKT after 15 min of incubation with SEW was blocked by pre-treatment of cells with the phosphoinositidyl inositol 3-kinase (PI3K) inhibitor LY294002 (Figure 3.2E-F). To test if AKT is directly involved in SEW-mediated protection against apoptosis, WT macrophages were incubated with an AKT inhibitor (AKT V) before exposure to TN and SEW. AKT V treatment alone appeared to increase the baseline level of apoptosis, although this did not reach statistical significance (Figure 3.2G-H). As previously, TN treatment significantly increased macrophage apoptosis and treatment of macrophages with SEW protected them against TN-induced apoptosis (Figure 3.2G-H). On the other hand, macrophages that were pre-treated with the AKT inhibitor were not

protected by SEW against TN-induced apoptosis, indicating that AKT activation is required for SEW's ability to prevent apoptosis in macrophages (Figure 3.2H). Together these results suggest that activation of the S1PR1 in macrophages confers protection through activation of the PI3K/AKT pathway.

Figure 3.2: S1PR1 activation in macrophages signals through the PI3K/AKT signaling pathway to protect against apoptosis

Thioglycollate-elicited mouse peritoneal macrophages were incubated with 1 μM FTY720 or 1 μM SEW2871 for 15 minutes or the indicated periods of time in the absence or presence of the PI3K inhibitor LY294002 ("LY"). "UN" designates control cells that received vehicle alone. Proteins were collected separated by SDS-PAGE and immunoblotting for p-AKT and total AKT was carried out as described in Materials and Methods. **A, C, E.** Representative blots showing p-AKT (Ser473) and total AKT levels in cells after FTY20 (A), SEW2871 in the absence (C) or presence (E) of LY. **B, D, F.** Quantification of A (n=3), C (n=4) and E (n=3) blots respectively, where each represents an independent experiment. **G,H.** Cells were incubated with tunicamycin (TN) and SEW2871 (SEW) as in Figure 3.1, with or without the AKT inhibitor AKT V (10μM). After 24 hrs cells were fixed and stained for TUNEL (green) and DAPI (blue). **G.** Representative images (40 x objective, scale bar: 50 μm). **H.** Quantification of TUNEL positive cells (%) after treatment with TN and SEW in presence or absence of AKT V (n=3). Results are shown as mean ± SEM. *$p<0.05$; **$p<0.01$; ***$p<0.001$ for comparisons indicated by the horizontal bars.

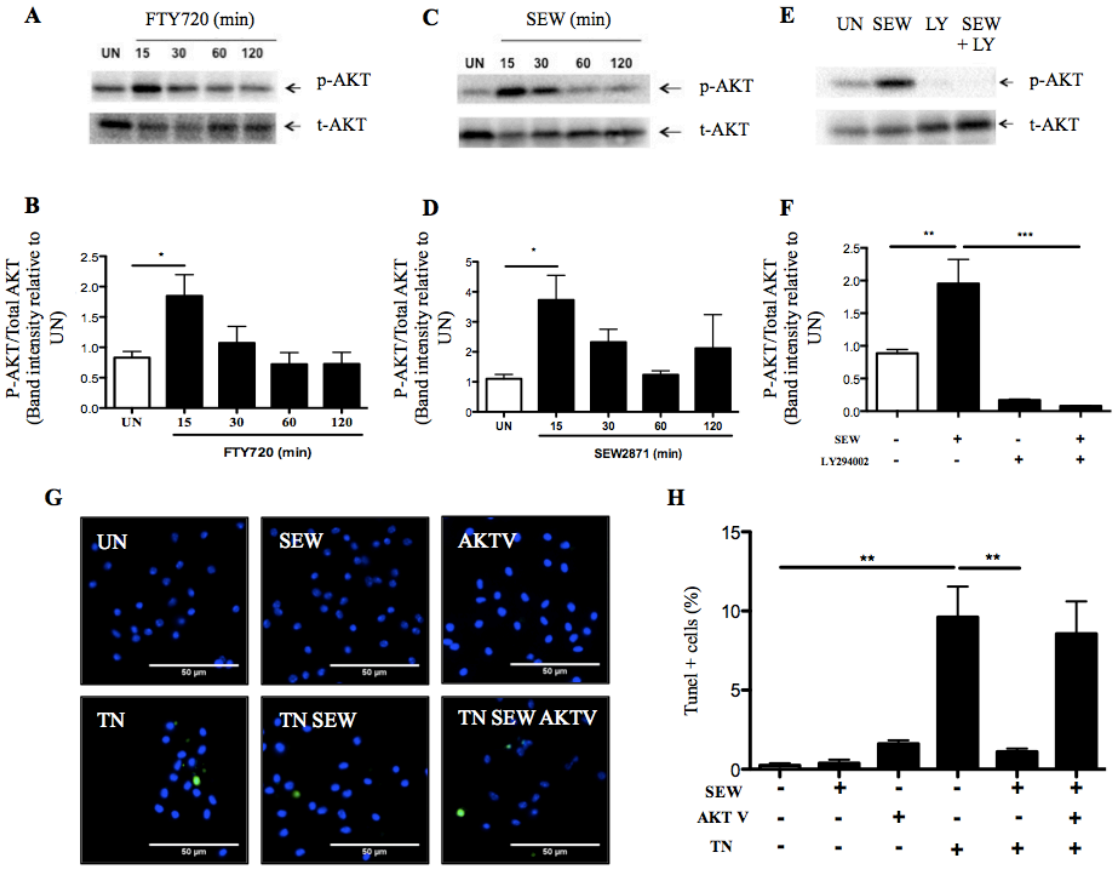
A
FTY720 (min)
UN 15 30 60 120
p-AKT
t-AKT
C
SEW (min)
UN 15 30 60 120
p-AKT
t-AKT
E
UN SEW LY SEW + LY
p-AKT
t-AKT
B
P-AKT/Total AKT (Band intensity relative to UN)
UN 15 30 60 120
FTY720 (min)
D
P-AKT/Total AKT (Band intensity relative to UN)
UN 15 30 60 120
SEW2871 (min)
F
P-AKT/Total AKT (Band intensity relative to UN)
SEW
LY294002
G
UN
SEW
AKTV
TN
TN SEW
TN SEW AKTV
H
Tunel + cells (%)
SEW
AKT V
TN

3.4.3 Effect of macrophage S1PR1 deficiency on HDL-mediated protection against apoptosis

To test the role of S1PR1 in protection of macrophages against apoptosis, we generated $S1PR1^{MKO}$ macrophages by mating S1PR1-floxed mice with Lys2-cre ($S1PR1^{wt/wt}$) mice in which Cre recombinase is expressed and able to excise the S1PR1 gene in macrophages and granulocytes (34). Recombination of the S1PR1 gene in macrophages $S1PR1^{MKO}$ compared to those from prepared from $S1PR1^{wt/wt}$ was confirmed by RT-PCR (Supplementary Figure 3.6). Consistent with the absence of S1PR1 expression, treatment of $S1PR1^{MKO}$ macrophages with SEW did not lead to increased p-AKT levels, whereas SEW treatment of control $S1PR1^{wt/wt}$ macrophages, exhibited increased p-AKT (Figure 3.3A-B) similar to that seen in WT macrophages (Figure 3.2C-F). Consistent with the lack of increase in AKT phosphorylation, treatment of $S1PR1^{MKO}$ macrophages with SEW did not protect them against TN-induced apoptosis whereas control $S1PR1^{wt/wt}$ macrophages were protected by SEW treatment (Figure 3.3C-D). HDL has been reported to carry S1P, the natural ligand of S1PR1, in plasma and HDL associated S1P has been reported to mediate some of HDL's effects on cells. Similar to the effects of SEW, treatment of control macrophages ($S1PR1^{wt/wt}$ mice) with HDL was able to protect them against TN-induced apoptosis (Figure 3.3E-F; Supplementary Figure 3.7). TN-induced apoptosis in $S1PR1^{MKO}$ macrophages to a similar degree as it did in control $S1PR1^{wt/wt}$ macrophages; however, HDL treatment did not suppress TN-induced apoptosis in S1PR1 deficient ($S1PR1^{MKO}$) (Figure 3.3E-F). These results show that S1PR1 activation can

protect macrophages against apoptosis possibly through AKT phosphorylation and that macrophage S1PR1 expression is required for HDL's anti-apoptotic effect.

Figure 3.3: HDL cannot protect S1PR1 deficient macrophages against tunicamycin-induced apoptosis

Thioglycollate-elicited peritoneal macrophages from $S1PR1^{wt/wt}$ and $S1PR1^{MKO}$ mice were incubated with 1 μM SEW2871 (SEW) for 15 minutes. Proteins were collected, separated by SDS-PAGE and immunoblotted for p-AKT and total AKT was carried out as described in Materials and Methods. **A.** Representative blot showing p-AKT (Ser473) and total AKT after SEW incubation. **B.** Quantification of band intensities. Results are shown as mean ± SEM (n=3). For apoptosis experiments (**C-F**), thioglycollate-elicited mouse peritoneal macrophages from $S1PR1^{wt/wt}$ and $S1PR1^{MKO}$ mice were incubated with tunicamycin (TN, 10 μg/mL) in the presence or absence of 1μM SEW (**C-D**) or 50 μg/mL HDL (**E-F**). After 24 hours, cells were fixed and stained for TUNEL (green) and DAPI (blue). Representative images of TUNEL/DAPI-stained $S1PR1^{wt/wt}$ (**C**) and $S1PR1^{MKO}$ (**D**) macrophages treated with TN and SEW are shown (40 x objective, scale bar: 50 μm) and the quantification of TUNEL positive cells (%) (n=3). Representative images of TUNEL-stained $S1PR1^{wt/wt}$ (**E**) and $S1PR1^{MKO}$ (**F**) macrophages treated with TN and HDL are shown (40 x objective, scale bar: 25 μm) and the quantification of TUNEL positive cells (%) (n=3). Results are shown as mean ± SEM.*$p<0.05$; **$p<0.01$; ***$p<0.001$.

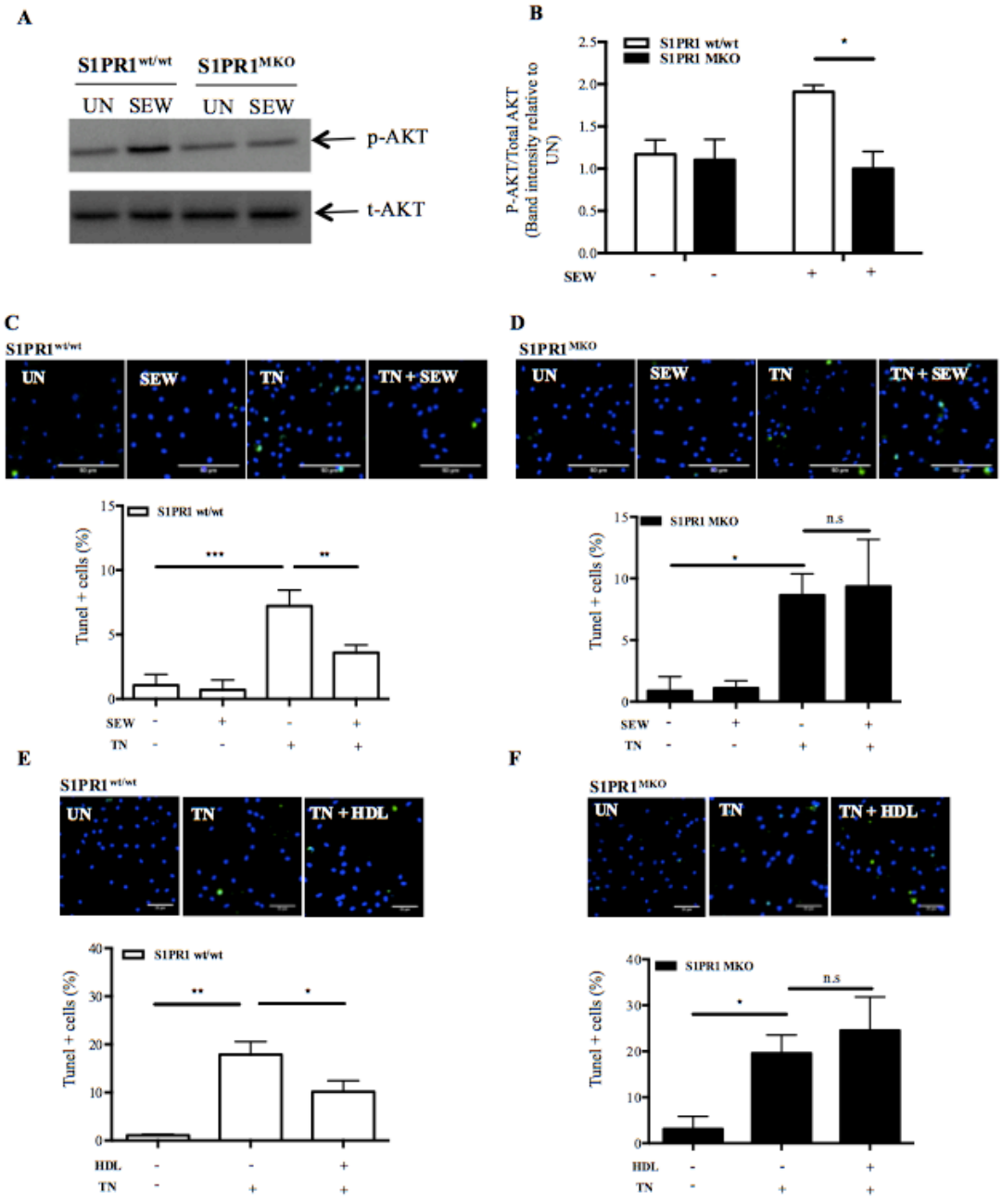
A
S1PR1wt/wt
S1PR1MKO
UN SEW UN SEW
p-AKT
t-AKT
B
S1PR1 wt/wt
S1PR1 MKO
P-AKT/Total AKT (Band intensity relative to UN)
SEW
C
S1PR1wt/wt
UN
SEW
TN
TN + SEW
Tunel + cells (%)
D
S1PR1MKO
n.s
E
S1PR1wt/wt
TN + HDL
HDL
TN
F
S1PR1MKO

3.4.4 Effect of macrophage S1PR1 deficiency on HF diet induced atherosclerosis in BM transplanted LDLR KO mice

To test the role of S1PR1 in macrophages on atherosclerosis development, we transplanted bone marrow (BM) from either $S1PR1^{MKO}$ or $S1PR1^{wt/wt}$ mice into lethally irradiated LDLR KO recipient mice (hereafter referred as $LDLR^{BM\ S1PR1\ MKO}$ and $LDLR^{BM\ S1PR1\ WT}$ mice) and induced atherosclerosis by feeding the BM transplanted mice a HF diet for 9 or 12 weeks.

To test if the expression of Cre recombinase would affect atherosclerosis development, we performed control BMT experiments where LDLR KO mice received either wild type ($LDLR^{BM\ WT}$) or Cre expressing BM ($LDLR^{BM\ S1PR1\ WT}$) and were fed a HF diet for 6 or 12 weeks. The $LDLR^{BM\ S1PR1\ WT}$ group did not show significant differences in total plasma cholesterol, atherosclerosis progression or necrotic core formation when compared to $LDLR^{BM\ WT}$ (Supplementary figure 3.8), indicating that Cre recombinase expression did not interfere with atherosclerosis development in the context of BM transplantation.

$LDLR^{BM\ S1PR1\ WT}$ and $LDLR^{BM\ S1PR1\ MKO}$ mice fed the HF diet for 9 or 12 weeks showed no differences in total cholesterol, free cholesterol, cholesterol ester, HDL cholesterol, and non-HDL cholesterol levels (Table 3.1). Triglyceride levels were slightly, though significantly lower in $LDLR^{BM\ S1PR1\ WT}$ mice fed the HF diet for 9 weeks, than on the $LDLR^{BM\ S1PR1\ WT}$ fed the HF diet for 12 weeks or the $LDLR^{BM\ S1PR1\ MKO}$ mice fed for either 9 or 12 weeks (Table 3.1). No differences in cholesterol distribution

between lipoproteins were seen between $LDLR^{BM\ S1PR1\ WT}$ or $LDLR^{BM\ S1PR1\ MKO}$ mice fed the HF diet for either 9 or 12 weeks (Supplementary figure 3.9).

Figures 3.4A and B show representative images of atherosclerotic plaques in the aortic sinus of 9 weeks HF diet-fed $LDLR^{BM\ S1PR1\ WT}$ and $LDLR^{BM\ S1PR1\ MKO}$ mice. Macrophage S1PR1 deficiency was accompanied by a significantly increased average plaque size in the aortic sinus after 9 weeks on a high fat diet (Figure 3.4A-C; average plaque sizes 81,000 ± 14,000 μm^2 for $LDLR^{BM\ S1PR1\ WT}$ and 122,000 ± 8,000 μm^2 for $LDLR^{BM\ S1PR1\ MKO}$ mice). Atherosclerotic plaques from 9 week HF diet-fed $LDLR^{BM\ S1PR1\ MKO}$ mice exhibited larger sized necrotic cores (average 23 ± 4 % of total plaque size) than similarly fed $LDLR^{BM\ S1PR1\ WT}$ mice (average 12 ± 4 % of total plaque size) (Figure 3.5A-C). TUNEL staining also revealed significantly increased (163 ± 11 vs 101 ± 17 /mm^2 of atherosclerotic plaque) accumulation of apoptotic nuclei in plaques from $LDLR^{BM\ S1PR1\ MKO}$ mice compared to $LDLR^{BM\ S1PR1\ WT}$ mice after 9 weeks of HF diet feeding (Figure 3.5G-I). Atherosclerotic plaques were larger and average plaque sizes were similar in $LDLR^{BM\ S1PR1\ WT}$ and $LDLR^{BM\ S1PR1\ MKO}$ mice fed the HF diet for 12 weeks (173,000 ± 15,000 μm^2 and 193,000 ± 21,000 μm^2 respectively; Figure 3.4D-F). Necrotic core sizes and numbers of apoptotic nuclei were increased after 12 weeks of HF diet feeding and although there appeared to be trends towards increased levels in $LDLR^{BM\ S1PR1\ MKO}$ mice compared to $LDLR^{BM\ S1PR1\ WT}$ mice after 12 weeks of HF diet feeding, differences did not reach statistical significance (Figure 3.5D-F and 3.5J-L). These results suggest that S1PR1 might play a role at early stages of plaque development and that it might do so by preventing macrophage apoptosis and necrotic core formation.

Table 3.1: Plasma lipids in LDLR$^{BM\ S1PR1\ WT}$ and LDLR$^{BM\ S1PR1\ MKO}$ fed a high fat diet for 9 or 12 weeks

Plasma was prepared from blood collected by cardiac puncture from HF diet fed-LDLR$^{BM\ S1PR1\ WT}$ and LDLR$^{BM\ S1PR1\ MKO}$ mice at the moment of harvest. Plasma lipids were determined as described in materials and methods. Results are expressed as mean ± SEM. Sample size is indicated in parenthesis on the group column. *p<0.05 vs 9 weeks LDLR$^{BM\ S1PR1\ WT}$.

	9 weeks		12 weeks	
	LDLR$^{BM\ S1PR1\ WT}$ (13)	**LDLR$^{BM\ S1PR1\ MKO}$ (14)**	**LDLR$^{BM\ S1PR1\ WT}$ (19)**	**LDLR$^{BM\ S1PR1\ MKO}$ (10)**
Total Cholesterol (mmol/l)	44.59 ± 4.90	49.21 ± 2.40	45.32 ± 3.73	40.20 ± 3.48
Unesterified Cholesterol (mmol/l)	9.87 ± 1.03	11.31 ± 0.46	10.26 ± 0.69	9.41 ± 1.09
Cholesterol Ester (mmol/l)	34.72 ± 4.02	37.90 ± 2.08	35.06 ± 3.87	30.78 ± 4.10
Triglycerides (mmol/l)	2.62 ± 0.27	3.75 ± 0.42*	4.29 ± 0.42	4.41 ± 0.56
HDL-cholesterol (mmol/l)	5.53 ± 0.33	6.15 ± 0.53	5.05 ± 0.28	5.75 ± 0.50
Non HDL-cholesterol (mmol/l)	39.07 ± 5.16	43.06 ± 2.62	40.28 ± 3.67	34.45 ± 3.35

Figure 3.4: S1PR1 deficiency in macrophages increases atherosclerosis in BM transplanted LDLR KO mice fed a HF diet for 9 weeks

Irradiated LDLR KO mice received bone marrow from either $S1PR1^{wt/wt}$ or $S1PR1^{MKO}$ mice and were fed a high fat diet for 9 (n=13-14) and 12 (n=19-10) weeks. **A-B**. Representative images of oil red O-stained aortic sinus cryosections of $LDLR\ KO^{BM\text{-}S1PR1\ wt}$ and $LDLR\ KO^{BM\text{-}S1PR1\ MKO}$ mice fed a HF diet for 9 weeks (5 x objective, scale bar: 100 μm). **C.** Quantification of plaque areas for n=13 and 14 mice respectively. Results are shown as scatter dot plot (lines: mean ± SEM). *$p<0.05$. **D-E**. Representative images of oil red O-stained aortic sinus cryosections of $LDLR\ KO^{BM\text{-}S1PR1\ wt}$ and $LDLR\ KO^{BM\text{-}S1PR1\ MKO}$ mice fed a HF diet for 12 weeks (5 x objective, scale bar: 100 μm). **F.** Quantification of plaque areas for n=9 and 10 mice, respectively. Results are shown as scatter dot plot (lines: mean ± SEM).

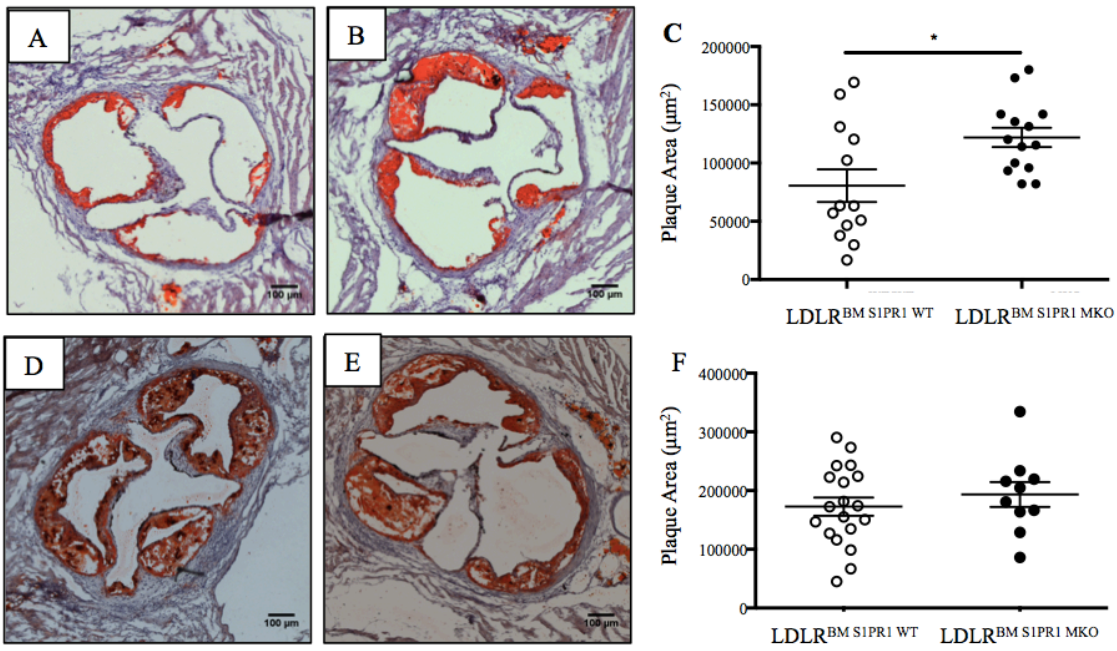
A
B
C
D
E
F
100 µm
Plaque Area (µm²)
200000
150000
100000
50000
0
*
LDLR BM S1PR1 WT
LDLR BM S1PR1 MKO
400000
300000
200000
100000

Figure 3.5: S1PR1 deficiency in macrophages increases necrotic core formation and atherosclerotic plaque apoptosis in BM transplanted LDLR KO mice fed a HF diet for 9 weeks

LDLR KO$^{BM\text{-}S1PR1\ wt}$ and LDLR KO$^{BM\text{-}S1PR1\ MKO}$ mice were fed a high fat diet for 9 (n=13-14) or 12 (n=19-10) weeks. Necrotic core was visualized in H&E stained cryosections and measured as described in the materials and methods. Representative images from LDLR KO$^{BM\text{-}S1PR1\ wt}$ and LDLR KO$^{BM\text{-}S1PR1\ MKO}$ mice fed a HF diet for 9 weeks (**A, B)** or 12 weeks (**D, E**) (5 x objective, scale bar: 100 μm). Quantification of relative necrotic core areas in 9 weeks fed (**C**) or 12 weeks fed mice (**F**). Results are shown as scatter dot plot (lines: mean ± SEM). Cryosections were stained for apoptotic nuclei by TUNEL (green) and counterstained for nuclei with DAPI (blue). Representative TUNEL/DAPI-stained images of aortic atherosclerotic plaque sections from LDLR KO$^{BM\text{-}S1PR1\ wt}$ and LDLR KO$^{BM\text{-}S1PR1\ MKO}$ mice fed a HF diet for 9 weeks (**G, H**) or 12 weeks (**J, K**) (20 x objective, scale bar: 50 μm). Quantification of TUNEL-positive nuclei per plaque area in mice fed the HF diet for 9 weeks (**I**) or 12 weeks (**L**) (n=10). Results are shown as scatter dot plot (lines: mean ± SEM). *$p<0.05$; **$p<0.01$.

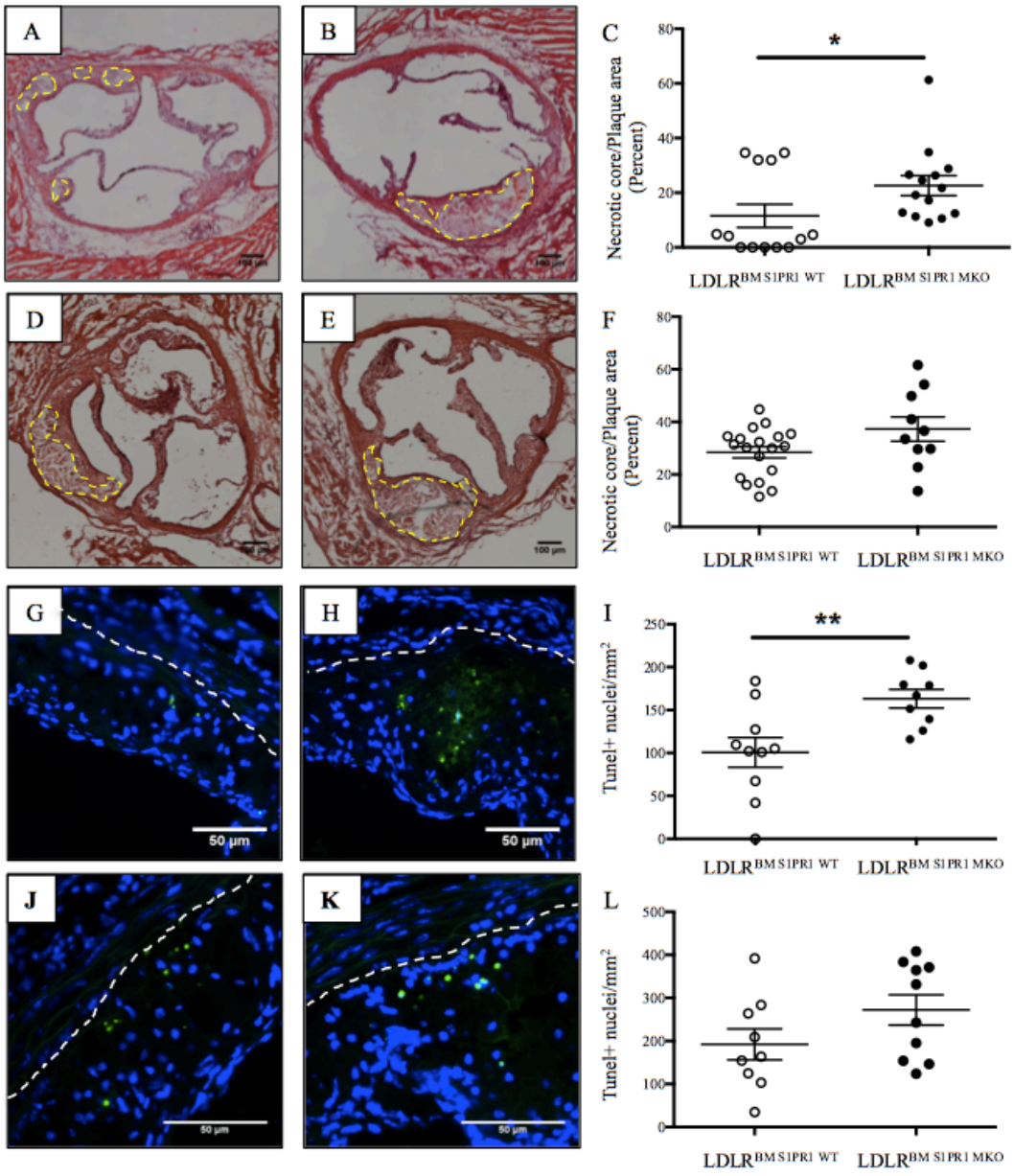
A
B
C
Necrotic core/Plaque area (Percent)
*
LDLR BM S1PR1 WT
LDLR BM S1PR1 MKO
D
E
F
Necrotic core/Plaque area (Percent)
LDLR BM S1PR1 WT
LDLR BM S1PR1 MKO
G
H
50 µm
I
Tunel+ nuclei/mm²
**
LDLR BM S1PR1 WT
LDLR BM S1PR1 MKO
J
K
L
Tunel+ nuclei/mm²
LDLR BM S1PR1 WT
LDLR BM S1PR1 MKO

3.5 Discussion

Our study is the first one to look into the role of macrophage S1PR1 in apoptosis and atherosclerosis development. Here we showed that activation of the S1PR1 protects macrophages against apoptosis induced by TN, and ER stress-inducing agent, or oxLDL, an oxidative stress-inducing agent (Figure 3.1) in a PI3K/AKT dependent manner (Figure 3.2). Macrophage S1PR1 expression is also required for HDL-mediated protection against apoptosis (Figure 3.3). We also showed that S1PR1 deficiency in macrophages increases atherosclerotic plaque sizes, apoptosis in atherosclerotic plaques and necrotic core sizes at early stages (after 9 weeks of HF diet feeding) of plaque development, but that these effects are lost at later stages of plaque development (Figure 3.4-3.5).

Sphingolipids are central regulators in critical cell processes such as survival, cell death and proliferation (35). Among the components of the sphingosine-1-phosphate rheostat, ceramide and sphingosine are usually associated with inhibition of proliferation and induction of apoptosis while S1P promotes cell growth and survival (36). S1P has been shown to protect keratinocytes, liver sinusoidal cells and cardiomyocytes against apoptosis (37-39). In endothelial cells, serum-deprivation induced reduction in cell survival was also prevented by incubation of the cells in the presence of reconstituted HDL containing S1P. By using specific inhibitors, the authors were able to identify receptor S1PR1 and 3 as the main mediators of the anti-apoptotic effect (40). Consistent with this, our data shows that specific activation of the S1PR1 in macrophages protects against apoptosis induced by both TN and oxLDL (Figure 3.1). Surprisingly, Chen and

colleagues have reported that oxLDL can protect macrophages against apoptosis by induction of an oscillatory increase in intracellular calcium concentration (41). The mechanism involved activation of sphingosine kinase 1 by oxLDL and the S1P-mediated release of calcium from intracellular stores (42). Hundal and colleagues have also reported similar results were oxLDL can inhibit macrophage apoptosis by sustaining AKT activation and B-cell lymphoma-extra large (Bcl-XL) levels (43). There are several factors that can account for these contradictory results including cell type used and experimental conditions although oxLDL concentration seems to be a key factor. Studies were protection has been reported used concentrations under 50 μg/mL, while apoptosis has been reported with concentrations equal or over 100 μg/mL, in agreement with our results (41-44).

Abundant literature has linked AKT activation to S1P's antiapoptotic signaling. Nofer and colleagues demonstrated that HDL-S1P treatment of endothelial cells could switch off the pro-apoptotic protein Bad and the subsequent activation of caspases 3 and 9, inhibiting apoptosis in an AKT activation-dependent manner (45). Likewise, sphingosine kinase 1 overexpression in endothelial cells protects them against apoptosis also by activating PI3K/AKT and up-regulating B-cell lymphoma 2 (Bcl-2) (46). Our results also indicate that protection seen after activation of the S1PR1 could be mediated by activation of the PI3K/AKT. In fact, inhibition of AKT phosphorylation effectively prevented apoptosis protection triggered by S1PR1 activation (Figure 3.2). In this context, it has been reported that S1P secreted by apoptotic cells increases survival by activation of PI3K, extracellular signal-regulated kinases 1/2 (ERK1/2) and Bcl-2 up-regulation in

macrophages (47). Up-regulation of myeloid cell leukemia 1 (Mcl-1) via PI3K and protein kinase C (PKC), and down-regulation of BIM via mitogen activated protein kinases (MAPK)/ERK1/2 have also been reported in endothelial cells exposed to FTY720 phosphate (48). Further experiments will help clarify the signaling pathways downstream of S1PR1 mediated AKT activation, leading to survival in macrophages.

S1P has been shown to mediate several of HDL's effects in cells types involved in atherosclerosis. HDL can inhibit SMCs migration in a response likely mediated by S1P since it was blocked when using a siRNA directed against the S1PR2 (49; 50). In endothelial cells, HDL-associated S1P modulates endothelial cell tube formation through activation of MAPK cascade therefore promoting angiogenesis (51). Here we show evidence suggesting that S1PR1 expression is required by HDL to protect macrophages against apoptosis induced by TN treatment (Figure 3.3). This result is consistent with our previous finding that activation of S1PR1 is required for HDL-mediated macrophage migration (30). That study also showed that agonists of the S1PR1 as well as knockout of the HDL receptor SR-B1 or inhibition of its lipid transfer activity prevented HDL induced macrophage migration. We also show that S1PR1 deficient macrophages express normal levels of *scarb-1* mRNA (Supplementary figure 3.10), which suggests that even though HDL is able to bind to its receptor, it cannot protect macrophages lacking S1PR1. Considering this along with the data presented here-in, it seems that a likely model for HDL signaling involves the SR-B1 mediated delivery of S1P to S1PR1, leading to the activation of PI3K/AKT signaling pathway, known in a number of cell types to be involved in cell migration as well as protection against apoptosis.

Macrophages are one of the main cell types involved in atherosclerosis development and based on our *in vitro* data, we were interested in exploring the importance of S1PR1 expression in macrophages on plaque formation. Analysis of LDLR KO mice reconstituted with BM from $S1PR1^{MKO}$ or control $S1PR1^{wt/wt}$ donors and then fed a high fat diet for 9 weeks showed that macrophage S1PR1 deficiency does not significantly alter plasma lipid composition (Table 3.1) but it significantly increases plaque development (Figures 3.4). Consistent with our data, Sattler and colleagues recently showed that HDL-associated S1P correlated negatively with the overall severity of coronary artery disease (CAD) and that low levels of HDL-bound S1P were predictive for CAD (52). The overall number of macrophages in lesions is a result of a balance between recruitment, emigration and local proliferation (53). Macrophage recruitment as previously described is a consequence of the inflammatory process activated by modified lipoprotein accumulation in the vessel wall (2). Both HDL and agonists of the S1PRs control macrophage migration so increased plaque size can be associated to defective emigration in the absence of macrophage S1PR1 (30). Macrophage proliferation has also been detected in atherosclerotic plaques and it could contribute to plaque size (54). Further experiments need to be performed to identify if this process contributes to plaque formation in our mouse model.

Macrophage apoptosis is an important feature of atherosclerotic plaque formation at all stages of the disease. Clearance of apoptotic cells, a process known as efferocytosis, prevents secondary necrosis and limits plaque growth (55). As the disease progresses, however, efferocytosis is thought to become defective promoting necrotic

core formation and plaque instability (56). Macrophage SR-B1 deficiency was recently reported to affect plaque efferocytosis. Macrophage SR-B1 deficiency promoted defective apoptotic cell clearance through activation of the Src/PI3K/ Ras-related C3 botulinum toxin substrate 1 (Rac1) pathway *in vitro*, resulting in larger necrotic cores *in vivo* (57). Similarly, macrophage S1PR1 deficiency in our BMT experiments resulted in increased necrotic core sizes after 9 weeks on a high fat diet compared to control condition (Figure 3.5). Furthermore, our results suggest that the increase in necrotic core size might be explained by an increase in plaque apoptosis due to macrophage S1PR1 deficiency, in agreement with our *in vitro* data. Similar to our results, administration of a S1PR1 agonist to LDLR KO mice fed a high fat diet significantly prevented atherosclerosis development without affecting plasma lipid composition (58). These effects of S1PR1 deficiency were absent in mice fed for 12 weeks, which had considerably larger sized plaques with larger necrotic cores and greater plaque apoptosis (Figure 3.4-3.5), suggesting that S1PR1 deficiency might play a more important role at earlier stages of plaque development, rather than after prolonged periods of time. A few other studies have also explored the role of other S1PRs in atherosclerosis development. Studies in S1PR2/apoE dKO mice suggest that opposite to S1PR1, S1PR2 acts as a pro-atherogenic factor promoting macrophage retention and cytokine release therefore increasing atherosclerosis. On the other hand, apoE KO mice deficient in S1PR3 did not show any effects on atherosclerosis development but macrophage content in the plaque was significantly reduced (59). We did not detect S1PR3 transcripts in control macrophages, nor did we see any increase in S1PR2 expression in cultured macrophages

lacking S1PR1 (Supplementary Figure 3.6) suggesting that there is no compensatory up-regulation of S1PR2 in S1PR1 deficient thioglycollate-elicited macrophages at least in culture. We cannot rule out the possibility that other S1PRs such as S1PR2 might increase in other types of macrophages or at some point during atherosclerosis development *in vivo*, which could influence plaque development and might contribute to the lack of effect of S1PR1 deficiency on atherosclerosis at the 12 week feeding period. Further studies are required to test this possibility.

In summary, based on our results we propose that the S1P/S1PR1 axis is important for HDL signaling in macrophages and plays a role in protection against apoptosis. In our working model, HDL would signal through SR-B1 while delivering S1P to S1PR1. The joint signaling through both SR-B1 and S1PR1 activates the PI3K/AKT axis playing a role in protection against atherosclerosis by preventing macrophage apoptosis and necrotic core formation. Further studies in other cell types involved in plaque development would help clarify the role of S1P in atheroprotection and open possibilities for future therapies.

3.6 References

1. Gimbrone MA, Jr., Topper JN, Nagel T, Anderson KR, Garcia-Cardena G: Endothelial dysfunction, hemodynamic forces, and atherogenesis. *Ann N Y Acad Sci* **902**:230-239; discussion 239-240, 2000.

2. Libby P, Ridker PM, Hansson GK: Progress and challenges in translating the biology of atherosclerosis. *Nature* **473**:317-325, 2011.

3. Tabas I: Macrophage apoptosis in atherosclerosis: consequences on plaque progression and the role of endoplasmic reticulum stress. *Antioxid Redox Signal* **11**:2333-2339, 2009.

4. Libby P, Geng YJ, Aikawa M, Schoenbeck U, Mach F, Clinton SK, Sukhova GK, Lee RT: Macrophages and atherosclerotic plaque stability. *Curr Opin Lipidol* **7**:330-335, 1996.

5. Maiolino G, Rossitto G, Caielli P, Bisogni V, Rossi GP, Calo LA: The role of oxidized low-density lipoproteins in atherosclerosis: the myths and the facts. *Mediators Inflamm* **2013**:714653, 2013.

6. Quinn MT, Parthasarathy S, Fong LG, Steinberg D: Oxidatively modified low density lipoproteins: a potential role in recruitment and retention of monocyte/macrophages during atherogenesis. *Proc Natl Acad Sci U S A* **84**:2995-2998, 1987.

7. Martinet W, Kockx MM: Apoptosis in atherosclerosis: focus on oxidized lipids and inflammation. *Curr Opin Lipidol* **12**:535-541, 2001.

8. Zhou AX, Tabas I: The UPR in atherosclerosis. *Semin Immunopathol* **35**:321-332, 2013.

9. Rigotti A, Trigatti B, Babitt J, Penman M, Xu S, Krieger M: Scavenger receptor BI--a cell surface receptor for high density lipoprotein. *Curr Opin Lipidol* **8**:181-188, 1997.

10. Trigatti B, Rayburn H, Vinals M, Braun A, Miettinen H, Penman M, Hertz M, Schrenzel M, Amigo L, Rigotti A, Krieger M: Influence of the high density lipoprotein receptor SR-BI on reproductive and cardiovascular pathophysiology. *Proc Natl Acad Sci U S A* **96**:9322-9327, 1999.

11. Braun A, Trigatti BL, Post MJ, Sato K, Simons M, Edelberg JM, Rosenberg RD, Schrenzel M, Krieger M: Loss of SR-BI expression leads to the early onset of occlusive atherosclerotic coronary artery disease, spontaneous myocardial infarctions, severe

cardiac dysfunction, and premature death in apolipoprotein E-deficient mice. *Circ Res* **90**:270-276, 2002.

12. Zhang S, Picard MH, Vasile E, Zhu Y, Raffai RL, Weisgraber KH, Krieger M: Diet-induced occlusive coronary atherosclerosis, myocardial infarction, cardiac dysfunction, and premature death in scavenger receptor class B type I-deficient, hypomorphic apolipoprotein ER61 mice. *Circulation* **111**:3457-3464, 2005.

13. Covey SD, Krieger M, Wang W, Penman M, Trigatti BL: Scavenger receptor class B type I-mediated protection against atherosclerosis in LDL receptor-negative mice involves its expression in bone marrow-derived cells. *Arterioscler Thromb Vasc Biol* **23**:1589-1594, 2003.

14. Zhang W, Yancey PG, Su YR, Babaev VR, Zhang Y, Fazio S, Linton MF: Inactivation of macrophage scavenger receptor class B type I promotes atherosclerotic lesion development in apolipoprotein E-deficient mice. *Circulation* **108**:2258-2263, 2003.

15. Rosenson RS, Brewer HB, Jr., Ansell BJ, Barter P, Chapman MJ, Heinecke JW, Kontush A, Tall AR, Webb NR: Dysfunctional HDL and atherosclerotic cardiovascular disease. *Nat Rev Cardiol* **13**:48-60, 2016.

16. Fuhrman B, Gantman A, Aviram M: Paraoxonase 1 (PON1) deficiency in mice is associated with reduced expression of macrophage SR-BI and consequently the loss of HDL cytoprotection against apoptosis. *Atherosclerosis* **211**:61-68, 2010.

17. Alewijnse AE, Peters SL: Sphingolipid signalling in the cardiovascular system: good, bad or both? *Eur J Pharmacol* **585**:292-302, 2008.

18. Schuchardt M, Tolle M, Prufer J, van der Giet M: Pharmacological relevance and potential of sphingosine 1-phosphate in the vascular system. *Br J Pharmacol* **163**:1140-1162, 2011.

19. Cahalan SM, Gonzalez-Cabrera PJ, Sarkisyan G, Nguyen N, Schaeffer MT, Huang L, Yeager A, Clemons B, Scott F, Rosen H: Actions of a picomolar short-acting S1P(1) agonist in S1P(1)-eGFP knock-in mice. *Nat Chem Biol* **7**:254-256, 2011.

20. Cuvillier O, Pirianov G, Kleuser B, Vanek PG, Coso OA, Gutkind S, Spiegel S: Suppression of ceramide-mediated programmed cell death by sphingosine-1-phosphate. *Nature* **381**:800-803, 1996.

21. Sanchez T, Hla T: Structural and functional characteristics of S1P receptors. *J Cell Biochem* **92**:913-922, 2004.

22. Poti F, Simoni M, Nofer JR: Atheroprotective role of high-density lipoprotein (HDL)-associated sphingosine-1-phosphate (S1P). *Cardiovasc Res* **103**:395-404, 2014.

23. Weigert A, Weis N, Brune B: Regulation of macrophage function by sphingosine-1-phosphate. *Immunobiology* **214**:748-760, 2009.

24. Nofer JR, Bot M, Brodde M, Taylor PJ, Salm P, Brinkmann V, van Berkel T, Assmann G, Biessen EA: FTY720, a synthetic sphingosine 1 phosphate analogue, inhibits development of atherosclerosis in low-density lipoprotein receptor-deficient mice. *Circulation* **115**:501-508, 2007.

25. Keul P, Tolle M, Lucke S, von Wnuck Lipinski K, Heusch G, Schuchardt M, van der Giet M, Levkau B: The sphingosine-1-phosphate analogue FTY720 reduces atherosclerosis in apolipoprotein E-deficient mice. *Arterioscler Thromb Vasc Biol* **27**:607-613, 2007.

26. Poti F, Costa S, Bergonzini V, Galletti M, Pignatti E, Weber C, Simoni M, Nofer JR: Effect of sphingosine 1-phosphate (S1P) receptor agonists FTY720 and CYM5442 on atherosclerosis development in LDL receptor deficient (LDL-R(-)/(-)) mice. *Vascul Pharmacol* **57**:56-64, 2012.

27. Blom T, Back N, Mutka AL, Bittman R, Li Z, de Lera A, Kovanen PT, Diczfalusy U, Ikonen E: FTY720 stimulates 27-hydroxycholesterol production and confers atheroprotective effects in human primary macrophages. *Circ Res* **106**:720-729, 2010.

28. Bolick DT, Srinivasan S, Kim KW, Hatley ME, Clemens JJ, Whetzel A, Ferger N, Macdonald TL, Davis MD, Tsao PS, Lynch KR, Hedrick CC: Sphingosine-1-phosphate prevents tumor necrosis factor-{alpha}-mediated monocyte adhesion to aortic endothelium in mice. *Arterioscler Thromb Vasc Biol* **25**:976-981, 2005.

29. Kimura T, Tomura H, Mogi C, Kuwabara A, Damirin A, Ishizuka T, Sekiguchi A, Ishiwara M, Im DS, Sato K, Murakami M, Okajima F: Role of scavenger receptor class B type I and sphingosine 1-phosphate receptors in high density lipoprotein-induced inhibition of adhesion molecule expression in endothelial cells. *J Biol Chem* **281**:37457-37467, 2006.

30. Al-Jarallah A, Chen X, Gonzalez L, Trigatti BL: High density lipoprotein stimulated migration of macrophages depends on the scavenger receptor class B, type I, PDZK1 and Akt1 and is blocked by sphingosine 1 phosphate receptor antagonists. *PLoS One* **9**:e106487, 2014.

31. Fuller M, Dadoo O, Serkis V, Abutouk D, MacDonald M, Dhingani N, Macri J, Igdoura SA, Trigatti BL: The effects of diet on occlusive coronary artery atherosclerosis

and myocardial infarction in scavenger receptor class B, type 1/low-density lipoprotein receptor double knockout mice. *Arterioscler Thromb Vasc Biol* **34**:2394-2403, 2014.

32. Trigatti BL, Mangroo D, Gerber GE: Photoaffinity labeling and fatty acid permeation in 3T3-L1 adipocytes. *J Biol Chem* **266**:22621-22625, 1991.

33. Van Vre EA, Ait-Oufella H, Tedgui A, Mallat Z: Apoptotic cell death and efferocytosis in atherosclerosis. *Arterioscler Thromb Vasc Biol* **32**:887-893, 2012.

34. Clausen BE, Burkhardt C, Reith W, Renkawitz R, Forster I: Conditional gene targeting in macrophages and granulocytes using LysMcre mice. *Transgenic Res* **8**:265-277, 1999.

35. Maceyka M, Harikumar KB, Milstien S, Spiegel S: Sphingosine-1-phosphate signaling and its role in disease. *Trends Cell Biol* **22**:50-60, 2012.

36. Maceyka M, Milstien S, Spiegel S: Sphingosine-1-phosphate: the Swiss army knife of sphingolipid signaling. *J Lipid Res* **50 Suppl**:S272-276, 2009.

37. Schmitz EI, Potteck H, Schuppel M, Manggau M, Wahydin E, Kleuser B: Sphingosine 1-phosphate protects primary human keratinocytes from apoptosis via nitric

oxide formation through the receptor subtype S1P(3). *Mol Cell Biochem* **371**:165-176, 2012.

38. Nowatari T, Murata S, Nakayama K, Sano N, Maruyama T, Nozaki R, Ikeda N, Fukunaga K, Ohkohchi N: Sphingosine 1-phosphate has anti-apoptotic effect on liver sinusoidal endothelial cells and proliferative effect on hepatocytes in a paracrine manner in human. *Hepatol Res* 2014.

39. Tao R, Hoover HE, Honbo N, Kalinowski M, Alano CC, Karliner JS, Raffai R: High-density lipoprotein determines adult mouse cardiomyocyte fate after hypoxia-reoxygenation through lipoprotein-associated sphingosine 1-phosphate. *Am J Physiol Heart Circ Physiol* **298**:H1022-1028, 2010.

40. Kimura T, Sato K, Malchinkhuu E, Tomura H, Tamama K, Kuwabara A, Murakami M, Okajima F: High-density lipoprotein stimulates endothelial cell migration and survival through sphingosine 1-phosphate and its receptors. *Arterioscler Thromb Vasc Biol* **23**:1283-1288, 2003.

41. Chen JH, Riazy M, Smith EM, Proud CG, Steinbrecher UP, Duronio V: Oxidized LDL-mediated macrophage survival involves elongation factor-2 kinase. *Arterioscler Thromb Vasc Biol* **29**:92-98, 2009.

42. Chen JH, Riazy M, Wang SW, Dai JM, Duronio V, Steinbrecher UP: Sphingosine kinase regulates oxidized low density lipoprotein-mediated calcium oscillations and macrophage survival. *J Lipid Res* **51**:991-998, 2010.

43. Hundal RS, Gomez-Munoz A, Kong JY, Salh BS, Marotta A, Duronio V, Steinbrecher UP: Oxidized low density lipoprotein inhibits macrophage apoptosis by blocking ceramide generation, thereby maintaining protein kinase B activation and Bcl-XL levels. *J Biol Chem* **278**:24399-24408, 2003.

44. Han CY, Pak YK: Oxidation-dependent effects of oxidized LDL: proliferation or cell death. *Exp Mol Med* **31**:165-173, 1999.

45. Nofer JR, Levkau B, Wolinska I, Junker R, Fobker M, von Eckardstein A, Seedorf U, Assmann G: Suppression of endothelial cell apoptosis by high density lipoproteins (HDL) and HDL-associated lysosphingolipids. *J Biol Chem* **276**:34480-34485, 2001.

46. Limaye V, Li X, Hahn C, Xia P, Berndt MC, Vadas MA, Gamble JR: Sphingosine kinase-1 enhances endothelial cell survival through a PECAM-1-dependent activation of PI-3K/Akt and regulation of Bcl-2 family members. *Blood* **105**:3169-3177, 2005.

47. Weigert A, Johann AM, von Knethen A, Schmidt H, Geisslinger G, Brune B: Apoptotic cells promote macrophage survival by releasing the antiapoptotic mediator sphingosine-1-phosphate. *Blood* **108**:1635-1642, 2006.

48. Rutherford C, Childs S, Ohotski J, McGlynn L, Riddick M, MacFarlane S, Tasker D, Pyne S, Pyne NJ, Edwards J, Palmer TM: Regulation of cell survival by sphingosine-1-phosphate receptor S1P1 via reciprocal ERK-dependent suppression of Bim and PI-3-kinase/protein kinase C-mediated upregulation of Mcl-1. *Cell Death Dis* **4**:e927, 2013.

49. Tamama K, Tomura H, Sato K, Malchinkhuu E, Damirin A, Kimura T, Kuwabara A, Murakami M, Okajima F: High-density lipoprotein inhibits migration of vascular smooth muscle cells through its sphingosine 1-phosphate component. *Atherosclerosis* **178**:19-23, 2005.

50. Damirin A, Tomura H, Komachi M, Liu JP, Mogi C, Tobo M, Wang JQ, Kimura T, Kuwabara A, Yamazaki Y, Ohta H, Im DS, Sato K, Okajima F: Role of lipoprotein-associated lysophospholipids in migratory activity of coronary artery smooth muscle cells. *Am J Physiol Heart Circ Physiol* **292**:H2513-2522, 2007.

51. Miura S, Fujino M, Matsuo Y, Kawamura A, Tanigawa H, Nishikawa H, Saku K: High density lipoprotein-induced angiogenesis requires the activation of Ras/MAP kinase

in human coronary artery endothelial cells. *Arterioscler Thromb Vasc Biol* **23**:802-808, 2003.

52. Sattler K, Lehmann I, Graler M, Brocker-Preuss M, Erbel R, Heusch G, Levkau B: HDL-bound sphingosine 1-phosphate (S1P) predicts the severity of coronary artery atherosclerosis. *Cell Physiol Biochem* **34**:172-184, 2014.

53. Moore KJ, Sheedy FJ, Fisher EA: Macrophages in atherosclerosis: a dynamic balance. *Nat Rev Immunol* **13**:709-721, 2013.

54. Robbins CS, Hilgendorf I, Weber GF, Theurl I, Iwamoto Y, Figueiredo JL, Gorbatov R, Sukhova GK, Gerhardt LM, Smyth D, Zavitz CC, Shikatani EA, Parsons M, van Rooijen N, Lin HY, Husain M, Libby P, Nahrendorf M, Weissleder R, Swirski FK: Local proliferation dominates lesional macrophage accumulation in atherosclerosis. *Nat Med* **19**:1166-1172, 2013.

55. Tabas I: Apoptosis and efferocytosis in mouse models of atherosclerosis. *Curr Drug Targets* **8**:1288-1296, 2007.

56. Schrijvers DM, De Meyer GR, Kockx MM, Herman AG, Martinet W: Phagocytosis of apoptotic cells by macrophages is impaired in atherosclerosis. *Arterioscler Thromb Vasc Biol* **25**:1256-1261, 2005.

57. Tao H, Yancey PG, Babaev VR, Blakemore JL, Zhang Y, Ding L, Fazio S, Linton MF: Macrophage SR-BI mediates efferocytosis via Src/PI3K/Rac1 signaling and reduces atherosclerotic lesion necrosis. *J Lipid Res* **56**:1449-1460, 2015.

58. Poti F, Gualtieri F, Sacchi S, Weissen-Plenz G, Varga G, Brodde M, Weber C, Simoni M, Nofer JR: KRP-203, sphingosine 1-phosphate receptor type 1 agonist, ameliorates atherosclerosis in LDL-R-/- mice. *Arterioscler Thromb Vasc Biol* **33**:1505-1512, 2013.

59. Keul P, Lucke S, von Wnuck Lipinski K, Bode C, Graler M, Heusch G, Levkau B: Sphingosine-1-phosphate receptor 3 promotes recruitment of monocyte/macrophages in inflammation and atherosclerosis. *Circ Res* **108**:314-323, 2011.

3.7 Supplementary materials and methods

3.7.1 Real time PCR

Thioglycollate-elicited macrophages were collected and plated overnight in DMEM supplemented with 10 % FBS, 2 mM L-glutamine, 50 μg/ml penicillin and 50 U/ml streptomycin. The next day, cells were washed and total RNA was extracted using the RNeasy mini kit (Qiagen, Toronto, ON, Canada). RNA integrity and concentration were evaluated by measuring the absorbance at 260/280 in a spectrophotometer. One μg of RNA was used to prepare cDNA using the Quantitec reverse transcription kit (Qiagen, Toronto, ON, Canada). Quantitative real-time- (qRT-) PCR was performed using the primers listed in supplementary Table 3.1 (1).

3.7.2 Lipoprotein cholesterol profile

Plasma was obtained as described and diluted 1:3 in FPLC buffer (154mM NaCl, 1mM EDTA pH 8) and 100 μl were subjected to fast protein liquid chromatography (FPLC) using a Tricorn Superose 6 10/30 HR column and AKTA FPLC system (GE Healthcare Life Sciences, Mississauga, ON, Canada). The total cholesterol content in each fraction was quantified using the Infinity Cholesterol assay kit (Thermo Fisher Scientific, Ottawa, ON, Canada) according to the manufacturer's protocol.

3.7.3 References

1. Li C, Yang G, Ruan J: Sphingosine kinase-1/sphingosine-1-phosphate receptor type 1 signalling axis is induced by transforming growth factor-beta1 and stimulates cell migration in RAW264.7 macrophages. Biochem Biophys Res Commun 426:415-420, 2012.

3.8 Supplementary data

Supplementary Table 3.2: Quantitative real-time- (qRT-) PCR primers

Target gene	Primer pair sequence
Mouse S1PR1	Forward 5-ACTTTGCGAGTGAGCTG-3 Reverse 5-AGTGAGCCTTCAGTTACAGC-3
Mouse S1PR2	Forward 5-TTCTGGAGGGTAACACAGTGGT-3 Reverse 5-ACACCCTTTGTATCAAGTGGCA-3
Mouse S1PR3	Forward 5-TGGTGTGCGGCTGTCTAGTCAA-3 Reverse 5-CACAGCAAGCAGACCTCCAGA-3
Mouse SR-B1	Forward 5-CAGGCTGTGGGAACTCTAGC-3 Reverse 5-GAAAAAGCGCCAGATACAGC-3
Mouse Glyceraldehyde 3-phosphate dehydrogenase (GAPDH)	Forward 5-ACCACAGTCCATGCCATCAC-3 Reverse 5-TCCACCACCCTGTTGCTGTA-3

Supplementary Figure 3.6: Relative expression of macrophage S1PR1 in different mouse strains

Mouse peritoneal macrophages were isolated and RNA extracted. Quantitative real time PCR from total cDNA was performed as described in the supplementary materials and methods. GAPDH was used as an internal control and all results are calculated relative to the control condition. **A.** Relative expression of S1PR1 in WT versus $S1PR1^{wt/wt}$. **B.** Relative expression of S1PR1 in $S1PR1^{wt/wt}$ versus $S1PR1^{MKO}$ macrophages. **C.** Relative expression of S1PR2 in WT, $S1PR1^{wt/wt}$ and $S1PR1^{MKO}$ macrophages. **D.** Relative expression of S1PR3 in WT, $S1PR1^{wt/wt}$ and $S1PR1^{MKO}$ macrophages, relative to lung expression levels. Results are expressed as mean ± SEM. ***$p<0.001$ (n= 3-4 per genotype. Lung sample n=1).

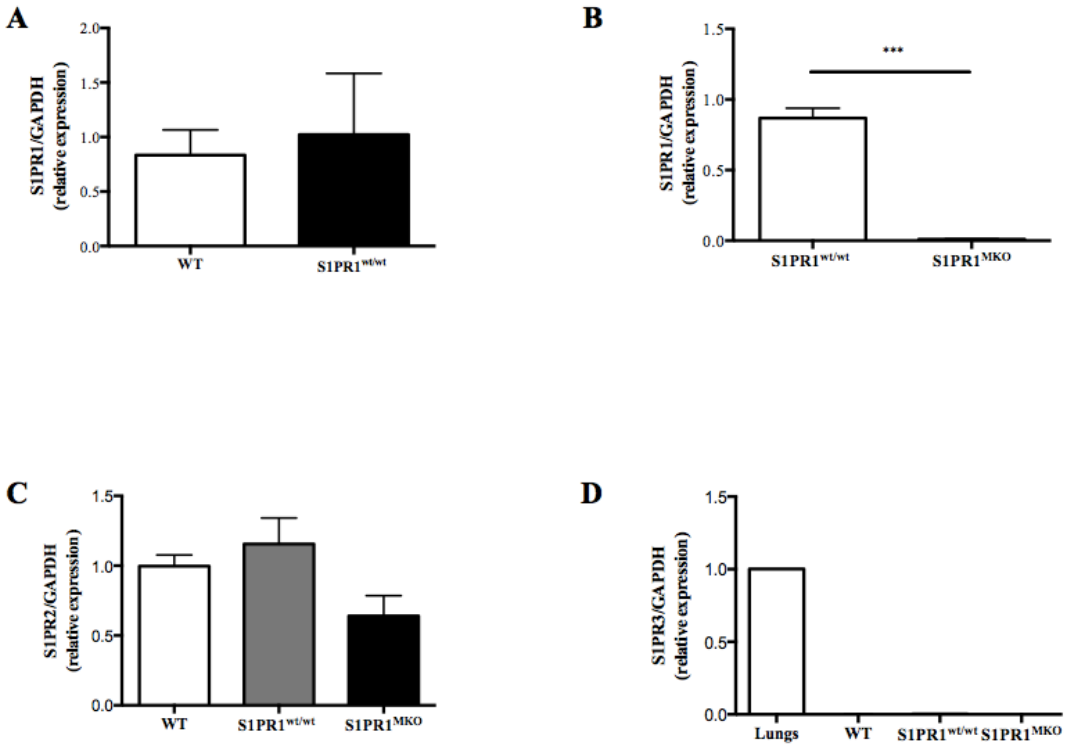
A
S1PR1/GAPDH
(relative expression)
2.0
1.5
1.0
0.5
0.0
WT
S1PR1wt/wt
B
S1PR1/GAPDH
(relative expression)
1.5
1.0
0.5
0.0
***
S1PR1wt/wt
S1PR1MKO
C
S1PR2/GAPDH
(relative expression)
1.5
1.0
0.5
0.0
WT
S1PR1wt/wt
S1PR1MKO
D
S1PR3/GAPDH
(relative expression)
1.5
1.0
0.5
0.0
Lungs
WT
S1PR1wt/wt
S1PR1MKO

Supplementary Figure 3.7: Evaluation of tunicamycin induced apoptosis in WT and S1PR1$^{+/+}$ macrophages

Mouse peritoneal macrophages were exposed to 10 μg/ml tunicamycin in the presence or absence of 50 μg/ml HDL. After 24 hrs cells were fixed and stained for TUNEL (green) and DAPI (blue) as described in Materials and methods. **A.** Representative images (40 x objective, scale bar: 25 μm). **B.** Quantification of TUNEL positive cells (%) after treatment with TN in the presence or absence of HDL. Results are shown as mean ± SEM (n=3). *p<0.05; **p<0.01; ***p<0.001 for comparisons indicated by the horizontal bars.

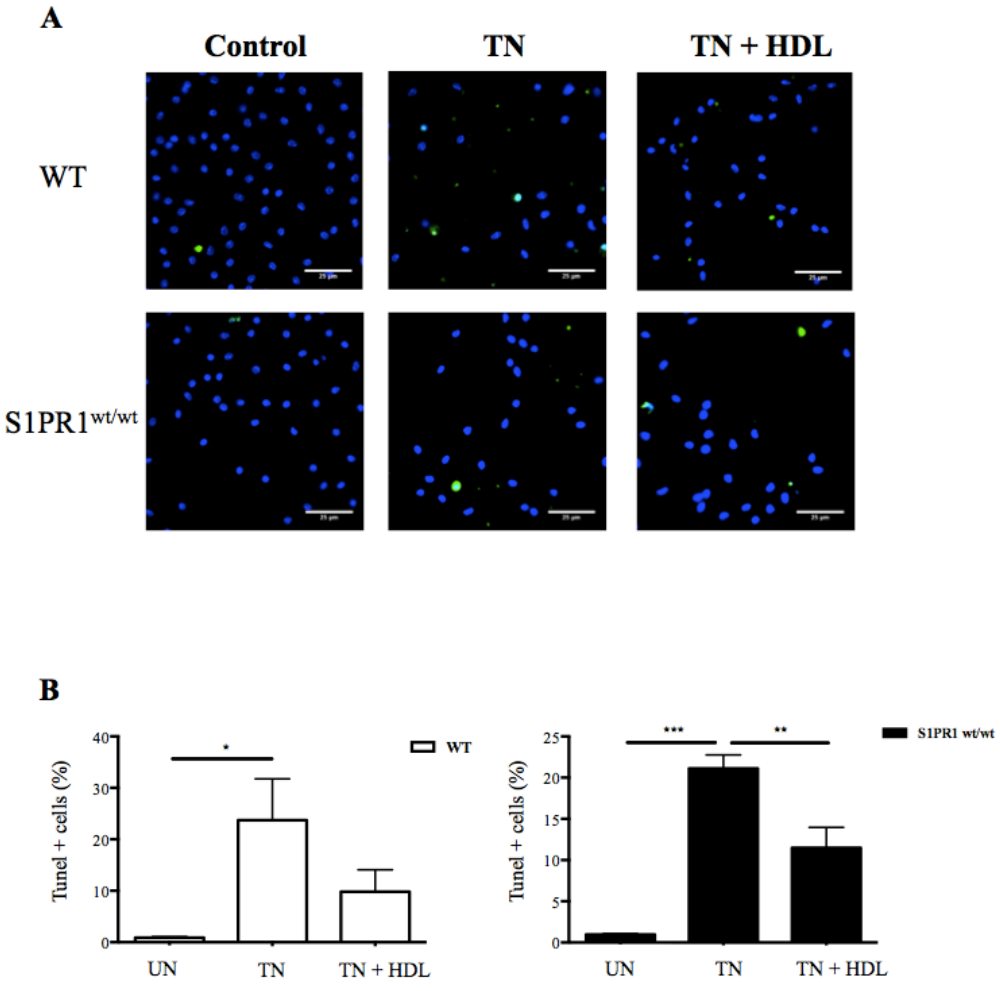
A
Control
TN
TN + HDL
WT
S1PR1wt/wt
B
Tunel + cells (%)
WT
S1PR1 wt/wt
UN
TN
TN + HDL
*
***
**

Supplementary Figure 3.8: Effect of Cre recombinase expression on atherosclerosis development in bone marrow-transplanted LDLR KO mice fed a high fat diet

Irradiated LDLR KO mice received bone marrow from either WT or S1PR1$^{wt/wt}$ mice and were fed a high fat diet for 6 (n=6-8) or 12 (n=7-8) weeks. **A.** Total plasma cholesterol for mice fed a HF diet for 6 weeks. **B**. Total plasma cholesterol for mice fed a HF diet for 12 weeks. Representative images from LDLR$^{BM\ WT}$ and LDLR$^{BM\ S1PR1\ WT}$ mice fed a HF diet for 6 weeks (**C, D)** or 12 weeks (**F, G**) (5 x objective, scale bar: 100 μm). Quantification of atherosclerotic plaque areas in 6 weeks fed (**E**) or 12 weeks fed mice (**H**). Results are presented a mean ± SEM. **I.** Quantification of relative necrotic core area in 12 weeks fed mice. Mice fed a HF diet for 6 weeks did not develop necrotic cores in the aortic sinus atherosclerotic plaque. Results are presented as scatter dot-plot (lines= mean ± SEM).

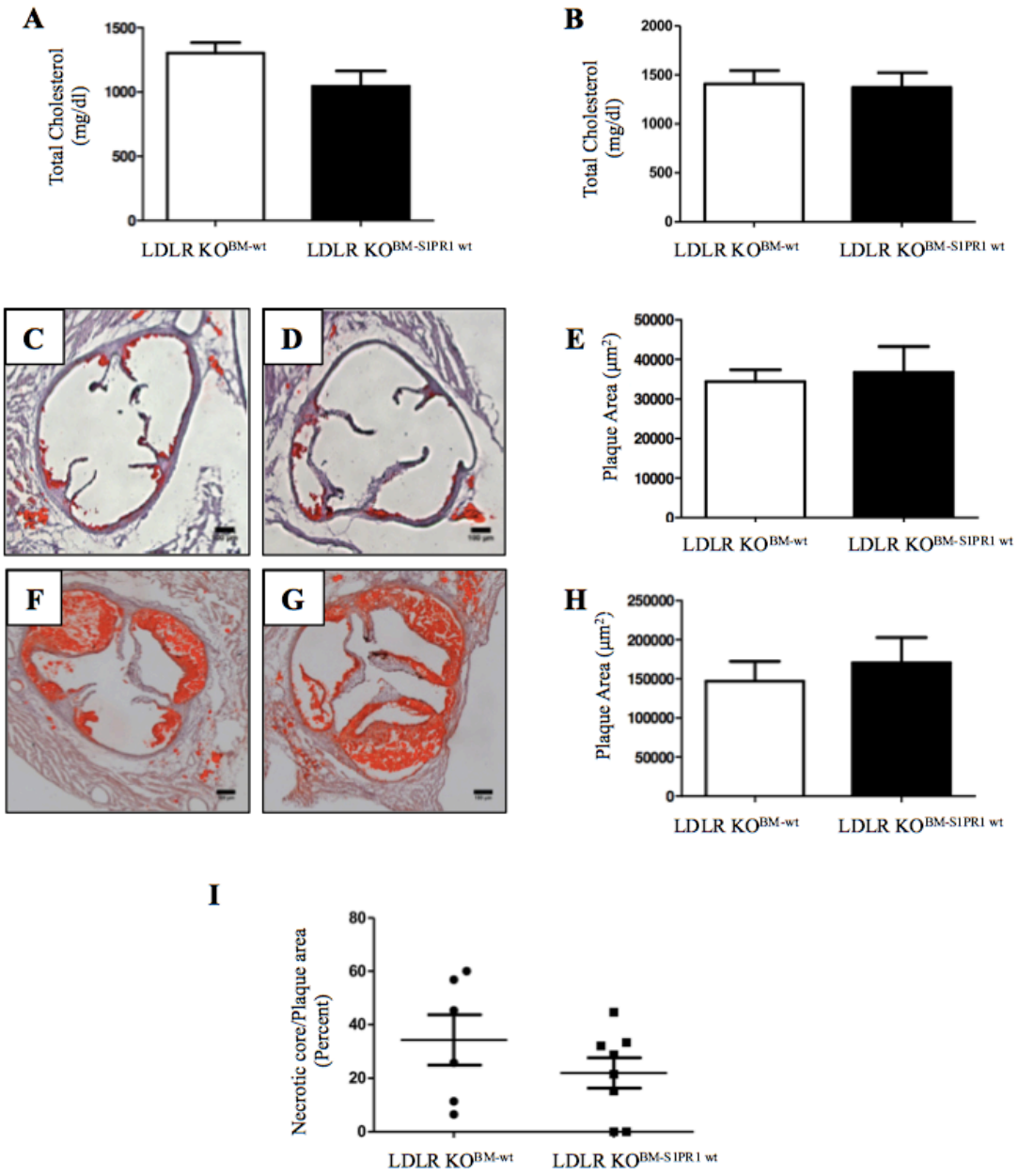
A
Total Cholesterol (mg/dl)
1500
1000
500
0
LDLR KO^BM-wt
LDLR KO^BM-S1PR1 wt
B
Total Cholesterol (mg/dl)
2000
1500
1000
500
0
LDLR KO^BM-wt
LDLR KO^BM-S1PR1 wt
C
D
E
Plaque Area (μm²)
50000
40000
30000
20000
10000
0
LDLR KO^BM-wt
LDLR KO^BM-S1PR1 wt
F
G
H
Plaque Area (μm²)
250000
200000
150000
100000
50000
0
LDLR KO^BM-wt
LDLR KO^BM-S1PR1 wt
I
Necrotic core/Plaque area (Percent)
80
60
40
20
0
LDLR KO^BM-wt
LDLR KO^BM-S1PR1 wt

Supplementary Figure 3.9: Lipoprotein profile in bone marrow-transplanted LDLR KO mice fed a high diet for 9 or 12 weeks

Irradiated LDLR KO mice received bone marrow from either S1PR1$^{wt/wt}$ or S1PR1^{MKO} mice and were fed a high fat diet for 9 or 12 weeks. Lipoproteins were separated by fast protein liquid chromatography (FPLC) as described in supplementary materials and methods. **A.** Plasma lipoprotein profile and cholesterol distribution per lipoprotein category of mice fed a high fat diet for 9 weeks. **B**. Plasma lipoprotein profile and cholesterol distribution per lipoprotein category of mice fed a high fat diet for 12 weeks. Results are shown as mean ± SEM for each fraction (n=3).

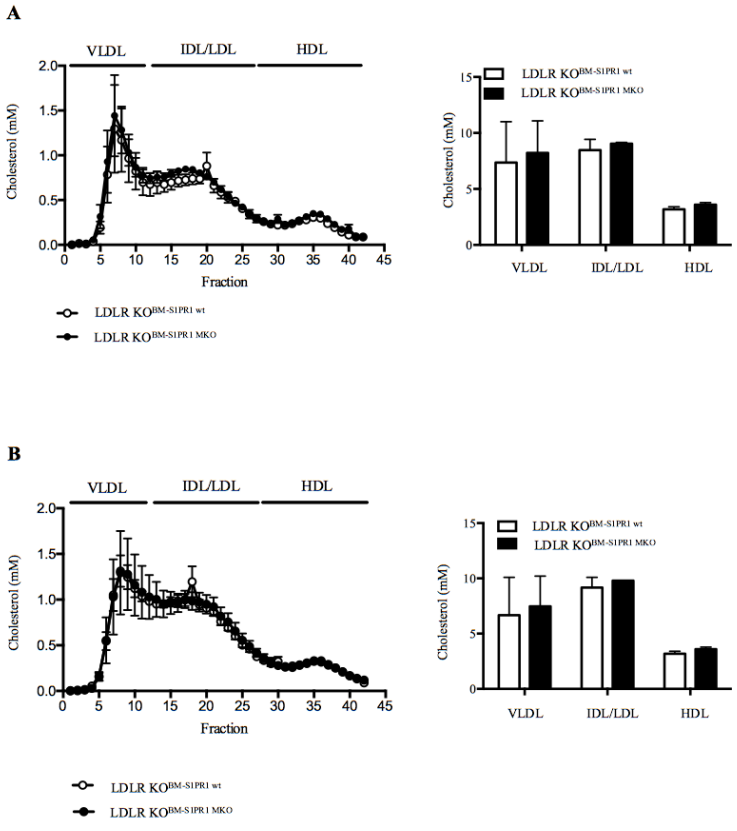

Supplementary Figure 3.10: Relative expression of macrophage SR-B1 mRNA in different mouse strains

Mouse peritoneal macrophages form WT, S1PR1$^{wt/wt}$ and S1PR1^{MKO} mice were isolated and RNA extracted. Quantitative real time PCR from total cDNA was performed as described in supplementary materials and methods. GAPDH was used as an internal control and the relative expression of SR-B1 was quantified relative to WT mice. Results are expressed as mean ± SEM (n=3 mice per genotype).

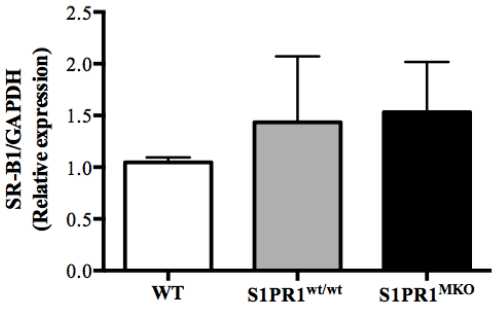

Chapter 4

Role of BH3-only protein BIM on macrophage apoptosis and necrotic core formation in atherosclerosis

Author list: Leticia Gonzalez, Pei Yu and Bernardo L. Trigatti.

Foreword:

This chapter continues to explore the role of HDL on preventing macrophage apoptosis, with emphasis on the role of the pro-apoptotic protein BIM as a downstream target of HDL and also the role of BIM in atherosclerosis development. We first start by showing that apoA1 deficiency renders LDLR KO mice more prone to atherosclerosis and necrotic core formation. Then, we were able to show that BIM deficiency in macrophages protects them against apoptosis and that HDL cannot further protect in the absence of BIM. Our data also suggests that HDL might be altering BIM protein levels instead of affecting its transcriptional levels. In the context of reduced circulating levels of HDL, BIM deficiency in the bone marrow compartment resulted in a reduction on both atherosclerotic plaque and necrotic core size.

This manuscript will be submitted for publication late 2016. Experiments were designed by Leticia Gonzalez and Pei Yu with guidance by Bernardo L. Trigatti. All the

data presented is the result of the combined work of Pei Yu and Leticia Gonzalez. Both authors contributed to animals work and sample collection equally. Pei Yu collected and analyzed the *in vitro* data, blood cell data and the atherosclerosis data. Leticia Gonzalez collected and analyzed the plasma data, gravimetric data and the TUNEL data. All data was interpreted under the guidance of Bernardo L. Trigatti. This version of the manuscript was written by Leticia Gonzalez with guidance from Bernardo L. Trigatti.

4.1 Abstract

Objective: Low levels of HDL cholesterol and apoA1 in circulation have been identified as risk factors for atherosclerosis development. Macrophage apoptosis had been identified as a major contributor towards necrotic core formation and the transition towards unstable plaques. Several factors have been suggested to induce macrophage apoptosis in the context of the atherosclerotic plaque, including endoplasmic reticulum (ER) stress and oxidized LDL, each of these factors are known to activate the pro-apoptotic protein BIM. HDL has been shown to protect cells against both ER stress- and oxidized LDL-induced apoptosis, suggesting that it might do so by manipulating BIM levels.

Methods and results: To test if HDL protected macrophages against apoptosis by manipulating intracellular levels of BIM, and to identify the role of BIM on atherosclerotic development, we first induced apoptosis in BIM KO macrophages. Macrophages lacking BIM were significantly protected against apoptosis and treatment with HDL was not able to further increase protection. HDL treatment was also able to reduce BIM protein levels in stressed macrophages, with no changes in mRNA hinting at post-translational effects. *In vivo*, BIM deficiency in the bone marrow compartment was associated with reduction in both atherosclerotic plaque and necrotic core sizes.

Conclusion: BIM deficiency in the bone marrow cells seems to be protective against atherosclerosis development, and HDL could be protecting macrophages against

apoptosis by manipulating BIM levels, however more studies are needed to fully understand the mechanism behind these observations.

Key words: atherosclerosis, high-density lipoprotein, BIM, macrophage apoptosis.

4.2 Introduction

High levels of low-density lipoprotein (LDL) cholesterol are associated with an increased risk for cardiovascular disease (1). In contrast, high-density lipoprotein (HDL) cholesterol levels are negatively correlated with the risk for coronary heart disease (CHD) (1). Likewise the plasma levels of apolipoprotein (apo) A1, the main protein component of HDL, are inversely associated with CHD risk (2). ApoA1 plays an important role in reverse cholesterol transport and it can mediate some of the atheroprotective actions of HDL (3). Reconstituted HDL containing apoA1 reduced vascular cell adhesion molecule 1 (VCAM-1) (4). Also, apoA1 administration to mice and humans prevented LDL oxidation (5). Studies have shown that a low level of apoA1 is an independent risk factor for CHD in patients not displaying the major risk factors like HDL cholesterol lower than 35 mg/dl (6). Low levels of apoA1 are also found in patients that survive myocardial infarction, even though HDL cholesterol levels were unchanged (7). More recently, the apoA1-75A allele was shown to be associated to lower risk of developing coronary artery disease due to an increase in serum concentration of apoA1 and HDL cholesterol (8). Overexpression of apoA1 in animal models has consistently been shown to have anti-

atherogenic effects. Hepatic overexpression of human apoA1 in mice reduced atherosclerosis in C57BL/6 mice fed an atherogenic diet (9) and apoE deficient mice (apoE KO) (10; 11). Regression of pre-established plaques due to liver expression of human apoA1 has also been reported in LDL receptor deficient mice (LDLR KO) (12).

Apoptosis during the course of atherosclerosis is a prominent event shaping plaque formation and contributing to necrotic core formation (13). Free cholesterol accumulation in foam cells has been suggested as one of the main mechanisms behind macrophage apoptosis in the atherosclerotic plaque (14). Accumulation of unesterified cholesterol in the cells alters the endoplasmic reticulum (ER) physicochemical properties causing ER stress (15). Atherosclerotic plaques from both humans and animals express markers in ER stress at different stages of plaque development (16; 17). Different mechanisms are involved in ER stress-induced apoptosis in macrophages. Prolonged expression of the ER chaperone CCAAT/enhancer binding protein homologous protein (CHOP) reportedly induces ER oxidase 1 α (ERO1α), increasing cytosolic calcium and triggering apoptosis (18). CHOP-induced expression of DNA damage-inducible protein 34 (GADD34) further increases protein translation due to de-phosphorylation of the eukaryotic initiation factor 2α (eIF2α), worsening ER stress and inducing apoptosis (19). Additionally, CHOP up-regulates the expression of the pro-apoptotic proteins p53 upregulated modulator of apoptosis (PUMA) and the BCL-2 homology domain 3 (BH3)-only protein, B-cell lymphoma 2 interacting mediator of cell death (BIM), leading to mitochondria-dependent apoptosis (20; 21). BIM is a member of the BH3-only family of pro-apoptotic proteins (22). BH3-only proteins respond to cell death signaling by

releasing the inhibition of Bcl-2-associated X protein (Bax) and Bcl-2 homologous antagonist/killer (Bak) by the pro-survival members of the B-cell lymphoma 2 (Bcl-2) family (22). BIM's pro-apoptotic capacity is controlled at the transcriptional and post-transcriptional levels. Apoptotic stimuli have been reported to induce BIM transcription through the activation of the forkhead-like transcription factor forkhead box O3 (FOXO3a) in several cell types including osteoblasts and hepatocytes (23; 24). On the other hand, in cells stimulated with growth factors BIM can be inactivated through extracellular signal-regulated kinases (ERK)-mediated phosphorylation, targeting BIM for proteasomal degradation (25-27).

Modified lipoproteins- including oxidized LDL (oxLDL)- are initiators of the development of atherosclerosis through the formation of macrophage foam cells (28). Oxysterols, the products of cholesterol oxidation found in oxLDL, are recognized as inducers of monocyte/macrophage apoptosis due to the activation of the mitochondrial death pathway (29). In this context, Rusiñol and colleagues demonstrated that oxysterol treatment of a macrophage-like cell line induced the degradation of AKT, up-regulating BIM among other effects (29). HDL has been shown to both inhibit LDL oxidation and also to prevent the pro-inflammatory effects triggered by oxLDL (30). HDL also prevented oxLDL-induced endothelial cell death by blocking CHOP activation (31). Finally, data from our laboratory suggests that HDL could protect macrophages from apoptosis by decreasing BIM levels (32). The aim of the present study is to study whether HDL protects macrophages by inducing changes in BIM levels and to assess the

impact of inactivation of BIM in bone marrow derived cells on atherosclerosis development.

4.3 Materials and methods

4.3.1 Materials

HDL was purchased from Alfa Aesar (Ward Hill, MA, USA). All other chemicals were purchased from Sigma Aldrich (St. Louis, Missouri, USA) unless indicated otherwise.

4.3.2 Mice

All procedures involving animals were approved by the McMaster University Animal Research Ethics Board and were in accordance with guidelines of the Canadian Council of Animal Care. All animals with the exception of BIM KO mice were bred and housed at the TaARI animal facility at McMaster University under controlled light (12 hours light/dark cycle) and temperature conditions, and had free access to normal chow diet (Harlan Teklad TD2918, Madison, WI, USA) and water. BIM deficient (BIM KO; B6.129S1-Bcl2l11$^{tm1.1Ast}$/J) mice were purchased from Jackson Laboratories (Bar Harbor, Maine, USA). ApoA1 deficient (apoA1 KO; B6.129P2-Apoa1^{tm1Unc}/J) used to generate apoA1/LDLR double knockout (dKO) mice were obtained from Jackson Laboratories

(Bar Harbor, Maine, USA). ApoA1 KO mice were bred to LDLR KO mice; double heterozygous offspring were bred back to LDLR KO mice to generate apoA1$^{+/-}$/LDLR$^{-/-}$ mice, which were intercrossed to generate apoA1$^{-/-}$/LDLR$^{-/-}$ (apoA1/LDLR dKO) mice. These were maintained by breeding homozygous mutant mice. For atherosclerosis and necrotic core formation studies, apoA1/LDLR dKO mice were placed on a diet containing 21% butter fat and 0.15% cholesterol (HF diet; Dyets Inc. 112286) for 10 weeks before harvest. After completion of the feeding period, mice were fasted for 4 hours prior to anesthesia and euthanasia. Blood samples were collected by cardiac puncture and tissues were perfused with heparinized saline (10 U/mL) followed by 10% formalin. Hearts were harvested, weighed and fixed overnight in 10% formalin prior to embedding in Cryomatrix (Thermo Fisher Scientific, Ottawa, Canada).

4.3.3 Cell preparation and cell culture

For *in vitro* experiments, mice were injected with 10% thioglycollate and at day 4 post-injection they were anesthetized and euthanized. Resident peritoneal macrophages were isolated by lavage in phosphate-buffered saline (PBS) containing 5 mM ethylenediaminetetraacetic acid (EDTA), centrifuged at 500xg and resuspended in Dulbecco's modified Eagle Medium (DMEM) supplemented with 3% newborn calf lipoprotein deficient serum (NCLPDS), 2 mM L-glutamine, 50 μg/ml penicillin and 50 U/ml streptomycin.

4.3.4 Bone marrow transplantation

Bone marrow (BM) was flushed out of femurs and tibias from male BIM KO or control wild type (WT) mice with Iscove's Modified Dulbecco's media (Gibco, Thermo Fisher, Ottawa, ON, Canada) containing 2% heat inactivated fetal bovine serum (FBS) supplemented with 2 mM L-glutamine, 50 μg/ml penicillin and 50 U/ml streptomycin. Recipient LDLR KO mice (10-12 weeks old, males) were exposed to 1400 rad of irradiation from a ^{137}Cs source using a Gammacel 3000/small animal irradiator. BM (3 x 10^6 cells/mouse) was injected by retro-orbital injection. Mice were allowed to recover for 4 weeks before being placed on the HF diet for 10 weeks as described above. After completion of the feeding period, mice were fasted for 4 hours prior to anesthesia and euthanasia. Heparinized blood was collected by cardiac puncture and plasma was obtained by centrifugation at 4000 rpm. Tissues were collected after in situ perfusion with 10 U/ml heparinized saline followed by 10% formalin, immersion fixed overnight in 10% formalin and embedded in Shandon Cryomatrix (Thermo Fisher Scientific, Ottawa, ON, Canada). Plasma and tissue samples were stored at -80 C until further analysis.

4.3.5 Plasma analysis

Plasma was obtained by centrifugation of blood at 4000 rpm for 15 minutes and stored at -80°C until further analysis. Commercial enzymatic assays were used to determine total cholesterol (Infinity Cholesterol Reagent, Thermo Fisher Scientific), free cholesterol

(Free Cholesterol E, Wako Diagnostics, Mountain view, CA, USA), triglycerides (L-type Triglyceride M, Wako Chemicals, Richmond, VA, USA) and HDL-Cholesterol (HDL-cholesterol E, Wako Diagnostics, Mountain view, CA, USA) in plasma, following the manufacture's protocols. Non-HDL cholesterol was calculated as the difference between total cholesterol and HDL cholesterol measurements. Cholesteryl ester levels were calculated as the difference between total cholesterol and free cholesterol measurements for each sample. Plasma glucose was measured using a commercial glucometer (Contour meter, Bayer).

4.3.6 Enzyme-linked immunosorbent assay

Plasma levels of interleukin (IL)-6 were measured using the ELISA Max Deluxe kit (BioLegend, San Diego, CA, USA).

4.3.7 Histology

Transverse cryosections of the aortic sinus (10 μm) were collected and stained with oil red O (ORO) to detect lipid deposition. Aortic sinus atherosclerosis was measured as previously described using quantitative morphometry with ImageJ software (33). For necrotic core sizes, aortic sinus cryosections were stained with hematoxylin/eosin (H&E) stain. The necrotic core area was defined as the a-nuclear and a-cellular area within the plaque and was normalized against the atherosclerotic plaque area. All images were

collected with a Zeiss Axiovert 200M inverted fluorescence microscope with a 5X objective (Carl Zeiss Canada Ltda., Toronto, Canada).

4.3.8 Immunofluorescence

For *in vitro* apoptosis experiments, macrophages were treated with HDL (50 μg/ml) in the presence or not of tunicamycin (TN, 10 μg/ml) for 24 hours at 37°C. Media was removed and cells were fixed with paraformaldehyde. Apoptosis was detected by staining macrophages with a rabbit anti-mouse cleaved caspase-3 antibody (1:1000; Cell Signaling Technology, Danvers, MA, USA), followed by anti-rabbit Alexa-488 secondary antibody (Life Technologies Inc, Burlington, ON, Canada). Nuclei were visualized with 4',6'-diamidino-2-plenylindole (DAPI). All images were captured using a Zeiss Axiovert 200M inverted fluorescence microscope with a 40 x objective (Carl Zeiss Canada Ltda., Toronto, Canada).

For detection of apoptosis in the atherosclerotic plaque, 10 μm cryosections were stained using the ApopTag In situ apoptosis detection kit (Millipore, Etobicoke, Canada). Nuclei were visualized with DAPI. All images were captured using a Zeiss Axiovert 200M inverted fluorescence microscope with a 20 x objective (Carl Zeiss Canada Ltda., Toronto, Canada). Numbers of apoptotic cells were normalized to atherosclerotic plaque area.

4.3.9 Real time PCR

Macrophages were treated with HDL (50 μg/ml) in the presence or not of tunicamycin (TN, 10 μg/ml) or thapsigargin (Thap, 5 mM) for 24 hours at 37°C. Total RNA was extracted from macrophages using the RNeasy Mini kit (Qiagen Inc., Toronto, ON, Canada) and quantified using a SpectraMax Plus384 spectrophotometer (Molecular Devices, Sunnyvale, California, USA). cDNA was obtained by reverse transcription from 1 μg of total RNA using the QuantiTec reverse transcription Kit (Qiagen Inc., Toronto, ON, Canada). Quantitative real time PCR was performed in an Applied Biosystems 7300 Real Time PCR system (Applied Biosystems, Foster City, California, USA) under default conditions. Primers used were as follow: BIM (forward) 5'-CGACAGTCTCAGGAGGAAC-3', (reverse) 5'-CCTTCTCCATACCAGACGCA-3' (34); GAPDH (forward) 5'-ACCACAGTCCATGCCATCAC-3', (reverse). All samples were run in triplicates and BIM expression in treated cells was compared to control samples and normalized to GAPDH expression.

4.3.10 SDS-PAGE and immunoblotting

Macrophages were treated with HDL (50 μg/ml) in the presence or not of tunicamycin (TN, 10 μg/ml) or thapsigargin (Thap, 5 mM) for 24 hours at 37°C. Proteins were collected in RIPA buffer supplemented with protease inhibitors (1mM PMSF, 1 μg/ml pepstatin A, 1 mg/ml leupeptin, 2 μg/ml aprotinin). Protein concentration was determine

using the BCA protein assay and 30 μg of protein were separated by dodecylsulfate-12% acrylamide gel electrophoresis (SDS-PAGE) and electrophoretically transferred to polyvinyldifluoride (PVDF) membranes. Membranes were blocked with 5% skim milk in TBST buffer (0.1% tween-20) followed by incubation with a rabbit anti-mouse BIM antibody (Cell Signaling Technology, Danvers, MA, USA). After incubation, membranes were washed and incubated with a horseradish peroxidase (HRP)-conjugated goat anti-rabbit antibody (Jackson Immunoresearch laboratory, West Grove, Pennsylvania, USA). HRP activity was detected using the Amersham Enhanced Chemiluminescence (ECL) kit (GE Healthcare Life Sciences Baie d'Urfe Quebec, Canada) and band intensity was measured using a Gel Doc imaging system (Bio-Rad laboratories, Hercules, California, USA).

4.3.11 Blood cell analysis

Blood was collected by cheek puncture from a subset of BMT animals prior to harvest. $CD11b^+$ (Rat anti-mouse CD11b antibody, APC conjugate; Life Technologies, Carlsbad, CA, USA), $B220^+$ (anti-human/mouse CD45R PerCP-Cyanine5.5; eBioscience, San Diego, CA, USA) and $CD3^+$ (FITC rat anti-mouse CD3 molecular complex; BD Pharmigen, San Jose, CA, USA) cells were assessed by flow cytometry on a BD LSR II flow cytometer. Red blood cells and dead cells were excluded from the analysis based on forward and side scatter plots.

4.3.12 Statistical analysis

Results are presented as mean ± SEM. Data was subjected to the D'Agostino & Pearson omnibus normality test prior to statistical analysis. Data fitting a normal distribution were compared using the Student's T test. If data did not pass the normality test, then it was analyzed using the Mann Whitney U test. For comparisons between more than two groups, data was analyzed by two-way ANOVA followed by the Sidak's multiple comparison test. All data analysis was done using the PRISM software (GraphPad Software Inc, La Jolla, CA, USA). $P<0.05$ was considered to be significant.

4.4 Results

4.4.1 Effect of macrophage BIM deficiency on tunicamycin-induced apoptosis

BIM plays a central role in oxysterols-induced apoptosis in macrophages (29). BIM is also activated in endoplasmic reticulum (ER) stress in different cells types including pancreatic islets, C2C12 murine myoblast cells and macrophages (20; 35; 36). Considering this, we decided to test if BIM was involved in ER-stress induced apoptosis in macrophages. To do so, mouse peritoneal macrophages from BIM KO and WT mice were isolated and treated with TN (10 μg/ml) in the presence or not of HDL (50 μg/ml) for 24 hours. WT macrophages and BIM KO macrophages show now difference in apoptosis susceptibility under control and HDL-treated conditions (Figure 4.1). TN

treatment resulted in dramatically increased levels of cleaved caspase-3 staining in WT macrophages, while co-incubation with HDL was able to significantly protect them. Macrophage BIM deficiency rendered cells significantly resistant and co-incubation with HDL did not further protect macrophages against TN-induced activation of caspase-3 (figure 4.1). Together, these results confirm that BIM plays an important role in the activation of apoptotic pathways by TN in macrophages.

Figure 4.1: Effect of BIM deficiency on tunicamycin-induced apoptosis in macrophages

Thioglycollate-elicited mouse peritoneal macrophages from WT and BIM KO mice were cultured overnight in 3% NCLPDS DMEM. The next day, cells were incubated with tunicamycin (10 μg/ml) in the presence or absence of HDL (10 μg/ml) for 24 hours. Cells were fixed in 4% paraformaldehyde and cell apoptosis was detected with a primary antibody against cleaved caspase-3 followed by a secondary antibody conjugated to Alexa 488 (green). DAPI was used as nuclear counterstain (blue). **A.** Representative images of macrophages stained for cleaved caspase-3 (40 x objective, scale bar: 20 μm). **B.** Quantification of cleaved caspase-3 positive cells (n=3). Results are shown as mean ± SEM (***$p<0.001$).

A

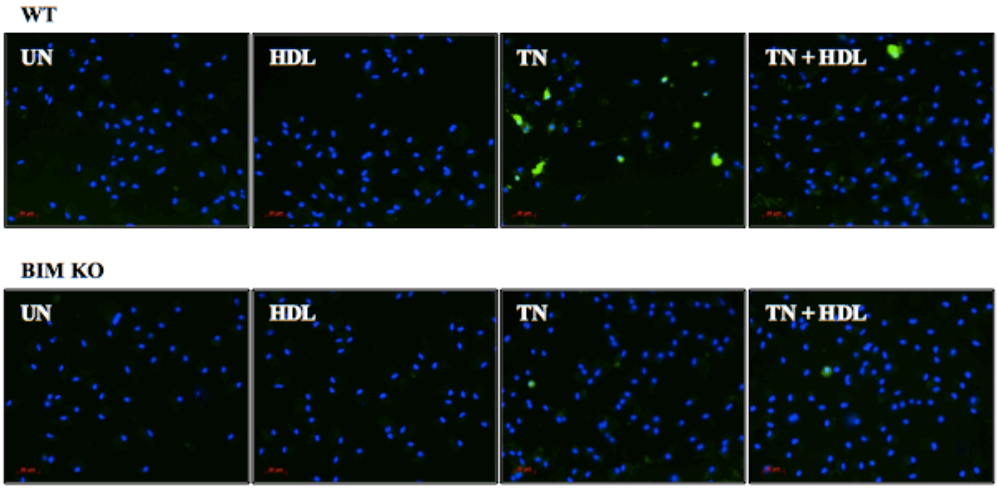
WT
UN
HDL
TN
TN + HDL
BIM KO
UN
HDL
TN
TN + HDL

B

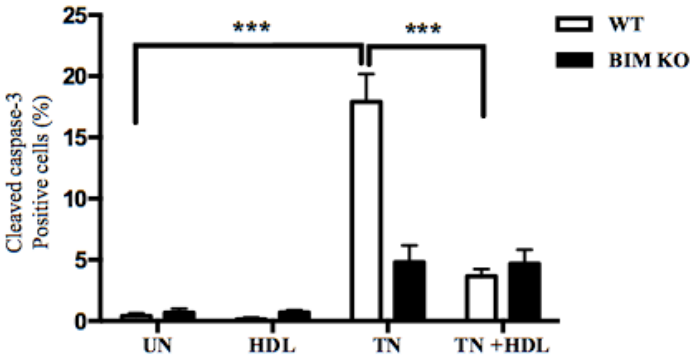
Cleaved caspase-3
Positive cells (%)
25
20
15
10
5
0
***
***
WT
BIM KO
UN
HDL
TN
TN +HDL

4.4.2 Effect of HDL-treatment on BIM expression in macrophages exposed to ER stress inducing agents

HDL has been reported to protect cells from ER stress-induced apoptosis without restoring ER functionality (37). To test whether changes in BIM levels are involved in HDL-mediated protection against apoptosis, WT peritoneal macrophages were incubated with TN or Thap in the presence or absence of HDL and proteins were collected for SDS-PAGE analysis. Figure 4.2A shows a blot for BIM and Mcl-1, with β-actin as the loading control. When macrophages were co-incubated with TN and HDL, a clear reduction in BIM levels can be seen. Similarly, HDL can also reduce BIM levels in cells treated with Thap. No significant changes in Mcl-1 were detected in any of the conditions tested. To verify if the reduction in BIM levels was associated with a reduction in *bim* transcription, mouse peritoneal macrophages were treated as above and total RNA was isolated for RT-PCR analysis of BIM and GAPDH transcript levels. HDL did not induce significant changes in *bim* transcription levels compared to TN- and Thap-treated conditions (figure 4.2B). Our results, though preliminary, suggest that HDL does not affect BIM gene expression but rather BIM protein levels.

Figure 4.2: Effect of HDL on BIM protein and mRNA levels in macrophages treated with tunicamycin and thapsigargin

Thioglycollate-elicited mouse peritoneal macrophages from WT mice were incubated with tunicamycin (10 μg/ml) or thapsigargin (5 μM) in the presence or not of HDL (10 μg/ml) for 24 hours. **A.** Proteins were collected in RIPA buffer (10 mM Tris-Cl pH8, 1 mM EDTA, 1 % Triton X-100, 0.1 % sodium deoxycolate, 0.1 % SDS, 140 mM NaCl) and separated by SDS-polyacrylamide gel electrophoresis (SDS-PAGE, 12% acrylamide) and transferred to a polyvinylidene fluoride (PVDF) membrane. Membranes were incubated with primary antibody overnight (BIM, Mcl-1, β-actin, 1:1000, Cell signaling) and bands were detected by chemiluminescence (n=1). **B.** Total RNA was collected using a commercial RNA extraction kit (RNeasy, Qiagen). RNA concentration was determined by absorbance and cDNA was prepared. BIM levels of expression were evaluated by real time PCR (n=3). Results are shown as mean ± SEM.

A

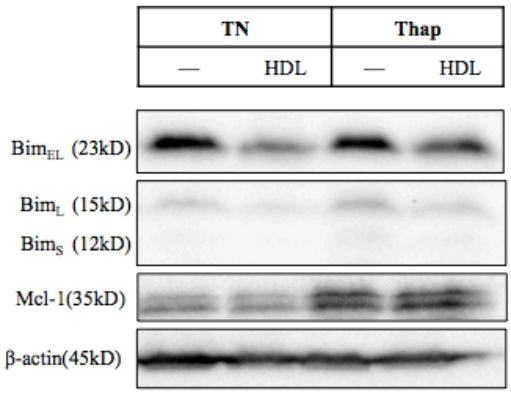
TN
Thap
—
HDL
—
HDL
Bim$_{EL}$ (23kD)
Bim$_{L}$ (15kD)
Bim$_{S}$ (12kD)
Mcl-1(35kD)
β-actin(45kD)

B

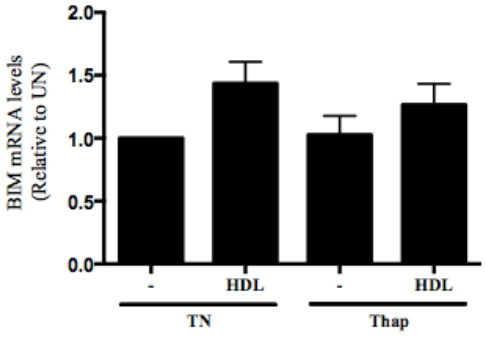
BIM mRNA levels
(Relative to UN)
2.0
1.5
1.0
0.5
0.0
-
HDL
-
HDL
TN
Thap

4.4.3 Effect of ApoA1 deficiency on plasma parameters in LDLR KO mice

To test if apoA1 deficiency, and the consequent reduction in HDL levels, would impact atherosclerosis development in LDLR KO mice, we fed LDLR KO and apoA1/LDLR dKO (referred to as ALdKO) mice a HF diet for 10 weeks before tissue and blood samples were collected. As expected, ALdKO mice fed a HF diet exhibited a 62% decrease in HDL-cholesterol compared to HF-diet fed control LDLR KO mice (Table 4.1). ALdKO mice fed a HF diet also showed a significant decrease in total cholesterol, unesterified cholesterol, cholesterol esters and non HDL-cholesterol while triglyceride levels remained unchanged (Table 4.1). No significant differences in IL-6 and glucose levels were found between HF diet fed-LDLR KO and ALdKO mice.

Table 4.1: Plasma parameters in LDLR KO and ALdKO mice fed a high fat diet for 10 weeks

Plasma was prepared from blood collected by cardiac puncture from LDLR KO and ALdKO mice fed a HF diet for 10 weeks. Plasma lipids and cytokine and glucose levels were determined as described in materials and methods. Results are expressed as mean ± SEM. Sample size is indicated in parenthesis on the group column: a, $p<0.05$ vs LDLR KO; b, $p<0.001$ vs LDLR KO, Student's T test.

	LDLR KO (20)	ALdKO (22)
Total Cholesterol (mmol/l)	43.47 ± 2.61	33.32 ± 2.83[a]
Free Cholesterol (mmol/l)	13.38 ± 0.83	10.67 ± 0.94[a]
Cholesterol Ester (mmol/l)	30.09 ± 1.97	22.65 ± 1.99[a]
Triglycerides (mmol/l)	3.55 ± 0.35	3.54 ± 0.62
HDL-cholesterol (mmol/l)	2.91 ± 0.20	1.10 ± 0.11[b]
Non HDL-cholesterol (mmol/l)	40.56 ± 2.58	32.22 ± 2.75[a]
IL-6 (pg/dl)	43.72 ± 13.52	62.41 ± 17.04
Glucose (mM)	12.07 ± 0.58	10.37 ± 0.93

4.4.4 Effect of ApoA1 deficiency on HF-diet induced atherosclerosis in LDLR KO mice

To test the effect of a lack of apoA1 on atherosclerosis development, ALdKO mice and LDLR KO mice fed a HF diet were euthanized after 10 weeks after the initiation of HF diet feeding. Figure 4.3A and 4.3B show representative images of atherosclerotic plaques in the aortic sinus of control LDLR KO and ALdKO mice. ApoA1 deficiency significantly increased the average size of the aortic sinus atherosclerotic plaque in LDLR KO mice fed a HF diet compared to control LDLR KO mice under the same feeding conditions (Figure 4.3C). Larger necrotic cores were also found in ALdKO mice fed a HF diet, compared to control HF-diet fed LDLR KO (Figure 4.3D-F). No differences were detected in numbers of apoptotic cells in the aortic sinus atherosclerotic plaque from the two groups of mice analyzed (Figure 4.3G-I). Altogether, our results confirm that ApoA1 deficiency is associated with lower levels of HDL cholesterol and the development of larger atherosclerotic plaques with bigger necrotic cores in the aortic sinus of HF diet fed LDLR KO mice.

Figure 4.3: Effect of ApoA1 deficiency on atherosclerosis and necrotic core development in LDLR KO mice fed a high fat diet

LDLR KO and ALdKO (ApoA1/LDLR dKO) mice were fed a high fat diet for 10 weeks before analysis (n=20-22). **A.** Cross sections from the aortic sinus of fixed hearts were collected. Representative images of oil red O-stained aortic sinus cryosections of LDLR KO and ALdKO mice are shown (5 x objective, scale bar: 100 μm). Plaque area is expressed in μm^2. **B.** Representative images of hematoxylin and eosin-stained aortic sinus cryosections of LDLR KO and ALdKO mice are shown (5 x objective, scale bar: 100 μm). Relative necrotic core area was expressed as percent of total plaque area. **C.** Representative images of TUNEL/DAPI-stained aortic sinus cryosections of LDLR KO and ALdKO mice (20 x objective, scale bar: 50 μm) and the respective quantification of TUNEL-positive nuclei per plaque area are shown (n=10). Results are shown as scatter dot plot (lines: mean ± SEM; *$p<0.05$, **$p<0.01$, Student's T test).

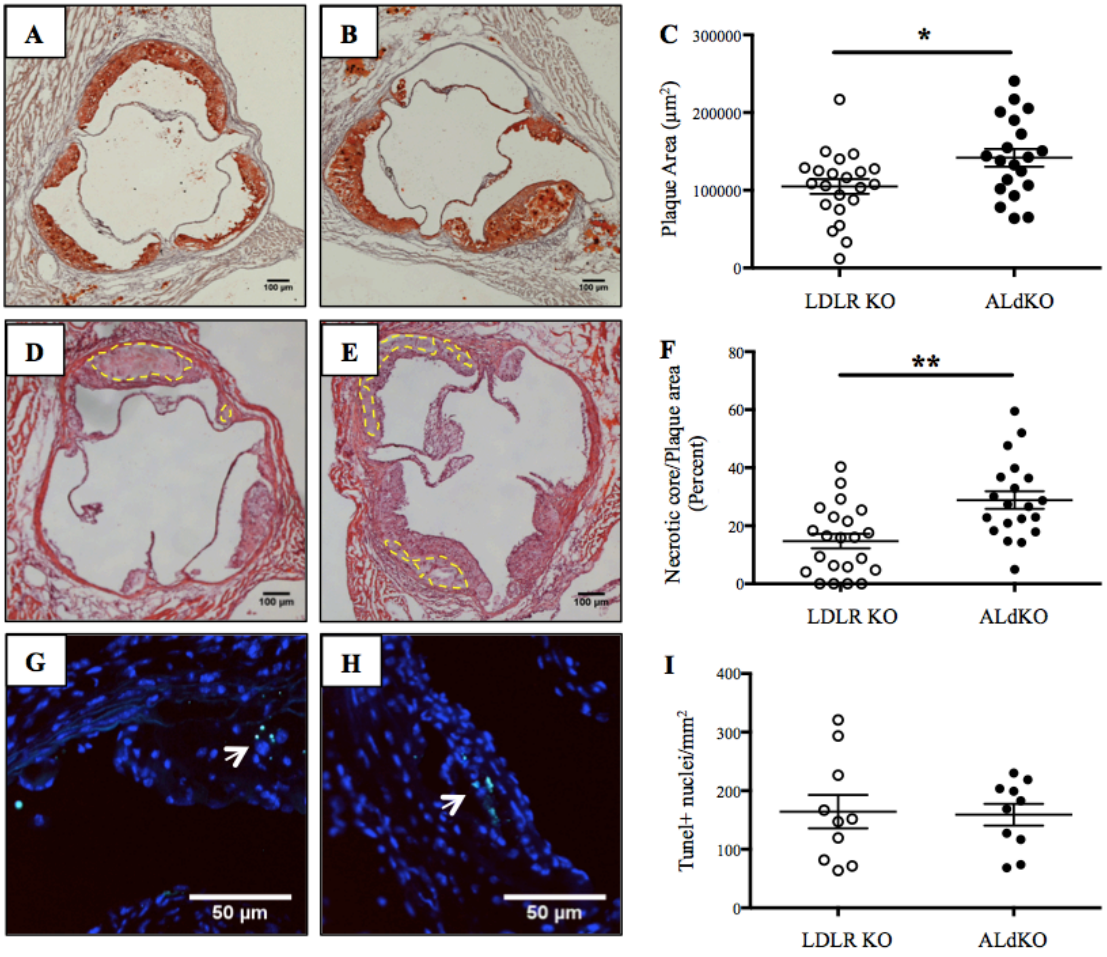
A
B
D
E
G
H
100 µm
50 µm
C
Plaque Area (µm²)
300000
200000
100000
0
*
LDLR KO
ALdKO
F
Necrotic core/Plaque area (Percent)
80
60
40
20
0
**
LDLR KO
ALdKO
I
Tunel+ nuclei/mm²
400
300
200
100
0
LDLR KO
ALdKO

4.4.5 Effect of BM BIM deficiency on plasma lipids in HF-diet fed ALdKO mice

To test if BIM influenced atherosclerosis development, we used bone marrow (BM) transplantation to generate ALdKO mice that lacked BIM exclusively in BM derived cells. Irradiated ALdKO mice were transplanted with BM from either WT (referred to as $ALdKO^{BM\text{-}WT}$) or BIM KO mice (referred to as $ALdKO^{BM\text{-}BIM\ KO}$) and atherosclerosis was induced by feeding BMT mice a HF diet. HF diet-fed $ALdKO^{BM\text{-}BIM\ KO}$ exhibited a ~ 45 % reduction in total cholesterol compared to HF diet-fed $ALdKO^{BM\text{-}WT}$ control mice (Table 4.2). Significant reductions in unesterified cholesterol, cholesterol esters, triglycerides and non-HDL cholesterol were also detected in the $ALdKO^{BM\text{-}BIM\ KO}$ group compared to $ALdKO^{BM\text{-}WT}$ controls, whereas no differences were detected in HDL cholesterol (Table 4.2).

Table 4.2: Plasma lipids in ALdKO$^{BM\text{-}WT}$ and ALdKO$^{BM\text{-}BIM\ KO}$ mice fed a high fat diet

Plasma was prepared from blood collected by cardiac puncture from HF diet fed-ALdKO$^{BM\text{-}WT}$ and ALdKO$^{BM\text{-}BIM\ KO}$ mice at the moment of harvest. Plasma lipids were determined as described in materials and methods. Results are expressed as mean ± SEM. Sample size is indicated in parenthesis on the group column: a, $p<0.01$; b, $p<0.001$.

	ALdKO$^{BM\text{-}WT}$ (13)	ALdKO$^{BM\text{-}BIM\ KO}$ (12)
Total Cholesterol (mmol/l)	30.62 ± 2.63	16.76 ± 1.81[b]
Free Cholesterol (mmol/l)	9.58 ± 0.61	5.33 ± 0.52[b]
Cholesterol Ester (mmol/l)	21.03 ± 2.15	11.42 ± 1.30[a]
Triglycerides (mmol/l)	5.24 ± 0.46	3.22 ± 0.36[a]
HDL-cholesterol (mmol/l)	1.28 ± 0.11	1.20 ± 0.13
Non HDL-cholesterol (mmol/l)	29.34 ± 2.61	15.56 ± 1.82[b]

4.4.6 Effect of BM BIM deficiency on atherosclerosis development in HF-diet fed ALdKO mice

Figure 4.4A and 4.4B shows representative images of atherosclerotic plaques in the aortic sinus of 10 week HF diet-fed ALdKO$^{BM\text{-}WT}$ and ALdKO$^{BM\text{-}BIM\ KO}$ mice. BIM deficiency in BM derived cells significantly reduced the average atherosclerotic plaque size in the ALdKO$^{BM\text{-}BIM\ KO}$ group compared the control ALdKO$^{BM\text{-}WT}$ fed the same diet (Figure 4.4C). Since BIM deficiency significantly protected macrophages against apoptosis (Figure 4.2), we tested the effect of BM BIM deficiency on necrotic core formation. To evaluate relative necrotic core size, area devoid of nuclei staining in ORO stained sections were measured and results were expressed as percent of plaque area. In figure 4.4, necrotic cores are outlined with a yellow dash line. BIM deficiency in the BM compartment reduced the absolute necrotic core size when compared with the ALdKO$^{BM\text{-}WT}$ group (not shown), however when normalized to plaque total cross sectional areas, there was a trend towards reduced relative necrotic core size in the mice with BM specific BIM deficiency which did not reach statistical significance ($p=0.0592$). Similarly, preliminary data on plaque apoptosis showed no significant differences in the numbers of apoptotic cells in the atherosclerotic plaques from both the ALdKO$^{BM\text{-}WT}$ and ALdKO$^{BM\text{-}BIM\ KO}$ groups (Figure 4.4D-F), although more samples need to be analyzed before a definitive conclusion can be drawn.

Figure 4.4: Effect of BIM deficiency in bone marrow-derived cells on atherosclerosis development in high fat diet-fed ALdKO mice

Irradiated ALdKO mice received bone marrow from either WT or BIM KO mice. Bone marrow transplanted mice were allowed to recover for 4 weeks before being fed a high fat diet for 10 weeks (n= 12-19). **A-B.** Cross sections from the aortic sinus of fixed hearts were collected. Representative images of oil red O-stained aortic sinus cryosections of ALdKO$^{BM\text{-}WT}$ and ALdKO$^{BM\text{-}BIM\ KO}$ mice (5 x objective, scale bar: 100 μm). **C.** Quantification of plaque area. Results are shown as scatter dot plot (lines: mean ± SEM). **p<0.01, Student's T test. **D**. Relative necrotic core area was expressed as percent of total plaque area (n=11-19). Results are shown as scatter dot plot (lines: mean ± SEM). P=0.0592, Student's T test. **E-F.** Cryosections were stained for apoptotic nuclei by TUNEL (green) and counterstained for nuclei with DAPI (blue). Representative TUNEL/DAPI-stained images of aortic atherosclerotic plaque sections from ALdKO$^{BM\text{-}WT}$ and ALdKO$^{BM\text{-}BIM\ KO}$ mice (20 x objective, scale bar: 50 μm). **G**. Quantification of TUNEL-positive nuclei per plaque area in mice fed the HF diet for 10 weeks (n=3-6). Results are shown as scatter dot plot (lines: mean ± SEM).

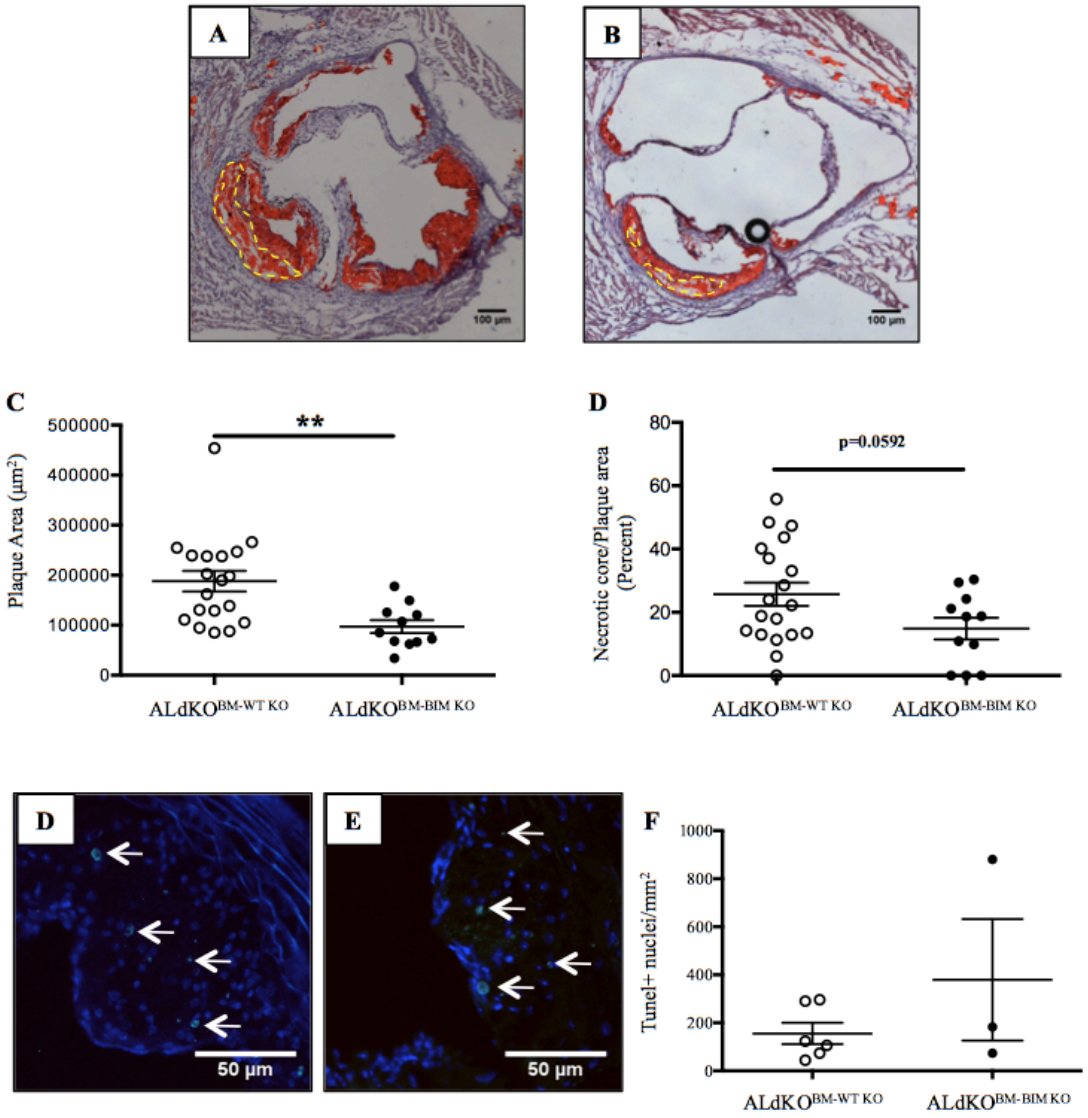
A
B
100 µm
100 µm
C
Plaque Area (µm²)
500000
400000
300000
200000
100000
0
**
ALdKO BM-WT KO
ALdKO BM-BIM KO
D
Necrotic core/Plaque area (Percent)
80
60
40
20
0
p=0.0592
ALdKO BM-WT KO
ALdKO BM-BIM KO
D
50 µm
E
50 µm
F
Tunel+ nuclei/mm²
1000
800
600
400
200
0
ALdKO BM-WT KO
ALdKO BM-BIM KO

4.4.7 Effect of BM BIM deficiency on white blood cell numbers and spleen size in HF-diet fed ALdKO mice

As previously mentioned, BIM is essential for the induction of apoptosis in hematopoietic cells (38). To test if inactivation of BIM in BM derived cells affected the numbers of circulating leukocytes in HF diet-fed ALdKO mice, we subjected white blood cells to flow cytometry analysis of CD11b, a marker of myeloid cells, cluster of differentiation 3 (CD3), a marker of T-lymphocytes and B220, a marker for B-lymphocytes. The average proportion of $B220^{+}$ cells was significantly increased by 23 % in $ALdKO^{BM\text{-}BIM\ KO}$ compared to $ALdKO^{BM\text{-}WT}$ control mice. A similar level of increase was observed in the average proportions of $CD3^{+}$ cells, but the difference was not statistically significant (Table 4.3). On the other hand, there was a 40 % reduction on the percentage of circulating $CD11b^{+}$ cells in $ALdKO^{BM\text{-}BIM\ KO}$ compared to $ALdKO^{BM\text{-}WT}$ control mice fed the same HF diet (Table 4.3). $ALdKO^{BM\text{-}BIM\ KO}$ mice also displayed larger spleens and increased SPW/BW ratio compared to the control $ALdKO^{BM\text{-}WT}$ mice (Table 4.4). The increase in spleen size might be related to an increase in circulating white blood cells.

Table 4.3: White blood cell numbers in ALdKO mice transplanted with WT and BIM KO bone marrow

Blood cells from HF diet fed-ALdKO$^{BM\text{-}BIM\ KO}$ and ALdKO$^{BM\text{-}WT}$ mice were analyzed by flow cytometry as described in Materials and Methods. Results are expressed as mean ± SEM. Sample size is indicated in parenthesis on the group column: a, $p<0.05$ vs ALdKO$^{BM\text{-}BIM\ KO}$, Mann Whitney test.

	ALdKO$^{BM\text{-}WT}$ (6)	ALdKO$^{BM\text{-}BIM\ KO}$ (3)
CD3$^+$ cells (%)	14.43 ± 0.95	17.47 ± 1.37
B220$^+$ cells (%)	53.72 ± 0.75	66.10 ± 2.59[a]
CD11b$^+$ cells (%)	33.45 ± 1.38	19.87 ± 2.07[a]

Table 4.4: Spleen size in ALdKO mice transplanted with WT and BIM KO bone marrow

Spleens from HF diet fed-ALdKO$^{BM\text{-}BIM\ KO}$ and ALdKO$^{BM\text{-}WT}$ mice were collected and weighed after 10 weeks on a high fat diet. Results are expressed as mean ± SEM. Sample size is indicated in parenthesis on the group column: a, $p<0.05$ vs ALdKO$^{BM\text{-}BIM\ KO}$, Mann Whitney test.

	ALdKO$^{BM\text{-}WT}$ (19)	ALdKO$^{BM\text{-}BIM\ KO}$ (12)
Body Weight (BW, g)	28.19 ± 0.63	25.83 ± 0.91[a]
Spleen Weight (SW, g)	0.102 ± 0.003	0.197 ± 0.012[b]
SW/BW	0.0040 ± 0.0002	0.0077 ± 0.0005[b]

4.5 Discussion

In the present study we show that ApoA1 deficiency results in the development of larger atherosclerotic plaques and necrotic cores in the aortic sinus of LDLR KO mice fed a HF diet, when compared to control LDLR KO mice fed the same diet. BIM deficiency significantly reduces macrophage susceptibility to apoptosis triggered by TN but HDL was not able to further reduce apoptosis levels in BIM KO cells. In the context of atherosclerosis development, BIM deficiency in BM derived cells was associated with protection against atherosclerosis development and smaller necrotic cores. Furthermore, preliminary data suggested that reduction in BIM protein levels but not *bim* expression might be involved in HDL's mechanism of protection against apoptosis.

In the mitochondria-dependent apoptotic pathway BH3-only proteins, including BIM, block the inhibitory action of pro-survival Bcl-2 proteins on Bax and Bak (22). BIM – along with PUMA – is also involved in controlling the death of activated T cells, a critical process for termination of immune responses (39). Moreover, BIM is critical in B-cell receptor (BCR)-mediated apoptosis of autoreactive B cells, an important step in the prevention of an autoimmune reaction (40). Our results show that BIM KO macrophages are protected against TN-induced apoptosis (figure 4.1). Similar results have been observed in BIM KO lymphocytes, which fail to undergo apoptosis under conditions of cytokine withdrawal (38). In the same context, cytokine deprivation in a pre-B cell line was associated with an increase in the intracellular levels of BIM (41). Our data also suggested that HDL could mediate macrophage protection against apoptosis by reducing

intracellular levels of BIM (figure 4.2). Previous studies have shown that phagocytosis-mediated apoptosis of macrophages involves up-regulation of BIM levels through the activation of Toll-like receptors (42). HDL has been reported to activate both AKT and MAPK signaling pathways in several cell types (43), including macrophages (44). Furthermore, HDL has been reported to induce cell survival and proliferation via activation of AKT signaling (45-47) and ERK1/2 (48). AKT activation has been reported to prevent cytokine withdrawal-mediated apoptosis by phosphorylating FOXO3a and inhibiting BIM expression in a murine pro-B cell line (41). Similarly, activation of ERK1/2 induced cell survival by phosphorylating BIM and targeting the protein for ubiquitination and proteasome degradation (25-27). These results together with ours suggest that HDL-mediated reduction of BIM levels in Thap- and TN-treated macrophages could be mediated by activation of one of these signaling pathways. Further experiments are required to corroborate this hypothesis.

Studies have demonstrated that apoA1 deficiency does not seem to be sufficient to cause atherosclerosis. ApoA1 KO mice fed a chow diet did not spontaneously develop atherosclerosis despite a clear reduction in HDL cholesterol levels (49). Even when challenged with an atherogenic diet, apoA1 KO mice will only develop small atherosclerotic lesions in the aortic sinus that are not significantly bigger than those found in wild type mice (49). In our study we decided to compare the impact of apoA1 deficiency – and the consequent reduction in HDL levels – in a pro-atherogenic background (LDLR KO) and under conditions where plasma cholesterol is significantly elevated, by feeding the animals a HF diet. Our data shows that apoA1 deficiency results

in reduced total cholesterol and HDL cholesterol levels compared with the control condition (Table 4.1). ApoA1 deficiency in transgenic mice expressing human ApoB (ApoA1 HuBTg) also correlated with a significant reduction in total cholesterol levels (50). Similar results were also reported in apoA1/LDLR dKO mice fed a diet consisting of 0.1% cholesterol and 10% palm oil for 16 weeks, where dKO mice presented significantly reduced total cholesterol levels compared to LDLR KO (51). Despite the reduction in circulating total cholesterol, apoA1 deficiency in LDLR KO mice significantly increased both atherosclerotic plaque and necrotic core sizes in the aortic sinus of mice fed a HF diet (Figures 4.3). ApoA1/LDLR dKO mice fed a chow diet were previously reported to develop significantly larger plaques compared to LDLR KO, although in this study levels of HDL cholesterol were relatively similar between both groups (52). ApoA1 HuBTg mice also developed increased atherosclerosis compared to HuBTg mice (50). Even though we detected an increase in necrotic core formation, there were no changes in the numbers of apoptotic cells in the aortic sinus atherosclerotic plaques from both groups (Figure 4.3). It is possible that the effect seen in atherosclerotic plaque and necrotic core formation are related to other anti-atherogenic properties of apoA1 – besides maintenance of HDL levels – such as its role in reverse cholesterol transport and anti-inflammatory properties (53).

BIM deficiency in BM transplanted apoA1/LDLR dKO mice fed a HF diet was associated with a reduction in total cholesterol levels due to reduced non-HDL cholesterol with no changes in HDL cholesterol (Table 4.2). ApoA1/LDLR dKO mice transplanted with BIM deficient BM also presented elevations in the percent of $CD3^+$ and $B220^+$ cells

in circulation (Table 4.3). Consistent with our results, Bouillet and colleagues first reported that BIM KO mice presented a significant increase in total number of B cells and mature T cells both in blood and spleen compartment (38). Along with increases in proportions of T and B cells, we also found that myeloid cells represent a reduced proportion of circulating leukocytes in apoA1/LDLR dKO mice lacking BIM in BM derived cells (Table 4.3). In contrast, others previously reported and increase in total numbers of circulating monocytes along with B and T lymphocytes in BIM KO mice (38). Additional work aimed at measurement of total leukocyte numbers in ALdKO$^{BM\text{-}BIM\ KO}$ and ALdKO$^{BM\text{-}WT}$ mice will resolve this discrepancy. The increased spleen sizes in ALdKO$^{BM\text{-}BIM\ KO}$ compared to ALdKO$^{BM\text{-}WT}$ mice (Table 4.4) are consistent with the increased spleen size of BIM KO mice previously reported and probably due to an increase in splenic leukocyte cell populations (38). The increased lymphocyte counts in the ALdKO$^{BM\text{-}BIM\ KO}$ mice may be responsible for the reduced levels of non-HDL cholesterol. Hypocholesterolemia has been previously described in leukemia patients – which present increased levels of white blood cells in circulation (54). The underlying mechanisms remain unclear, but may be related to elevated LDLR activity reported in leukemia cells (55; 56).

In early lesions, macrophage apoptosis and prompt clearance of dead cells limits plaque growth (57). As disease develops, defective clearance of apoptotic cells and the consequent accumulation of apoptotic macrophages promote plaque growth and necrotic core formation (57). Transplantation of Bax deficient bone marrow into LDLR KO mice reduced macrophage apoptosis and was associated with an increase in aortic root lesions

sizes (58). Likewise, ApoE KO mice lacking $p19^{Arf}$ - a cell cycle regulator- exhibit increased atherosclerosis and attenuated macrophage apoptosis (59). On the other hand, inactivation of the pro-survival protein apoptosis inhibitor of macrophage (AIM) in LDLR KO mice results in reduced atherosclerosis due to increased atherosclerosis due to increased macrophage apoptosis (60). In our hands, BIM deficiency in BM derived cells in apoA1/LDLR dKO mice was associated with reduced levels of atherosclerosis in the aortic sinus and smaller necrotic cores (Figure 4.4). Gautier and colleagues tested the effect of overexpressing human Bcl-2 in macrophages on an ApoE KO background and showed that inhibition of apoptosis at early stages (5 weeks on high fat diet) significantly increased atherosclerosis development; however after 15 weeks of diet lesions appeared significantly smaller when compared to ApoE KO mice (61). According to their data, the shift in response to atherosclerosis development would happen around 10 weeks of high fat diet feeding, which is consistent with our findings (61).

In summary, we have shown that HDL might be protecting macrophages from apoptosis by decreasing intracellular BIM levels. In the context of atherosclerosis, BIM deficiency in the bone marrow compartment positively impacts atherosclerosis development, reducing both atherosclerotic plaque and necrotic core size in apoA1/LDLR dKO fed a HF diet, suggesting that in the presence of low levels of circulating HDL, absence of BIM is protective.

4.6 References

1. Gordon T, Castelli WP, Hjortland MC, Kannel WB, Dawber TR: High density lipoprotein as a protective factor against coronary heart disease. The Framingham Study. *Am J Med* **62**:707-714, 1977.

2. Rader DJ, Hoeg JM, Brewer HB, Jr.: Quantitation of plasma apolipoproteins in the primary and secondary prevention of coronary artery disease. *Ann Intern Med* **120**:1012-1025, 1994.

3. Hoekstra M, Van Eck M: Mouse models of disturbed HDL metabolism. *Handb Exp Pharmacol* **224**:301-336, 2015.

4. Dimayuga P, Zhu J, Oguchi S, Chyu KY, Xu XO, Yano J, Shah PK, Nilsson J, Cercek B: Reconstituted HDL containing human apolipoprotein A-1 reduces VCAM-1 expression and neointima formation following periadventitial cuff-induced carotid injury in apoE null mice. *Biochem Biophys Res Commun* **264**:465-468, 1999.

5. Navab M, Hama SY, Cooke CJ, Anantharamaiah GM, Chaddha M, Jin L, Subbanagounder G, Faull KF, Reddy ST, Miller NE, Fogelman AM: Normal high density lipoprotein inhibits three steps in the formation of mildly oxidized low density lipoprotein: step 1. *J Lipid Res* **41**:1481-1494, 2000.

6. Francis MC, Frohlich JJ: Coronary artery disease in patients at low risk--apolipoprotein AI as an independent risk factor. *Atherosclerosis* **155**:165-170, 2001.

7. Franzen J, Fex G: Low serum apolipoprotein A-I in acute myocardial infarction survivors with normal HDL cholesterol. *Atherosclerosis* **59**:37-42, 1986.

8. Liao B, Cheng K, Dong S, Liu H, Xu Z: Effect of apolipoprotein A1 genetic polymorphisms on lipid profiles and the risk of coronary artery disease. *Diagn Pathol* **10**:102, 2015.

9. Rubin EM, Krauss RM, Spangler EA, Verstuyft JG, Clift SM: Inhibition of early atherogenesis in transgenic mice by human apolipoprotein AI. *Nature* **353**:265-267, 1991.

10. Plump AS, Scott CJ, Breslow JL: Human apolipoprotein A-I gene expression increases high density lipoprotein and suppresses atherosclerosis in the apolipoprotein E-deficient mouse. *Proc Natl Acad Sci U S A* **91**:9607-9611, 1994.

11. Paszty C, Maeda N, Verstuyft J, Rubin EM: Apolipoprotein AI transgene corrects apolipoprotein E deficiency-induced atherosclerosis in mice. *J Clin Invest* **94**:899-903, 1994.

12. Tangirala RK, Tsukamoto K, Chun SH, Usher D, Pure E, Rader DJ: Regression of atherosclerosis induced by liver-directed gene transfer of apolipoprotein A-I in mice. *Circulation* **100**:1816-1822, 1999.

13. Viola J, Soehnlein O: Atherosclerosis - A matter of unresolved inflammation. *Semin Immunol* **27**:184-193, 2015.

14. Maxfield FR, Tabas I: Role of cholesterol and lipid organization in disease. *Nature* **438**:612-621, 2005.

15. Li Y, Ge M, Ciani L, Kuriakose G, Westover EJ, Dura M, Covey DF, Freed JH, Maxfield FR, Lytton J, Tabas I: Enrichment of endoplasmic reticulum with cholesterol inhibits sarcoplasmic-endoplasmic reticulum calcium ATPase-2b activity in parallel with increased order of membrane lipids: implications for depletion of endoplasmic reticulum calcium stores and apoptosis in cholesterol-loaded macrophages. *J Biol Chem* **279**:37030-37039, 2004.

16. Myoishi M, Hao H, Minamino T, Watanabe K, Nishihira K, Hatakeyama K, Asada Y, Okada K, Ishibashi-Ueda H, Gabbiani G, Bochaton-Piallat ML, Mochizuki N, Kitakaze M: Increased endoplasmic reticulum stress in atherosclerotic plaques associated with acute coronary syndrome. *Circulation* **116**:1226-1233, 2007.

17. Zhou J, Lhotak S, Hilditch BA, Austin RC: Activation of the unfolded protein response occurs at all stages of atherosclerotic lesion development in apolipoprotein E-deficient mice. *Circulation* **111**:1814-1821, 2005.

18. Li G, Mongillo M, Chin KT, Harding H, Ron D, Marks AR, Tabas I: Role of ERO1-alpha-mediated stimulation of inositol 1,4,5-triphosphate receptor activity in endoplasmic reticulum stress-induced apoptosis. *J Cell Biol* **186**:783-792, 2009.

19. Marciniak SJ, Yun CY, Oyadomari S, Novoa I, Zhang Y, Jungreis R, Nagata K, Harding HP, Ron D: CHOP induces death by promoting protein synthesis and oxidation in the stressed endoplasmic reticulum. *Genes Dev* **18**:3066-3077, 2004.

20. Puthalakath H, O'Reilly LA, Gunn P, Lee L, Kelly PN, Huntington ND, Hughes PD, Michalak EM, McKimm-Breschkin J, Motoyama N, Gotoh T, Akira S, Bouillet P, Strasser A: ER stress triggers apoptosis by activating BH3-only protein Bim. *Cell* **129**:1337-1349, 2007.

21. Ghosh AP, Klocke BJ, Ballestas ME, Roth KA: CHOP potentially co-operates with FOXO3a in neuronal cells to regulate PUMA and BIM expression in response to ER stress. *PLoS One* **7**:e39586, 2012.

22. Akiyama T, Tanaka S: Bim: guardian of tissue homeostasis and critical regulator of the immune system, tumorigenesis and bone biology. *Arch Immunol Ther Exp (Warsz)* **59**:277-287, 2011.

23. Kawamura N, Kugimiya F, Oshima Y, Ohba S, Ikeda T, Saito T, Shinoda Y, Kawasaki Y, Ogata N, Hoshi K, Akiyama T, Chen WS, Hay N, Tobe K, Kadowaki T, Azuma Y, Tanaka S, Nakamura K, Chung UI, Kawaguchi H: Akt1 in osteoblasts and osteoclasts controls bone remodeling. *PLoS One* **2**:e1058, 2007.

24. Barreyro FJ, Kobayashi S, Bronk SF, Werneburg NW, Malhi H, Gores GJ: Transcriptional regulation of Bim by FoxO3A mediates hepatocyte lipoapoptosis. *J Biol Chem* **282**:27141-27154, 2007.

25. Ley R, Balmanno K, Hadfield K, Weston C, Cook SJ: Activation of the ERK1/2 signaling pathway promotes phosphorylation and proteasome-dependent degradation of the BH3-only protein, Bim. *J Biol Chem* **278**:18811-18816, 2003.

26. Akiyama T, Bouillet P, Miyazaki T, Kadono Y, Chikuda H, Chung UI, Fukuda A, Hikita A, Seto H, Okada T, Inaba T, Sanjay A, Baron R, Kawaguchi H, Oda H, Nakamura K, Strasser A, Tanaka S: Regulation of osteoclast apoptosis by ubiquitylation of proapoptotic BH3-only Bcl-2 family member Bim. *EMBO J* **22**:6653-6664, 2003.

27. Luciano F, Jacquel A, Colosetti P, Herrant M, Cagnol S, Pages G, Auberger P: Phosphorylation of Bim-EL by Erk1/2 on serine 69 promotes its degradation via the proteasome pathway and regulates its proapoptotic function. *Oncogene* **22**:6785-6793, 2003.

28. Lusis AJ: Atherosclerosis. *Nature* **407**:233-241, 2000.

29. Rusinol AE, Thewke D, Liu J, Freeman N, Panini SR, Sinensky MS: AKT/protein kinase B regulation of BCL family members during oxysterol-induced apoptosis. *J Biol Chem* **279**:1392-1399, 2004.

30. Elsoe S, Ahnstrom J, Christoffersen C, Hoofnagle AN, Plomgaard P, Heinecke JW, Binder CJ, Bjorkbacka H, Dahlback B, Nielsen LB: Apolipoprotein M binds oxidized phospholipids and increases the antioxidant effect of HDL. *Atherosclerosis* **221**:91-97, 2012.

31. Muller C, Salvayre R, Negre-Salvayre A, Vindis C: HDLs inhibit endoplasmic reticulum stress and autophagic response induced by oxidized LDLs. *Cell Death Differ* **18**:817-828, 2011.

32. Al-Jarallah A. Insights into the development of atherosclerosis and coronary artery disease: studies from gene targeted mice lacking the high density receptor, SR-BI.McMaster University, Hamilton, ON, Canada, 2012

33. Fuller M, Dadoo O, Serkis V, Abutouk D, MacDonald M, Dhingani N, Macri J, Igdoura SA, Trigatti BL: The effects of diet on occlusive coronary artery atherosclerosis and myocardial infarction in scavenger receptor class B, type 1/low-density lipoprotein receptor double knockout mice. *Arterioscler Thromb Vasc Biol* **34**:2394-2403, 2014.

34. Liang M, Russell G, Hulley PA: Bim, Bak, and Bax regulate osteoblast survival. *J Bone Miner Res* **23**:610-620, 2008.

35. Morishima N, Nakanishi K, Tsuchiya K, Shibata T, Seiwa E: Translocation of Bim to the endoplasmic reticulum (ER) mediates ER stress signaling for activation of caspase-12 during ER stress-induced apoptosis. *J Biol Chem* **279**:50375-50381, 2004.

36. Wali JA, Rondas D, McKenzie MD, Zhao Y, Elkerbout L, Fynch S, Gurzov EN, Akira S, Mathieu C, Kay TW, Overbergh L, Strasser A, Thomas HE: The proapoptotic BH3-only proteins Bim and Puma are downstream of endoplasmic reticulum and mitochondrial oxidative stress in pancreatic islets in response to glucotoxicity. *Cell Death Dis* **5**:e1124, 2014.

37. Puyal J, Petremand J, Dubuis G, Rummel C, Widmann C: HDLs protect the MIN6 insulinoma cell line against tunicamycin-induced apoptosis without inhibiting ER stress and without restoring ER functionality. *Mol Cell Endocrinol* **381**:291-301, 2013.

38. Bouillet P, Metcalf D, Huang DC, Tarlinton DM, Kay TW, Kontgen F, Adams JM, Strasser A: Proapoptotic Bcl-2 relative Bim required for certain apoptotic responses, leukocyte homeostasis, and to preclude autoimmunity. *Science* **286**:1735-1738, 1999.

39. Bauer A, Villunger A, Labi V, Fischer SF, Strasser A, Wagner H, Schmid RM, Hacker G: The NF-kappaB regulator Bcl-3 and the BH3-only proteins Bim and Puma control the death of activated T cells. *Proc Natl Acad Sci U S A* **103**:10979-10984, 2006.

40. Enders A, Bouillet P, Puthalakath H, Xu Y, Tarlinton DM, Strasser A: Loss of the pro-apoptotic BH3-only Bcl-2 family member Bim inhibits BCR stimulation-induced apoptosis and deletion of autoreactive B cells. *J Exp Med* **198**:1119-1126, 2003.

41. Dijkers PF, Birkenkamp KU, Lam EW, Thomas NS, Lammers JW, Koenderman L, Coffer PJ: FKHR-L1 can act as a critical effector of cell death induced by cytokine withdrawal: protein kinase B-enhanced cell survival through maintenance of mitochondrial integrity. *J Cell Biol* **156**:531-542, 2002.

42. Kirschnek S, Ying S, Fischer SF, Hacker H, Villunger A, Hochrein H, Hacker G: Phagocytosis-induced apoptosis in macrophages is mediated by up-regulation and activation of the Bcl-2 homology domain 3-only protein Bim. *J Immunol* **174**:671-679, 2005.

43. Nofer JR: Signal transduction by HDL: agonists, receptors, and signaling cascades. *Handb Exp Pharmacol* **224**:229-256, 2015.

44. Al-Jarallah A, Chen X, Gonzalez L, Trigatti BL: High density lipoprotein stimulated migration of macrophages depends on the scavenger receptor class B, type I, PDZK1 and Akt1 and is blocked by sphingosine 1 phosphate receptor antagonists. *PLoS One* **9**:e106487, 2014.

45. Xu J, Qian J, Xie X, Lin L, Zou Y, Fu M, Huang Z, Zhang G, Su Y, Ge J: High density lipoprotein protects mesenchymal stem cells from oxidative stress-induced apoptosis via activation of the PI3K/Akt pathway and suppression of reactive oxygen species. *Int J Mol Sci* **13**:17104-17120, 2012.

46. Xu J, Qian J, Xie X, Lin L, Ma J, Huang Z, Fu M, Zou Y, Ge J: High density lipoprotein cholesterol promotes the proliferation of bone-derived mesenchymal stem cells via binding scavenger receptor-B type I and activation of PI3K/Akt, MAPK/ERK1/2 pathways. *Mol Cell Biochem* **371**:55-64, 2012.

47. Nofer JR, Levkau B, Wolinska I, Junker R, Fobker M, von Eckardstein A, Seedorf U, Assmann G: Suppression of endothelial cell apoptosis by high density lipoproteins (HDL) and HDL-associated lysosphingolipids. *J Biol Chem* **276**:34480-34485, 2001.

48. Tao R, Hoover HE, Honbo N, Kalinowski M, Alano CC, Karliner JS, Raffai R: High-density lipoprotein determines adult mouse cardiomyocyte fate after hypoxia-reoxygenation through lipoprotein-associated sphingosine 1-phosphate. *Am J Physiol Heart Circ Physiol* **298**:H1022-1028, 2010.

49. Li H, Reddick RL, Maeda N: Lack of apoA-I is not associated with increased susceptibility to atherosclerosis in mice. *Arterioscler Thromb* **13**:1814-1821, 1993.

50. Voyiaziakis E, Goldberg IJ, Plump AS, Rubin EM, Breslow JL, Huang LS: ApoA-I deficiency causes both hypertriglyceridemia and increased atherosclerosis in human apoB transgenic mice. *J Lipid Res* **39**:313-321, 1998.

51. Zabalawi M, Bhat S, Loughlin T, Thomas MJ, Alexander E, Cline M, Bullock B, Willingham M, Sorci-Thomas MG: Induction of fatal inflammation in LDL receptor and ApoA-I double-knockout mice fed dietary fat and cholesterol. *Am J Pathol* **163**:1201-1213, 2003.

52. Moore RE, Kawashiri MA, Kitajima K, Secreto A, Millar JS, Pratico D, Rader DJ: Apolipoprotein A-I deficiency results in markedly increased atherosclerosis in mice lacking the LDL receptor. *Arterioscler Thromb Vasc Biol* **23**:1914-1920, 2003.

53. Navab M, Reddy ST, Van Lenten BJ, Fogelman AM: HDL and cardiovascular disease: atherogenic and atheroprotective mechanisms. *Nat Rev Cardiol* **8**:222-232, 2011.

54. Naik PP, Ghadge MS, Raste AS: Lipid profile in leukemia and Hodgkin's disease. *Indian J Clin Biochem* **21**:100-102, 2006.

55. Vitols S, Gahrton G, Bjorkholm M, Peterson C: Hypocholesterolaemia in malignancy due to elevated low-density-lipoprotein-receptor activity in tumour cells: evidence from studies in patients with leukaemia. *Lancet* **2**:1150-1154, 1985.

56. Goncalves RP, Rodrigues DG, Maranhao RC: Uptake of high density lipoprotein (HDL) cholesteryl esters by human acute leukemia cells. *Leuk Res* **29**:955-959, 2005.

57. Andres V, Pello OM, Silvestre-Roig C: Macrophage proliferation and apoptosis in atherosclerosis. *Curr Opin Lipidol* **23**:429-438, 2012.

58. Liu J, Thewke DP, Su YR, Linton MF, Fazio S, Sinensky MS: Reduced macrophage apoptosis is associated with accelerated atherosclerosis in low-density lipoprotein receptor-null mice. *Arterioscler Thromb Vasc Biol* **25**:174-179, 2005.

59. Gonzalez-Navarro H, Abu Nabah YN, Vinue A, Andres-Manzano MJ, Collado M, Serrano M, Andres V: p19(ARF) deficiency reduces macrophage and vascular smooth muscle cell apoptosis and aggravates atherosclerosis. *J Am Coll Cardiol* **55**:2258-2268, 2010.

60. Arai S, Shelton JM, Chen M, Bradley MN, Castrillo A, Bookout AL, Mak PA, Edwards PA, Mangelsdorf DJ, Tontonoz P, Miyazaki T: A role for the apoptosis inhibitory factor AIM/Spalpha/Api6 in atherosclerosis development. *Cell Metab* **1**:201-213, 2005.

61. Gautier EL, Huby T, Witztum JL, Ouzilleau B, Miller ER, Saint-Charles F, Aucouturier P, Chapman MJ, Lesnik P: Macrophage apoptosis exerts divergent effects on atherogenesis as a function of lesion stage. *Circulation* **119**:1795-1804, 2009.

Chapter 5: Discussion

The main focus of this thesis is to study the role of the S1P receptors in protection against atherosclerosis, with special emphasis in macrophage apoptosis and necrotic core formation. In particular, the participation of the S1P receptor, S1PR1, in macrophages is explored in order to understand the contribution of this signaling pathway to apoptosis protection and atherosclerotic plaque development. Chapters 2 and 3 explore the participation of the S1P receptors signaling in regulating atherosclerosis development and necrotic core formation. In chapter 2, diet-induced atherosclerotic plaque and necrotic core formation are evaluated in the context of diabetes. In this study, STZ-treated SR-B1 KO/apoE-hypo mice were fed a HFC diet to induce atherosclerosis in order to evaluate atherosclerotic plaque development under conditions of hyperglycemia. To evaluate the participation of the S1P signaling axis in this context, mice were treated with the S1P receptor agonist FTY720, in the drinking water. In chapter 3, the role of the S1P receptor, S1PR1, in macrophages in apoptosis protection, atherosclerotic plaque development and necrotic core formation was studied. The ability of the S1P/S1PR1 signaling axis to protect macrophages against apoptosis and the connection between HDL and S1PR1 signaling was tested as well. Chapter 4 is also focused on macrophage apoptosis but it is aimed to study in more details the role of the pro-apoptotic protein BIM in HDL-mediated protection against cell death. The participation of BIM in atherosclerotic plaque and necrotic core formation was studied *in vivo* in the context of

low levels of circulating HDL, in HF diet-fed apoA1/LDLR dKO mice. Overall, this thesis provides insights into a role for S1P receptor signaling, particularly S1PR1 in protection against macrophage apoptosis and the pathology of atherosclerosis.

5.1 Summary of the results presented in Chapters 2-4

Chapter 2 of this thesis describes the effect of diabetes on the development of atherosclerosis in HFC diet-fed SR-B1 KO/apoE-hypo mice. Diabetes was induced by multiple low-dose injections of STZ to SR-B1 KO/apoE-hypo mice. After confirming hyperglycemia, mice were placed on a high fat/high cholesterol (HFC) diet in order to induce atherosclerosis development. STZ-treated, HFC diet-fed SR-B1 KO/apoE-hypo mice developed substantial atherosclerotic plaques and increased necrotic core sizes in the aortic sinus compared to control normoglycemic, HFC diet-fed SR-B1 KO/apoE-hypo mice. Unexpectedly, diabetes did not significantly affect the development of CA atherosclerosis but it increased platelet accumulation in atherosclerotic CAs of mice fed an HFC diet. STZ-treated, HFC diet-fed mice also exhibited extensive myocardial fibrosis compared to normoglycemic controls. Hyperglycemia was also associated with a significant reduction in survival compared to control-treated mice, when both were challenged with the HFC diet. FTY720 was administered in the drinking water in order to evaluate the effects of S1PR signaling on atherosclerosis development in the context of diabetic atherosclerosis. FTY720 treatment did not affect the development of hyperglycemia in the STZ treated mice. It was able to reduce some of diabetes' effects

on atherosclerosis progression. Treatment with FTY720 reduced the sizes of the atherosclerotic plaques and necrotic cores within those plaques, in the aortic sinus of diabetic SR-B1 KO/apoE-hypo mice fed a HFC diet. It also slightly reduced the numbers of occluded CAs accompanied by a greater reduction in platelet accumulation in atherosclerotic CAs. The reduction in necrotic core sizes detected in FTY720-treated, HFC diet-fed diabetic mice was also accompanied by a reduction in apoptosis in the aortic sinus atherosclerotic plaques. Despite the beneficial effects, however, FTY720 treatment did not translated into an extended survival.

Chapter 3 explores the role of the macrophage S1PR1 in atherosclerosis development focusing on macrophage apoptosis protection. Selective activation of the S1PR1 in macrophages protected them against different pro-apoptotic stimuli in a PI3K/AKT dependent manner. Furthermore, macrophage S1PR1 deficiency affected HDL's ability to protect macrophages against apoptosis. This is consistent with the idea that S1P, a bioactive lipid carried by HDL, and the ligand for S1PR1, mediates many of HDL's signaling effects in target cells. To study the role of macrophage S1PR1 in atherosclerosis development, LDLR KO mice were transplanted with S1PR1 deficient or control BM and atherosclerosis was induced by feeding a high fat, western type (HF) diet. A lack of S1PR1 in macrophages was associated with increased atherosclerotic plaque and necrotic core sizes in the aortic sinus in mice after 9 weeks on a HF diet. The increased necrotic core sizes found in the HF diet-fed LDLR KO mice transplanted with S1PR1 deficient BM was also associated with increased numbers of $TUNEL^+$ nuclei in the aortic sinus atherosclerotic plaque. When mice were fed for a longer period of time

(12 weeks), atherosclerotic plaque sizes, necrotic core sizes and numbers of apoptotic cells in atherosclerotic plaques all increased, however no significant difference were detected between the mice transplanted with S1PR1 deficient BM and control BM, suggesting that macrophage S1PR1 signaling pathway might play a less important role in later stages of plaque development.

HDL-mediated protection of macrophages against apoptosis (Al-Jarallah, 2012; Yu, 2016) and regulation of cell survival by S1P/S1PR1 (Rutherford et al., 2013), have both been reported to involve regulation of BIM levels in the cell. In chapter 4, we tested the role of BIM on macrophage apoptosis and atherosclerosis development in the context of low levels of HDL-cholesterol. BIM deficient macrophages were significantly more resistant to TN-induced apoptosis compared to control macrophages and HDL did not further protect cells under the same pro-apoptotic conditions. Preliminary data also showed that HDL might reduce BIM levels at the protein levels in pro-apoptotic conditions. Reduced levels of circulating HDL in HF diet-fed apoA1/LDLR dKO mice translated into low levels of total cholesterol but increased atherosclerotic plaque and necrotic core sizes in the aortic sinus. To evaluate the role of BIM in atherosclerosis development in the context of low HDL-cholesterol, apoA1/LDLR dKO mice were transplanted with BIM deficient or control BM and fed a HF diet to induce atherosclerosis. BIM deficiency in the BM compartment resulted in the development of smaller atherosclerotic plaques in the aortic sinus and a trend towards a reduction in the size of necrotic cores within the atherosclerotic plaque, compared with control HF diet-fed BMT mice. A reduction in the proportion of $CD11b^{+}$ cells (monocytes/macrophages)

in circulation was also detected, while the percentage $B220^+$ cells was increased, however further experiments are needed to clarify if this might contribute to the reduction detected in atherosclerotic plaque sizes.

5.2 Implications of the results obtained and future directions

Despite the inverse correlation existing between HDL cholesterol and the CVD risk, there is cumulative evidence showing that simple increasing HDL-cholesterol does not protect against CVD (Nofer, 2013). For example, the AIM-HIGH and HPS2-THRIVE trials used niacin as a means to increase HDL cholesterol but failed to report a reduction in cardiovascular risk (Group, 2013; Investigators et al., 2011). Similar results were also obtained in acute coronary syndrome patients treated with inhibitors of CETP, despite the significant increase detected in HDL cholesterol (Barter et al., 2007; Schwartz et al., 2012). These results shed light on the possibility that other components of HDL might be contributing to the anti-atherogenic properties of this lipoprotein and S1P, a lysosphingolipid carried by HDL in circulation, has risen as a strong candidate that could be playing a relevant role in HDL's atheroprotective effects (Nofer, 2015). The potential anti-atherogenic properties of S1P and its receptors have been widely explored *in vitro* in endothelial cells and smooth muscle cells, with fewer studies addressing its role in macrophages (Poti et al., 2014). Animal studies, on the other hand, have been less conclusive and the outcome can be both anti- or pro-atherogenic depending on the S1P receptor activated (Poti et al., 2014).

FTY720 treatment has been shown to reduce atherosclerosis development in apoE KO and LDLR KO mice fed a HFC diet in a process mainly dependent on its effect on lymphocyte counts (Keul et al., 2007; Nofer et al., 2007). Consistent with these results, diabetic SR-B1 KO/apoE-hypo mice treated with FTY720 were significantly protected against atherosclerotic plaque development in the aortic sinus and also presented reduced necrotic core sizes in the aortic sinus plaque (chapter 2). The reduction in atherosclerotic plaque sizes might be attributed to a reduction in lymphocyte counts as previously reported. On the other hand, others have reported that complete lymphocyte deficiency (by deletion of RAG2) did not alter coronary artery atherosclerosis development in a related strain of mice, the SR-B1/apoE dKO mice (Karackattu et al., 2005). Alternatively, the effect of FTY720 on atherosclerosis could involve changes in the migration of macrophages. We have previously reported that S1PR agonists including FTY720 can induce macrophage migration, suggesting that FTY720 administration might trigger changes in monocyte/macrophage migration patterns that affect atherosclerotic plaque growth (Al-Jarallah et al., 2014). Others have reported that under certain experimental conditions, HDL can trigger the migration of macrophages out of atherosclerotic plaques, limiting plaque growth and favoring plaque regression (Feig et al., 2011b). The contribution of macrophage migration to the arrest in plaque growth detected in our model could be tested using fluorescently labeled beads to specifically mark phagocytic cells (including monocyte derived macrophages) as previously described (Feig et al., 2011a; Pei et al., 2013). In order to test if FTY720 favors emigration of macrophage from established plaques, mice with size-matched plaques can be injected

with fluorescent beads followed by treatment with FTY720. Appearance of beads in circulation and/or quantification of remaining beads in the atherosclerotic plaque could be measured.

FTY720 only slightly affected CA atherosclerosis, but significantly reduced platelet accumulation in atherosclerotic CA and myocardial fibrosis (chapter 2). Studies have shown that platelets deficient in sphingosine kinase 1 are less capable to aggregate and form thrombi (Munzer et al., 2014). Reduction in thrombus formation after FTY720 treatment has also been reported in a model of ischemic stroke in mice (Kraft et al., 2013). Considering that FTY720 is known to induce internalization of the S1PR1 (Matloubian et al., 2004), and even though it is not clear if S1P can directly act upon platelets, it is possible that the reduction in platelet aggregation seen in treated HFC diet-fed diabetic SR-B1 KO/apoE-hypo is related to the ability of FTY720 to directly reduce platelet activation. Platelet function (aggregation and thrombus formation) after FTY720 treatment could be tested *in vitro* in a flow chamber as described by Münzer and colleagues (Munzer et al., 2014) in order to evaluate if this could contribute to the reduction in aggregated platelets found in diabetic mice treated with FTY720. Another possibility that could be explored is to test if FTY720 treatment affects platelets numbers in our model. S1P, through the activation of S1PR1, regulates thrombopoiesis by modulating proplatelet formation and shedding, and acute administration of S1PR1 agonists significantly increases platelet counts (Zhang et al., 2012). Based on this information, another important experiment would be to investigate if the reduction in

platelet aggregation detected in FTY720-treated diabetic mice could be a consequence of the reduction in platelet counts, due to internalization of the S1PR1.

Myocardial fibrosis is an important feature of diabetic cardiomyopathy and consistent with the results shown on this thesis, several studies have shown that fibrosis in the heart of diabetic patients can occur independent of CA atherosclerosis (Russo and Frangogiannis, 2016). Considering this, the reduction in fibrosis seen under treatment with FTY720 might be related to a direct effect of this drug on cardiac fibroblasts, as described by Liu and colleagues in a mouse model of hypertension (Liu et al., 2013) so it would interesting to tests this changes in our model of diabetic cardiomyopathy. Despite the beneficial effects of FTY720 treatment described in this thesis, no improvement in survival was detected, despite previous studies where improvement of cardiac function and survival were reported in SR-B1 KO/apoE-hypo mice treated with a lower dose of FTY720 (Wang et al., 2014). The improvement in survival, however, was not accompanied by a reduction in atherosclerosis, a feature achieved by the dose used on this thesis (Wang et al., 2014). To fully comprehend the extent of FTY720 effects of diabetic cardiomyopathy, it would be useful to try multiple doses of FTY720 in order to achieve not only reduction in atherosclerosis but also improvement in cardiac function. Similarly, we could treat the animals with receptor-specific agonists, like SEW271, to dissect the individual role of S1PR1 in this pathology. FTY720 has been reported to have opposing effects in terms of S1PR1 activation. In the short term, FTY720 acts as an agonist, activating S1PR1 signaling; however after prolonged exposure, it acts as a functional antagonist, inducing receptor internalization and degradation (Oo et al., 2011). If

activation of S1PR1 were behind the atheroprotective effects of FTY720 treatment, then the use of S1PR1 KO mice would help differentiate between effects of receptor down-regulation from effects of receptor activation in the context of diabetic atherosclerosis.

In chapter 2, this thesis looked in more details at the role of S1PR1 in macrophage apoptosis and its impact on atherosclerosis development. In agreement with studies in endothelial cells (Kimura et al., 2003), activation of the S1PR1 axis in macrophages was protective against apoptosis. S1PR1 was also required for the ability of HDL to protect macrophages against apoptosis. Although we were able to show that S1PR1 signaling leading to protection against apoptosis involved activation of PI3K/AKT, it would be interesting to know in more detail the pathway followed after S1PR1 activation leading to cell survival. Previous studies in fibroblasts suggested that activation of the S1PR1 led to cell survival by suppressing BIM accumulation through ERK activation and by increasing Mcl-1 through PI3K/PKC (Rutherford et al., 2013). Cell survival in response to overexpression of SphK1 in endothelial cells was also associated with PI3K/AKT activation and modulation of Bcl-2 and BIM (Limaye et al., 2005). A combination of antibodies and specific inhibitors could be used to test if any of these proteins/signaling pathways are also playing a role in macrophage survival. The data showed on chapter 3 suggests that BIM potentially plays an important role in ER stress-triggered apoptosis and that it may be regulated by HDL treatment and involved in HDL dependent apoptosis protection (Al-Jarallah, 2012). How does HDL control intracellular BIM levels? In non-apoptotic cells, BIM is found sequestered by the microtubular dynein motor complex (Luciano et al., 2003), but under pro-apoptotic conditions, regulation of intracellular

levels of BIM seems to be mediated by ERK1/2-mediated phosphorylation and proteasomal degradation (Ley et al., 2003; Luciano et al., 2003). HDL has been reported to activate MAPK activity (Nofer, 2015), including ERK1/2, at least in certain cell types (Zhang et al., 2007). Whether it does so in macrophages remains to be tested, although this suggests that proteasomal degradation of BIM after activation of HDL signaling pathways might be a mechanism worth exploring in macrophages.

Consistent with results seen in chapter 2, macrophage S1PR1 deficiency results in increased atherosclerotic plaques and necrotic core sizes in the aortic sinus, confirming the protective role of the S1P/S1PRs signaling in protection against atherosclerosis but also suggesting that this protective role might be more important at early stages rather than in advanced plaques (chapter 3). By using the fluorescent beads technique previously mentioned we could also test if macrophage migration is affected *in vivo* in the context of S1PR1 deficiency and how it relates to atherosclerotic plaque growth. It would also be of interest to test multiple time points in atherosclerosis development to clarify the dynamics of plaque progression e.g. the shifting point where S1PR1 stops being protective, changes in plaque composition that might explain the shift in the response towards S1PR1 signaling, etc.

In terms of necrotic core formation, the results presented on this thesis show that FTY720 treatment resulted in a reduction in the number of apoptotic nuclei detected in the atherosclerotic plaque, while macrophage S1PR1 deficiency resulted in an increase in numbers of $TUNEL^+$ cells in the atherosclerotic plaque. Previous studies have suggested that increased plaque apoptosis contributes to necrotic core formation when paired with

deficient clearance of dead cells (Seimon and Tabas, 2009). S1P and the S1PR1 have been recently reported to play an important role in efferocytosis. Apoptotic cell-derived S1P, by interacting with S1PR1, was reported to activate the erythropoietin (EPO)/EPO receptor axis in macrophages, inducing the expression of phagocytic receptors such as MerTK. This result suggests that S1PR1 deficiency in the macrophages not only would contribute to necrotic core formation by increasing macrophage apoptosis but also it negatively impacts clearance. It would be interesting to see if S1PR1 might influence SR-B1's ability to mediate clearance of apoptotic cells by phagocytes as well (Tao et al., 2015). To test for changes in efferocytosis, we could co-stain for apoptosis and macrophage markers and the look for macrophages containing apoptotic nuclei in the cytoplasm. We could also seek to detect if either absence of S1PR1 in macrophages or treatment with FTY720, or a more selective S1PR1 agonist such as SEW2871, result in changes in the levels of expression of other factor known to be involved in efferocytosis like MerTK, component 1 q subcomponent a chain (C1q) and lysophosphatidylcholine (lysoPC) (Thorp and Tabas, 2009). Changes in efferocytosis can also be detected in $S1PR1^{MKO}$ mice by peritoneal lavage as previously described (Friggeri et al., 2011). In the context of S1PR1 deficiency in macrophages, we could also test for changes in SR-B1 protein levels or subcellular location.

Some other important questions that need to be explored are: does HDL interact directly with S1PR1? Does it interact with SR-B1 and then leads to S1PR1 activation? And if so, how does HDL interaction with SR-B1 lead to activation of S1PR1 signaling? Does SR-B1 signaling depend on S1PR1 or does it signal independently? Our data

suggests that HDL signaling leading to protection of macrophages against apoptosis requires SR-B1 (Al-Jarallah, 2012) and S1PR1 (chapter 2) since HDL mediated protection against apoptosis is blocked when this agents are not present. Thus, in terms of macrophage survival, this suggests that SR-B1 requires S1PR1 signaling, although others have suggested that SR-B1 may elicit potentially S1PR1 independent signaling pathways (Mineo and Shaul, 2013). One potential pathway by which HDL interacting with SR-B1 might lead to activation of S1PR1 signaling in by SR-B1-mediated transfer of S1P from HDL to cells, making it available for activation of S1PR1. SR-B1 has been reported to facilitate the transfer of lipids from bound HDL with broad specificity for different types of lipids although the ability to transfer S1P has not been confirmed (Thuahnai et al., 2001). The ability of SR-B1 to transfer lipids is explained by the presence of a hydrophobic tunnel predicted in SR-B1 to span the region involved in HDL binding to the membrane (Neculai et al., 2013). We have shown that HDL induced macrophage migration, a process inhibited not only by S1PR1 antagonists but also by a small molecule inhibitor that selectively prevents SR-B1 mediated lipid transfer from HDL without disrupting HDL binding, which is consistent with the model that SR-B1 may mediate S1P transfer from HDL to S1PR1. To test this model further studies are required. These include first directly demonstrating that SR-B1 mediates S1P uptake from bound HDL. In this context, preliminary data from our laboratory shows that HDL treated with S1P lyase (S1P depleted HDL) cannot protect wild type macrophages against TN-induced apoptosis (Kelvyn Fernandes and Bernardo Trigatti, unpublished data), similar to the results obtained in S1PR1-deficient macrophages, further suggesting that

HDL may be delivering S1P in order to activate S1PR1. Another important experiment is to test if SR-B1 and S1PR1 may physically co-localize or interact in some way. Both SR-B1 and S1PR1 have been described to localize in caveolae, suggesting that the receptors might be in close proximity on the cell surface, facilitating their interaction (Babitt et al., 1997; Igarashi and Michel, 2000; Means et al., 2008). S1PR1 deficiency does not alter the mRNA levels of *scarb-1* in macrophages (Supplementary Figure 3.10) but it could affect SR-B1 stability on the cell membrane and/or its interaction with PDZK1, which remains to be tested. Finally, it would also be important to test if mutant forms of SR-B1, defective in lipid transfer, would affect HDL's ability to induce migration of macrophages and protect against macrophage apoptosis.

Based on the results presented in this thesis along with previous findings, we propose a model in which SR-B1 and S1PR1 are localized in close proximity in the cell membrane, facilitating the delivery of HDL-bound S1P to the membrane through the interaction of HDL with SR-B1. S1P can then activate S1PR1 and the PI3K/AKT signaling pathway leading to protection of macrophages against apoptosis. BIM inactivation also plays a role in HDL-mediated protection against macrophage apoptosis; however further studies are required to identify the signaling pathways leading to HDL-mediated changes in BIM levels (Figure 5.1).

Figure 5.1: Working model of HDL-mediated protection of macrophages against apoptosis

HDL activates S1PR1 by delivering S1P in close proximity of the receptor, inducing activation of the PI3K/AKT signaling pathway, which results in protection of macrophages against TN- and oxLDL-induced apoptosis. Activation of the PI3K/AKT signaling pathway may lead to changes in BIM protein levels, leading to protection against apoptosis. Activation of SR-B1 by HDL has also been reported to protect against macrophage apoptosis in a PDZK1 dependent manner. HDL does not protect S1PR1 deficient macrophages against apoptosis, suggesting that HDL requires both signaling axes in order to protect macrophages and raising the possibility of a connection between both signaling pathways.

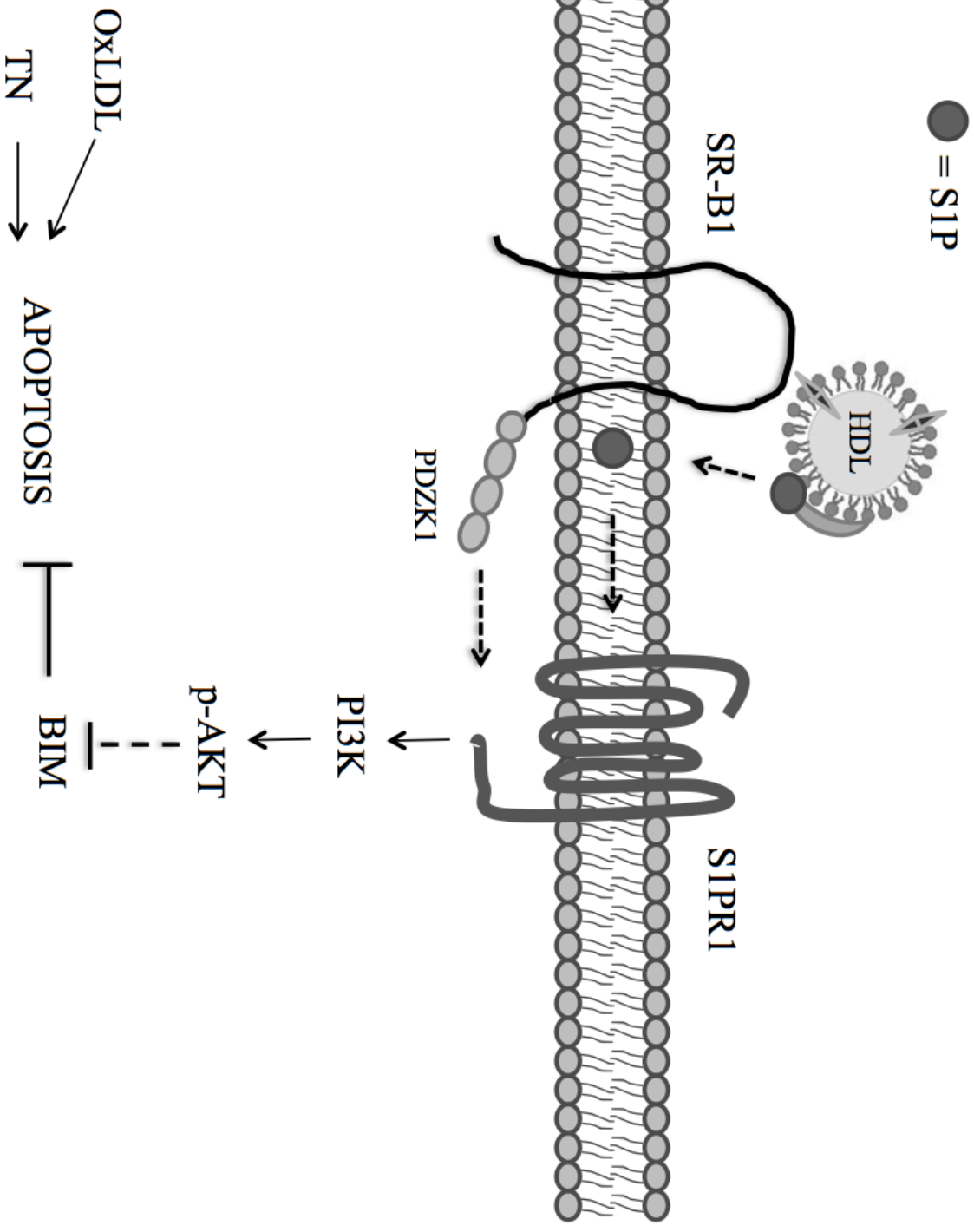
= S1P
SR-B1
HDL
PDZK1
S1PR1
PI3K
p-AKT
BIM
APOPTOSIS
TN
OxLDL

5.3 Conclusions

The results presented in this thesis explore for the importance of the S1PR signaling, particularly S1PR1 in macrophage apoptosis and atherosclerosis development. The S1P/S1PR1 axis in directly involved in protection of macrophages against apoptosis in a PI3K/AKT dependent manner. S1PR1 deficiency also negatively impacts HDL's ability to prevent cell death in macrophages suggesting that signaling through this receptor is not only crucial for HDL-induced migration, as previously reported, but also important in HDL-mediated cell survival. S1PR1 in macrophages seems to play a role in controlling plaque growth during early stages, reducing plaque apoptosis and necrotic core formation. Similar protective effects are also seen in the context of diabetes, where an S1PR agonist was able to protect against atherosclerosis progression. A reduction in the levels of the pro-apoptotic protein BIM has been suggested to play an important role in HDL dependent protection of macrophages against apoptosis *in vitro* and inactivation of BIM in bone marrow derived cells is associated with reduced high fat diet induced atherosclerosis development in apoA1/LDLR dKO mice. However effects of an absence of BIM in bone marrow derived cells other than macrophages cannot be ruled out and further experiments are needed to clarify the mechanisms involved in atheroprotection and its role in macrophages, in particular in plaque apoptosis, as well as how it fits in the SR-B1/S1PR1 signaling pathway activated by HDL.

References

Acton, S., Rigotti, A., Landschulz, K.T., Xu, S., Hobbs, H.H., and Krieger, M. (1996). Identification of scavenger receptor SR-BI as a high density lipoprotein receptor. Science *271*, 518-520.

Al-Jarallah, A. (2012). Insights into the development of atherosclerosis and coronary artery disease: studies from gene targeted mice lacking the high density receptor, SR-BI (McMaster University, Hamilton, ON, Canada).

Al-Jarallah, A., Chen, X., Gonzalez, L., and Trigatti, B.L. (2014). High density lipoprotein stimulated migration of macrophages depends on the scavenger receptor class B, type I, PDZK1 and Akt1 and is blocked by sphingosine 1 phosphate receptor antagonists. PloS one *9*, e106487.

Alewijnse, A.E., and Peters, S.L. (2008). Sphingolipid signalling in the cardiovascular system: good, bad or both? European journal of pharmacology *585*, 292-302.

Allende, M.L., Yamashita, T., and Proia, R.L. (2003). G-protein-coupled receptor S1P1 acts within endothelial cells to regulate vascular maturation. Blood *102*, 3665-3667.

Arai, S., Shelton, J.M., Chen, M., Bradley, M.N., Castrillo, A., Bookout, A.L., Mak, P.A., Edwards, P.A., Mangelsdorf, D.J., Tontonoz, P.*, et al.* (2005). A role for the apoptosis

inhibitory factor AIM/Spalpha/Api6 in atherosclerosis development. Cell metabolism *1*, 201-213.

Arai, T., Wang, N., Bezouevski, M., Welch, C., and Tall, A.R. (1999). Decreased atherosclerosis in heterozygous low density lipoprotein receptor-deficient mice expressing the scavenger receptor BI transgene. The Journal of biological chemistry *274*, 2366-2371.

Argraves, K.M., Sethi, A.A., Gazzolo, P.J., Wilkerson, B.A., Remaley, A.T., Tybjaerg-Hansen, A., Nordestgaard, B.G., Yeatts, S.D., Nicholas, K.S., Barth, J.L.*, et al.* (2011). S1P, dihydro-S1P and C24:1-ceramide levels in the HDL-containing fraction of serum inversely correlate with occurrence of ischemic heart disease. Lipids in health and disease *10*, 70.

Assmann, G., and Nofer, J.R. (2003). Atheroprotective effects of high-density lipoproteins. Annu Rev Med *54*, 321-341.

Babitt, J., Trigatti, B., Rigotti, A., Smart, E.J., Anderson, R.G., Xu, S., and Krieger, M. (1997). Murine SR-BI, a high density lipoprotein receptor that mediates selective lipid uptake, is N-glycosylated and fatty acylated and colocalizes with plasma membrane caveolae. The Journal of biological chemistry *272*, 13242-13249.

Barter, P.J., Caulfield, M., Eriksson, M., Grundy, S.M., Kastelein, J.J., Komajda, M., Lopez-Sendon, J., Mosca, L., Tardif, J.C., Waters, D.D.*, et al.* (2007). Effects of torcetrapib in patients at high risk for coronary events. N Engl J Med *357*, 2109-2122.

Beriault, D.R., and Werstuck, G.H. (2012). The role of glucosamine-induced ER stress in diabetic atherogenesis. Exp Diabetes Res *2012*, 187018.

Birker-Robaczewska, M., Studer, R., Haenig, B., Menyhart, K., Hofmann, S., and Nayler, O. (2008). bFGF induces S1P1 receptor expression and functionality in human pulmonary artery smooth muscle cells. Journal of cellular biochemistry *105*, 1139-1145.

Bot, M., Van Veldhoven, P.P., de Jager, S.C., Johnson, J., Nijstad, N., Van Santbrink, P.J., Westra, M.M., Van Der Hoeven, G., Gijbels, M.J., Muller-Tidow, C.*, et al.* (2013). Hematopoietic sphingosine 1-phosphate lyase deficiency decreases atherosclerotic lesion development in LDL-receptor deficient mice. PloS one *8*, e63360.

Braun, A., Trigatti, B.L., Post, M.J., Sato, K., Simons, M., Edelberg, J.M., Rosenberg, R.D., Schrenzel, M., and Krieger, M. (2002). Loss of SR-BI expression leads to the early onset of occlusive atherosclerotic coronary artery disease, spontaneous myocardial infarctions, severe cardiac dysfunction, and premature death in apolipoprotein E-deficient mice. Circ Res *90*, 270-276.

Briand, O., Lestavel, S., Pilon, A., Torpier, G., Fruchart, J.C., and Clavey, V. (2003). SR-BI does not require raft/caveola localisation for cholesteryl ester selective uptake in the human adrenal cell line NCI-H295R. Biochim Biophys Acta *1631*, 42-50.

Brindley, D.N. (2004). Lipid phosphate phosphatases and related proteins: signaling functions in development, cell division, and cancer. Journal of cellular biochemistry *92*, 900-912.

Brundert, M., Ewert, A., Heeren, J., Behrendt, B., Ramakrishnan, R., Greten, H., Merkel, M., and Rinninger, F. (2005). Scavenger receptor class B type I mediates the selective uptake of high-density lipoprotein-associated cholesteryl ester by the liver in mice. Arteriosclerosis, thrombosis, and vascular biology *25*, 143-148.

Bui, Q.T., Prempeh, M., and Wilensky, R.L. (2009). Atherosclerotic plaque development. Int J Biochem Cell Biol *41*, 2109-2113.

Cai, S., Khoo, J., and Channon, K.M. (2005). Augmented BH4 by gene transfer restores nitric oxide synthase function in hyperglycemic human endothelial cells. Cardiovasc Res *65*, 823-831.

Camerer, E., Regard, J.B., Cornelissen, I., Srinivasan, Y., Duong, D.N., Palmer, D., Pham, T.H., Wong, J.S., Pappu, R., and Coughlin, S.R. (2009). Sphingosine-1-phosphate

in the plasma compartment regulates basal and inflammation-induced vascular leak in mice. The Journal of clinical investigation *119*, 1871-1879.

Cardilo-Reis, L., Gruber, S., Schreier, S.M., Drechsler, M., Papac-Milicevic, N., Weber, C., Wagner, O., Stangl, H., Soehnlein, O., and Binder, C.J. (2012). Interleukin-13 protects from atherosclerosis and modulates plaque composition by skewing the macrophage phenotype. EMBO Mol Med *4*, 1072-1086.

Chen, S., Yang, J., Xiang, H., Chen, W., Zhong, H., Yang, G., Fang, T., Deng, H., Yuan, H., Chen, A.F.*, et al.* (2015). Role of sphingosine-1-phosphate receptor 1 and sphingosine-1-phosphate receptor 2 in hyperglycemia-induced endothelial cell dysfunction. Int J Mol Med *35*, 1103-1108.

Chinnaiyan, A.M. (1999). The apoptosome: heart and soul of the cell death machine. Neoplasia *1*, 5-15.

Christoffersen, C., Jauhiainen, M., Moser, M., Porse, B., Ehnholm, C., Boesl, M., Dahlback, B., and Nielsen, L.B. (2008). Effect of apolipoprotein M on high density lipoprotein metabolism and atherosclerosis in low density lipoprotein receptor knock-out mice. The Journal of biological chemistry *283*, 1839-1847.

Christoffersen, C., Obinata, H., Kumaraswamy, S.B., Galvani, S., Ahnstrom, J., Sevvana, M., Egerer-Sieber, C., Muller, Y.A., Hla, T., Nielsen, L.B.*, et al.* (2011). Endothelium-

protective sphingosine-1-phosphate provided by HDL-associated apolipoprotein M. Proceedings of the National Academy of Sciences of the United States of America *108*, 9613-9618.

Connelly, M.A., De La Llera-Moya, M., Peng, Y., Drazul-Schrader, D., Rothblat, G.H., and Williams, D.L. (2003). Separation of lipid transport functions by mutations in the extracellular domain of scavenger receptor class B, type I. The Journal of biological chemistry *278*, 25773-25782.

Cory, S., and Adams, J.M. (2002). The Bcl2 family: regulators of the cellular life-or-death switch. Nat Rev Cancer *2*, 647-656.

Covey, S.D., Krieger, M., Wang, W., Penman, M., and Trigatti, B.L. (2003). Scavenger receptor class B type I-mediated protection against atherosclerosis in LDL receptor-negative mice involves its expression in bone marrow-derived cells. Arterioscler Thromb Vasc Biol *23*, 1589-1594.

Cuvillier, O., Pirianov, G., Kleuser, B., Vanek, P.G., Coso, O.A., Gutkind, S., and Spiegel, S. (1996). Suppression of ceramide-mediated programmed cell death by sphingosine-1-phosphate. Nature *381*, 800-803.

Daniels, T.F., Killinger, K.M., Michal, J.J., Wright, R.W., Jr., and Jiang, Z. (2009). Lipoproteins, cholesterol homeostasis and cardiac health. Int J Biol Sci *5*, 474-488.

Daum, G., Grabski, A., and Reidy, M.A. (2009). Sphingosine 1-phosphate: a regulator of arterial lesions. Arteriosclerosis, thrombosis, and vascular biology *29*, 1439-1443.

Deevska, G.M., and Nikolova-Karakashian, M.N. (2011). The twists and turns of sphingolipid pathway in glucose regulation. Biochimie *93*, 32-38.

Dole, V.S., Matuskova, J., Vasile, E., Yesilaltay, A., Bergmeier, W., Bernimoulin, M., Wagner, D.D., and Krieger, M. (2008). Thrombocytopenia and platelet abnormalities in high-density lipoprotein receptor-deficient mice. Arteriosclerosis, thrombosis, and vascular biology *28*, 1111-1116.

Du, X.L., Edelstein, D., Dimmeler, S., Ju, Q., Sui, C., and Brownlee, M. (2001). Hyperglycemia inhibits endothelial nitric oxide synthase activity by posttranslational modification at the Akt site. The Journal of clinical investigation *108*, 1341-1348.

Duan, J., Dahlback, B., and Villoutreix, B.O. (2001). Proposed lipocalin fold for apolipoprotein M based on bioinformatics and site-directed mutagenesis. FEBS letters *499*, 127-132.

Duenas, A.I., Aceves, M., Fernandez-Pisonero, I., Gomez, C., Orduna, A., Crespo, M.S., and Garcia-Rodriguez, C. (2008). Selective attenuation of Toll-like receptor 2 signalling may explain the atheroprotective effect of sphingosine 1-phosphate. Cardiovasc Res *79*, 537-544.

Elmore, S. (2007). Apoptosis: a review of programmed cell death. Toxicol Pathol *35*, 495-516.

Feig, J.E., Parathath, S., Rong, J.X., Mick, S.L., Vengrenyuk, Y., Grauer, L., Young, S.G., and Fisher, E.A. (2011a). Reversal of hyperlipidemia with a genetic switch favorably affects the content and inflammatory state of macrophages in atherosclerotic plaques. Circulation *123*, 989-998.

Feig, J.E., Rong, J.X., Shamir, R., Sanson, M., Vengrenyuk, Y., Liu, J., Rayner, K., Moore, K., Garabedian, M., and Fisher, E.A. (2011b). HDL promotes rapid atherosclerosis regression in mice and alters inflammatory properties of plaque monocyte-derived cells. Proceedings of the National Academy of Sciences of the United States of America *108*, 7166-7171.

Feng, B., Yao, P.M., Li, Y., Devlin, C.M., Zhang, D., Harding, H.P., Sweeney, M., Rong, J.X., Kuriakose, G., Fisher, E.A.*, et al.* (2003). The endoplasmic reticulum is the site of cholesterol-induced cytotoxicity in macrophages. Nat Cell Biol *5*, 781-792.

Fox, T.E., Bewley, M.C., Unrath, K.A., Pedersen, M.M., Anderson, R.E., Jung, D.Y., Jefferson, L.S., Kim, J.K., Bronson, S.K., Flanagan, J.M.*, et al.* (2011). Circulating sphingolipid biomarkers in models of type 1 diabetes. Journal of lipid research *52*, 509-517.

Friggeri, A., Banerjee, S., Biswas, S., de Freitas, A., Liu, G., Bierhaus, A., and Abraham, E. (2011). Participation of the receptor for advanced glycation end products in efferocytosis. Journal of immunology *186*, 6191-6198.

Fuller, M., Dadoo, O., Serkis, V., Abutouk, D., MacDonald, M., Dhingani, N., Macri, J., Igdoura, S.A., and Trigatti, B.L. (2014). The effects of diet on occlusive coronary artery atherosclerosis and myocardial infarction in scavenger receptor class B, type 1/low-density lipoprotein receptor double knockout mice. Arterioscler Thromb Vasc Biol *34*, 2394-2403.

Funk, S.D., Yurdagul, A., Jr., and Orr, A.W. (2012). Hyperglycemia and endothelial dysfunction in atherosclerosis: lessons from type 1 diabetes. Int J Vasc Med *2012*, 569654.

Garcia, J.G., Verin, A.D., and Schaphorst, K.L. (1996). Regulation of thrombin-mediated endothelial cell contraction and permeability. Semin Thromb Hemost *22*, 309-315.

Genest, J.J., Jr., Martin-Munley, S.S., McNamara, J.R., Ordovas, J.M., Jenner, J., Myers, R.H., Silberman, S.R., Wilson, P.W., Salem, D.N., and Schaefer, E.J. (1992). Familial lipoprotein disorders in patients with premature coronary artery disease. Circulation *85*, 2025-2033.

Gerrity, R.G., Natarajan, R., Nadler, J.L., and Kimsey, T. (2001). Diabetes-induced accelerated atherosclerosis in swine. Diabetes *50*, 1654-1665.

Gleissner, C.A., Sanders, J.M., Nadler, J., and Ley, K. (2008). Upregulation of aldose reductase during foam cell formation as possible link among diabetes, hyperlipidemia, and atherosclerosis. Arteriosclerosis, thrombosis, and vascular biology *28*, 1137-1143.

Gonzalez-Diez, M., Rodriguez, C., Badimon, L., and Martinez-Gonzalez, J. (2008). Prostacyclin induction by high-density lipoprotein (HDL) in vascular smooth muscle cells depends on sphingosine 1-phosphate receptors: effect of simvastatin. Thromb Haemost *100*, 119-126.

Group, H.T.C. (2013). HPS2-THRIVE randomized placebo-controlled trial in 25 673 high-risk patients of ER niacin/laropiprant: trial design, pre-specified muscle and liver outcomes, and reasons for stopping study treatment. Eur Heart J *34*, 1279-1291.

Hadi, H.A., Carr, C.S., and Al Suwaidi, J. (2005). Endothelial dysfunction: cardiovascular risk factors, therapy, and outcome. Vascular health and risk management *1*, 183-198.

Hammad, S.M., Crellin, H.G., Wu, B.X., Melton, J., Anelli, V., and Obeid, L.M. (2008). Dual and distinct roles for sphingosine kinase 1 and sphingosine 1 phosphate in the response to inflammatory stimuli in RAW macrophages. Prostaglandins Other Lipid Mediat *85*, 107-114.

Hansson, G.K., and Libby, P. (2006). The immune response in atherosclerosis: a double-edged sword. Nature reviews Immunology *6*, 508-519.

Hegele, R.A. (2009). Plasma lipoproteins: genetic influences and clinical implications. Nat Rev Genet *10*, 109-121.

Hetz, C. (2012). The unfolded protein response: controlling cell fate decisions under ER stress and beyond. Nat Rev Mol Cell Biol *13*, 89-102.

Hla, T., Galvani, S., Rafii, S., and Nachman, R. (2012). S1P and the birth of platelets. J Exp Med *209*, 2137-2140.

Holland, W.L., Miller, R.A., Wang, Z.V., Sun, K., Barth, B.M., Bui, H.H., Davis, K.E., Bikman, B.T., Halberg, N., Rutkowski, J.M.*, et al.* (2011). Receptor-mediated activation of ceramidase activity initiates the pleiotropic actions of adiponectin. Nature medicine *17*, 55-63.

Holm, T.M., Braun, A., Trigatti, B.L., Brugnara, C., Sakamoto, M., Krieger, M., and Andrews, N.C. (2002). Failure of red blood cell maturation in mice with defects in the high-density lipoprotein receptor SR-BI. Blood *99*, 1817-1824.

Igarashi, J., and Michel, T. (2000). Agonist-modulated targeting of the EDG-1 receptor to plasmalemmal caveolae. eNOS activation by sphingosine 1-phosphate and the role of

caveolin-1 in sphingolipid signal transduction. The Journal of biological chemistry *275*, 32363-32370.

Igarashi, J., Miyoshi, M., Hashimoto, T., Kubota, Y., and Kosaka, H. (2007). Statins induce S1P1 receptors and enhance endothelial nitric oxide production in response to high-density lipoproteins. Br J Pharmacol *150*, 470-479.

Imasawa, T., Koike, K., Ishii, I., Chun, J., and Yatomi, Y. (2010). Blockade of sphingosine 1-phosphate receptor 2 signaling attenuates streptozotocin-induced apoptosis of pancreatic beta-cells. Biochemical and biophysical research communications *392*, 207-211.

Investigators, A.-H., Boden, W.E., Probstfield, J.L., Anderson, T., Chaitman, B.R., Desvignes-Nickens, P., Koprowicz, K., McBride, R., Teo, K., and Weintraub, W. (2011). Niacin in patients with low HDL cholesterol levels receiving intensive statin therapy. N Engl J Med *365*, 2255-2267.

Ito, K., Anada, Y., Tani, M., Ikeda, M., Sano, T., Kihara, A., and Igarashi, Y. (2007). Lack of sphingosine 1-phosphate-degrading enzymes in erythrocytes. Biochemical and biophysical research communications *357*, 212-217.

Jarvisalo, M.J., Jartti, L., Nanto-Salonen, K., Irjala, K., Ronnemaa, T., Hartiala, J.J., Celermajer, D.S., and Raitakari, O.T. (2001). Increased aortic intima-media thickness: a marker of preclinical atherosclerosis in high-risk children. Circulation *104*, 2943-2947.

Jarvisalo, M.J., Putto-Laurila, A., Jartti, L., Lehtimaki, T., Solakivi, T., Ronnemaa, T., and Raitakari, O.T. (2002). Carotid artery intima-media thickness in children with type 1 diabetes. Diabetes *51*, 493-498.

Jian, B., de la Llera-Moya, M., Ji, Y., Wang, N., Phillips, M.C., Swaney, J.B., Tall, A.R., and Rothblat, G.H. (1998). Scavenger receptor class B type I as a mediator of cellular cholesterol efflux to lipoproteins and phospholipid acceptors. The Journal of biological chemistry *273*, 5599-5606.

Karackattu, S.L., Picard, M.H., and Krieger, M. (2005). Lymphocytes are not required for the rapid onset of coronary heart disease in scavenger receptor class B type I/apolipoprotein E double knockout mice. Arteriosclerosis, thrombosis, and vascular biology *25*, 803-808.

Keul, P., Lucke, S., von Wnuck Lipinski, K., Bode, C., Graler, M., Heusch, G., and Levkau, B. (2011). Sphingosine-1-phosphate receptor 3 promotes recruitment of monocyte/macrophages in inflammation and atherosclerosis. Circulation research *108*, 314-323.

Keul, P., Tolle, M., Lucke, S., von Wnuck Lipinski, K., Heusch, G., Schuchardt, M., van der Giet, M., and Levkau, B. (2007). The sphingosine-1-phosphate analogue FTY720 reduces atherosclerosis in apolipoprotein E-deficient mice. Arteriosclerosis, thrombosis, and vascular biology *27*, 607-613.

Kimura, T., Mogi, C., Tomura, H., Kuwabara, A., Im, D.S., Sato, K., Kurose, H., Murakami, M., and Okajima, F. (2008). Induction of scavenger receptor class B type I is critical for simvastatin enhancement of high-density lipoprotein-induced anti-inflammatory actions in endothelial cells. Journal of immunology *181*, 7332-7340.

Kimura, T., Sato, K., Kuwabara, A., Tomura, H., Ishiwara, M., Kobayashi, I., Ui, M., and Okajima, F. (2001). Sphingosine 1-phosphate may be a major component of plasma lipoproteins responsible for the cytoprotective actions in human umbilical vein endothelial cells. The Journal of biological chemistry *276*, 31780-31785.

Kimura, T., Sato, K., Malchinkhuu, E., Tomura, H., Tamama, K., Kuwabara, A., Murakami, M., and Okajima, F. (2003). High-density lipoprotein stimulates endothelial cell migration and survival through sphingosine 1-phosphate and its receptors. Arteriosclerosis, thrombosis, and vascular biology *23*, 1283-1288.

Kimura, T., Tomura, H., Mogi, C., Kuwabara, A., Damirin, A., Ishizuka, T., Sekiguchi, A., Ishiwara, M., Im, D.S., Sato, K.*, et al.* (2006). Role of scavenger receptor class B type I and sphingosine 1-phosphate receptors in high density lipoprotein-induced inhibition of

adhesion molecule expression in endothelial cells. The Journal of biological chemistry *281*, 37457-37467.

Kingwell, B.A., Chapman, M.J., Kontush, A., and Miller, N.E. (2014). HDL-targeted therapies: progress, failures and future. Nat Rev Drug Discov *13*, 445-464.

Kischkel, F.C., Hellbardt, S., Behrmann, I., Germer, M., Pawlita, M., Krammer, P.H., and Peter, M.E. (1995). Cytotoxicity-dependent APO-1 (Fas/CD95)-associated proteins form a death-inducing signaling complex (DISC) with the receptor. The EMBO journal *14*, 5579-5588.

Klingenberg, R., Nofer, J.R., Rudling, M., Bea, F., Blessing, E., Preusch, M., Grone, H.J., Katus, H.A., Hansson, G.K., and Dengler, T.J. (2007). Sphingosine-1-phosphate analogue FTY720 causes lymphocyte redistribution and hypercholesterolemia in ApoE-deficient mice. Arteriosclerosis, thrombosis, and vascular biology *27*, 2392-2399.

Knorr, M., Locher, R., Vogt, E., Vetter, W., Block, L.H., Ferracin, F., Lefkovits, H., and Pletscher, A. (1988). Rapid activation of human platelets by low concentrations of low-density lipoprotein via phosphatidylinositol cycle. Eur J Biochem *172*, 753-759.

Kocher, O., and Krieger, M. (2009). Role of the adaptor protein PDZK1 in controlling the HDL receptor SR-BI. Current opinion in lipidology *20*, 236-241.

Kocher, O., Yesilaltay, A., Cirovic, C., Pal, R., Rigotti, A., and Krieger, M. (2003). Targeted disruption of the PDZK1 gene in mice causes tissue-specific depletion of the high density lipoprotein receptor scavenger receptor class B type I and altered lipoprotein metabolism. The Journal of biological chemistry *278*, 52820-52825.

Kocher, O., Yesilaltay, A., Shen, C.H., Zhang, S., Daniels, K., Pal, R., Chen, J., and Krieger, M. (2008). Influence of PDZK1 on lipoprotein metabolism and atherosclerosis. Biochimica et biophysica acta *1782*, 310-316.

Kontush, A., Lindahl, M., Lhomme, M., Calabresi, L., Chapman, M.J., and Davidson, W.S. (2015). Structure of HDL: particle subclasses and molecular components. Handbook of experimental pharmacology *224*, 3-51.

Kozarsky, K.F., Donahee, M.H., Glick, J.M., Krieger, M., and Rader, D.J. (2000). Gene transfer and hepatic overexpression of the HDL receptor SR-BI reduces atherosclerosis in the cholesterol-fed LDL receptor-deficient mouse. Arteriosclerosis, thrombosis, and vascular biology *20*, 721-727.

Kozarsky, K.F., Donahee, M.H., Rigotti, A., Iqbal, S.N., Edelman, E.R., and Krieger, M. (1997). Overexpression of the HDL receptor SR-BI alters plasma HDL and bile cholesterol levels. Nature *387*, 414-417.

Kraft, P., Gob, E., Schuhmann, M.K., Gobel, K., Deppermann, C., Thielmann, I., Herrmann, A.M., Lorenz, K., Brede, M., Stoll, G.*, et al.* (2013). FTY720 ameliorates acute ischemic stroke in mice by reducing thrombo-inflammation but not by direct neuroprotection. Stroke *44*, 3202-3210.

Krishna, S.M., Seto, S.W., Moxon, J.V., Rush, C., Walker, P.J., Norman, P.E., and Golledge, J. (2012). Fenofibrate increases high-density lipoprotein and sphingosine 1 phosphate concentrations limiting abdominal aortic aneurysm progression in a mouse model. Am J Pathol *181*, 706-718.

Kumar, A., and Saba, J.D. (2009). Lyase to live by: sphingosine phosphate lyase as a therapeutic target. Expert Opin Ther Targets *13*, 1013-1025.

Landschulz, K.T., Pathak, R.K., Rigotti, A., Krieger, M., and Hobbs, H.H. (1996). Regulation of scavenger receptor, class B, type I, a high density lipoprotein receptor, in liver and steroidogenic tissues of the rat. The Journal of clinical investigation *98*, 984-995.

Ley, R., Balmanno, K., Hadfield, K., Weston, C., and Cook, S.J. (2003). Activation of the ERK1/2 signaling pathway promotes phosphorylation and proteasome-dependent degradation of the BH3-only protein, Bim. The Journal of biological chemistry *278*, 18811-18816.

Li, H., Zhu, H., Xu, C.J., and Yuan, J. (1998). Cleavage of BID by caspase 8 mediates the mitochondrial damage in the Fas pathway of apoptosis. Cell *94*, 491-501.

Liao, X., Sharma, N., Kapadia, F., Zhou, G., Lu, Y., Hong, H., Paruchuri, K., Mahabeleshwar, G.H., Dalmas, E., Venteclef, N.*, et al.* (2011). Kruppel-like factor 4 regulates macrophage polarization. The Journal of clinical investigation *121*, 2736-2749.

Libby, P. (2009). Molecular and cellular mechanisms of the thrombotic complications of atherosclerosis. Journal of lipid research *50 Suppl*, S352-357.

Libby, P., Ridker, P.M., and Hansson, G.K. (2011). Progress and challenges in translating the biology of atherosclerosis. Nature *473*, 317-325.

Limaye, V., Li, X., Hahn, C., Xia, P., Berndt, M.C., Vadas, M.A., and Gamble, J.R. (2005). Sphingosine kinase-1 enhances endothelial cell survival through a PECAM-1-dependent activation of PI-3K/Akt and regulation of Bcl-2 family members. Blood *105*, 3169-3177.

Liu, J., Thewke, D.P., Su, Y.R., Linton, M.F., Fazio, S., and Sinensky, M.S. (2005). Reduced macrophage apoptosis is associated with accelerated atherosclerosis in low-density lipoprotein receptor-null mice. Arteriosclerosis, thrombosis, and vascular biology *25*, 174-179.

Liu, W., Zi, M., Tsui, H., Chowdhury, S.K., Zeef, L., Meng, Q.J., Travis, M., Prehar, S., Berry, A., Hanley, N.A.*, et al.* (2013). A novel immunomodulator, FTY-720 reverses existing cardiac hypertrophy and fibrosis from pressure overload by targeting NFAT (nuclear factor of activated T-cells) signaling and periostin. Circ Heart Fail *6*, 833-844.

Liu, Y., Wada, R., Yamashita, T., Mi, Y., Deng, C.X., Hobson, J.P., Rosenfeldt, H.M., Nava, V.E., Chae, S.S., Lee, M.J.*, et al.* (2000). Edg-1, the G protein-coupled receptor for sphingosine-1-phosphate, is essential for vascular maturation. The Journal of clinical investigation *106*, 951-961.

Locksley, R.M., Killeen, N., and Lenardo, M.J. (2001). The TNF and TNF receptor superfamilies: integrating mammalian biology. Cell *104*, 487-501.

Luciano, F., Jacquel, A., Colosetti, P., Herrant, M., Cagnol, S., Pages, G., and Auberger, P. (2003). Phosphorylation of Bim-EL by Erk1/2 on serine 69 promotes its degradation via the proteasome pathway and regulates its proapoptotic function. Oncogene *22*, 6785-6793.

Lucke, S., and Levkau, B. (2010). Endothelial functions of sphingosine-1-phosphate. Cellular physiology and biochemistry : international journal of experimental cellular physiology, biochemistry, and pharmacology *26*, 87-96.

Lusis, A.J. (2000). Atherosclerosis. Nature *407*, 233-241.

Maahs, D.M., West, N.A., Lawrence, J.M., and Mayer-Davis, E.J. (2010). Epidemiology of type 1 diabetes. Endocrinol Metab Clin North Am *39*, 481-497.

Mahajan-Thakur, S., Bohm, A., Jedlitschky, G., Schror, K., and Rauch, B.H. (2015). Sphingosine-1-Phosphate and Its Receptors: A Mutual Link between Blood Coagulation and Inflammation. Mediators Inflamm *2015*, 831059.

Manning-Tobin, J.J., Moore, K.J., Seimon, T.A., Bell, S.A., Sharuk, M., Alvarez-Leite, J.I., de Winther, M.P., Tabas, I., and Freeman, M.W. (2009). Loss of SR-A and CD36 activity reduces atherosclerotic lesion complexity without abrogating foam cell formation in hyperlipidemic mice. Arteriosclerosis, thrombosis, and vascular biology *29*, 19-26.

Matloubian, M., Lo, C.G., Cinamon, G., Lesneski, M.J., Xu, Y., Brinkmann, V., Allende, M.L., Proia, R.L., and Cyster, J.G. (2004). Lymphocyte egress from thymus and peripheral lymphoid organs is dependent on S1P receptor 1. Nature *427*, 355-360.

Means, C.K., Miyamoto, S., Chun, J., and Brown, J.H. (2008). S1P1 receptor localization confers selectivity for Gi-mediated cAMP and contractile responses. The Journal of biological chemistry *283*, 11954-11963.

Mineo, C., and Shaul, P.W. (2013). Regulation of signal transduction by HDL. Journal of lipid research *54*, 2315-2324.

Mineo, C., Yuhanna, I.S., Quon, M.J., and Shaul, P.W. (2003). High density lipoprotein-induced endothelial nitric-oxide synthase activation is mediated by Akt and MAP kinases. The Journal of biological chemistry *278*, 9142-9149.

Miura, S., Fujino, M., Matsuo, Y., Kawamura, A., Tanigawa, H., Nishikawa, H., and Saku, K. (2003). High density lipoprotein-induced angiogenesis requires the activation of Ras/MAP kinase in human coronary artery endothelial cells. Arteriosclerosis, thrombosis, and vascular biology *23*, 802-808.

Moore, K.J., Sheedy, F.J., and Fisher, E.A. (2013). Macrophages in atherosclerosis: a dynamic balance. Nature reviews Immunology *13*, 709-721.

Morigi, M., Angioletti, S., Imberti, B., Donadelli, R., Micheletti, G., Figliuzzi, M., Remuzzi, A., Zoja, C., and Remuzzi, G. (1998). Leukocyte-endothelial interaction is augmented by high glucose concentrations and hyperglycemia in a NF-kB-dependent fashion. The Journal of clinical investigation *101*, 1905-1915.

Munzer, P., Schmid, E., Walker, B., Fotinos, A., Chatterjee, M., Rath, D., Vogel, S., Hoffmann, S.M., Metzger, K., Seizer, P.*, et al.* (2014). Sphingosine kinase 1 (Sphk1) negatively regulates platelet activation and thrombus formation. Am J Physiol Cell Physiol *307*, C920-927.

Murphy, A.J., Woollard, K.J., Hoang, A., Mukhamedova, N., Stirzaker, R.A., McCormick, S.P., Remaley, A.T., Sviridov, D., and Chin-Dusting, J. (2008). High-density lipoprotein reduces the human monocyte inflammatory response. Arterioscler Thromb Vasc Biol *28*, 2071-2077.

Myoishi, M., Hao, H., Minamino, T., Watanabe, K., Nishihira, K., Hatakeyama, K., Asada, Y., Okada, K., Ishibashi-Ueda, H., Gabbiani, G.*, et al.* (2007). Increased endoplasmic reticulum stress in atherosclerotic plaques associated with acute coronary syndrome. Circulation *116*, 1226-1233.

Neculai, D., Schwake, M., Ravichandran, M., Zunke, F., Collins, R.F., Peters, J., Neculai, M., Plumb, J., Loppnau, P., Pizarro, J.C.*, et al.* (2013). Structure of LIMP-2 provides functional insights with implications for SR-BI and CD36. Nature *504*, 172-176.

Niessen, F., Furlan-Freguia, C., Fernandez, J.A., Mosnier, L.O., Castellino, F.J., Weiler, H., Rosen, H., Griffin, J.H., and Ruf, W. (2009). Endogenous EPCR/aPC-PAR1 signaling prevents inflammation-induced vascular leakage and lethality. Blood *113*, 2859-2866.

Nofer, J.R. (2013). Hyperlipidaemia and cardiovascular disease: the quantity does not turn into quality! Current opinion in lipidology *24*, 366-368.

Nofer, J.R. (2015). Signal transduction by HDL: agonists, receptors, and signaling cascades. Handbook of experimental pharmacology *224*, 229-256.

Nofer, J.R., Bot, M., Brodde, M., Taylor, P.J., Salm, P., Brinkmann, V., van Berkel, T., Assmann, G., and Biessen, E.A. (2007). FTY720, a synthetic sphingosine 1 phosphate analogue, inhibits development of atherosclerosis in low-density lipoprotein receptor-deficient mice. Circulation *115*, 501-508.

Nofer, J.R., Brodde, M.F., and Kehrel, B.E. (2010). High-density lipoproteins, platelets and the pathogenesis of atherosclerosis. Clin Exp Pharmacol Physiol *37*, 726-735.

Nofer, J.R., Kehrel, B., Fobker, M., Levkau, B., Assmann, G., and von Eckardstein, A. (2002). HDL and arteriosclerosis: beyond reverse cholesterol transport. Atherosclerosis *161*, 1-16.

Nofer, J.R., Levkau, B., Wolinska, I., Junker, R., Fobker, M., von Eckardstein, A., Seedorf, U., and Assmann, G. (2001). Suppression of endothelial cell apoptosis by high density lipoproteins (HDL) and HDL-associated lysosphingolipids. The Journal of biological chemistry *276*, 34480-34485.

Nofer, J.R., van der Giet, M., Tolle, M., Wolinska, I., von Wnuck Lipinski, K., Baba, H.A., Tietge, U.J., Godecke, A., Ishii, I., Kleuser, B.*, et al.* (2004). HDL induces NO-dependent vasorelaxation via the lysophospholipid receptor S1P3. The Journal of clinical investigation *113*, 569-581.

Nofer, J.R., and van Eck, M. (2011). HDL scavenger receptor class B type I and platelet function. Current opinion in lipidology *22*, 277-282.

Nugent, D., and Xu, Y. (2000). Sphingosine-1-phosphate: characterization of its inhibition of platelet aggregation. Platelets *11*, 226-232.

Okajima, F. (2002). Plasma lipoproteins behave as carriers of extracellular sphingosine 1-phosphate: is this an atherogenic mediator or an anti-atherogenic mediator? Biochim Biophys Acta *1582*, 132-137.

Oo, M.L., Chang, S.H., Thangada, S., Wu, M.T., Rezaul, K., Blaho, V., Hwang, S.I., Han, D.K., and Hla, T. (2011). Engagement of S1P(1)-degradative mechanisms leads to vascular leak in mice. The Journal of clinical investigation *121*, 2290-2300.

Orr, A.W., Hastings, N.E., Blackman, B.R., and Wamhoff, B.R. (2010). Complex regulation and function of the inflammatory smooth muscle cell phenotype in atherosclerosis. J Vasc Res *47*, 168-180.

Pappu, R., Schwab, S.R., Cornelissen, I., Pereira, J.P., Regard, J.B., Xu, Y., Camerer, E., Zheng, Y.W., Huang, Y., Cyster, J.G.*, et al.* (2007). Promotion of lymphocyte egress into blood and lymph by distinct sources of sphingosine-1-phosphate. Science *316*, 295-298.

Park, L., Raman, K.G., Lee, K.J., Lu, Y., Ferran, L.J., Jr., Chow, W.S., Stern, D., and Schmidt, A.M. (1998). Suppression of accelerated diabetic atherosclerosis by the soluble receptor for advanced glycation endproducts. Nature medicine *4*, 1025-1031.

Pei, Y., Chen, X., Aboutouk, D., Fuller, M.T., Dadoo, O., Yu, P., White, E.J., Igdoura, S.A., and Trigatti, B.L. (2013). SR-BI in bone marrow derived cells protects mice from diet induced coronary artery atherosclerosis and myocardial infarction. PLoS One *8*, e72492.

Pitson, S.M. (2011). Regulation of sphingosine kinase and sphingolipid signaling. Trends Biochem Sci *36*, 97-107.

Poti, F., Costa, S., Bergonzini, V., Galletti, M., Pignatti, E., Weber, C., Simoni, M., and Nofer, J.R. (2012). Effect of sphingosine 1-phosphate (S1P) receptor agonists FTY720 and CYM5442 on atherosclerosis development in LDL receptor deficient (LDL-R(-)/(-)) mice. Vascul Pharmacol *57*, 56-64.

Poti, F., Gualtieri, F., Sacchi, S., Weissen-Plenz, G., Varga, G., Brodde, M., Weber, C., Simoni, M., and Nofer, J.R. (2013). KRP-203, sphingosine 1-phosphate receptor type 1 agonist, ameliorates atherosclerosis in LDL-R-/- mice. Arteriosclerosis, thrombosis, and vascular biology *33*, 1505-1512.

Poti, F., Simoni, M., and Nofer, J.R. (2014). Atheroprotective role of high-density lipoprotein (HDL)-associated sphingosine-1-phosphate (S1P). Cardiovasc Res *103*, 395-404.

Renard, C.B., Kramer, F., Johansson, F., Lamharzi, N., Tannock, L.R., von Herrath, M.G., Chait, A., and Bornfeldt, K.E. (2004). Diabetes and diabetes-associated lipid abnormalities have distinct effects on initiation and progression of atherosclerotic lesions. The Journal of clinical investigation *114*, 659-668.

Rigotti, A., Miettinen, H.E., and Krieger, M. (2003). The role of the high-density lipoprotein receptor SR-BI in the lipid metabolism of endocrine and other tissues. Endocr Rev *24*, 357-387.

Rigotti, A., Trigatti, B.L., Penman, M., Rayburn, H., Herz, J., and Krieger, M. (1997). A targeted mutation in the murine gene encoding the high density lipoprotein (HDL) receptor scavenger receptor class B type I reveals its key role in HDL metabolism. Proc Natl Acad Sci U S A *94*, 12610-12615.

Rivera, J., Proia, R.L., and Olivera, A. (2008). The alliance of sphingosine-1-phosphate and its receptors in immunity. Nature reviews Immunology *8*, 753-763.

Ron, D., and Walter, P. (2007). Signal integration in the endoplasmic reticulum unfolded protein response. Nat Rev Mol Cell Biol *8*, 519-529.

Rosenblat, M., Gaidukov, L., Khersonsky, O., Vaya, J., Oren, R., Tawfik, D.S., and Aviram, M. (2006). The catalytic histidine dyad of high density lipoprotein-associated serum paraoxonase-1 (PON1) is essential for PON1-mediated inhibition of low density lipoprotein oxidation and stimulation of macrophage cholesterol efflux. The Journal of biological chemistry *281*, 7657-7665.

Russo, I., and Frangogiannis, N.G. (2016). Diabetes-associated cardiac fibrosis: Cellular effectors, molecular mechanisms and therapeutic opportunities. J Mol Cell Cardiol *90*, 84-93.

Rutherford, C., Childs, S., Ohotski, J., McGlynn, L., Riddick, M., MacFarlane, S., Tasker, D., Pyne, S., Pyne, N.J., Edwards, J.*, et al.* (2013). Regulation of cell survival by sphingosine-1-phosphate receptor S1P1 via reciprocal ERK-dependent suppression of Bim and PI-3-kinase/protein kinase C-mediated upregulation of Mcl-1. Cell death & disease *4*, e927.

Rye, K.A., Clay, M.A., and Barter, P.J. (1999). Remodelling of high density lipoproteins by plasma factors. Atherosclerosis *145*, 227-238.

Saelens, X., Festjens, N., Vande Walle, L., van Gurp, M., van Loo, G., and Vandenabeele, P. (2004). Toxic proteins released from mitochondria in cell death. Oncogene *23*, 2861-2874.

Sanchez, T., and Hla, T. (2004). Structural and functional characteristics of S1P receptors. Journal of cellular biochemistry *92*, 913-922.

Sanna, M.G., Wang, S.K., Gonzalez-Cabrera, P.J., Don, A., Marsolais, D., Matheu, M.P., Wei, S.H., Parker, I., Jo, E., Cheng, W.C.*, et al.* (2006). Enhancement of capillary leakage and restoration of lymphocyte egress by a chiral S1P1 antagonist in vivo. Nature chemical biology *2*, 434-441.

Sattler, K., Lehmann, I., Graler, M., Brocker-Preuss, M., Erbel, R., Heusch, G., and Levkau, B. (2014). HDL-bound sphingosine 1-phosphate (S1P) predicts the severity of coronary artery atherosclerosis. Cellular physiology and biochemistry : international journal of experimental cellular physiology, biochemistry, and pharmacology *34*, 172-184.

Sattler, K.J., Elbasan, S., Keul, P., Elter-Schulz, M., Bode, C., Graler, M.H., Brocker-Preuss, M., Budde, T., Erbel, R., Heusch, G.*, et al.* (2010). Sphingosine 1-phosphate levels in plasma and HDL are altered in coronary artery disease. Basic research in cardiology *105*, 821-832.

Scanu, A.M., and Edelstein, C. (2008). HDL: bridging past and present with a look at the future. FASEB journal : official publication of the Federation of American Societies for Experimental Biology *22*, 4044-4054.

Schuchardt, M., Tolle, M., Prufer, J., and van der Giet, M. (2011). Pharmacological relevance and potential of sphingosine 1-phosphate in the vascular system. British journal of pharmacology *163*, 1140-1162.

Schwartz, G.G., Olsson, A.G., Abt, M., Ballantyne, C.M., Barter, P.J., Brumm, J., Chaitman, B.R., Holme, I.M., Kallend, D., Leiter, L.A.*, et al.* (2012). Effects of dalcetrapib in patients with a recent acute coronary syndrome. N Engl J Med *367*, 2089-2099.

Seimon, T., and Tabas, I. (2009). Mechanisms and consequences of macrophage apoptosis in atherosclerosis. Journal of lipid research *50 Suppl*, S382-387.

Sevvana, M., Ahnstrom, J., Egerer-Sieber, C., Lange, H.A., Dahlback, B., and Muller, Y.A. (2009). Serendipitous fatty acid binding reveals the structural determinants for ligand recognition in apolipoprotein M. J Mol Biol *393*, 920-936.

Shih, D.M., Gu, L., Xia, Y.R., Navab, M., Li, W.F., Hama, S., Castellani, L.W., Furlong, C.E., Costa, L.G., Fogelman, A.M.*, et al.* (1998). Mice lacking serum paraoxonase are susceptible to organophosphate toxicity and atherosclerosis. Nature *394*, 284-287.

Singleton, P.A., Dudek, S.M., Chiang, E.T., and Garcia, J.G. (2005). Regulation of sphingosine 1-phosphate-induced endothelial cytoskeletal rearrangement and barrier enhancement by S1P1 receptor, PI3 kinase, Tiam1/Rac1, and alpha-actinin. FASEB

journal : official publication of the Federation of American Societies for Experimental Biology *19*, 1646-1656.

Skoura, A., Michaud, J., Im, D.S., Thangada, S., Xiong, Y., Smith, J.D., and Hla, T. (2011). Sphingosine-1-phosphate receptor-2 function in myeloid cells regulates vascular inflammation and atherosclerosis. Arteriosclerosis, thrombosis, and vascular biology *31*, 81-85.

Smythies, L.E., White, C.R., Maheshwari, A., Palgunachari, M.N., Anantharamaiah, G.M., Chaddha, M., Kurundkar, A.R., and Datta, G. (2010). Apolipoprotein A-I mimetic 4F alters the function of human monocyte-derived macrophages. Am J Physiol Cell Physiol *298*, C1538-1548.

Stoneman, V., Braganza, D., Figg, N., Mercer, J., Lang, R., Goddard, M., and Bennett, M. (2007). Monocyte/macrophage suppression in CD11b diphtheria toxin receptor transgenic mice differentially affects atherogenesis and established plaques. Circulation research *100*, 884-893.

Summers, S.A. (2010). Sphingolipids and insulin resistance: the five Ws. Current opinion in lipidology *21*, 128-135.

Swirski, F.K., Libby, P., Aikawa, E., Alcaide, P., Luscinskas, F.W., Weissleder, R., and Pittet, M.J. (2007). Ly-6Chi monocytes dominate hypercholesterolemia-associated

monocytosis and give rise to macrophages in atheromata. The Journal of clinical investigation *117*, 195-205.

Tabas, I. (2010a). Macrophage death and defective inflammation resolution in atherosclerosis. Nature reviews Immunology *10*, 36-46.

Tabas, I. (2010b). The role of endoplasmic reticulum stress in the progression of atherosclerosis. Circulation research *107*, 839-850.

Tabas, I., Garcia-Cardena, G., and Owens, G.K. (2015). Recent insights into the cellular biology of atherosclerosis. The Journal of cell biology *209*, 13-22.

Tacke, F., Alvarez, D., Kaplan, T.J., Jakubzick, C., Spanbroek, R., Llodra, J., Garin, A., Liu, J., Mack, M., van Rooijen, N.*, et al.* (2007). Monocyte subsets differentially employ CCR2, CCR5, and CX3CR1 to accumulate within atherosclerotic plaques. The Journal of clinical investigation *117*, 185-194.

Takeya, H., Gabazza, E.C., Aoki, S., Ueno, H., and Suzuki, K. (2003). Synergistic effect of sphingosine 1-phosphate on thrombin-induced tissue factor expression in endothelial cells. Blood *102*, 1693-1700.

Takuwa, N., Du, W., Kaneko, E., Okamoto, Y., Yoshioka, K., and Takuwa, Y. (2011). Tumor-suppressive sphingosine-1-phosphate receptor-2 counteracting tumor-promoting

sphingosine-1-phosphate receptor-1 and sphingosine kinase 1 - Jekyll Hidden behind Hyde. Am J Cancer Res *1*, 460-481.

Tamama, K., Tomura, H., Sato, K., Malchinkhuu, E., Damirin, A., Kimura, T., Kuwabara, A., Murakami, M., and Okajima, F. (2005). High-density lipoprotein inhibits migration of vascular smooth muscle cells through its sphingosine 1-phosphate component. Atherosclerosis *178*, 19-23.

Tao, H., Yancey, P.G., Babaev, V.R., Blakemore, J.L., Zhang, Y., Ding, L., Fazio, S., and Linton, M.F. (2015). Macrophage SR-BI mediates efferocytosis via Src/PI3K/Rac1 signaling and reduces atherosclerotic lesion necrosis. Journal of lipid research *56*, 1449-1460.

Tauseef, M., Kini, V., Knezevic, N., Brannan, M., Ramchandaran, R., Fyrst, H., Saba, J., Vogel, S.M., Malik, A.B., and Mehta, D. (2008). Activation of sphingosine kinase-1 reverses the increase in lung vascular permeability through sphingosine-1-phosphate receptor signaling in endothelial cells. Circulation research *103*, 1164-1172.

Thorp, E., Cui, D., Schrijvers, D.M., Kuriakose, G., and Tabas, I. (2008). Mertk receptor mutation reduces efferocytosis efficiency and promotes apoptotic cell accumulation and plaque necrosis in atherosclerotic lesions of apoe-/- mice. Arteriosclerosis, thrombosis, and vascular biology *28*, 1421-1428.

Thorp, E., Li, G., Seimon, T.A., Kuriakose, G., Ron, D., and Tabas, I. (2009). Reduced apoptosis and plaque necrosis in advanced atherosclerotic lesions of Apoe-/- and Ldlr-/- mice lacking CHOP. Cell metabolism *9*, 474-481.

Thorp, E., and Tabas, I. (2009). Mechanisms and consequences of efferocytosis in advanced atherosclerosis. J Leukoc Biol *86*, 1089-1095.

Thuahnai, S.T., Lund-Katz, S., Williams, D.L., and Phillips, M.C. (2001). Scavenger receptor class B, type I-mediated uptake of various lipids into cells. Influence of the nature of the donor particle interaction with the receptor. The Journal of biological chemistry *276*, 43801-43808.

Tolle, M., Pawlak, A., Schuchardt, M., Kawamura, A., Tietge, U.J., Lorkowski, S., Keul, P., Assmann, G., Chun, J., Levkau, B.*, et al.* (2008). HDL-associated lysosphingolipids inhibit NAD(P)H oxidase-dependent monocyte chemoattractant protein-1 production. Arteriosclerosis, thrombosis, and vascular biology *28*, 1542-1548.

Trigatti, B., Rayburn, H., Vinals, M., Braun, A., Miettinen, H., Penman, M., Hertz, M., Schrenzel, M., Amigo, L., Rigotti, A.*, et al.* (1999). Influence of the high density lipoprotein receptor SR-BI on reproductive and cardiovascular pathophysiology. Proc Natl Acad Sci U S A *96*, 9322-9327.

Trigatti, B.L., Krieger, M., and Rigotti, A. (2003). Influence of the HDL receptor SR-BI on lipoprotein metabolism and atherosclerosis. Arterioscler Thromb Vasc Biol *23*, 1732-1738.

Tsukano, H., Gotoh, T., Endo, M., Miyata, K., Tazume, H., Kadomatsu, T., Yano, M., Iwawaki, T., Kohno, K., Araki, K.*, et al.* (2010). The endoplasmic reticulum stress-C/EBP homologous protein pathway-mediated apoptosis in macrophages contributes to the instability of atherosclerotic plaques. Arteriosclerosis, thrombosis, and vascular biology *30*, 1925-1932.

Ulrych, T., Bohm, A., Polzin, A., Daum, G., Nusing, R.M., Geisslinger, G., Hohlfeld, T., Schror, K., and Rauch, B.H. (2011). Release of sphingosine-1-phosphate from human platelets is dependent on thromboxane formation. Journal of thrombosis and haemostasis : JTH *9*, 790-798.

van der Stoep, M., Korporaal, S.J., and Van Eck, M. (2014). High-density lipoprotein as a modulator of platelet and coagulation responses. Cardiovasc Res *103*, 362-371.

Van Eck, M., Bos, I.S., Hildebrand, R.B., Van Rij, B.T., and Van Berkel, T.J. (2004). Dual role for scavenger receptor class B, type I on bone marrow-derived cells in atherosclerotic lesion development. Am J Pathol *165*, 785-794.

Van Eck, M., Hoekstra, M., Hildebrand, R.B., Yaong, Y., Stengel, D., Kruijt, J.K., Sattler, W., Tietge, U.J., Ninio, E., Van Berkel, T.J.*, et al.* (2007). Increased oxidative stress in scavenger receptor BI knockout mice with dysfunctional HDL. Arteriosclerosis, thrombosis, and vascular biology *27*, 2413-2419.

Venkataraman, K., Thangada, S., Michaud, J., Oo, M.L., Ai, Y., Lee, Y.M., Wu, M., Parikh, N.S., Khan, F., Proia, R.L.*, et al.* (2006). Extracellular export of sphingosine kinase-1a contributes to the vascular S1P gradient. The Biochemical journal *397*, 461-471.

Vinals, M., Xu, S., Vasile, E., and Krieger, M. (2003). Identification of the N-linked glycosylation sites on the high density lipoprotein (HDL) receptor SR-BI and assessment of their effects on HDL binding and selective lipid uptake. The Journal of biological chemistry *278*, 5325-5332.

Viswambharan, H., Ming, X.F., Zhu, S., Hubsch, A., Lerch, P., Vergeres, G., Rusconi, S., and Yang, Z. (2004). Reconstituted high-density lipoprotein inhibits thrombin-induced endothelial tissue factor expression through inhibition of RhoA and stimulation of phosphatidylinositol 3-kinase but not Akt/endothelial nitric oxide synthase. Circulation research *94*, 918-925.

Voulgari, C., Papadogiannis, D., and Tentolouris, N. (2010). Diabetic cardiomyopathy: from the pathophysiology of the cardiac myocytes to current diagnosis and management strategies. Vascular health and risk management *6*, 883-903.

Wang, G., Kim, R.Y., Imhof, I., Honbo, N., Luk, F.S., Li, K., Kumar, N., Zhu, B.Q., Eberle, D., Ching, D.*, et al.* (2014). The immunosuppressant FTY720 prolongs survival in a mouse model of diet-induced coronary atherosclerosis and myocardial infarction. Journal of cardiovascular pharmacology *63*, 132-143.

Wang, L., Connelly, M.A., Ostermeyer, A.G., Chen, H.H., Williams, D.L., and Brown, D.A. (2003). Caveolin-1 does not affect SR-BI-mediated cholesterol efflux or selective uptake of cholesteryl ester in two cell lines. Journal of lipid research *44*, 807-815.

Weigert, A., Johann, A.M., von Knethen, A., Schmidt, H., Geisslinger, G., and Brune, B. (2006). Apoptotic cells promote macrophage survival by releasing the antiapoptotic mediator sphingosine-1-phosphate. Blood *108*, 1635-1642.

Weigert, A., Weis, N., and Brune, B. (2009). Regulation of macrophage function by sphingosine-1-phosphate. Immunobiology *214*, 748-760.

Werstuck, G.H., Khan, M.I., Femia, G., Kim, A.J., Tedesco, V., Trigatti, B., and Shi, Y. (2006). Glucosamine-induced endoplasmic reticulum dysfunction is associated with accelerated atherosclerosis in a hyperglycemic mouse model. Diabetes *55*, 93-101.

Whetzel, A.M., Bolick, D.T., Srinivasan, S., Macdonald, T.L., Morris, M.A., Ley, K., and Hedrick, C.C. (2006). Sphingosine-1 phosphate prevents monocyte/endothelial interactions in type 1 diabetic NOD mice through activation of the S1P1 receptor. Circulation research *99*, 731-739.

Wilkerson, B.A., Grass, G.D., Wing, S.B., Argraves, W.S., and Argraves, K.M. (2012). Sphingosine 1-phosphate (S1P) carrier-dependent regulation of endothelial barrier: high density lipoprotein (HDL)-S1P prolongs endothelial barrier enhancement as compared with albumin-S1P via effects on levels, trafficking, and signaling of S1P1. The Journal of biological chemistry *287*, 44645-44653.

Winer, N., and Sowers, J.R. (2004). Epidemiology of diabetes. J Clin Pharmacol *44*, 397-405.

Wong, N.D. (2014). Epidemiological studies of CHD and the evolution of preventive cardiology. Nat Rev Cardiol *11*, 276-289.

Wu, W., Mosteller, R.D., and Broek, D. (2004). Sphingosine kinase protects lipopolysaccharide-activated macrophages from apoptosis. Mol Cell Biol *24*, 7359-7369.

Wu, Z., Wagner, M.A., Zheng, L., Parks, J.S., Shy, J.M., 3rd, Smith, J.D., Gogonea, V., and Hazen, S.L. (2007). The refined structure of nascent HDL reveals a key functional domain for particle maturation and dysfunction. Nat Struct Mol Biol *14*, 861-868.

Xu, J., Qian, J., Xie, X., Lin, L., Ma, J., Huang, Z., Fu, M., Zou, Y., and Ge, J. (2012). High density lipoprotein cholesterol promotes the proliferation of bone-derived mesenchymal stem cells via binding scavenger receptor-B type I and activation of PI3K/Akt, MAPK/ERK1/2 pathways. Mol Cell Biochem *371*, 55-64.

Yan, S.D., Schmidt, A.M., Anderson, G.M., Zhang, J., Brett, J., Zou, Y.S., Pinsky, D., and Stern, D. (1994). Enhanced cellular oxidant stress by the interaction of advanced glycation end products with their receptors/binding proteins. The Journal of biological chemistry *269*, 9889-9897.

Yatomi, Y., Ruan, F., Hakomori, S., and Igarashi, Y. (1995). Sphingosine-1-phosphate: a platelet-activating sphingolipid released from agonist-stimulated human platelets. Blood *86*, 193-202.

Yu, P. (2016). The high density lipoprotein and atherosclerosis.

Yuhanna, I.S., Zhu, Y., Cox, B.E., Hahner, L.D., Osborne-Lawrence, S., Lu, P., Marcel, Y.L., Anderson, R.G., Mendelsohn, M.E., Hobbs, H.H.*, et al.* (2001). High-density lipoprotein binding to scavenger receptor-BI activates endothelial nitric oxide synthase. Nature medicine *7*, 853-857.

Zeadin, M.G., Petlura, C.I., and Werstuck, G.H. (2013). Molecular mechanisms linking diabetes to the accelerated development of atherosclerosis. Can J Diabetes *37*, 345-350.

Zernecke, A., Shagdarsuren, E., and Weber, C. (2008). Chemokines in atherosclerosis: an update. Arteriosclerosis, thrombosis, and vascular biology *28*, 1897-1908.

Zhang, B., Tomura, H., Kuwabara, A., Kimura, T., Miura, S., Noda, K., Okajima, F., and Saku, K. (2005a). Correlation of high density lipoprotein (HDL)-associated sphingosine 1-phosphate with serum levels of HDL-cholesterol and apolipoproteins. Atherosclerosis *178*, 199-205.

Zhang, L., Orban, M., Lorenz, M., Barocke, V., Braun, D., Urtz, N., Schulz, C., von Bruhl, M.L., Tirniceriu, A., Gaertner, F.*, et al.* (2012). A novel role of sphingosine 1-phosphate receptor S1pr1 in mouse thrombopoiesis. The Journal of experimental medicine *209*, 2165-2181.

Zhang, Q., Zhang, Y., Feng, H., Guo, R., Jin, L., Wan, R., Wang, L., Chen, C., and Li, S. (2011). High density lipoprotein (HDL) promotes glucose uptake in adipocytes and glycogen synthesis in muscle cells. PloS one *6*, e23556.

Zhang, S., Picard, M.H., Vasile, E., Zhu, Y., Raffai, R.L., Weisgraber, K.H., and Krieger, M. (2005b). Diet-induced occlusive coronary atherosclerosis, myocardial infarction, cardiac dysfunction, and premature death in scavenger receptor class B type I-deficient, hypomorphic apolipoprotein ER61 mice. Circulation *111*, 3457-3464.

Zhang, Y., Ahmed, A.M., McFarlane, N., Capone, C., Boreham, D.R., Truant, R., Igdoura, S.A., and Trigatti, B.L. (2007). Regulation of SR-BI-mediated selective lipid uptake in Chinese hamster ovary-derived cells by protein kinase signaling pathways. Journal of lipid research *48*, 405-416.

Zhou, A.X., and Tabas, I. (2013). The UPR in atherosclerosis. Seminars in immunopathology *35*, 321-332.

Zhu, W., Saddar, S., Seetharam, D., Chambliss, K.L., Longoria, C., Silver, D.L., Yuhanna, I.S., Shaul, P.W., and Mineo, C. (2008). The scavenger receptor class B type I adaptor protein PDZK1 maintains endothelial monolayer integrity. Circulation research *102*, 480-487.